Dissertation

The hPGDS-PGD_2-DP1-DP2 axis in innate immunity and pulmonary inflammation

submitted by

Sonja RITTCHEN, BSc, MSc

for the Academic Degree of

Doctor of Philosophy

(PhD)

at the

Medical University of Graz

Otto Loewi Research Center

for Vascular Biology, Immunology and Inflammation,

Division of Pharmacology

under the supervision of

Prof. Dr. Akos Heinemann

2020

Declaration

I hereby declare that this thesis is my own original work and that I have fully acknowledged by name all of those individuals and organizations that have contributed to the research for this thesis. Due acknowledgement has been made in the text to all other material used. Throughout this thesis and in all related publications I followed the "Standards of Good Scientific Practice and Ombuds Committee at the Medical University of Graz".

Graz, 23. November 2020

Location, date

Signature

Disclosures

Parts of my dissertation have been published in:

(1) Rittchen, S; Heinemann, A Therapeutic Potential of Hematopoietic Prostaglandin D_2 Synthase in Allergic Inflammation. Cells. 2019; 8(6)

(2) Rittchen, S; Rohrer, K; Platzer, W; Knuplez, E; Bärnthaler, T; Marsh, LM; Atallah, R; Sinn, K; Klepetko, W; Sharma, N; Nagaraj, C; Heinemann, A Prostaglandin D_2 strengthens human endothelial barrier by activation of E-type receptor 4. Biochem Pharmacol. 2020 Oct 7; 114277

All of the above mentioned co-authors have explicitly agreed to the use of their data in this thesis.

Collaborations

- Jasmin Strutz and Gernot Desoye, Department of Gynaecology, Medical University of Graz – Spheroid sprouting assay (protocol and assistance)
- Nassim Ghaffari Tabrizi-Wizsy, Otto Loewi Research Center, Division of –Immunology and Pathophysiology, Medical University of Graz – CAM assay (protocol and assistance)
- Nerea Ferreirós and Daniel Kratz, Institute of Clinical Pharmacology, Goethe-University Frankfurt, Pharmazentrum Frankfurt/ZAFES, Frankfurt, Germany – LC/MS (sample preparation, measurements and results)
- Walter Klepetko and Katharina Sinn, Division of Thoracic Surgery, Medical University of Vienna – donor lung material
- Leigh Marsh, Ludwig Boltzmann Institute for Lung Vascular Research, Graz – EP4 and DP1 receptor staining on human lung sections
- Rudolf Schicho, Department of Pharmacology, Medical University of Graz – C57BL/6j mice

Acknowledgements

First of all, I would like to thank my supervisor Akos Heinemann for taking me in and enabling me to work on these great projects throughout my PhD. I cannot say how grateful I am for your genuine support and that your door is always open, but I especially value your open mind for suggestions. Thanks for giving me the freedom to explore and grow with my projects.

My special thanks go to Katharina Jandl, who guided and encouraged me throughout my PhD - not only on a professional level. Thanks for your friendship, help, concern, support, knowledge, scientific advice and many, many more things you did for me that never failed to cheer me up and bring me back on track.

I would like to thank Rufina Schuligoi and the members of my thesis committee Gernot Desoye and Grazyna Kwapiszewska for their valuable scientific advice and contributions to my projects. Additionally, I want to thank Nassim Ghaffari Tabrizi-Wizsy for offering me the opportunity to use the CAM assay and introducing me to the technique.

The past four years at the Otto Loewi Research Center, Division of Pharmacology were busy, educational, sometimes nerve wrecking, but first and foremost inspirational and a lot of fun – in brief, the best place to conduct my PhD thesis. All this would not have been possible without my amazing friends and co-workers: Kathrin, Georg Richtig, Georg Racic, David, Ilse, Wolfgang, Thomas, Iris, Bernhard, Melanie, Eva, Athina, Reham, Sabine, Julia, July and everyone else! I'm grateful for your friendship, endless support, pep talks and excellent technical assistance.

Further, I would like to express my gratitude to Simon Phipps for accepting me as visiting PhD student in his group. I have benefitted in so many ways from my stay in Brisbane – professionally and personally - it was a very fruitful stay, indeed. Special thanks go to my lab mates Mary, Natasha, Lisa, Bodie, Ridwan, Mahfuz, Al Amin and Ismail for making me feel welcome from the beginning. Ashik, I have no words to say how thankful I am to you. I miss your valuable

knowledge and our scientific and non-scientific discussions – it was always a pleasure working with you. You were the best supervisor I could have wished for!

Many thanks also go to my sister and Theresa for their company, support and for providing me with food whenever I didn't have time to cook. Ines, I cannot tell you how much I value our conversations and the time we spend together.

My PhD life would have been very dull without my precious friends: the Biochem Crew, who shared so many challenges with me – it's good to have someone in the same boat. My Kremser girls - thanks for always having an open ear and magnificent suggestions. Die Kärntner, who I have spent countless fun nights and days with. Thanks also to my Australian flatmates and friends for making my stay so much more fun. You all have become such a big part of my life – a big thanks for your support, fun times and cheering me up!

Last but not least, I greatly appreciate all the support and help I get from my parents, but also their concern and advice - thank you for your trust and making everything possible. This small note of thanks doesn't come close to how grateful I am! Also, thanks Tasi for keeping me sane.

My PhD work was funded by the doctorate program "Molecular Fundamentals of Inflammation" (DK MOLIN, FWF, W1241) and the Medical University of Graz. My research stay in Simon Phipps' Respiratory Immunology group at QIMR Berghofer Institute, Brisbane, Australia was supported by an EMBO Short-term Fellowship (8109) and by the doctorate program MOLIN (FWF, W1241).

It is good to have an end to journey toward;
But it is the journey that matters, in the end.

- Ursula K. Le Guin

Table of contents

DECLARATION II

DISCLOSURES III

ACKNOWLEDGEMENTS IV

TABLE OF CONTENTS VII

ABBREVIATIONS XIII

ZUSAMMENFASSUNG 1

ABSTRACT 3

1. INTRODUCTION 5

1.1. PROSTAGLANDIN D_2 GENERATION AND SIGNALLING 5

1.1.1. THE CYCLOOXYGENASE PATHWAY 5

1.1.2. HPGDS – THE RATE LIMITING ENZYME OF PGD_2 PRODUCTION 7

1.1.3. IDENTIFICATION OF POTENTIAL PROSTAGLANDIN SOURCES 8

Immune cells *8*

Parenchymal cells *11*

1.1.4. DP RECEPTOR SIGNALLING AND FUNCTION 11

DP1 receptor in pulmonary inflammation *12*

DP2 receptor in pulmonary inflammation *13*

1.1.5. NON-DP RECEPTOR-MEDIATED PGD_2-INDUCED EFFECTS 14

1.2. PULMONARY ENDOTHELIUM 15

1.2.1. ENDOTHELIAL BARRIER FUNCTION 16

1.2.2. PROSTAGLANDINS REGULATE ENDOTHELIAL BARRIER FUNCTION 16

Prostaglandin E_2 *17*

Prostaglandin D_2 *17*

1.2.3. VASCULAR LEAKAGE IN AIRWAY INFLAMMATION 18

1.2.4. VASCULAR DYSFUNCTION AS A RESULT OF DE-REGULATED ANGIOGENESIS 19

1.3. MONONUCLEAR PHAGOCYTES AS INFLAMMATORY MODULATORS 21

1.3.1. THE MONONUCLEAR PHAGOCYTE SYSTEM 21

Circulating monocytes *21*

Monocyte-derived macrophages *23*

1.3.2. ORIGIN AND FUNCTION OF PULMONARY MACROPHAGES 24

1.3.3. POTENTIAL AS PROSTAGLANDIN D_2 SOURCES AND TARGETS 25

1.3.4. RESPONSE TO PULMONARY INFECTION AND INJURY 26

1.3.5. MACROPHAGES ARE CENTRAL MODULATORS OF PULMONARY TISSUE REPAIR, REGENERATION AND REMODELLING 28

Repair and regeneration *29*

Pathological remodelling *30*

1.4. RESPIRATORY INFLAMMATORY DISORDERS – PROSTAGLANDIN D_2 AS THERAPEUTIC TARGET 31

1.4.1. ACUTE RESPIRATORY INFLAMMATION 31

1.4.2. CHRONIC PULMONARY INFLAMMATION 33

Pulmonary fibrosis *33*

Allergic asthma and rhinitis *34*

Chronic obstructive pulmonary disease (COPD) *36*

1.4.3. ONGOING CLINICAL STUDIES ABOUT THE HPGDS-PGD_2-DP1-DP2 AXIS AS THERAPEUTIC TARGET 36

DP2 receptor *36*

DP1 receptor *37*

Hematopoietic PGD synthase *38*

1.5. AIMS OF THE DISSERTATION 39

PART I – E-TYPE 4 RECEPTOR MEDIATES PGD_2-INDUCED ENHANCEMENT OF PULMONARY ENDOTHELIAL BARRIER FUNCTION 39

PART II – CHARACTERIZATION OF NOVEL PROSTAGLANDIN SOURCES IN LPS-INDUCED INFLAMMATION 39

PART III – PGD_2-DP2 ACTIVATION ON HUMAN IL-4 POLARIZED MONOCYTE-DERIVED MACROPHAGES ABROGATES ANGIOGENIC POTENTIAL OF CONDITIONED MEDIUM 39

2. MATERIALS AND METHODS 40

2.1 ETHICAL APPROVALS 40

Human ethics. *40*

Animal ethics. *40*

2.2 CELL CULTURE 40

Endothelial cell culture. *40*

EP4-knock down in primary human microvascular endothelial cells. *41*

Isolation of peripheral blood leukocytes. 41
Generation of human monocyte-derived macrophages. 42
Stimulation of MDM with PGD_2, BW245c or DK-PGD_2 and collection of conditioned medium. 42
Broncho-alveolar lavage (BAL) fluid collection and culturing of mononuclear cells. 43
2.3 CELLULAR ASSAYS 44
Electric Impedance Cell-substrate Sensing (ECIS). 44
Thrombin barrier disruption assay. 44
Cell cycle analysis. 45
Spheroid sprouting assay with human pulmonary microvascular endothelial cells. 45
Platelet aggregation. 46
2.4 MICROSCOPY AND BIOCHEMICAL METHODS 46
Immunofluorescence staining for microscopy. 46
F-actin / VE-cadherin staining in human endothelial cells. 47
Quantification of endothelial monolayer integrity after VE-cadherin/F-actin staining. 47
EP4 / DP1 staining. 48
hPGDS staining. 48
In Situ hybridization (ISH). 49
Real time quantitative PCR. 50
Western blotting. 52
Flow cytometry and FACS. 54
Myeloid cell sorting from whole lung single cell suspension. 55
PGD_2 and PGE_2 detection in conditioned medium. 57
Pierce BCA protein assay. 57
Determination of lipid mediators in conditioned medium with LC/MS. 58
2.5 *IN VIVO* AND *EX VIVO* MODELS 59
Animal housing. 59
LPS-induced lung inflammation model. 59
Ovalbumin-induced allergic airway inflammation. 59
Bleomycin-induced pulmonary fibrosis (chronic inflammation). 59
Chicken chorioallantoic membrane (CAM) angiogenesis assay. 60
2.6 STATISTICAL ANALYSIS 60
3. RESULTS 62
3.1. PART I: E-TYPE 4 RECEPTOR MEDIATES PGD_2-INDUCED ENHANCEMENT OF PULMONARY ENDOTHELIAL BARRIER FUNCTION 62

PGD_2 and DP1 agonist BW245c but not DP2 agonist DK-PGD_2 concentration-dependently enhanced human microvascular endothelial barrier 62

PGD_2 and DP1 agonist BW245c protect human microvascular endothelial cell barrier 64

DP1 antagonism but not DP2 antagonism partially reduces PGD_2-induced barrier enhancement 66

PGD_2 does not enhance HPMEC barrier function through activation of PPARγ, TP receptors or cyclooxygenases 67

Inhibition of adenylate cyclase and PKA does not ablate PGD_2 or BW245c-induced HPMEC barrier enhancement. 68

Human endothelial cells express very low basal levels of DP1 but much higher EP4 receptor mRNA and protein 71

Blockade of EP4 receptors abrogates PGD_2 and BW245c barrier enhancement and protection against thrombin-induced barrier disruption 71

Transient EP4 receptor knock-down in HPMECs diminishes barrier enhancement by PGD_2 and BW245c 75

PGE_2 and PGD_2 affect AKT phosphorylation but not VE-cadherin, focal adhesion kinase or paxillin phosphorylation in HPMEC. 78

PGD_2 and BW245c also promote human pulmonary artery endothelial cell barrier function through EP4-activation 79

3.2. PART II: CHARACTERIZATION OF NOVEL PROSTAGLANDIN SOURCES IN LPS-INDUCED INFLAMMATION 82

hPGDS expression in human circulating leukocytes and mononuclear phagocytes reveals potential PGD_2 sources 82

Murine monocytes, macrophages, neutrophils and mast cells sorted from the mouse lung express hPGDS on mRNA and protein level. 83

Evaluation of monocytes and macrophages as prostanoid sources in bleomycin-induced pulmonary fibrosis 86

Mononuclear cells collected with BALF from LPS-induced acute pulmonary inflammation but not OVA-induced allergic inflammation release PGD_2 88

Ex vivo LPS/IFN-γ stimulated murine monocytes and macrophages sorted from the healthy lung release significant amounts of prostaglandins. 90

Human peripheral blood monocytes and monocyte-derived macrophages release PGD_2 and PGE_2 after LPS/IFN-γ, but not IL-4 stimulation. 91

Human monocytes surpass monocyte-derived macrophages as prostaglandin sources after LPS/IFN-γ at all time points 93

Monocyte-derived PGE_2 affects endothelial cell barrier function 94

Human peripheral blood monocytes and monocyte-derived macrophages constitutively express hPGDS 96

In human mononuclear phagocytes, LPS/IFN-γ activation initiates rapid COX-2 upregulation, while hPGDS is downregulated after 24 h on mRNA level 97

Neutrophils sorted from mice with LPS-induced pulmonary inflammation release significant levels of PGD_2. 101

Murine monocytes and macrophages require the presence of LPS/IFN-γ to induce PG production, while repeated stimulation reduces PGD_2 but not PGE_2 release 102

Human neutrophils neither express relevant levels of hPGDS nor release PGD_2 after LPS stimulation *IN VITRO*. 105

3.3. PART III: PGD_2-DP2 ACTIVATION ON HUMAN IL-4 POLARIZED MONOCYTE-DERIVED MACROPHAGES ABROGATES ANGIOGENIC POTENTIAL OF CONDITIONED MEDIUM 106

PGD_2 significantly promotes HPMEC wound healing capacity, while PGD_2 stimulation of human MDM delays wound closure. 106

PGD_2 modifies primary human M2-like monocyte-derived macrophage morphology, but not CD206, CD80 or CD163 expression 107

PGD_2-primed M2-like macrophages differentially regulate HPMEC wound healing 109

PGD_2 stimulation of IL-4 polarized MDM reduces sprouting of HPMEC and angiogenesis in the CAM angiogenesis assay 111

Repeated PGD_2 stimulation during polarization of MDM derived from healthy or atopic donors results only in minor changes of their angiogenic secretome 113

DP2 activation on human MDM in the presence of IL-4 reduces angiogenic properties of conditioned media 116

Conditioned medium from DP receptor agonist-treated, IL-4 polarized human monocyte-derived macrophages differentially affects HPMEC resistance 116

DP1 and DP2 receptor activation on human IL-4 polarized macrophages differentially affect angiogenic secretome of macrophages 117

4. DISCUSSION 119

4.1 PART I: E-type receptor 4 mediates PGD_2 enhancement of pulmonary endothelial barrier function 119

4.2 PART II: Characterization of novel prostaglandin sources in LPS-induced inflammation 124

4.3 PART III: PGD_2-DP2 ACTIVATION ON HUMAN IL-4 POLARIZED MONOCYTE-DERIVED MACROPHAGES ABROGATES ANGIOGENIC POTENTIAL OF CONDITIONED MEDIUM 129

5. CONCLUSION 133

6. REFERENCES 135

APPENDIX XII

7.1 MATERIALS & EQUIPMENT XII

Abbreviations

AA	arachidonic acid
AC	adenylate cyclase
AF	Alexa Fluor (fluorophore)
AKT	protein kinase B
APC	antigen presenting cell / fluorophore
ARDS	acute respiratory distress syndrome
BAL	broncho-alveolar lavage
bFGF	basic fibroblast growth factor
Ca^{2+}	calcium ion
CAM	chorioallantoic membrane
cAMP	cyclic adenosine monophosphate
CD	cluster of differentiation
COPD	chronic obstructive pulmonary disease
COX	cyclooxygenase
Cy	cyanine (fluorophore)
CRTH2	chemoattractant receptor-homologous molecule on Th2
DAG	diacylglycerol
DAMP	danger-associate molecular pattern
DP	D-type prostanoid receptor
ELISA	enzyme-linked immunosorbent assay
eNOS	endothelial nitric oxide synthase
EP	E-type prostanoid receptor
F-actin	filamentous actin
FACS	fluorescence-activated cell sorting
FCS	fetal calf serum
FMO	fluorescence minus one
GAPDH	glyceraldehyde dehydrogenase
GPCR	G-protein coupled receptor
HPAEC	human pulmonary artery endothelial cells
HDMEC	human dermal microvascular endothelial cells
hPGDS	hematopoietic prostaglandin D synthase
HPMEC	human pulmonary microvascular endothelial cells
HSC	hematopoietic stem cell
IC	isotype control
ICS	inhaled corticosteroids
IFN	interferon
Ig	immunoglobin
IL	interleukin
iNOS	inducible nitric oxide synthase

IPF	idiopathic pulmonary fibrosis
LPS	lipopolysaccharide
LPGDS	lipocalin-type prostaglandin D synthase
Ly6C	lymphocyte antigen 6 complex locus C1
NSAID	nonsteroidal anti-inflammatory drug
MAPK	mitogen-activated protein kinase
M-CSF	macrophage-colony stimulating factor
MDM	monocyte-derived macrophage
MOX	methoxylamine oxide
mPGES	microsomal PGE synthase
NK cells	natural killer cells
OVA	ovalbumin
PAMP	pathogen-associate molecular pattern
P/S	penicillin/streptomycin
PBMC	peripheral blood mononuclear cells
PBS	phosphate-buffered saline
PI3K	phostphatidyl inositol 3 kinase
PE	phycoerythrin (fluorophore)
PerCP	peridinin chlorophyll protein (fluorophore)
PG	prostaglandin
PKA/C	protein kinase A/C
PMNL	polymorphonuclear leucocytes
PPAR	peroxisome proliferator-activated receptor
PVDF	polyvinylidene diflouride
qRT-PCR	quantitative reverse transcription polymerase chain reaction
rh	recombinant human
ROS	reactive oxygen species
RPMI	Roswell Park Memorial Institute (medium)
RT	room temperature
S1P	sphingosine-1-phosphate
SEM	standard error of the mean
TLR	Toll-like receptor
TNF	tumour necrosis factor
TP	thromboxane receptor
VE-cad	vascular endothelial cadherin
VEGF	vascular endothelial growth factor

Zusammenfassung

Atemwegserkrankungen stellen eine große Belastung für die öffentliche Gesundheit dar und zählen weltweit zu den führenden Ursachen für Tod und Beeinträchtigung. Es ist inzwischen weithin anerkannt, dass das angeborene Immunsystem, eine zentrale Rolle bei der Modulation der Entzündung in der Lunge spielt. Bis heute fehlen uns noch spezifische Anhaltspunkte, um eine Überaktivierung oder eine anormale Funktion des angeborenen Immunsystems zu begrenzen. Prostaglandin (PG) D_2 ist ein Lipidmediator, der verschiedene inflammatorische Wirkungen ausübt, darunter die Rekrutierung und Aktivierung von Immunzellen, die Verengung der Bronchien und Hyperaktivierung der Atemwege. Aus diesem Grund besteht ein immenses Interesse daran, die PGD_2-Produktion zu hemmen, um Lungenentzündungen zu mindern. Allerdings sind die von PGD_2 induzierten Effekte deutlich komplexer als bisher angenommen. Ihre Wirkung hängt von vielen Faktoren ab, was eine eindeutige funktionelle Klassifizierung erschwert. Aus diesem Grund ist diese Doktorarbeit der Erweiterung des Wissens über PGD_2-induzierte Effekte im Zusammenhang mit pulmonalen Entzündungen gewidmet.

Im ersten Teil dieser Arbeit fanden wir heraus, dass PGD_2 und der DP1-Agonist BW245c die pulmonale und dermale mikrovaskuläre Endothelzellbarrierefunktion verstärkt und vor einer Thrombin-induzierten Durchlässigkeit schützt. Diese Effekte wurden nur in geringem Ausmaß durch die Aktivierung des DP1-Rezeptors und unabhängig von cAMP/PKA vermittelt. Im Gegensatz dazu konnten wir zeigen, dass der EP4 rezeptor für die Barriereverstärkung durch PGD_2 und BW245c zuständig war. Diese Daten zeigen einen neuen Mechanismus, durch den PGD_2 Entzündungsprozesse in der Lunge beeinflussen kann und hebt die Rolle der EP4-Rezeptoren für die Funktion der menschlichen Endothelzelle hervor.

Mastzellen wurden wiederholt als primäre PGD_2-Quellen identifiziert; ihre Beteiligung an einer akuten Entzündung ist jedoch aufgrund ihrer geringen Anzahl bei nichtallergischen entzündlichen Reaktionen eher unwahrscheinlich. Daher bestand das zweite Ziel dieser Arbeit darin, das Potenzial humaner Leukozyten als Prostaglandinquellen *in vitro* sowie in murinen Modellen der Lungenentzündung zu untersuchen. Tatsächlich wurden signifikante Mengen von PGD_2 von humanen und murinen Monozyten und Makrophagen, die mit bakteriellem

Lipopolysaccharid (LPS) und Interferon (IFN)-γ stimuliert wurden, freigesetzt. Zusammenfassend lässt sich sagen, dass Monozyten, Makrophagen und eventuell Neutrophile als Prostaglandinquelle fungieren und in der Lage sind, zu erhöhten PGD_2-Werten bei akuter Lungenentzündung beizutragen.

Als nächstes untersuchten wir die Rolle der DP Rezeptor-Aktivierung auf Makrophagen und der regenerativen Funktion hinsichtlich der Bildung neuer Blutgefäße. Makrophagen beeinflussen nicht nur die frühe Phase der Entzündung, sondern auch die Gewebsregeneration, die ein entscheidender Schritt zu einer normalen Lungenfunktion ist. Hier fanden wir heraus, dass die DP2-Rezeptor-Aktivierung auf IL-4-polarisierten Makrophagen die Gefäßneubildung reduziert. Eine gestörte Gefäßregeneration und die daraus resultierende vaskuläre Dysfunktion trägt häufig zur Vernarbung der Atemwege bei. Diese Erkenntnisse stellen somit einen vielversprechenden therapeutischen Ansatz zur Behandlung von Atemwegserkrankungen dar.

Zusammengefasst verdeutlichen diese Daten einige der weitreichenden Funktionen von PGD_2 auf das angeborene Immunsystem, einschließlich der neuen Erkenntnisse, dass PGD_2 durch die Aktivierung des EP4-Rezeptors wirken kann, dass Monozyten bedeutende Mengen an PGD_2 freisetzen und dass PGD_2-DP2 Aktivierung einen Einfluss auf Makrophagen und ihr gefäßneubildendes Potenzial hat. Dieses gesammelte Wissen wird in der Zukunft wertvoll sein, um gezielte entzündungshemmende oder regenerative Therapien für Atemwegserkrankungen zu entwickeln.

Abstract

Respiratory diseases pose a great burden on public health and are among the leading causes of death and disability worldwide. It has now been widely accepted that innate immunity, at its centre alveolar macrophages, plays a pivotal role in modulating pulmonary inflammation. To-date, we still lack specific targets to limit hyper-activation or aberrant function of innate immunity. Prostaglandin (PG) D_2 is a potent lipid mediator exerting various inflammatory actions including recruitment and activation of immune cells, broncho-constriction and airway hyper-reactivity. Due to this, there has been immense interest in limiting PGD_2 production and signalling to alleviate pulmonary inflammation, especially for patients suffering from allergic asthma. Yet, PGD_2-induced effects have proven to be more complex than previously thought. Its action depends on many factors, thereby further complicating a definite functional classification. On these grounds, this PhD thesis is dedicated to expanding the knowledge about PGD_2-elicited effects in the context of pulmonary inflammation.

In the first part of this thesis, we found that PGD_2 and the DP1 agonist BW245c potently increased pulmonary and dermal microvascular endothelial cell barrier function and protected against thrombin-induced barrier disruption. Surprisingly, these effects were mediated only to a minor extent through DP1 receptor activation and were independent from cAMP/PKA activation, as it has been previously published for DP1-related barrier enhancement. In contrast, we could prove that EP4 receptor activation was pivotal for barrier enhancement by PGD_2 and BW245c. These data demonstrate a novel mechanism by which PGD_2 may modulate pulmonary inflammation and emphasizes the role of EP4 receptors in human endothelial cell function.

Mast cells are believed to be the primary PGD_2 sources; however, their involvement in acute inflammation is rather unlikely due to their low numbers in non-allergic settings. In the second part of this thesis, we evaluated the potential of monocytes and macrophages as prostaglandin sources *in vitro* as well as in murine models of lung inflammation. Remarkably, PGD_2 and PGE_2 release by human monocytes significantly surpassed the levels observed for monocyte-derived macrophages after LPS/IFN-γ stimulation. *In vivo* data confirmed that monocytes and macrophages act as potent PG source and are capable of contributing to elevated PGD_2 levels in acute pulmonary

inflammation, but not allergic inflammation. Further investigation will be necessary to delineate how to exploit the therapeutic potential of this finding.

In the third part, we explored the role of DP2 receptor activation on macrophages and their regenerative function, i.e. the formation of new vessels. Macrophages not only influence the early phase of inflammation but also actively participate in the regeneration of epithelial and endothelial layers, which is a critical step towards restored lung function. We found that PGD_2-DP2 receptor activation on IL-4 polarized human monocyte-derived macrophages reduced sprout formation of human pulmonary microvascular endothelial cells and angiogenesis in the chicken CAM assay. Deregulated angiogenesis and resulting vascular dysfunction often contribute to airway and tissue remodelling, thus, posing a promising therapeutic approach to ameliorate acute and chronic airway inflammation.

Summing up, these data clarify some of the vast functions of PGD_2 on the innate immune system including the novel findings that i) PGD_2 is able to act through EP4 receptor activation, ii) monocytes release significant levels of PGD_2 and iii) PGD_2-DP2 signalling on macrophages modulates their angiogenic potential. Further investigation is required to explore the therapeutic relevance of these findings, but this knowledge will be valuable in the future to develop targeted anti-inflammatory or regenerative therapies for respiratory diseases.

1. Introduction

1.1. Prostaglandin D_2 generation and signalling

Prostaglandins (PG), thromboxane (TX), leukotriene (LT) and lipoxin (LX) belong to the family of eicosanoids, which are a group of molecules derived from the C_{20} fatty acid arachidonic acid. Eicosanoids are potent bioactive mediators that mainly act in an auto- or paracrine fashion by influencing target cell function through activation of specific G-protein-coupled receptors (GPCRs). PG and TX are referred to as prostanoids and are synthesised by the cyclic pathway (3). At the onset of inflammation or external assault, PGD_2 is one of the first mediators released by various cell types. PGD_2 is an inflammatory lipid mediator influencing a vast array of (patho-) physiological functions within the body; however, PGD_2-mediated effects remain quite controversial and vary strongly between animal species, tissue and experimental settings (1,4). Consequently, it is important to harvest collective knowledge about origin, spacio-temporal qualities of release as well as target receptors and cells to explore its therapeutic potential in inflammatory disorders.

1.1.1. The Cyclooxygenase pathway

In the first step of PG synthesis, phospholipase A_2 (PLA_2) catalyses the release of arachidonic acid from cellular phospholipid membranes. There are various PLA_2 with different functions and regulatory properties known to-date, which has been thoroughly reviewed (5). The most relevant phospholipase for PG synthesis, however, is the cytosolic PLA_2 that can be activated by Ca^{2+}-ionophores, enhanced serine phosphorylation induced by various stimuli, including zymosan, a structural component of the cell wall from yeast, but may also be hormone-mediated through e.g. epinephrine (6). Arachidonic acid is a substrate for constitutively expressed cyclooxygenase (COX)-1 as well as COX-2, which is inducible upon inflammatory stimulation (7). Both COX enzymes have a dual function with cyclooxygenase and peroxidase activity and are able to catalyse the isomerization of arachidonic acid to PGH_2 with PGG_2 as intermediate. PGH_2 further acts as substrate for various prostanoid synthases, including rate-limiting enzymes for PGD_2 production, hematopoietic and lipocalin-type PGD synthases (**Figure 1**).

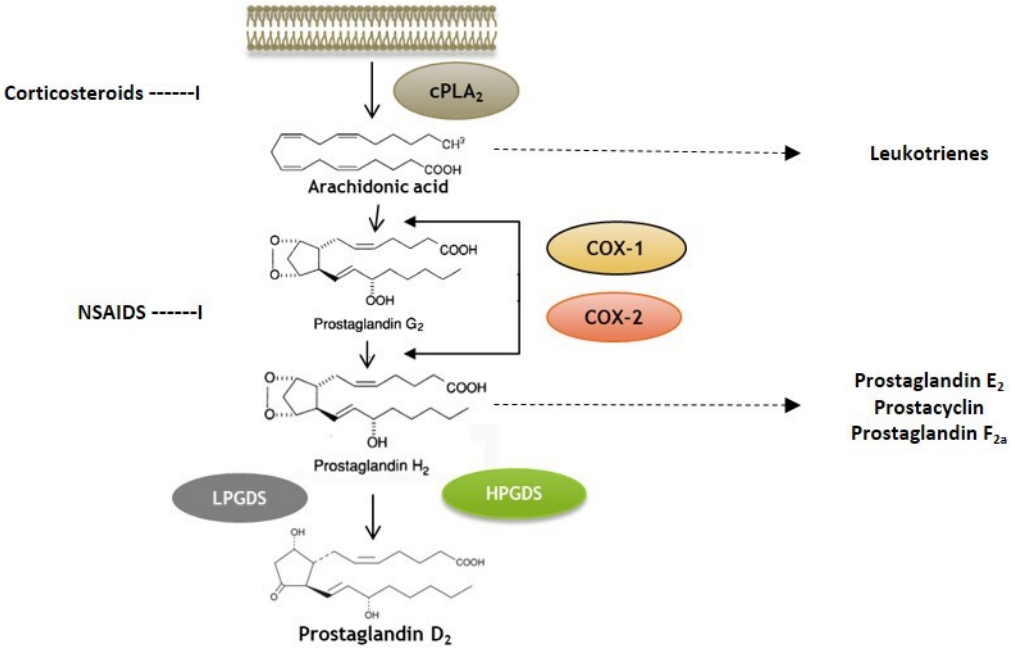

Figure 1. Generation of Prostaglandin D_2 with the arachidonic acid/cyclooxygenase pathway. Corticosteroids impair release of arachidonic acid from phospholipid membranes, while NSAIDs target further downstream by inhibiting COX function. Arachidonic acid serves as precursor for leukotrienes and PGH_2 precedes PGD_2 but also PGE_2, PGI_2 and $PGF_{2\alpha}$. $cPLA_2$: cytosolic phospholipase A_2, COX: cyclooxygenase, LPGDS: lipocalin-type PGD synthase, hPGDS: hematopoietic PGD synthase, NSAIDs: non-steroidal anti-inflammatory drugs.

Microsomal PGE synthase 1 (mPGES-1), microsomal PGE synthase 2 (mPGES-2), and cytosolic PGE synthase (cPGES) catalyse the generation of PGE_2; hematopoietic and lipocalin-type PGD synthase affords PGD_2 formation; thromboxane A synthase catalyses the generation of TXA_2/TXB_2 and prostacyclin synthase is responsible for the generation of PGI_2 (8). Each of these lipid mediators has a specific immunomodulatory function and depending on the cell type and microenvironment, differential expression of rate-limiting enzymes may change prostanoid production profile of a cell. An imbalance between intracellular prostanoids, e.g. the ratio between PGE_2 and PGD_2, can be crucial for the development of many diseases including bronchial asthma (9). Notably, COX inhibition prevents the production of all prostaglandins, while specific inhibition of unfavourable lipid mediator signalling e.g. by targeting hPGDS-dependent PGD_2 production would keep physiological functions of beneficial mediators like PGE_2 and prostacyclin intact. Importantly, prostaglandins have a short half-life, i.e. for PGD_2 it is about 30 min in plasma before it is rapidly metabolized by enzymatic or non-enzymatic pathways. Several bioactive

degradation products of PGD_2 such as 13,14-dihydro-15-keto-PGD_2, 11β-PGF_{2a}, PGJ_2, Δ^{12}-PGD_2 and 15-deoxy-$\Delta^{12,14}$-PGD_2 also modulate inflammation (10).

1.1.2. hPGDS – the rate limiting enzyme of PGD_2 production

Some parts of this section have been published previously in adapted form (1). Two distinct rate-limiting PGD synthases have been identified: Lipocalin-type PGD synthase (LPGDS) and hematopoietic PGD synthase (hPGDS), which differ vastly in origin, structure, tissue distribution and function. By measuring urinary PGD metabolites in hPGDS or LPGDS knock-out mice it could be determined that about 90 % of the systemic PGD_2 biosynthesis is dependent on the hPGDS pathway and only partially due to conversion by LPGDS or spontaneous non-enzymatic conversion (11,12). LPGDS is primarily expressed in the central nervous system and the reproductive tract from where it is secreted into cerebrospinal fluid and the bloodstream. Notably, LPGDS function is independent from reduced glutathione (GSH) as a co-factor (13). In contrast, hPGDS (a Sigma-class glutathione transferase) is expressed in peripheral tissues and catalyses the isomerization of PGH_2 to PGD_2 using GSH and Ca^{2+} or Mg^{2+} as cofactors (14). The hPGDS enzyme forms a homodimer with 23 kDa subunits whereby each subunit requires one GSH (15). Site-directed mutagenesis indicated that Lys112, Cys156, and Lys198 are involved in the binding of PGH_2, Trp104 is pivotal for structural integrity of the catalytic centre for GSH-transferase and PGD synthase activities, and Tyr8 and Arg14 are essential for functional activation of the GSH thiol group (16). Indeed, LPGDS is quite different in terms of catalytic properties, amino acid sequence, tertiary structure, evolutional origin, chromosomal localization, tissue distribution and purpose – a good example of functional convergence (13). A number of naturally occurring hPGDS enzyme variants have been described with differences in thermal stability and GST-activity. A highly stable hPGDS isoenzyme (Val187Ile) was identified in African Americans, which was associated with reduced colorectal cancer risk (17). Whether specific hPGDS variants are more frequent in allergic disease or other inflammatory disorders has not been clarified to date. Functional coupling between COX-2 and hPGDS as well as a possible role of hPGDS membrane translocation in modulation of PGD_2 synthesis has been reported (18). Further, it has been suggested that hPGDS activity is dependent on pH as it impacts H^+ abstraction from the GSH thiol group (14). Zhao et al. could show that reactive oxygen species (ROS) are crucial for proper hPGDS function. Selective

inhibition of NADPH oxidase-2 in murine bone marrow-derived macrophages ablated bacterial lipopolysaccharide (LPS)-induced production of PGD_2 but not PGE_2 (19). In line with this, the transcription factor nuclear-erythroid-2 p45-related factor (Nrf2) in combination with peroxiredoxin 1 and 6 regulated PGD_2 production by hPGDS in murine bone marrow-derived macrophages (20). Activation of the Toll-like receptor 4 and subsequent oxidative stress trigger nuclear factor-κB signalling and peroxiredoxin 6 phosphorylation, a bifunctional enzyme with glutathione peroxidase and phospholipase A_2 activity, which in turn activates NADPH oxidase-2 (21). This also highlights the importance of NADPH oxidase-2 in maintaining cellular glutathione levels to facilitate hPGDS function. Nrf2 has been reported to start a positive feedback induction of LPGDS by hPGDS-derived PGD_2 and 15-deoxy-Δ12,14-PGJ_2 in murine macrophages, which initiated resolution of LPS-induced lung inflammation in mice (22). In human eosinophils, PGD_2 synthesis was located at the nuclear envelope and was associated with intracellular lipid bodies (23). Correspondingly, inhibition of hPGDS-PGD_2 production with HQL-79 reduced lipid body formation in eosinophils.

1.1.3. Identification of potential prostaglandin sources

Some parts of this section have been published previously (1). Various cells are able to produce PGD_2 after different stimuli. Expression of the hematopoietic PGD synthase is a good first indication whether a cell is capable of producing PGD_2. Interestingly, hPGDS is differentially expressed in peripheral tissues and expression levels in cell types also vary between species and diseases. In the rat, hPGDS could be identified on protein level in spleen, bone marrow, liver, colon, small intestine, skin and thymus, while the highest expression of hPGDS mRNA in human tissue was detected in macrophages, placenta, intestine, adipose tissue and foetal liver (24). In the following section current literature describing hPGDS expression and PGD_2 production by murine or human immune or parenchymal cells will be discussed.

Immune cells

Cells of the mononuclear phagocyte system will be addressed separately in section 1.2.3.

Mast cells are mainly tissue-resident cells in the skin and mucosal surfaces and can be found with increased abundance in allergic and asthmatic patients (25–27). These cells have been described multiple times as the key PGD_2 sources in allergic disease. Upon allergen-induced cross-linking of Fcε-bound IgE human mast cells release high local concentrations (40 ng/million cells) of PGD_2 (28). The hPGDS transcript is enriched in human and murine tissue-resident mast cells as compared to other cells analysed (29). PGD_2 generation in isolated human lung mast cells mainly depends on COX-1 and hPGDS but not LPGDS, while COX-2 was absent both at baseline and after LPS or stem cell factor stimulation (30). Higher numbers of hPGDS but not LPGDS expressing mast cells could be found in the nasal mucosa of patients with allergic rhinitis (31). Other infiltrating cells included eosinophils, macrophages and lymphocytes. In mice, lung tumour-infiltrating c-Kit^+/FcE-RI^+ mast cells showed up positive for hPGDS in immunofluorescence microscopy (30,32).

Granulocytes are short-lived cells of the innate immune system with a characteristically lobed nucleus. They received their name from carrying granules with antimicrobial peptides and cytotoxic proteins. Influx of eosinophil granulocytes is as hallmark of allergic inflammation where they contribute to elevated mucus production, airway hyper-reactivity and tissue remodelling in asthma (33,34). Activated eosinophils secrete various cytotoxic proteins and pro-inflammatory mediators that drive Th2-type inflammation including IL-4, IL-5, IL-10 and IL-13 (35). Eosinophils express both DP receptors on their cell surface, whereby receptor activation by PGD_2 modulates eosinophil survival, migration and activation (36–38). Under certain circumstances, f.e. after eotaxin (23) or lysin-aspirin stimulation (39), eosinophils themselves may act as PGD_2 sources. Human peripheral blood eosinophils and murine bone marrow-derived eosinophils have been reported to constitutively express hPGDS and release PGD_2 in a HQL-79-sensitive manner (23). Likewise, infiltrating eosinophils in the nasal mucosa of patients with allergic rhinitis express hPGDS (31). Feng et al. observed that human peripheral blood eosinophils from patients with aspirin-exacerbated respiratory disease express significantly higher levels of hPGDS than eosinophils from asthmatic or healthy subjects (39).

Basophils have attracted notice primarily in allergic responses despite their relatively low numbers in comparison with mast cells and eosinophils (40–43). PGD_2-DP2 acts as potent chemoattractant and activator for basophils which may result in basophil accumulation at sites of inflammation (44). Comparable to mast cells, IgE-receptor cross-linking activates basophils and

initiates secretion of various cytokines favouring a type-2 inflammation including IL-4 (40). Murine basophils express hPGDS on mRNA and protein level, whereby sensitization with anti-TNP-IgE and subsequent stimulation with TNP-OVA triggered PGD_2 and PGE_2 release at similar levels (45). The same study could show that primary human basophils release PGD_2 after priming with IL-3, sensitization and stimulation with anti-human IgE, but no PGE_2 could be detected. Recently, another group found that autocrine PGD_2 production and CXCR4-dependent stimulation of basophils can be reversed by using a specific hPGDS inhibitor (HPGDS inhibitor I, Cayman) in a mouse model of systemic lupus erythematosus (46).

Neutrophils comprise the most abundant cell population of peripheral blood leukocytes and play a central role in acute bacterial infections and type-1 inflammatory reactions (47). HPGDS expression in neutrophils has been identified in a murine model of LPS-induced lung inflammation (48), however, PGD_2 production by neutrophils has not been fully characterized yet.

Lymphocytes are key players of adaptive immunity and immunological memory. The DP2 receptor has been first described in Th2 cells, resulting in the synonym chemoattractant receptor homologous molecule expressed on Th2 cells (CRTH2) and highlights the functional importance of PGD_2 for these cell population (49). It has been reported that PGD_2 signalling mainly influences Th2 and group 2 innate lymphoid cell (ILC2) function (49,50). Stimulation of $hPGDS^+DP2^+$ Th2 cells from healthy adults with a combination of OKT3 (monoclonal anti-CD3 antibody) and KOLT-2 (monoclonal anti-CD28 antibody) induced the release of up to 30 ng PGD_2/ml ($5x10^6$ cells) (51). These $hPGDS^+CRTH2^+$ Th2, but not Th1 cells, express hPGDS, which was confirmed by flow cytometry, and Western and Northern blotting. Further, $CD161^+$/$hPGDS^+$ Th2 cells release higher levels of type-2 inflammation promoting IL-5 and IL-13 (52).

Class 2 innate lymphocytes (ILC2) can be found in the lung, skin and gut and play an important role in the development of type 2 inflammation (53). PGD_2 has been shown to regulate the function, migration and accumulation of ILC2s during pulmonary inflammation whereby DP2 is now one of the key cell surface markers for this lymphoid cell population (54). Recently, it was shown that autocrine PGD_2 production facilitates ILC2 function and activation. Human ILC2s express hPGDS on mRNA level and release up to 1.5 ng/ml PGD_2 ($5x\ 10^5$ cells) after stimulation with IL-33, IL-25 and TSLP. Maric et al. could prove that disruption of endogenous PGD_2

production with a COX-1/2 or hPGDS inhibitor KMN-698 reduced IL-5 and IL-13 secretion, CD25 upregulation and PGD_2 production (50).

Parenchymal cells

Epithelial cells align at tissue surfaces throughout the body and form a tight barrier to keep out external factors and pathogens. Particularly at mucosal surfaces, epithelial cells actively participate in the development and progression of inflammation, e.g. during allergic response (55). In a neonatal mouse model of viral bronchiolitis, bronchial epithelial cells upregulated hPGDS and released up to 1500 pg PGD_2/ml 24 h after pneumonia virus of mice infection (56). In line with this, changes in the lipidomic profile of rhinovirus-infected airway epithelial cells including an increase in PGD_2 release could be documented (57). Interestingly, there seems to be a strong connection between epithelial-derived PGD_2 and viral infections which could also be important in the development of future therapeutics.

Endothelial cells line the inner wall of blood vessels and form a semi-permeable barrier. More about endothelial barrier function and its influence on pulmonary inflammation can be found in **Section 1.2**. No studies could prove so far that endothelial cells express hPGDS. Conversely, some studies presented evidence of LPGDS-derived PGD_2 production by endothelial cells (58,59). Notably, LPGDS knock-out mice but not hPGDS knock-out mice display a cardiovascular phenotype (11). In the vasculature, autocrine LPGDS-derived PGD_2 seems to be crucial in protection from hypertension and thrombogenesis.

Smooth muscle cell hyperplasia and -sensitivity is a characteristic feature of airway remodelling, e.g. in asthmatics. Recently, microarray, RT-qPCR and Western blot results revealed an increased hPGDS expression in bronchial smooth muscle tissue of ovalbumin-challenged mice (60). Whether this is also relevant for other pulmonary inflammatory diseases remains to be investigated.

1.1.4. DP receptor signalling and function

PGD_2 exerts its function primarily through activation of two distinct G-protein coupled receptors (GPCR), DP1 and DP2, but has also been reported to activate TP receptors and PPARγ at higher concentrations (**Figure 2**).

GPCRs, also referred to as 7-transmembrane (7TM) receptors, represent one of the largest and most important membrane protein family in terms of medical drug discovery (61,62). Signalling *via* GPCRs requires the integral membrane-spanning receptor as well as intracellular components associated with the receptor, referred to as heterotrimeric G-proteins. Heterotrimeric G-proteins consist of three subunits – G_{α}, G_{β} and G_{γ}. There are four major subtypes of Gα subunits with different functions as known so far, including cyclic AMP (cAMP) synthase stimulatory ($G_{\alpha,s}$), cAMP synthase inhibitory ($G_{\alpha,i}$), phospholipase C_{β} activating ($G_{\alpha,q}$) and actin cytoskeleton regulatory ($G_{\alpha,12/13}$) G_{α} subtypes (63). Ligand binding induces activation and conformational change of 7TM receptors which results in stabilization and modified affinity for heterotrimeric G-proteins at the cytosolic tail (64). As a result, exchange of guanosine tri-phosphate (GTP) for guanosine di-phosphate (GDP) at the Gα subunit is initiated and causes the dissociation of the G_{α} from $G_{\beta\gamma}$ subunits, which are able to independently mediate downstream signalling. GPCRs do not always exclusively bind one set of trimeric G-proteins, thus, can also be associated with different subtypes. The family of G_{α} subunits, though, determines downstream signalling whereby $G_{\alpha,s}$ induce cAMP generation, $G_{\alpha,i}$ inhibits cAMP generation, $G_{\alpha,q}$ induces the cleavage of phosphatidyl-inositol bis-phosphate into diacylglycerol and inositol tri-phosphate and increases Ca^{2+} levels, while $G_{\alpha,12/13}$ influences the cytoskeleton, e.g. by activation of small GTPase Rho. The G_{β} and G_{γ} subunits primarily act as heterodimers that function as secondary messengers and are thus able to modulate e.g. phospholipase and ion channel function (65). This wide range of physiological and pathophysiological effects modulated by GPCRs has a major impact on a various number of conditions and poses great possibilities in medical therapy (66).

DP1 receptor in pulmonary inflammation

The first G-protein coupled PGD_2 receptor to be discovered was D-type prostanoid receptor 1 (DP1). DP1 is widely expressed and can be found on platelets, eosinophils, basophils, monocytes, macrophages, endothelial cells, epithelial cells, Th1, Th2 cells (10,36,51,56,67,68). PGD_2 or PGD_2-derived metabolites, such as Δ^{12}-PGD_2 and PGJ_2, are able to bind DP1 which is coupled to a $G_{\alpha,s}$ subunit. Adenylyl cyclase activation results in elevated cAMP levels and activation of cAMP-dependent enzymes including protein kinase A (PKA) (69). Activation of DP1 receptor downstream signalling has been linked to both pro- and anti-inflammatory effects. DP1-mediated

responses include inhibition of platelet aggregation and induction of vaso- and bronchodilatation (70). In fact, most anti-inflammatory effects of PGD_2 have been linked to DP1 receptor activation on immune, epithelial or endothelial cells (48,56,68,71). In the context of pulmonary inflammation, however, PGD_2-DP1 activation has also been linked to inducing cough in guinea pigs (72), mucus production and airway hyper-reactivity in a mouse model of allergic asthma (73) as well as neutrophil infiltration in acute lung injury (67). Further, blockade of DP1 receptor was able to prevent rhinitis, conjunctivitis and pulmonary inflammation in guinea pigs (74). In total, DP1 receptor signalling remains a controversial therapeutic target in pulmonary inflammation and seems to be highly dependent on pathological settings.

DP2 receptor in pulmonary inflammation

More recently, a second G protein-coupled PGD_2 receptor termed DP2 was identified, originally named chemoattractant receptor-homologous molecule expressed on Th2 cells (CRTH2). It is expressed on Th2 cells, ILC2, eosinophils, basophils, dendritic cells, airway smooth muscle cells, airway epithelial cells, monocytes and macrophages (37,49,50,56,60,67). Further, the PGD_2-derived metabolites PGJ_2, Δ^{12}-PGJ_2, Δ^{12}-PGD_2, 15-deoxy-$\Delta^{12,\,14}$-PGJ_2, 15-deoxy-$\Delta^{12,\,14}$-PGD_2, 13, 14-dihydro-15-keto-PGD_2 (DK-PGD_2), 9α,11β-PGF_2, $PGF_{2\alpha}$ have also been described to favour DP2 over DP1 receptor activation (10,75,76). Receptor activation triggers GTP-GDP exchange at the associated $G_{\alpha,i}$ subunit, which in turn inhibits adenylyl cyclase and decreases intracellular cAMP levels (49). The $G_{\beta\gamma}$ subunit activates phospholipase C_β which generates diacylglycerol and inositol triphosphate resulting in elevated Ca^{2+} levels (77). Increase in intracellular calcium-ion levels is associated with immune-cell activation, migration, shape change, chemotaxis and degranulation. Additionally, DP2 receptor has been described to activate phosphatidyl inositol 3 kinase (PI_3K), phospholipase C (PLC) and p38MAP kinase pathway in a pertussis toxin-insensitive way, thus pointing to activation of $G_{\alpha,q}$. $G_{\alpha,q}$ activation has been shown to influence e.g. eosinophil shape change (78). DP2 has been mentioned to mediate a plethora of pro-inflammatory reactions (79). In pulmonary inflammation or more specifically in allergic inflammation, DP2 activation has been linked to inducing immune cell migration, respiratory burst of eosinophils as well as histamine and cytokine release (80). Further, DP2 activation promotes

smooth muscle cell proliferation and, thus, contributes to airway hyper-responsiveness and remodelling (81).

Recently, it has also been reported that DP1 and DP2 modulate each other's signalling capacity by formation of heteromers (82). In HEK cells expressing both DP receptors, DP1 receptor amplified DP2-induced Ca^{2+} release, which was mediated by $G_{\alpha,q/11}$. However, the potential of DP1/DP2 heterodimer formation and its effect on inflammatory responses still requires further investigation.

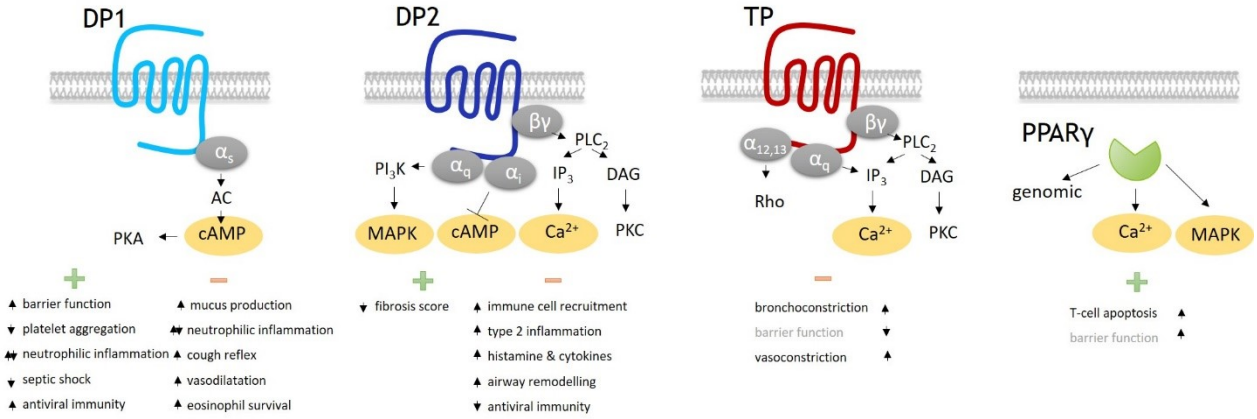

Figure 2. Receptors involved in PGD_2-mediated signalling and function. Summary of beneficial (green plus) or detrimental (orange minus) PGD_2-induced functions in inflammation. TP and PPARγ-mediated effects on barrier functions (grey) have not been linked to PGD_2 activation yet. DP: D-type prostaglandin receptor, TP: thromboxane receptor, PPARγ: peroxisome proliferator-activated receptor-γ, PKA/PKC: protein kinase A/C, cAMP: cyclic adenosine monophosphate, AC: adenylyl cyclase, PI_3K: phosphatidyl inositol 3 kinase, PLC: phospholipase C, IP_3: inositol triphosphate, DAG: diacylglycerol, Rho: Rho GTPase, MAPK: mitogen-activated protein kinase.

1.1.5. Non-DP receptor-mediated PGD_2-induced effects

Over the past years, PGD_2 has become quite infamous for its promiscuity in receptor binding. PGD_2 has the capacity to bind to nearly all prostanoid receptors although with lower affinity than DP receptors (83), which very likely results in additional synergistic or opposing effects to DP receptor activation. Suganami et al. confirmed that prostanoid receptors are able to adapt their conformation to facilitate binding of different ligands (84). DP1 and the PGE_2 receptor EP2

developed by gene tandem duplication (85); therefore, they are structurally very similar and PGD_2 is also able to activate EP2 receptors to some extent. PGD_2 as well as 15d-PGJ_2 is able to activate peroxisome proliferator-activated receptor γ (PPARγ) in the micro-molar range (86,87). Activation of PPARγ receptor by 15-d-PGJ_2, and to a small extent also PGD_2, is involved in vascular smooth muscle cell remodelling via activation of PPARγ and PPARδ but not DP receptor activation (88). Additionally, several studies reported that PGD_2 in micro-molar range acts as thromboxane receptor (TP) agonist and modulates the vascular tone in this manner. PGD_2-induced TP receptor activation caused pulmonary vasoconstriction in sheep, when intravenously administered (4) but also constricted airways, pulmonary arteries and veins in guinea pigs (89).

It is still unclear, why PGD_2 acts pro-inflammatory in one setting while it has anti-inflammatory actions in others. A thorough understanding of which receptors are targeted by PGD_2 on various cell types as well as which dosage range triggers certain effects, will help to improve therapeutic development.

1.2. Pulmonary endothelium

Throughout the body, endothelial cells form a solid barrier between circulation and interstitial space, thereby keeping extravasation of plasma proteins or circulatory cells at bay. Macrovascular endothelial cells line pulmonary arteries and veins, while microvascular endothelial cells line the capillaries and are subject to much higher blood pressure. Dependent on vascular type and location in the lung, heterogeneous endothelial cell populations show differences in permeability, signal transduction, proliferation and expression of adhesion molecules (90). Vascular homeostasis is preserved by various endothelial cell functions: endothelial cells oppose haemostasis by exerting anti-coagulant and fibrinolytic function, modulate the vascular tone by secretion of nitric oxide and endothelin-1 and disarm circulating leukocytes (91). On the other hand, tissue injury or inflammation initiates expression of leukocyte adhesion molecules, cytokines and chemokines by activated endothelial cells which is often accompanied by endothelial barrier disruption.

1.2.1. Endothelial barrier function

Endothelial cells form a strong, dynamic barrier that constantly undergoes mechanic and, occasionally, inflammatory stress. These circumstances require a selective permeability that prevents excessive plasma and leukocyte extravasation but at the same time provides surrounding tissues with nutrients. Pulmonary endothelial cells form a continuous layer characterized by cells closely aligned next to each other with inter-endothelial connections gradually increasing the smaller the vessel diameter. Indeed, microvascular endothelial cells form a far more restrictive barrier than macrovascular endothelial cells, facilitated by high basal cAMP concentrations and resulting in stabilization of cortical actin structures and adherens junctions in a PKA-dependent manner (92). Inter-endothelial tight and adherens junctions aid the connection between cells, while focal adhesion points tether endothelial cells to extracellular matrix components (93). The major component of endothelial adherens junctions is vascular endothelial (VE)-cadherin, which forms adhesive trans-dimers between monomers located on adjacent cells in a Ca^{2+}-dependent manner (94). The VE-cadherin cytoplasmic tail is associated with ß-catenin, γ-catenin (plakoglobin) and p120-catenin, which enables interaction with the actin cytoskeleton *via* actin binding proteins, thus stabilizing cell-cell junctions (95). Proper assembly of adherens junctions and endothelial barrier requires VE-cadherin; consequently, deletion of VE-cadherin is embryonically lethal in mice due to incomplete vascular development (96). Regulation of the endothelial barrier is maintained by a range of exogenous and endogenous agents (97) and is especially critical in limiting inflammatory reaction in tissues constantly exposed to external factors and pathogens such as the lung (98).

1.2.2. Prostaglandins regulate endothelial barrier function

Next to attraction and activation of immune cells, prostaglandins influence the vascular response during inflammation. PGs modulate the integrity of endothelial barrier during acute bacterial or viral infection; hence, they participate in regulating oedema formation and leukocyte infiltration.

Prostaglandin E_2

PGE_2 is among the most abundant PGs in the human body and is a structural isomer of PGD_2. Like PGD_2, it is derived from PGH_2 whereby its generation is facilitated by the action of PGE synthases: microsomal PGE synthases (mPGES-1 and mPGES-2) and cytosolic PGE synthase (cPGES). PGE_2 exerts its functions through activation of four GPCRs, E-type receptor 1-4 (EP 1-4), each of which are coupled to different downstream signalling cascades. While endothelial barrier function is not subject to regulation by G_q-coupled EP1 and $G_{\alpha,i}$-coupled EP3 receptor activation (99), we could show that PGE_2 enforced human pulmonary microvascular endothelial barrier function via EP4 activation and reduced leukocyte adhesion to endothelial cells (100). Further, PGE_2-EP4 stimulation protected against thrombin- and LPS-induced barrier disruption in human endothelium (100) and ameliorated acute lung injury in mice (101). The exact mechanism of EP4 receptor-mediated barrier enhancement still needs further investigation as none of the generally induced signalling cascades, including cAMP, eNOS, Rac1, PI3K, p38, ERK1/2, seem to be related to this effect (102).

Prostaglandin D_2

Most studies consider PGD_2 as barrier protective agent. Notably, DP1 agonism reduced vascular hyper-permeability in a mouse model of systemic anaphylaxis (103). This study could also show that genetic loss of DP1 receptor increases vascular permeability in mice. Further, PGD_2, DP1 agonism and 15-deoxy-$\Delta^{12,14}$-prostaglandin J_2 (15d-PGJ_2) attenuated leukocyte infiltration by improving endothelial barrier in a murine model of acute lung injury (48). In line with this, PGD_2 and DP1 agonist BW245c have been shown to promote endothelial barrier function in human dermal microvascular endothelial cells via cyclic AMP-PKA-Tiam1-Rac1 (68) and in a mouse model of acute lung injury (104). As mentioned above, PGD_2 and its metabolite 15d-PGJ_2 are able to activate PPARγ receptors in the micro-molar range (86,87). This might also affect PGD_2-mediated barrier effects because loss of PPARγ signalling in endothelial cells caused vascular leakage in PPARγ knock-out mice (105) and compromised barrier function in human brain microvascular endothelial cells, where PPARγ antagonism suppressed the expression of tight junction proteins (106). Furthermore, as PGD_2 in micro-molar range acts as pulmonary

vasoconstrictor through TP receptors (4,89), changes in endothelial barrier function might be induced in this manner. Some studies have already indicated that PGD_2 may bind with low affinity to EP4 receptors in human embryonic kidney (HEK) cells overexpressing the EP4 receptor (83,107). Consequently, Lydford et al. indirectly concluded from pharmacological studies using rabbit saphenous vein that (i) the DP1 antagonist BWA868c has some affinity for EP4 receptors and (ii) PGD_2 as well as BW245c-induced vasorelaxation was likely to be mediated through EP4 receptor activation (108). In contrast, clinical application of niacin, used as dietary supplement, is limited due to severe side effects including PGD_2-mediated facial flushing, which could be attenuated by combining niacin with an DP1 antagonist (109). These studies highlight the promiscuity of PGD_2 in prostaglandin receptor activation relevant to the regulation of vascular function.

1.2.3. Vascular leakage in airway inflammation

Vascular leakage is a hallmark of inflammatory reactions (**Figure 3**) whereby its characteristics depend on the severity and duration of the insult. Critical factors of barrier disruption are rearrangement of the actin cytoskeleton and loss of junctional integrity allowing the formation of gaps in the endothelial cell lining. In extreme cases, such as anaphylactic responses, systemic breakdown of vascular integrity occurs (97,110). In both, acute lung injury and respiratory distress syndrome, protection and enhanced recovery of endothelial barrier have great potential to limit pulmonary oedema and influx of inflammatory cells (111). But also in chronic pulmonary inflammation vascular leakage is an issue as it is accompanied by continuous leukocyte transmigration, tissue remodelling and inflammatory progression (112). At the early state of inflammation, local mediators released by activated resident cells, including macrophages and epithelial cells, induce a transient reduction of barrier function. External barrier disrupting agents such as bacterial LPS may also directly induce endothelial permeability. Part of this early response is activation of endothelial cells resulting in adhesion and transmigration of leukocytes. Recruited immune cells are able to modulate vascular leakage by releasing histamine, IL-6 and TNF-α and/or PGE_2 and sphingosine-1-phosphate that have barrier disruptive or protective effects, respectively (93). Additionally, thrombin as central player of haemostasis initiates platelet aggregation, endothelial cell activation, barrier disruption and leukocyte recruitment (113). Receptor activation

on endothelial cells leads to Rho-dependent actin stress fibre formation followed by Rac-dependent cell rounding and retraction, whereby cdc42 was not critical in the response to thrombin (114). Prolonged dysfunction of endothelial cell lining results in aggravated oedema, leukocyte extravasation and exacerbation of the inflammatory response. This primarily happens in the microvasculature, or more specifically in post-capillary venules (115), making microvascular endothelial cells an interesting target for barrier-enhancing therapy.

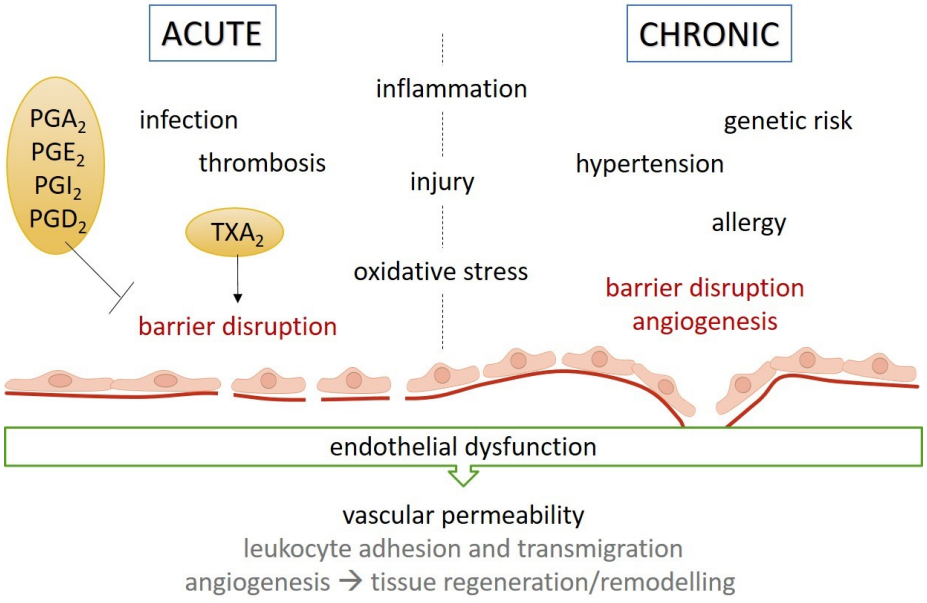

Figure 3. Endothelial dysfunction in acute and chronic inflammation. Lipid mediators are capable of protecting or inducing endothelial barrier disruption during inflammatory settings. NO: nitric oxide.

1.2.4. Vascular dysfunction as a result of de-regulated angiogenesis

If inflammation persists, angiogenic factors add up to inflammatory stimuli and, in combination, give rise to vascular dysfunction and/or remodelling. In chronic pulmonary inflammation vascular dysfunction appears in different flavours including loss of microvessels, deregulated angiogenesis and pathologic remodelling (116). Here, we will focus on alveolar and bronchial microvasculature since these regions are most severely affected in pulmonary diseases.

Barrier disruptive agents and oxidative stress instigate endothelial cell dysfunction, prolonged vascular leakage and endothelial cell apoptosis potentially resulting in loss of microvessels. Functional re-vascularization of alveoli after injury is required for tissue regeneration

but often affected by sustained inflammation. In mouse model of influenza infection-induced acute lung injury, a specific endothelial cell heterogeneity could be characterized, whereby a novel highly proliferative endothelial cell population was contributing to alveolar re-vascularization (117). Understanding how alveolar re-vascularization or loss of microvessels affect re-establishment of gas exchange and lung regeneration still requires further investigation but poses great therapeutic potential. Vasculopathy in chronic inflammation is often characterized by a heterogeneity of microvasculature density throughout the lung. In pulmonary fibrosis, an initial expansion of microvessels has been reported followed by a decline as the degree of scarring increased, whereby in severe fibrotic spots hardly any microvessels could be found (118). There are speculations about whether angiogenic factors such as vascular endothelial growth factor (VEGF) protect the alveolar wall and favour regeneration, although their role in fibrosis is controversial. In line with this, VEGF levels were significantly lower in BAL fluid of patients with idiopathic pulmonary fibrosis (119). Further, inflammatory mediators such as TNF-a, IL-1ß and IL-6 induce VEGF expression in alveolar epithelial cells (120), which might however be affected in fibrotic tissue. A similar heterogeneity in vascular distribution could be observed in COPD pathology: a vessel loss and reduced VEGF expression in emphysematous lesions (121). In contrast, it has been quite consistently reported that bronchial mucosa of asthmatic patients shows an increased vascular density accompanied by higher expression levels of VEGF, whereby bronchial vasculature is more permeable (122). Sustained vascular leakage in combination with angiogenic factors may substantiate further sprouting and migration of endothelial cells giving rise to new vessels (neo-angiogenesis) necessary for tissue repair but, if incomplete, may also cause vascular dysfunction (116).

There are only a few studies that investigated the role of PGD_2 signalling on angiogenesis. Murata et al. could see a strong anti-angiogenic effect of PGD_2-DP1 signalling in mice, supposedly through a barrier promoting effect (123). Further, endothelial LPGDS-derived PGD_2 reduced tumorigenic properties of associated endothelial cells such as hyper-permeability, angiogenesis and endothelial-to-mesenchymal transition (59). In contrast, PGE_2 has been clearly linked to promoting angiogenesis and cancer growth (124–126).

1.3. Mononuclear phagocytes as inflammatory modulators

1.3.1. The mononuclear phagocyte system

Monocytes and macrophages as well as dendritic cells belong to a network of cells that has been termed the mononuclear phagocyte (MNP) system. As the name already suggests, members of this system are professional phagocytes and are able to remove debris, apoptotic cells and other external antigens by means of phagocytosis. MNPs play a vital role in homeostasis, e.g. phagocytosis of excess mucus during steady state, as well as immunity by constantly surveying the pulmonary environment for potential threats such as intruding microorganisms or other antigens. The process of phagocytosis involves migration to apoptotic cells or pathogens triggered by chemotactic agents, recognition of 'eat me' signals such as extensive display of phosphatidylserine on the cell surface or pathogen-associated molecules and engulfment of said object. Shortly, phagocytosis can be divided into four main steps: (i) recognition of the target particles, (ii) initiation of the internalization machinery, (iii) phagosome formation and (iv) digestion of particle in phagolysosomes (127). To efficiently perform these tasks, MNPs have been equipped with danger- (DAMP) and pathogen-associated molecular pattern (PAMP) receptors including Toll-like receptors (TLR), which allow them to recognize hazardous or microorganism-associated molecular structures to initiate the inflammatory process, when necessary (128,129). MNPs share many characteristics, however, each cell type is specialized in certain tasks. Monocytes may serve as precursors of monocyte-derived macrophages and dendritic cells but foremost they are potent effectors of the inflammatory response by generating large amounts of reactive oxygen species, nitric oxide and inflammatory cytokines (130). Macrophages are an immensely heterogeneous population, but are specialized in phagocytosis and act as central modulators of innate inflammation (131), whereas the primary function of dendritic cells is to connect innate with adaptive immune response by activating naïve T cells (132).

Circulating monocytes

In humans, monocytes are characterized by differential expression of CD14, a co-receptor of Toll-like receptor 4 (TLR4), and CD16, the Fcγ receptor III. Using these surface markers, the monocyte population can be divided into three subsets with distinct immune functions: classical

monocytes with high CD14 but no or low CD16 expression (Ly6c^{high} monocytes in mice), intermediate monocytes with less CD14 and moderate CD16 expression and a non-classical subset with low CD14 but high CD16 expression (Ly6c^{low} in mice) (133). Among these, classical CD14^{high}CD16^{low} monocytes comprise the majority of peripheral blood monocytes. In adults, monocytes originate from hematopoietic stem cells in the bone marrow that further differentiate into common myeloid progenitors, which also give rise to neutrophils, dendritic cells, erythrocytes and megakaryocytes, and subsequently to granulocyte-monocyte or monocyte-dendritic cell progenitors (134). Chemoattractants, including chemokine [C-C motif] ligands CCL2 and CCL7, are necessary for successful egress of classical monocytes from the bone marrow but also for efficient chemotaxis to inflammatory sites (135). Fully differentiated monocytes are released into the bloodstream where they may circulate for several days. Unless inflammatory stimuli are received, monocytes remain in the vascular system. Non-classical monocytes, on the one hand, patrol the vasculature, providing immune surveillance and interacting with endothelial cells, while, on the other hand, intermediate and classical monocytes have mostly been linked to inflammatory processes (136). In the healthy lung, monocytes comprise only a minor part of MNPs, whereby the presence of tissue monocytes derived from classical monocytes has been proposed in murine lungs (137). Notably, lung migratory tissue monocytes were found either patrolling large vessels, or located at the interface between lung capillaries and alveoli where they participate in immune surveillance of the lung (138). A study looking into monocytes and monocyte-derived populations in lungs of healthy human subjects found mostly CD14^{+}CD16^{+} intermediate monocytes in bronchial wash and broncho-alveolar lavage, while in endo-bronchial biopsies only CD14^{+} classical monocytes are present, indicating distinct residency of these cells also in the healthy lung (139). In lung injury or inflammation, however, peripheral blood monocytes are recruited to inflammatory lesions, where they are able to differentiate into both - macrophages and dendritic cells - upon stimulation with macrophage colony stimulating factor (M-CSF) or granulocyte/macrophage colony stimulating factor (GM-CSF), respectively (140). But besides serving as progenitor cells, monocytes are able to release tremendous amounts of cytokines upon inflammatory stimulation, thereby actively participating in the reaction. LPS is a bacterial endotoxin originating from gram-negative bacteria which activates TLR4 downstream signalling, thereby inducing also NADPH oxidase (NOX) 2, that is needed for ROS production (141). CD14,

another pattern recognition receptor, and LPS-binding protein (LBP) recognize LPS and act as co-receptor for the TLR4/MD-2 heterodimer (142). Downstream signalling events are triggered, including activation of nuclear factor κB (NFκB), phosphatidyl inositol 3-kinase (PI3K) and activation of the mitogen-activated protein kinase (MAPK) pathway resulting in upregulation of pro-inflammatory cytokines and products needed for ROS production. LPS-CD14/TLR4 mediated signalling triggers the release of a plethora of inflammatory cytokines including TNF-α, IL-10, IL-1β, IL-6, IL-8 (143,144) as well as lipid mediators, i.e. PGE_2, in human monocytes (145).

Monocyte-derived macrophages

In general, alveolar macrophages are derived from embryonic precursor cells as mentioned previously; however, inflammatory assault throughout life as well as aging increases the proportion of monocyte-derived macrophages in the lung (146,147). In this process, monocytes are recruited to inflammatory sites, migrate through the vascular wall and differentiate into monocyte-derived macrophages upon stimulation with growth factors including M-CSF (148). Patient-derived peripheral blood monocytes are easily obtained, hence, *in vitro* differentiation of monocytes into monocyte-derived macrophages has become a common, reliable tool in immunological research to model and investigate infiltrating macrophage function (149). Macrophages come in many different flavours even though historically, there was a strict classification of macrophage polarization states, e.g. through surface marker expression. Ongoing research was able to identify more and more combinations of cellular functions with surface markers which hampers a clear classification between cell types and suggests a 'spectral' range of polarization states (150,151). Nevertheless, it has proven useful to define two opposing phenotypes of activated macrophages when looking at pro- or anti-inflammatory stimuli. Guilliams & van de Laar refer to this model as 'discrete polarization model' whereby stimulation of monocyte-derived macrophages with IFN-γ and bacterial endotoxins like LPS generates a pro-inflammatory, pathogen killing phenotype, while stimulation with IL-4, IL-10 or IL-13 induces a wound healing, tissue remodelling phenotype. Inflammatory macrophages, previously referred to as M1 macrophages, express inducible nitric oxide synthase (iNOS) and produce high levels of reactive oxygen species which facilitates their effector function against pathogens. Further, activation of pathogen recognition receptors (PRR) causes enhanced secretion of inflammatory cytokines including IL-1, IL-6 and tumour necrosis

factor, TNF-α (141). Inflammatory polarization in macrophages is characterized by up-regulation of surface molecules including MHC class II and B-7 (CD86/CD80) (141,152), upregulation of pro-inflammatory cytokines but also metabolic reprogramming in favour of glycolysis (153). Macrophages adapt their phenotype throughout the inflammatory process in a dynamic manner, whereby the environmental factors influence their function, but they actively modulate inflammatory outcome in the course of it. As inflammation progresses, apoptotic and necrotic cells accumulate and macrophages, as main phagocytic cell, are responsible for efficient clearance of cellular debris (efferocytosis). The process of efferocytosis triggers an anti-inflammatory programme in macrophages (154), thereby contributing to initiation of a phenotypic switch to an alternatively activated phenotype (155), originally referred to as M2 macrophages. Anti-inflammatory or type-2 cytokines such as IL-4 and IL-13, which may also be released by macrophages themselves, activate IL-4 receptor α (IL-4Rα), the phosphorylation of signal transducer and activator of transcription (STAT) 6 and adenosine monophosphate-activated kinase (AMPK) resulting in the upregulation of arginase 1, TGF-β, IL-10 and mannose receptor (CD206) expression, amongst others (156,157). Arginase 1 is an enzyme needed for extracellular matrix production and remodelling, while IL-10 and TGF-β have anti-inflammatory effects but also influence tissue regeneration. Additionally, arginase counteracts IFN-γ-induced upregulation of iNOS resulting in impaired ROS production (157). These processes reinforce the anti-inflammatory polarization state and function. Conclusively, alternatively activated macrophages are specialized in phagocytosis, but also release factors to promote wound healing and tissue regeneration.

1.3.2. Origin and function of pulmonary macrophages

In the lung, at least three types of resident macrophages can be found including interstitial, bronchial and alveolar macrophages (158). For a long time has been considered that all tissue macrophages originate from circulating monocytes, therefore, being descendants of bone marrow hematopoietic stem cells (159). Indeed, most adult tissue macrophages are a self-replicating population with specific function that are derived from embryonic cells rather than from circulating monocytes (160). In mice, alveolar macrophages develop from foetal monocytes that populate alveoli shortly after birth and become self-maintaining throughout life (161). Residing in alveoli,

they are the predominant phagocytic cells in the alveolar space, where they are highly exposed to external factors. Interestingly, alveolar macrophages are characterized by a low inflammatory profile: they express high levels of CD206 as well as CD200 receptor, which has been associated with an anti-inflammatory polarization state and inhibition of Toll-like receptor activation (162), respectively. Several processes have been suggested how resident alveolar macrophages are kept in an anti-inflammatory polarization state and how they contribute to a non-inflammatory environment in the healthy lung to avoid excess immune response to injury or antigens - see review by Hussell and Bell (163). Besides alveolar macrophages, which comprise the majority of resident macrophages in the lung, interstitial macrophages are found that have been linked to antigen presentation and a lower phagocytic activity (164). Up to now, it is still controversial where interstitial macrophages originate from. Interstitial macrophages have higher turnover rates in comparison to alveolar macrophages suggesting a continuous replacement of interstitial macrophages by circulating monocytes (165). As mentioned above, in the healthy lung the majority of alveolar macrophages are derived from embryonic progenitors, which are also able to proliferate and repopulate alveoli after depletion. However, if there is a genotoxic injury of resident macrophages or an ongoing inflammation, circulating monocytes are recruited and migrate across the vascular barrier, differentiate into monocyte-derived macrophages and may outcompete resident macrophages (160). This suggests a complex and crucial role of macrophage heterogeneity in health and disease and emphasizes the need of a well-balanced state between resident and monocyte-derived macrophages in the lung.

1.3.3. Potential as Prostaglandin D_2 sources and targets

In 1989, Urade et al. reported that hPGDS-expressing macrophages and dendritic cells in spleen, thymus, Peyer's patch of the intestine, submucosal layer of the stomach and in the liver are likely the major source of PGD_2 in the rat (166). *In vitro* cultured human monocytes have been reported a release of PGD_2 in a femtomol-range, suggesting that those cells should have the machinery to produce PGD_2, if activated accordingly (167). In current literature, monocytes have not been considered as PGD_2 sources yet. Further, human monocytes express both DP1 and DP2/CRTH2 receptors but show only minor response to activation (67).

Multiple studies showed hPGDS expression in murine bone marrow-derived macrophages whereby these cells released up to 20 ng PGD_2/ml ($1x10^6$ cells) upon stimulation with LPS or Zymosan A (19,168–170). In allergic rhinitis patients, hPGDS expressing macrophages were reported in nasal mucosa (31). Further, pulmonary macrophages in acute respiratory distress syndrome (67) and human adipose tissue macrophages (171) stained positive for hPGDS. Another study could show that hPGDS, but not LPGDS-targeting siRNA as well as co-treatment with HQL-79, a hPGDS inhibitor, but not AT-56, a LPGDS inhibitor, attenuated PGD_2 production by mouse bone marrow-derived macrophages (19). Recently, Henkel et al. showed that human monocyte-derived macrophages co-stimulated with IL-4 and house dust mite allergen produce PGD_2 (172). Human macrophages express both DP receptors and activation with PGD_2 triggers a chemotactic response and the release of several inflammatory mediators (67).

As prototype of an antigen presenting cell, dendritic cells have been considered as potential PGD_2 source in current literature (166). Interestingly, there is a relationship between increased hPGDS mRNA levels in murine DCs and a Th2-biased response (173). Although PGD_2 production by mouse bone marrow-derived DCs was not measured, the Th2 bias to the immune response was blunted after transfection of these cells with hPGDS-specific siRNA. Additionally, peripheral blood DCs as well as tissue plasmacytoid and myeloid DCs in atopic dermatitis patients stained positive for hPGDS (174). In the same study, human monocyte-derived DCs released up to 250 pg PGD_2/ $1x10^6$ cells after LPS stimulation, while LPS caused a downregulation of hPGDS expression after 6 h. Interestingly, primary synovial fluid DCs express much higher hPGDS levels than monocyte-derived DCs, but hPGDS expression decreases in synovial fluid DCs after 2 days in culture (175). Concerning DCs as target cells of PGD_2, it seems to impact the differentiation and function of human monocyte-derived dendritic cells by affecting antigen processing and presentation, which caused a bias in T-cell maturation towards Th2 cells in a DP1 receptor-dependent manner (176).

1.3.4. Response to pulmonary infection and injury

During infection or after injury, macrophage and epithelial cell cross-talk initiates release of pro-inflammatory cytokines by both cell types such as IL-1β, TNF-α, IL-6, macrophage inflammatory protein (MIP), CCL2, CCL5, CXCL8, KC (177–179). CCL2 attracts circulating

monocytes among other leukocytes, recruiting them to sites of inflammation. While undifferentiated monocytes are found in circulation, a semi-differentiated monocyte/macrophage population is capable of leaving the vasculature close to inflammatory loci where they are able to differentiate into monocyte-derived effector cells (148). As mentioned above, monocyte-derived macrophages accompany alveolar macrophages in modulating acute inflammation, sometimes overpowering resident macrophage function, as their pro-inflammatory programme is more pronounced.

In acute influenza A infections as an example for viral infections, alveolar macrophages recognize the virus and initiate IFN-ß production, thereby boosting antiviral immunity (180). Expression of CD200 and TGF-ß by alveolar macrophages, which are also exposed on the apical side of airway epithelial cells, appears to be pivotal to limit influenza infection and initiate tissue repair (181). Monocyte-derived macrophages may persist after pulmonary infection for a longer period and provide an immunological memory to protect from future infections (182). Notably, PGE_2 upregulation in alveolar macrophages inhibits IFN-ß production and impairs viral clearance (183). On the other hand, influenza A induces a collagenase membrane-tethered matrix metalloprotease in macrophages, which results in dysregulated extracellular matrix (ECM) proteolysis, tissue damage and even mortality (184). Further, a high number of recruited macrophages during influenza infection may increase alveolar epithelial cell injury and apoptosis (185). These observations corroborate a central role of macrophages in viral infections of the lung.

Alveolar macrophages are able to control subclinical bacterial infections, however, if they fail to eradicate the intruders, neutrophils are recruited for assistance. Depletion of alveolar macrophages or genetic modification of alveolar macrophage microbicidal capacity in mice resulted in a higher susceptibility to develop *S.pneumonia*-induced inflammation (186). These mice suffer from pronounced and prolonged neutrophilic inflammation and impaired efferocytosis, whereas bacterial clearance was unchanged. In contrast, some reports have linked monocyte recruitment and differentiation into monocyte-derived macrophages to detrimental effects during acute pulmonary inflammation. Monocyte depletion before LPS-induced lung injury alleviated symptoms in mice by suppressing neutrophil influx next to reducing IL-17 and HMGB1 expression (187). In contrast to the previously mentioned study, depletion of pulmonary macrophages has been found to reduce the severity of inflammatory response in LPS-induced lung injury potentiated by

exogenous PGD_2 (67). Interestingly, monocyte depletion did not result in amelioration of symptoms in an experimental human model of pulmonary inflammation (188), leaving unrequited whether monocytes/macrophages are beneficial or detrimental in human disease.

Chronic pulmonary inflammation is frequently associated with macrophage dysfunction including impaired efferocytosis, aberrant cytokine secretion and polarization (189–191). A mainly anti-inflammatory, M2-like polarization state in combination with limited inflammatory function such as reduced ROS and IFN production leads to inadequate anti-bacterial and -viral immunity. This impairment may contribute to exacerbations of chronic pulmonary disease, e.g. in allergic asthma (191).

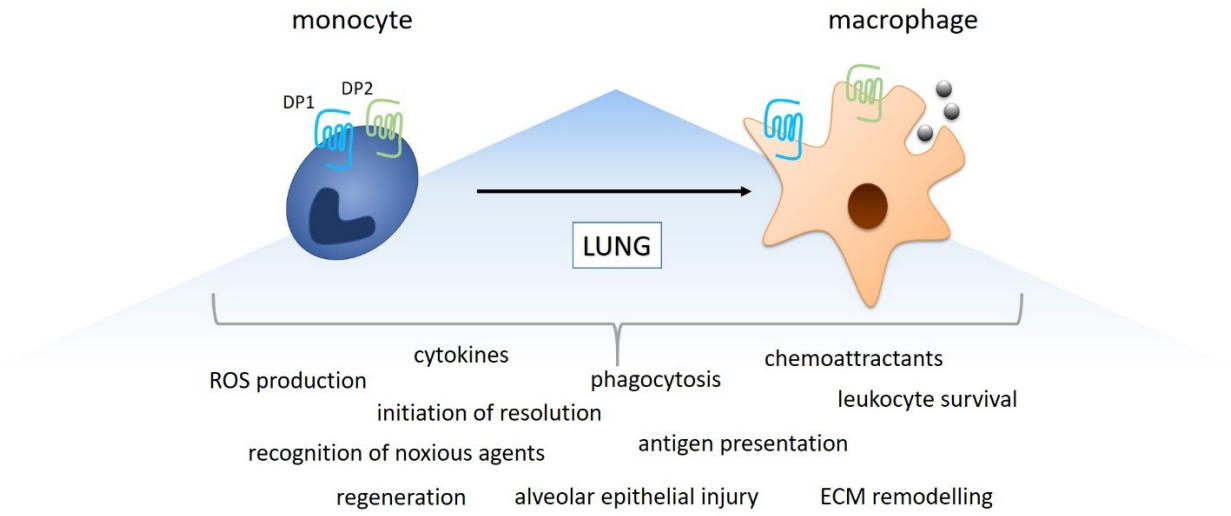

Figure 4. Monocytes and macrophages as central modulators of pulmonary immunity. ROS – reactive oxygen species, ECM – extracellular matrix.

1.3.5. Macrophages are central modulators of pulmonary tissue repair, regeneration and remodelling

In the late phase of inflammation, efferocytosis of cellular debris and initiation of an anti-inflammatory programme is necessary for the recovery of normal lung function. Alternatively-activated macrophages release growth factors including, but not limited to, VEGF, IL-10 and TGF-β in a controlled fashion to enable regeneration of airways (192). If dysregulated, however, excess release of macrophage-derived factors may lead to pathogenic changes in the lung tissue, as an example excess TGF-β leads to the development of fibrotic lesions.

Repair and regeneration

As mentioned above, macrophages not only influence the early phase of inflammation but also actively participate in the late or resolution phase. This includes regeneration and repair of epithelial and endothelial barrier which is a critical step towards normal lung function. Efferocytosis initiates a switch in macrophage phenotype and induces anti-inflammatory but also tissue repair genes. As a result, airway macrophages release a wide array of cytokines and growth factors to modulate restorative processes including keratinocyte growth factor, VEGF, epidermal growth factor, heparin-binding epidermal growth factor-like growth factor, platelet-derived growth factor (PDGF), GM-CSF and fibroblast growth factors (FGF) 2 and 10 (193). After lung injury, wound closure relies on generation and deposition of ECM proteins such as collagens and fibronectin around the damaged area. Th2 cytokines including IL-4, IL-13 and TGF-ß limit inflammation while activating matrix production by macrophages and myofibroblasts (181). ECM material in combination with newly formed blood vessels form a granulation tissue which serves as a scaffold during tissue regeneration (194). In allergic asthma, IL-10$^+$ macrophages have been associated with better prognosis, while CD206$^+$ macrophages have been related to the opposite (195). IL-10 is a crucial mediator in the resolution of airway inflammation as it reduces nitric oxide production and induces suppressor of cytokine signalling (SOCS)-3 (196). At the same time, alternatively-activated macrophage-derived factors, including IL-10 and TGF-β, promote wound healing and angiogenesis (197). Macrophages secrete a plethora of pro- and anti-angiogenic growth factors (198). VEGF-A release by monocyte-derived macrophages during early stage of tissue regeneration is critical to achieve sufficient vascularization and healing. Further, macrophages are able to secrete high levels of matrix metalloproteinases (MMPs) to modulate vascularization and ECM composition (199). Once more, apoptotic cells are responsible for a change in macrophage function resulting in a pro-angiogenic phenotype. S1P derived from apoptotic cells upregulates COX-2 and PGE_2 production in macrophages while downregulating PGD synthase. In turn, macrophage-derived PGE_2 stimulates endothelial cell migration and angiogenesis (200). Another factor expressed by macrophages, amphiregulin, has been directly linked to restoring lung function during viral infection in mice (201), however, also activates fibroblast proliferation, migration and differentiation (202).

Pathological remodelling

Tissue repair is a tightly regulated process, on the one hand, to guarantee functional recovery but, on the other hand, to avoid excess proliferation of cells and scarring of tissue, i.e pathological remodelling. In chronic inflammatory conditions, constant tissue injury by infiltrating leukocytes and ROS production in parallel with insufficient or dysregulated tissue repair may impair lung function and gas exchange. Interestingly, an imbalance between pro- and anti-inflammatory polarization state of macrophages has been observed in prolonged pulmonary inflammation and linked to excessive tissue remodelling (192). Higher numbers of alternatively-activated, often dysfunctional macrophages are present in chronic pulmonary disease such as allergic asthma, COPD and idiopathic pulmonary fibrosis (203). These macrophages are inefficient in phagocytosis but release an array of inflammatory and pro-fibrotic mediators and thus fail to facilitate inflammatory resolution. Phagocytosis of apoptotic cells initiates VEGF secretion by recruited macrophages (204), therefore, impaired phagocytic capacity might limit VEGF secretion and endothelial cell proliferation and regeneration. Moreover, recruited and resident macrophages play distinct roles in pathological remodelling. Deficiency of CCR2, a chemoattractant receptor primarily expressed on classical monocytes, ameliorated bleomycin-induced pulmonary fibrosis in mice by reducing alveolar macrophage-derived MMP expression. Lungs from $CCR2^{-/-}$ mice showed less collagen deposition, hydroxyproline content and reduced MMP activity (205). Excess MMP activity has been linked to emphysema but also to modulating angiogenic and regenerative processes. Several matrix degradation products, including endostatin and angiostatin, contribute to epithelial injury and potentially impair normal angiogenic wound healing (206,207). Dysregulated expression of MMPs and/or their inhibitors by macrophages poses a certain threat of pathological remodelling. Further, alveolar macrophages are potent sources of TGF-β (208), a tightly regulated factor that plays a central role in pathological remodelling by promoting airway smooth muscle cell proliferation (209), differentiation of pulmonary fibroblasts into myofibroblasts and epithelial-to-mesenchymal-transition (210). In contrast, TGF-β seems crucial to preserve development and homeostasis of alveolar macrophages and protects from age-related emphysema by suppressing MMP-12 expression (211) which indicates a delicate balance between beneficial and detrimental effects of TGF-β on tissue remodelling. In COPD, the underlying mechanisms of emphysema are

not completely understood to-date, however, macrophage-derived IL-13 and chitinase 1 appear to be involved in disease progression (212).

A tight regulation of pro- and anti-angiogenic factors as well as ECM processing is necessary to facilitate wound healing without aberrant angiogenesis and scarring. Macrophages are involved in most of the processes of lung repair but also pathological remodelling. Conclusively, modulation of macrophage function poses a good future target to tackle pathological remodelling in the lung.

1.4. Respiratory inflammatory disorders – Prostaglandin D_2 as therapeutic target

Respiratory diseases pose a great burden on public health and count to the leading causes of death and disability worldwide. According to the European Lung White Book published by the European Respiratory Society, lower respiratory infections are the most common cause of sick leave and account for millions of deaths worldwide. To be more accurate, a study published in 2019 stated alarming numbers saying that 3 million people die from chronic obstructive pulmonary disease, 4 million die from lower respiratory tract infections and/or pneumonia and 1.76 million die from lung cancer worldwide every year (213); however, many more live with impairments due to lung disease for many years, some even from early childhood on. Current estimates suggest that 300 million people suffer from asthma, with allergic asthma being one of the most common chronic childhood diseases, whereby populations living in high income countries show a higher prevalence (214). This causes not only limited quality of life for a huge part of the population but also accounts for a massive financial burden on the community. As a result, much effort has been put into prevention and treatment of respiratory diseases, however, due to the multifactorial and complex nature of pulmonary inflammatory disorders current approaches still lack efficient and targeted therapy.

1.4.1. Acute respiratory inflammation

Acute respiratory inflammation is most commonly caused by bacterial or viral infection or tissue injury caused by e.g. acid aspiration. It is characterized by critical respiratory impairment, hypoxia and decreased lung compliance. The most severe form of acute pulmonary inflammation

is termed acute respiratory distress syndrome (ARDS) which typically affects lower airways and is associated with multiple risk factors that trigger severe hypoxemia and respiratory failure (215). With sepsis and pneumonia being the leading causes of ARDS there is a mortality of 30 – 50 % in affected patients (WHO, 2014), whereby mechanic ventilation is still common as standard therapy for critical cases. The pathological progression of ARDS can be divided into early or exudative and late or fibro-proliferative phase, which differ in cellular composition and pathological function (216). Common characteristics of the early phase include endothelial and epithelial injury and permeability, alveolar oedema, impaired gas exchange and neutrophil influx (217,218). The later phase involves efferocytosis of apoptotic cells, proliferation of fibroblasts, regeneration of epithelial and endothelial barrier, formation of new blood vessels and extracellular matrix deposition (216).

During the early phase of acute pulmonary inflammation, tissue resident alveolar macrophages are activated and their function often accompanied by pro-inflammatory monocyte-derived macrophages which results in release of IFNs, TNF-α and various pro-inflammatory interleukins (219). Activation of Toll-like receptor 4 by bacterial lipopolysaccharide has been reported to directly induce rate-limiting enzyme-dependent PGD_2 and PGE_2 production in various cells including bone marrow-derived murine macrophages (168) but also indirectly through neutrophil recruitment and generation of reactive oxygen species. Oxidative stress in the lung may also trigger non-enzymatic production of PGD_2 in macrophages and mast cells whereby urinary eicosanoids including PGD_2 metabolites are considered as biomarkers for ARDS (220). There is evidence for an indirect link between increased PGD_2 levels and neutrophil influx mediated by macrophages as neutrophils are not directly attracted or activated by PGD_2; however, exogenous PGD_2 exacerbated neutrophilic inflammation in a mouse model of LPS-induced lung injury by activation DP receptors on macrophages (67). The same study could show that also in human cells DP1 as well as DP2 receptor activation on monocyte-derived macrophages resulted in prolonged neutrophil survival and increased chemotaxis. Notably, also more infiltrating cells expressing hPGDS could be observed in ARDS patients (67).

In contrast, various other studies suggested that PGD_2 limits inflammation in ALI/ARDS. Inflammation appears more severe during the onset phase in hPGDS knock-out mice, whereby DP1 agonism rescued this phenotype (48,221). During the early phase of acute lung inflammation,

endothelial cell integrity and barrier function are tightly regulated but often affected, resulting in leukocyte and plasma extravasation (97). It has been reported that LPGDS as well as hPGDS-derived PGD_2 is able to strengthen endothelial barrier function thereby alleviating inflammatory response in a mouse model of acute lung injury (48,68,104). Another study suggested that resolvin D1 induced COX2-PGD_2 expression, which resulted in less neutrophil infiltration and reduced TNF-α levels in a model of LPS-induced lung injury in rats (222). Further, there are indications that DP1 activation is crucial for initiation of the resolution phase and efficient macrophage clearance (221). Sarashina et al. published a study, which may explain some of the discrepancies observed by different studies: In a murine model of skin inflammation they identified a protective role of PGD_2 by enhancing endothelial barrier function, while in the later phase PGD_2-DP2 activation induced leukocyte chemotaxis and infiltration (223).

In the future, research might have to focus on interfering at different phases of acute pulmonary inflammation to achieve a more efficient treatment i.e. allowing PGD_2/PGE_2 induced barrier enhancement in the early phase and ablate PGD_2-DP2 induced inflammatory cell attraction in late phase.

1.4.2. Chronic pulmonary inflammation

Pulmonary fibrosis

Idiopathic pulmonary fibrosis (IPF) is a chronic progressive disease where ongoing inflammation promotes proliferation of fibroblasts, deposition of extracellular matrix and tissue remodelling, ultimately leading to impaired gas exchange and pulmonary compliance (224). Patients suffer from respiratory insufficiency and many even require transplantation. Besides genetic prevalence, pulmonary injury or inflammation can foster the development of fibrotic lesions, whereby fibro-proliferation may occur as early as 24 h after inflammatory onset in ARDS patients (225). Many factors affect disease progression including the innate immune response mediated by macrophages and neutrophils (181). There is strong evidence for the involvement of prostaglandins in pulmonary fibrosis. Recently, a study could show that inhibition of eicosanoid degradation has an anti-fibrotic effect mediated primarily through PGE_2 (226). Inhibition of an eicosanoid-degrading enzyme, 15-PGDH, resulted in less collagen deposition, epithelial apoptosis

and fibroblast proliferation as well as amelioration of lung function. Interestingly, published literature also suggests a protective role for PGD_2 in pulmonary fibrosis. In the presence of apoptotic cells, macrophages inhibit TGF-β-induced epithelial to mesenchymal transition, a critical factor of tissue remodelling seen in pulmonary fibrosis, by secretion of PGD_2, PGE_2 and hepatic growth factor (169). This effect could be reversed by COX-2 inhibition in macrophages or DP1 or EP4 receptor blockade in epithelial cells. Further, introduction of hPGDS over-expressing fibroblasts reduced basic fibroblast growth factor (bFGF) expression and pulmonary oedema in mice (227). In line with this, Kida et al. could show that hPGDS knock out mice suffer from a more severe bleomycin-induced lung inflammation and fibrosis characterized by more collagen deposition, vascular permeability as well as higher levels of TNF-α, MCP-1, COX-2 (228). This effect seems to be mediated through DP2 signalling as similar results in the murine model of bleomycin-induced pulmonary fibrosis could be observed in DP2 knock out mice. These mice not only showed a higher mortality, more collagen deposition and total protein in the lung but also less IL-6, IL-10, IFN-γ and IL-17A in BAL fluid (229).

Allergic asthma and rhinitis

Some parts of this section have been published in adapted form (1).

Asthma is a chronic respiratory disease characterized by airway hyper-responsiveness and airflow obstruction. To-date, reasonably good standard-of-care therapy is available for most asthmatics, however, new drugs are needed for severe and poorly controlled asthma aiming to replace oral corticosteroids, which have various adverse effects (230). PGD_2 has been detected in human airways during acute allergen challenge and severe asthma whereby disease severity has been shown to correlate with PGD_2 levels (9,231,232). PGD_2 acts as a chemoattractant and activator of Th2 cells, eosinophils and basophils, which is primarily mediated by DP2 activation (49). The role of DP1 in asthma remains elusive; however, DP1 agonism attenuated type 2 inflammation in preclinical models of asthma (71). In contrast, PGD_2 and the DP1 agonist BW245c trigger smooth muscle contraction and bronchoconstriction in micro-molar concentrations via activation of the thromboxane receptor (233). Further, PGD_2-DP1 signalling but not PGD_2-DP2 signalling induced cough in guinea pigs (72). Hence, both PGD_2 receptors, DP1 and DP2, have emerged as potential drug targets for the treatment of allergic asthma (77,234–236). In combination

with allergen exposure and genetic risk factors, lower respiratory viral infections in early childhood have been linked to a higher prevalence of developing asthma in later life as well as disease progression and acute asthmatic exacerbations in the established disease (237). PGD_2 production is elevated in viral respiratory infections and in turn promotes disease severity via DP2 (56). This recent study also showed that hPGDS expressing immune cells were recruited immediately after infection while at later time points bronchial epithelial cells upregulated hPGDS and PGD_2 production. Further, allergic inflammation is characterized by eosinophil influx and activation resulting in ongoing inflammation and tissue damage. High PGD_2 levels prolong eosinophil survival via the DP1 receptor and attract more eosinophils and Th2 cells via DP2 from the bloodstream (36,49). In aspirin-exacerbated respiratory disease or allergic inflammation, hPGDS-expressing eosinophils are able to release PGD_2, which could be attenuated with the hPGDS inhibitor HQL-79 (23,39). Basophils have also been suggested as potential PGD_2 sources in IgE-mediated inflammation (45). ILC2s are potent drivers of type-2 inflammation and have been of great interest lately. Inhibition of autocrine PGD_2 production in human ILC2s with hPGDS inhibitor KMN-698 reduced ILC2 activation as well as IL-5 and IL-13 release (50). In allergic rhinitis, infiltrating immune cells expressed hPGDS but not LPGDS in the nasal mucosa (31). Inhibition of PGD_2 production with hPGDS inhibitor TAS-204 or TFC-007 suppressed nasal blockage, nasal airway resistance and eosinophil infiltration in antigen-challenged guinea pigs (238,239). Treatment with hPGDS inhibitor HQL-79 suppressed OVA-induced allergic airway inflammation in wild type and also in hPGDS transgenic mice (18). HQL-79 has originally been developed as histamine receptor 1 antagonist, however, in the same study they could show that the effect was also present in histamine receptor 1 knock-out mice claiming that it can be attributed to reduction of PGD_2 synthesis. Severe asthma often involves airway remodelling including smooth muscle cell hyper-proliferation and activity. PGD_2 promotes smooth muscle cell proliferation via DP2 activation and contributes to a hyper-responsive phenotype typical for asthmatic patients (60,81). To conclude, blocking PGD_2 biosynthesis has been considered as therapeutic approach to treat allergic asthma in several studies.

Chronic obstructive pulmonary disease (COPD)

Inhalation of tobacco smoke or other biomaterials is the most common cause of COPD. Constant challenge with noxious particles causes chronic bronchitis with mucus hypersecretion and bronchial wall thickening and/or alveolar wall destruction, referred to as emphysema. As a result, patients suffer from airflow limitation and symptoms including dyspnoea, cough and sputum hyper-production (213). Inflammatory drivers of the disease are activated macrophages, neutrophils and lymphocytes, primarily cytotoxic T-cells, all of which release inflammatory mediators, oxidants and proteases. Indeed, neutrophil elastase and macrophage proteinases seem to be the primary effectors of lung destruction resulting in epithelial and endothelial cell death (240). Thus, oxidative stress and chronic inflammation associated with COPD also instigate vascular dysfunction and cardiovascular risk (241).

Further, cigarette smoke interferes with lung lipid metabolism in mice, including upregulation the cyclooxygenase pathway and PGE_2 and PGD_2 release, amongst others (242). Fibroblast senescence seems to be accelerated by excess production of PGE_2 in COPD patients (243), whereby subsequent deficiency of parenchymal ECM has been linked to progression of emphysema. The involvement of PGD_2 in COPD pathology remains unclear; however, due to compelling evidence of DP2-driven inflammation in pulmonary diseases, several studies were initiated. Indeed, DP2 antagonists AM156 and AM206 ameliorated neutrophil and lymphocyte recruitment as well as airway epithelial thickening and mucus hyper-production in mice (244). Novartis started a clinical trial for patients suffering from eosinophilic COPD with DP2 antagonist fevipiprant in 2019, however, this trial has been terminated without having shown significant improvement (ClinicalTrials.gov Identifier: NCT03810183). Further, DP2 antagonist AZD1981 resulted in no beneficial clinical effect in patients with moderate to severe COPD (245).

1.4.3. Ongoing clinical studies about the hPGDS-PGD_2-DP1-DP2 axis as therapeutic target

DP2 receptor

DP2 receptor antagonism has been of great interest as potential treatment in eosinophilic asthma, type 2 inflammation and for asthmatic conditions uncontrolled by standard therapy such

as low-dose inhaled corticosteroids (ICS) and/or β_2-agonists (246). The most promising candidate to date is the Novartis drug fevipiprant (QAW039), which reached Phase III in several ongoing clinical studies (247). Fevipiprant prevented human ILC2 activation (248), eosinophil migration (249) and reduced airway smooth muscle mass in patients with asthma (250). In Phase II studies, fevipiprant had limited efficacy in mild-to-moderate asthma, however, it improved forced expiratory volume in patients with moderate-to-severe asthma (251). Great effort was put into investigating fevipiprant in childhood asthma (NCT03650400) and adults with eosinophilic asthma (NCT03989635) amongst others, nevertheless, Novartis terminated all clinical trials in December 2019 due to limited efficacy. Additional DP2 antagonists that have been explored in clinical trials with focus on asthma are OC000459 (252), AZD1981 (253), setipiprant (254), BI671800 (255) and AMG853, a dual CRTH2 and DP receptor antagonist (256). OC000459 treatment resulted in reduced eosinophil numbers in sputum, occurrence of respiratory infections and improved quality of life, while, in contrast, AZD1981, BI671800 and AMG853 were less effective. In sum, recent clinical phase 3 studies on CRTH2 fevipiprant were not as outstanding as expected; however, exacerbation rates could be reduced by 22 % in patients with type 2-high allergic asthma, which is not trivial and might still offer a benefit to some (257). Beyond allergic inflammation in the lung, DP2 receptor has been reported to be involved in COPD and pulmonary fibrosis, while no clinical studies have been conducted looking into DP2 blockade in acute lung inflammation or fibrosis to this date. DP2 antagonist AZD1981 had no beneficial effect in patients with moderate-to-severe COPD (245). A clinical trial to study oral doses of fevipiprant in COPD patients with eosinophilia (NCT03810183) has been initiated in 2019; however, the trial was terminated in June 2020 and no results were posted.

DP1 receptor

In pulmonary disease, the role of DP1 receptor signalling remains controversial. A clearer picture could be seen in studies investigating PGD_2-induced facial flushing as adverse reaction to niacin, an efficient lipid-modifying drug. Administration of laropiprant (MK-0524), an inverse agonist and antagonist of DP1 receptor signalling, antagonised these unwanted symptoms (258). Additional treatment with aspirin did not further reduce residual flushing, thereby excluding involvement of other mediators downstream of the COX-pathway (259). Nasal congestion in

respiratory inflammation results from tissue oedema and vasodilation in the nasal mucosa, similar to facial flushing in niacin reports. Studies in healthy volunteers showed that laropiprant (MK-0524) alleviated nasal congestion (260), while clinical studies of DP1 antagonist laropiprant showed that it had no beneficial effect on nasal score and symptoms in asthmatic and allergic rhinitis patients (261). In contrast, a novel DP1 antagonist, ONO-4053, was deemed safe and more effective in improving nasal congestion and histamine-related symptoms such as sneezing, than leukotriene receptor antagonists in a Phase II clinical trial with allergic rhinitis patients (262).

Hematopoietic PGD synthase

Some parts of this section have been published in adapted form (1).

Collectively, clinical studies looking into pulmonary inflammatory disorders, mainly allergic asthma, indicate an involvement of both DP receptors in driving inflammation and debilitating symptoms (263). As a result, several patents and patent applications for hPGDS inhibitors as therapeutic option in allergic inflammation, asthma, chronic obstructive pulmonary disease and other inflammatory diseases have been initiated to allow blockade of PGD_2-elicited signalling (264–266). Even though several compounds targeting hPGDS-dependent PGD_2 synthesis are commercially available, only few reports on clinical studies evaluating hPGDS inhibitor safety and efficacy can be found. In 2015, a phase I clinical trial (NCT 02397005) was initiated to evaluate tolerability and pharmacokinetics of the selective and reversible hPGDS inhibitor ZL-2102 as therapeutic approach for COPD, asthma and idiopathic pulmonary fibrosis (267). At this time, no results of this study have been published yet. Beyond pulmonary inflammation, hPGDS has been considered as therapeutic target in Duchenne's muscular dystrophy as previous studies observed increased PGD_2 levels in myonecrotic areas and urinary tetranor-PGD metabolite in Duchenne's patients. Building up on these findings, another phase I clinical trial investigating safety and pharmacokinetics of hPGDS inhibitor TAS-205 in 23 boys with Duchenne's muscular dystrophy was completed in 2018 (268). HPGDS inhibitor TAS-205 was verified over various dose ranges and was judged safe and tolerable in patients with Duchenne's muscular dystrophy. Urinary PGD-metabolite was significantly reduced following treatment whereby urinary PGE_2 metabolite levels were unchanged. In this dose range, hPGDS inhibitor TAS-205 was well tolerated with significant and specific biological activity in patients.

1.5. Aims of the dissertation

PGD_2 is involved in many inflammatory responses and exerts both, pro- and anti-inflammatory action depending on brief or sustained stimulation, target cells and species. As a result, many findings are still inconclusive or contradictory, requiring further investigation to fully exploit its therapeutic potential. This thesis consists of three parts, all aiming to explore and describe the effects of PGD_2 on the innate immune response in pulmonary inflammation.

Therefore, the aims of this thesis were as following:

PART I – E-type 4 receptor mediates PGD_2-induced enhancement of pulmonary endothelial barrier function

- To elucidate, which receptor is activated by PGD_2 on primary human pulmonary microvascular endothelial cells (HPMEC)
- To investigate the effect of PGD_2 on HPMEC barrier function and its therapeutic potential in limiting oedema formation

PART II – Characterization of novel prostaglandin sources in LPS-induced inflammation

- To identify, which cell type is the major source of PGD_2 in LPS-induced inflammation
- To investigate LPS-induced regulation of hPGDS, the rate-limiting enzyme of PGD_2 production, in human monocytes and macrophages
- To explore the potential of human monocytes and macrophages as PGD_2 sources

PART III – PGD_2-DP2 activation on human IL-4 polarized monocyte-derived macrophages abrogates angiogenic potential of conditioned medium

- To explore, whether DP receptor activation on human macrophages affects HPMEC regeneration and angiogenesis
- To delineate, which receptor, DP1 or DP2, is involved in these processes and how

2. Materials and Methods

A detailed list of chemicals, reagents, equipment, antibodies and compounds can be found in the appendix section of this thesis. Some parts of this section have been published in adapted form (2).

2.1 Ethical Approvals

Human ethics. All experiments involving primary cells from human subjects were approved by the Institutional Review Board of the Medical University of Graz (EK 17-291 ex 05/06). All volunteers signed an informed consent. Human lung tissue samples were obtained from downsized non-tumourous, non-transplanted donor lungs from patients who underwent lung transplantation at the Department of Surgery, Division of Thoracic Surgery, Medical University of Vienna, Austria. The institutional ethics committee approved the protocol and tissue usage (976/2010), and patient consent was obtained before lung transplantation. A detailed description on how the explanted lungs were sampled and stored can be found elsewhere (269).

Animal ethics. All studies involving animal experiments were approved by the Animal Ethics Committee of the Austrian Federal Ministry of Science and Research (protocol numbers are indicated for respective experiments) and carried out in line with the European Community's Council Directive. OVA-induced allergic inflammation model with BALB/c mice was performed in 2016 (Robert Frei, protocol numbers: BMWF-66.010/0094- II/3b/2013; BMWFW-66.010/0020-WF/V/3b/2015), LPS-induced pulmonary inflammation model with BALB/c mice was performed in 2016 (Katharina Jandl, protocol number: BMWFW-66.010/0046- II/3b/2013). Bleomycin-induced fibrosis mouse model (C57BL/6j mice) was performed in 2019 (Thomas Bärnthaler, protocol number: BMWFW-66.010/0119-V/3b/2018) and LPS-induced mouse model with C57BL/6 was performed in 2020 (Amendment to protocol number: BMWFW-66.010/0119-V/3b/2018).

2.2 Cell culture

Endothelial cell culture. Human pulmonary microvascular endothelial cells (HPMEC, Lonza, Basel, Switzerland or PromoCell, Heidelberg, Germany), dermal microvascular endothelial

cells (HDMEC, PromoCell, Heidelberg, Germany) or pulmonary artery endothelial cells (HPAEC, Lonza, Basel, Switzerland) were cultured in corresponding complete medium in T75 Corning CellBind flasks pre-coated with attachment factor solution (PeloBiotech, Bavaria, Germany) or 1 % gelatine (Sigma-Aldrich) solution. A list of endothelial cell donors used for experiments can be found in **Table 1**. Cells were passaged when 80 % confluence was reached, detached with Trypsin/EDTA solution from respective company (PromoCell or Lonza) while cells from passage 4 to 9 were used for experiments.

EP4-knock down in primary human microvascular endothelial cells. EP4 knock-down in human pulmonary microvascular endothelial cells was performed as described previously (99). Briefly, HPMEC were seeded onto gelatine-coated 6 well plates (Corning CellBind) and transfected for 48 h with Lipofectamine RNAiMAX (ThermoFisherScientific, Massachusetts, USA) according to the manufacturer's instructions when they reached 60-70 % confluence. Each experimental set-up consisted of untreated, mock-transfected (Lipofectamine only), non-targeting control siRNA (50 nM) and specific PTGER4-targeting siRNA (50 nM PTGER4 FlexiTube-GeneSolution, Qiagen, Hilden, Germany) transfected cells as well as additional wells (control and EP4-specific siRNA) for knock-down control via qPCR or Western blotting. After 48 h transfection, cells were either collected in TriReagent for mRNA extraction, protein lysis buffer (4 M Urea in Tris/HCl ph 8 with 1 % SDS) for Western blotting or detached using trypsin/EDTA and seeded onto gelatine-coated 8W10E+ polycarbonate ECIS arrays. Cells were left to adhere in EBM-2 basal medium for 5 h and ECIS experiments were performed as described above. For immunofluorescent staining after knock-down, cells were grown and directly transfected in 8-well chamber slides (LabTek II).

Isolation of peripheral blood leukocytes. Approximately 70 ml of whole blood from healthy donors were collected in 3.8 % sodium citrate (1:10) and spun down at 400 x g for 20 min with low brake. Donors were selected independently of sex and age; however, it was noted whether a symptomatic allergy existed. After aspiration of platelet-rich plasma, 6 ml of 6% dextran was added to remaining blood cells, filled up to 50 ml with 0.9 % saline solution and incubated at room temperature for 30 min to facilitate erythrocyte sedimentation. The upper phase after dextran

sedimentation was transferred carefully onto 15 ml of histopaque-1077 and spun at 400 x g for 20 min with low brake. This density-gradient centrifugation step separates peripheral blood mononuclear cells (PBMC) containing B- and T-lymphocytes as well as NK cells and monocytes from polymorphonuclear leukocytes (PMNL) containing granulocytes. The PMNL pellet was resuspended in 10 ml 0.2 % saline solution, topped up with 10 ml of 1.6% saline solution and filled up to 30 ml with HBSS. After centrifugation, PBMC and PMNL cell number was determined using Kimura stain and a Neubauer counting chamber. For certain experiments, peripheral blood monocytes and eosinophils were enriched from the PBMC or PMNL fractions using either monocyte isolation kit II or eosinophil isolation kit (Miltenyi Biotech), respectively, according to the manufacturer's instructions.

Generation of human monocyte-derived macrophages. PBMC obtained from buffy coats were counted with a haemocytometer, resuspended in pre-warmed adhesion medium (RPMI supplemented with 5 % human AB serum, non-essential aminoacids, sodium pyruvate, HEPES and 1 % penicillin/streptomycin (P/S)) at a concentration of 10 Mio cells/ml and seeded onto CellBind plates (6-well plate: 2 ml cell suspension/well, 12-well plate: 1 ml cell suspension/well, 24-well plate: 0.5 ml cell suspension/well) for 1 h at 37 °C in humidified atmosphere with 5 % CO_2. Subsequently, non-adherent cells were aspirated, the wells were washed 3-5 times with 1 ml HBSS and differentiation medium containing 10 % foetal calf serum (FCS), 1 % P/S and 20 ng/ml rh M-CSF (6-well plate: 2 ml/well, 12-well plate: 1 ml/well) was added to the enriched monocyte population. Differentiation medium was changed every 2–3 days until macrophages were fully differentiated (day 6 – 8) which was determined by observing the cells' morphology. Following *in vitro* differentiation of monocytes, differentiation medium was replaced by activation medium without rh M-CSF. To acquire classically activated macrophages, MDM were incubated for 48 h with activation medium (RPMI with 10 % FCS, 1 % P/S) supplemented with 20 ng/ml rh IFN-y and 100 ng/ml LPS. To obtain macrophages with alternative phenotype, the medium was supplemented with 20 ng/ml rh IL-4 or IL-10 for 48 h.

Stimulation of MDM with PGD_2, BW245c or DK-PGD_2 and collection of conditioned medium. To evaluate the effect of monocyte-derived macrophages on endothelial cell function,

fully differentiated MDM were activated for 24 h to either pro- or anti-inflammatory phenotype or directly stimulated with PGD_2 or DP agonists (1 µM or vehicle) three consecutive times (Figure 5). One hour after 3rd agonist-treatment, activation medium (RPMI + 10 % FCS + 1 % P/S + supplements) was replaced by RPMI after a 3x PBS wash. Conditioned medium was collected after 3 h incubation with activated cells and stored at -70 °C. As RPMI control, an empty well received the same treatments as macrophages stimulated with 1 µM PGD_2 or agonists.

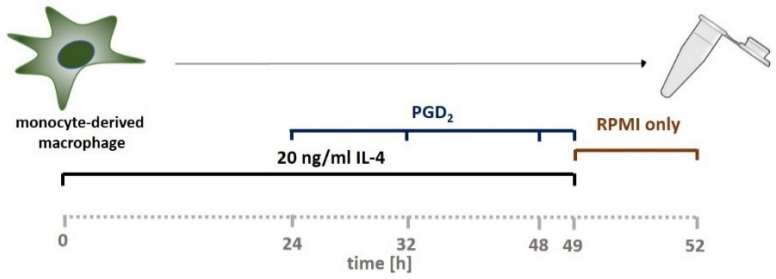

Figure 5. Schematic showing MDM activation and treatment with PGD_2 or DP agonists.

Broncho-alveolar lavage (BAL) fluid collection and culturing of mononuclear cells. OVA mice (n = 5), LPS mice (n = 5) and naïve mice (3-month-old BALB/c mice, n = 5) were anesthetized with an overdose of Ketamine/Xylazine working solution (10 mg/ml Ketasol, 1 mg/ml Rompun). Thorax was opened, trachea exposed and a tracheal cannula (1.20x40mm needle) inserted and fixed with a thread. The lung was lavaged 8-times with 1 ml ice cold BAL buffer (PBS^- with 0.6 mM EDTA) and collected in a Falcon tube on ice. BAL fluid was spun down at 400 x g for 5 min at room temperature and resuspended in 1 ml BAL buffer. Erythrocytes were lysed by adding 5 ml of NH_4Cl_2 lysis buffer on ice (5 min). Cells were washed with 5 ml BAL buffer followed by centrifugation at 400 x g for 5 min and resuspended in 1 ml BAL buffer. The number of viable cells was evaluated with Trypan blue. Additionally, mononuclear cells were morphologically identified and the ratio to total cells was determined. Cells were resuspended in adherence medium to get a final concentration of 0.3 million mononuclear cells / ml. Subsequently, 150 000 mononuclear cells from LPS and OVA or 75 000 from naïve mice per well were seeded in a 48-well plate (CellBind). After 1.5 h incubation at 37 °C non-adherent cells were washed off (3 x 500 µl wash buffer) and medium was replaced by activation medium (RPMI, 10 % FCS, 1 %

P/S). Cells were cultured at 0.15 million mononuclear cells / ml medium. Conditioned medium was collected after 4 and 18 h and amount of PGD_2 released into the culture medium was evaluated with a MOX-PGD_2 ELISA kit (CaymanChem).

2.3 Cellular assays

Electric Impedance Cell-substrate Sensing (ECIS). Endothelial cells were seeded at a density of 60 000 – 80 000 / 400 µl complete medium / well onto 8W10E$^+$ polycarbonate arrays (AppliedBiophysics, NY, USA) pre-coated with 10 mM L-cysteine in sterile water, followed by coating with 1 % gelatine solution and grown until confluence for 2 to 3 days. An ECIS® Z-Theta device (AppliedBiophysics, NY, USA) was used for online monitoring of resistance changes within the cellular monolayer. Prior to treatment, cells were serum starved in EBM-2 basal medium (PromoCell or Lonza) supplemented with 2 % FCS for 1 h, followed by baseline measurement for 2 h. Endothelial resistance was monitored continuously throughout pre-treatment with antagonists for 30 min and stimulation with PGD_2 or other agonists dissolved in EBM-2 basal medium with 2 % FCS for 24 h. A list of all agonists and antagonists used in this study are summarized in **Table 2**. Each treatment was performed in duplicate and normalized resistance for each well was recorded every 30 s for 20 h (4.5 h displayed for clarity) after agonist addition. Monocyte-conditioned medium used for ECIS barrier determination was diluted 1:20, while macrophage-conditioned medium was used at 1:4. To observe the effect of macrophage-conditioned medium on endothelial wound healing, cells were seeded onto 8W10E$^+$ polycarbonate arrays (AppliedBiophysics), starved in EBM-2 basal medium with 2 % FCS and baseline recorded for 2 h. Monolayer disruption for the wound healing assay (4 s, 3000 µA, 48 GHz) preceded direct addition of pre-warmed conditioned medium or treatments to achieve a 1:1 mixture in the wells.

Thrombin barrier disruption assay. Lab-Tek II CC^2 8-chamber well slides (ThermoFisher Scientific) were pre-coated with 1 % gelatine solution followed by seeding of 60 000 – 80 000 endothelial cells / well. When confluence was reached, cells were serum starved in EBM-2 basal medium with 2 % FCS for 30 min followed by incubation with EP4 receptor antagonist ONO-AE3-208 or vehicle for 20 min. Subsequently, endothelial cells were treated with indicated concentrations of PGD_2, PGE_2 or agonists for 15 min before cells were challenged with 0.5 U/ml

recombinant human thrombin (15 min). All incubations were performed at 37 °C, 5 % CO_2 and humidified atmosphere. Cells were washed once with pre-warmed Hepes-buffered saline and fixed in 3.8 % formalin solution (CarlRoth, Karlsruhe, Germany) for 10 min at room temperature.

Cell cycle analysis. Endothelial cells were seeded at a density of 75 000 – 80 000/well onto pre-coated CellBind 6-well plates and incubated overnight. After 1 h starvation (EBM-2 medium + 2 % FCS), macrophage-conditioned medium was added at a ratio of 1:10 or 1:5, while 100x concentrated PGD_2 solution was prepared to achieve a final concentration of 3 µM per well. Cells were incubated for additional 24 h before collection with Trypsin/EDTA. Ethanol fixation was performed over night at 4 °C, followed by Propidium Iodide (PI) staining (1 % FCS, 0.05 mg/ml PI, 0.1 mg/ml RNase A in PBS) for 1 h at 37 °C. PI staining was evaluated with FACS Canto II (emission filter B 585_42-A) by recording 50 000 events/condition.

Spheroid sprouting assay with human pulmonary microvascular endothelial cells. Spheroid sprouting assay was adapted for HPMEC from a previously published study (270). Cells were cultured as described above until 80 % confluence was reached and cells were detached using Trypsin/EDTA. Cell number was determined using Trypan blue and a Neubauer counting chamber. For spheroids, cells were resuspended in 0.25 % methylcellulose working solution in EBM-2 basal medium (PromoCell) at a density of 4 x 10^4 cells/ml and evenly distributed on the lid of a non-adherent plastic dish using a multichannel pipette to get 1000 cells in a 25 µl drop. Plates were inverted and incubated overnight with humid atmosphere at 37 °C. Next day, spheroids were harvested with Hank' buffered saline solution containing 10 % FCS and centrifuged at 500 x g for 3 min without brake. Supernatant was aspirated and spheroids gently loosened by tapping followed by addition of 0.7 % methylcellulose solution containing 40 % FCS, $NaHCO_3$ (15.6 mg/ml) for osmolarity, type-1 collagen (end concentration 2 mg/ml, rat tail collagen I, Corning) and NaOH (1 M) to balance the acidic pH. Spheroids were seeded in a volume of 500 µl into 24 well plates. After 2 h of collagen polymerization, stimulation media (M119 media with 10 % new born calf serum, 10 % human AB serum and 1 % P/S) containing compounds or conditioned media was added. A combination of 10 ng/ml TNF-α (Reliatech), 25 ng/ml VEGF-A (Reliatech) and 10 ng/ml FGF-2

(bFGF, Sigma-Aldrich) was used as positive control. Cumulative spheroid length [µm] was measured using ImageJ software by a blinded operator not familiar with tested substances.

Platelet aggregation. Washed platelets were obtained from platelet rich plasma (citrated blood) from healthy donors by centrifugation at 700 x g for 15 min without break, followed by two washing steps in wash buffer (140 mM NaCl, 10 mM $NaHCO_3$, 2.5 mM KCl, 0.9 mM Na_2HPO_4 * 2 H_2O, 2.1 mM $MgCl_2$, 22 mM $C_6H_5Na_3O_7$, 0.055 mM D-glucose monohydrate and 0.35 % bovine serum albumin; pH 6.5) as previously described (271). Platelets were resuspended in Tyrode buffer and platelet aggregation was determined using the 4-channel platelet aggregometer APACT4004 (LabiTec, Ahrensburg, Germany). Aggregation of washed platelets was recorded after addition of pro-aggregatory stimulation with adenosine diphosphate (ADP; Probe & Go, Osburg, Germany, 5-20 µM to induce ~30-40% aggregation) with constant stirring at 37 °C. Platelets were pre-treated with vehicle (EtOH) or 100 nM ONO-AE3-208 for 10 min followed by addition of 30 nM PGD_2 or vehicle (EtOH) for 5 min before stimulation with ADP/fibrinogen (F4129-1G, Fraction I, type III: from human plasma, Sigma Aldrich, Missouri, USA, 1 µg/ml). Aggregation was measured as increase in light transmission for 300 seconds and the maximum percentage (%) of aggregation obtained for each treatment was plotted.

2.4 Microscopy and biochemical methods

Immunofluorescence staining for microscopy. Following fixation with 3.7 % formalin solution for 10 min at room temperature, cells were washed and permeabilized with 0.1 % TritonX-100 in phosphate buffered saline for 10-15 min. Non-specific binding was blocked by incubation with 10 % normal goat serum (Sigma Aldrich, Missouri, USA) and 1 % bovine serum albumin in PBS for 30 min. Subsequently, primary antibody was diluted in antibody diluent (blocking solution diluted 1:10 with PBS) and added (100 µl/well or slide) for 1 h at room temperature. Cells were washed three times with PBS and incubated with respective secondary antibody (1:500, ThermoFisher Scientific) with or without Texas Red-X-conjugated phalloidin (1:40, ThermoFisher Scientific) for 30 min at room temperature. Slides were mounted with VectaShield / DAPI fluorescence mounting medium and images were taken using an Olympus IX70 fluorescence

microscope with an Olympus UPlanApo-20x, 40x or 60x lens. Controls included unstained cells, stained with isotype and secondary antibody only.

F-actin / VE-cadherin staining in human endothelial cells. After thrombin barrier disruption assay, cells were fixed and subjected to F-actin / VE-cadherin staining to determine monolayer integrity. Primary mouse anti-human VE-cadherin antibody (sc-9989, SantaCruz, TX, USA) was diluted 1:200 in antibody solution and incubated for 1 h at room temperature followed by incubation with secondary AF488-conjugated goat anti-mouse antibody and Texas-Red-conjugated phalloidin for 30 min.

Quantification of endothelial monolayer integrity after VE-cadherin/F-actin staining. Fiji ImageJ software was used for counting and to reduce the background noise. Cropped cells at image edges were excluded from quantification. To visualize the protective effect of PGD_2, BW245c, DK-PGD_2 and PGE_2, 5 images per well were taken (20x magnification) of 5 independent experiments by one operator, while scoring of barrier integrity was performed by another operator unfamiliar with experimental treatments. The percentage of cells with disrupted barrier was estimated using VE-cadherin staining at cell periphery. In vehicle-treated cells, peripheral VE-cadherin forms a thin, but continuous line between neighbouring cells. Stimulation with a barrier-enhancing agent such as PGE_2 strengthens this VE-cadherin junctional zone, which appears now brighter, wider and more uniform. At the same time, actin fibres are assembled at cell periphery to support VE-cadherin junctional complexes. Challenge with a barrier-disrupting agent such as thrombin leads to Rho-dependent stress fibre formation and Rac-dependent cell rounding and retraction. In the immunofluorescence images, this was observed as reduction of cortical F-actin staining, appearance of F-actin stress fibres throughout the cell body and, in its most severe form, stress fibres close to the nuclei. Further, actin polymerization causes cellular contraction, which causes intercellular gaps. Therefore, three parameters were considered to evaluate endothelial monolayer integrity: 1) percentage of cells with stress fibres covering >80 % of cytoplasmic area and/or stress fibres close to the nucleus, 2) number of inter-endothelial gaps normalized to total number of nuclei per field and 3) VE-cadherin staining at cell periphery, where a cell with less than 60 % continuous circumferential VE-Cadherin staining was considered as ‘cell with disrupted

barrier'. One data point corresponds to the mean value of 5 images per well (>250 cells). Schematic drawing of F-actin and VE-cadherin changes and one example to demonstrate how cells were counted can be found in Figure 6A and B, respectively.

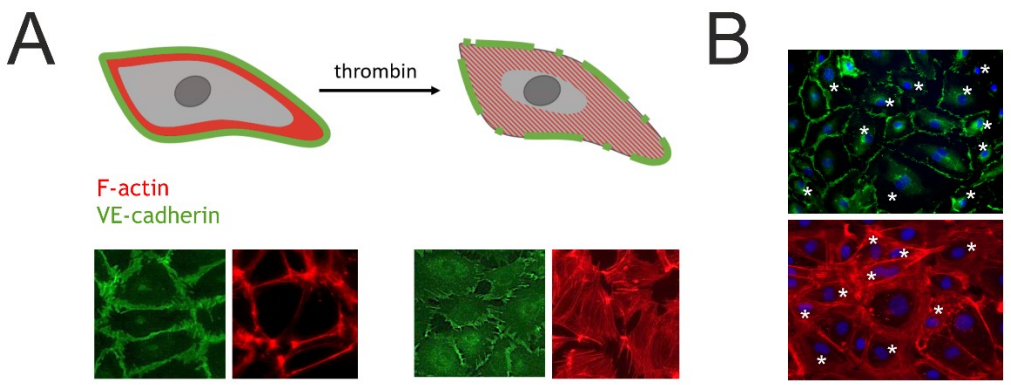

Figure 6. Quantification of endothelial monolayer integrity. A) Schematic drawing of peripheral F-actin fibres and VE-cadherin at steady state (left) and after treatment with a barrier disrupting agent (right). (B) Evaluation strategy of cells judged as positive for stress fibres or disrupted barrier indicated with an asterisk. Adapted from (2).

EP4 / DP1 staining. To visualize EP4 and DP1 receptor expression on HPMEC, cells were incubated with primary rabbit anti-DP1 (1:200, CaymanChem) for 1 h after fixation and blockade of unspecific binding, without prior permeabilization. Subsequently, cells were permeabilized with 0.1 % Triton-X, blocked for additional 30 min and incubated with primary mouse anti-EP4 (1:200, SantaCruz) for 1 h. Secondary goat anti-mouse AF647, goat anti-rabbit AF488 and Texas-Red-conjugated phalloidin were added for 30 min in the dark. To check anti-DP1 functionality, eosinophils from the PMNL fraction of healthy human blood were fixed in 3.7 % formalin solution, spun down using a cytospin device (600 rpm for 3 min) and stained with anti-DP1 as depicted above.

hPGDS staining. 500 000 peripheral blood monocytes/well, isolated from PBMC fraction by negative selection using Monocyte Isolation Kit II (Miltenyi), were seeded into Poly-L-Lysine pre-coated Lab-Tek II CC^2 8-well chamber slides (ThermoFisher Scientific) and left for 4 h to adhere. For MDM staining, 250 000 monocytes/well were seeded into Poly-L-Lysine pre-coated 8-well chamber slides and incubated for 6-8 days to generate fully differentiated MDM. Additionally,

human peripheral blood neutrophils were seeded as described for monocytes and subsequently subjected to staining. Briefly, cells were fixed with 3.8 % formalin solution for 15 min before proceeding to hPGDS staining. Following permeabilization and blocking, cells were stained with primary mouse anti-human hPGDS (1:100, Novus Bioscience) for 1 h at room temperature and subsequently with secondary AF488-conjugated goat anti-mouse antibody (1:500, ThermoFisher Scientific) and TexasRed-conjugated phalloidin for 30 min at room temperature in the dark.

***In Situ* hybridization (ISH).** ISH was conducted with the RNAscope kit (Cat#322360) for hPGDS (ACDBio, Newark, Calif) according to the manufacturer's protocol. Briefly, lung slides were deparaffinised with xylene and 99.9 % EtOH followed by drying in a pre-heated oven. Subsequently, slides were transferred to a steamer containing MilliQ water for acclimatization, before antigen retrieval with 10 mM Citrate buffer pH 6 was performed by microwaving at 850 W for 10 min. Slides were rinsed with MilliQ water and equilibrated with 99.9 % EtOH for 3 min before being dried in an oven at 37 °C. Each section was treated with protease plus (RNAScope kit), covered and incubated in the oven humidity tray at 40 °C for 20 min. Again, slides were rinsed with MilliQ water, placed back onto the slide rack and probe was added (RNAscope Probe- Mm-Hpgds, Cat#413391). The rack was placed back into the oven and probe hybridization was performed at 40 °C for 2 h. RNAscope wash buffer was diluted with MilliQ water and pre-warmed to 37 °C. Slides were transferred one by one to wash buffer and incubated for 2 min at room temperature with occasional agitation. This step was repeated once more. Next, slides were incubated with amplifier 1 for 30 min, amplifier 2 for 15 min, amplifier 3 for 30 min, amplifier 4 for 15 min, amplifier 5 for 45 min and amplifier 6 for 15 min. Amplification steps 1 to 4 were performed at 40 °C while steps 5-6 were performed at room temperature. In between amplification steps slides were washed twice in wash buffer for 2 min each. Finally, sections were incubated with detection reagent (Fast Red-A to Fast Red-B in a 1:60 ratio, 60 µl per section) in the humidity control tray for 10 min at room temperature. Slides were washed in MilliQ water. Following ISH, slides were incubated with blocking solution (10 % goat serum and 1 % BSA in PBS) for 1 h and stained with rabbit anti-CD68 (ab125212, Abcam, 1:200) overnight in a humid chamber at room temperature. Next day, slides were incubated with goat anti-rabbit AF488-conjugated secondary

antibody (1:300) for 3 h at room temperature in the dark. Slides were mounted with Vectamount and imaged with a NIKON A1 confocal microscope at 20x magnification.

Immunohistochemical staining of human lung sections. This staining was performed by our collaborators at the Ludwig Boltzmann Institute for Lung Vascular Research. Formalin-fixed, paraffin-embedded lung sections (2.5 µm thick) were prepared and stained with an ImmPRESS Polymer Detection Kit (VectorLaboratories, CA, USA). Briefly, lung sections were deparaffinised, rehydrated, immersed in citrate buffer (DAKO, 8388682; Agilent, CA, USA) and heated in a 95 °C waterbath for 20 min. Next, sections were incubated with 3 % H_2O_2 in methanol (Merck, NJ, USA) for 20 min. After washing, unspecific binding was blocked with 2.5 % normal horse serum for 20 min, followed by incubation with 3 % BSA for 30 min in a humid chamber. Mouse anti-vWF (1:1000, Dako, A0082), rabbit anti-DP1 (1:50, 101640, CaymanChem) and rabbit anti-EP4 (1:200, ab133170, Abcam, Cambride, UK) were diluted in 3 % BSA and consecutive sections from 4 different donors were stained over night at 4 °C. The following day, sections were washed and corresponding ImmPRESS reagent peroxidase solutions (VectorLaboratories, anti-rabbit MP-7401, anti-mouse MP-7402) added for 30 min at room temperature. Colour was developed with Nova Red substrate (VectorLaboratories, SK-4805). Sections were counter-stained with hemalaun, dehydrated and mounted with a Xylol-based medium. All slides were scanned using an Olympus VS120 slide scanning microscope (Olympus, Tokyo, Japan) at 40x magnification and images extracted using OlyVIA Software (Olympus).

Real time quantitative PCR. For RNA isolation, samples collected and stored in TriReagent (ThermoFisher Scientific or Sigma-Aldrich) were thawed on ice. Phase separation was achieved by addition of 80-200 µl chloroform for 3 min at room temperature and centrifugation at 12 000 rpm for 15 min at 4 °C. Upper aqueous phase containing RNA was transferred to a new tube and precipitation was induced by adding 99.9 % EtOH. Remaining phenol phase was saved and frozen at -80°C for protein extraction. Samples were further purified with a RNeasy Mini Kit (Qiagen) according to the protocol and RNA was eluted in 20-30 µl RNAse-free water. 0.3 to 1 µg of RNA was reverse transcribed using iScript cDNA Synthesis Kit (Bio-Rad, CA, USA) or high capacity

cDNA synthesis kit (ThermoFisher Scientific) according to the manufacturer's instructions. Resulting cDNA was diluted with 30 to 80 µl ddH_2O and used for quantitative RT-PCR experiments. SsoAdvanced™ Universal SYBR® Green Supermix (Bio-Rad) in combination with PrimePCR™ SYBR® Green Assay primers for indicated genes (BioRad) were used. A reverse transcription control was performed by mixing 1 µl RNA from randomly chosen samples, adding the reaction mix but no reverse transcriptase. Additionally, reverse transcription and negative control (ddH_2O) were run in parallel during each qPCR run. The standard PCR run was programmed for 10 µl volumes according to suggestions from BioRad: 2 min – 95°C, 39 to 55 repeats of 5 s – 95°C and 30 s of 60 °C, melting curve: 5 s – 95 °C, 5 s – 65 °C, 0.5 °C increments. DeltaCq values for the genes were calculated by subtracting corresponding gene Cq from GAPDH Cq values. Some results were plotted as $2^{(\Delta Cq)}$ (normalization to housekeeping gene) or $2^{(\Delta\Delta Cq)}$ (additional normalization to vehicle or naïve control) values.

EP4, DP1 and DP2 mRNA expression. For evaluation of receptor mRNA expression levels and knock-down efficiency, cells were collected either directly or after 48 h transfection in TriReagent (Sigma-Aldrich). Messenger RNA was extracted, and cDNA generated as described above. Samples were run in duplicates, PTGER4 normalized to GAPDH Cq values and results are shown as percentage of control siRNA. To evaluate DP1, DP2 and EP4 receptor mRNA expression levels in HPMEC, HDMEC and HPAEC, RNA was extracted, and cDNA generated from unstimulated cells as described above. Validated PrimePCR™ SYBR® Green Assay primers for human PTGER4, PTGDR, PTGDR2 and GAPDH (Bio-Rad) were used. Additionally, cDNA from human peripheral blood monocytes was used to check functionality of DP1 and DP2 primer pairs.

*hPGDS, mPTGES-1, LPGDS and COX-2 mRNA expression***.** Fully differentiated MDM were collected in 200 µl TriReagent at indicated time points after activation and stored at -70 °C until further use. Additionally, monocytes isolated with the Monocyte Isolation Kit II were used for RNA extraction and RT-qPCR (0.5 to 1 million cells per condition). The 20 µl reaction mix from cDNA synthesis was diluted with 30 µl (monocytes) or 50 µl (macrophages) RNAse free water. HPGDS, COX-2, mPTGES-1, LPGDS and GAPDH gene expression was detected using validated BioRad primers and a SYBR green reaction mix.

hPGDS, mPTGES-1, COX-2 and LPGDS mRNA expression in murine myeloid populations. Myeloid cells sorted from vehicle or LPS mice were collected and stored in TriReagent at -70 °C until further use. Briefly, neutrophil, macrophage, monocyte and mast cell samples from vehicle and LPS mice (2-4 mice per processing day) were thawed and processed simultaneously on the same day. Phase separation was achieved by addition of chloroform and centrifugation as described above. Aqueous phase was transferred to a new tube and RNA precipitated by addition of the same volume of 2-propanol and incubation for 5 min at room temperature. Samples were centrifuged at maximum speed (14 000 x g) for 10 min and supernatant aspirated. Pellet was washed twice with 75 % molecular grade EtOH and air dried. RNA was resuspended in 11 µl nuclease free water and concentration determined *via* nanodrop. 5 µl of RNA solution from each sample was reverse transcribed using the High capacity cDNA kit (ThermoFisher, 5 µl per reaction) and resulting cDNA diluted with 25 µl nuclease free water. 3 µl of sample cDNA was assayed in a 10 µl PCR reaction (SYBR green mix, BioRad) along with primer pairs listed in **Table 3**. Linearity of primer pair response was previously confirmed using a sample from LPS stimulated murine liver single cell suspension (data not shown), which was also run in parallel to each PCR reaction as positive control. The standard PCR protocol as described above was used with 55 repeats of annealing and extension.

Western blotting. Lysates were sonicated (4 cycles at 40 % power for 10 s each), spun down at 12 000 rpm for 10 min at 4 °C and the supernatant was used for Western blotting. Between 15 to 30 µg protein (as determined with a BCA assay) was loaded onto a precast gel (4-20 %) and proteins separated with 225 V for 45 min. Following a 10 min wash in MilliQ water, protein bands were transferred onto a PVDF membrane with help of an iBlot gel transfer device (Thermofisher Scientific). Subsequently, unspecific binding was blocked with 5 % milk in TBST buffer on a shaker at room temperature for 1 h and the membrane was incubated with primary antibodies at indicated concentrations overnight. Next day after washing three times with TBST buffer, the membrane was incubated with horseradish peroxidase-conjugated secondary antibody (1:5000 in 5 % milk) for 1.5 h. Bands were visualized by incubation for 5 min with Clarity™ Western ECL Blotting Substrate (BioRad) and subsequently evaluated with a BioRad chemiluminescence detector and corresponding Software (ImageViewer).

Monocytes and macrophages. Cell lysates were collected from monocytes or macrophages seeded in a 6-well plate (~ 1 – 2 x 10^6 cells) by addition of 120 µl protein lysis buffer (10 mM Hepes, 1 mM EDTA, 1 % Triton, 1 mM sodium-orthovanadate, 7.5 µl protease inhibitor cocktail (Sigma)) and scraping off cells. After blotting and blocking, the membrane was incubated with primary rabbit anti-human hPGDS (LSBio, 1 µg/ml), rabbit anti-human COX-2 (1:1000) in 1 % milk in washing buffer or rabbit anti-human GAPDH (1:3000) in 5 % milk at 4 °C overnight. The membrane was washed and incubated with stripping buffer (Restore PLUS Western blot stripping buffer, Thermofisher Scientific) for 15 min at room temperature, blocked for 1 h with 5 % milk and incubated with primary rabbit anti-LPGDS antibody overnight.

HPMEC PG receptor expression. Cell lysates were collected in 100 µl protein lysis buffer (10 mM Hepes, 1 mM EDTA, 1 % Triton-X, 1 mM sodium-orthovanadate, 7.5 µl protease inhibitor cocktail) or a 1:1 mixture of 8 M Urea buffer in Tris/HCl pH 8 and RIPA buffer with protease/phosphatase inhibitor with 1 % SDS and stored at -70 °C until further use. After blotting and blocking, the membrane was incubated with primary rabbit anti-human EP4 (Santa Cruz, sc-20677, 1:200) in 5 % milk at 4 °C overnight. Next day, the membrane was incubated with horseradish peroxidase-conjugated secondary goat anti-rabbit HRP-conjugated antibody (Jackson ImmunoResearch, 111-035-045, 1:5000) for 1.5 h. After detection, the membrane was washed for 30 min with stripping buffer (65.2 mM Tris/HCl with 2 % SDS pH 6.9 with 100 nM β-mercaptoethanol) at 50 °C with shaking, washed three times with TBST buffer for 10 min, blocked for 30 min at room temperature with 5 % milk and subsequently incubated with primary rabbit anti-human DP1 (CaymanChem, 101640, 1:200), primary rat anti-DP2 (SantaCruz, BM16, 1:200) or mouse anti-human β-actin (BioTechne, Minnesota, USA, NB600-501, 1:5000) and corresponding secondary antibody on the following day (horseradish peroxidase-conjugated secondary goat anti-mouse (Jackson ImmunoResearch, 115-035-062), goat anti-rabbit (Jackson ImmunoResearch, 111-035-045, 1:5000) or goat anti-rat (Jackson ImmunoResearch, 112-035-003, 1:5000) for 1.5 h.

HPMEC phospho-protein evaluation. For investigation of VE-cadherin, focal adhesion kinase, paxillin and AKT phosphorylation, HPMEC were seeded into 6-well CellBind plates and

grown until confluent. Cells were starved in EBM-MV2 basal medium supplemented with 2 % FCS for 1 h, incubated with 300 nM ONO-AE3-208 or vehicle for 20 min and subsequently stimulated with indicated concentrations of PGD_2 or PGE_2 for 30 min. After washing with HBSS, protein lysates were collected in 120 µl RIPA buffer with protease/phosphatase inhibitor cocktail (100x Halt Protease and Phosphatase inhibitor cocktail, ThermoFisher Scientific, Massachusetts, USA) and stored at -70 °C. For Western blotting, 15 µg protein were loaded onto the gel after sonication and centrifugation. A list of antibodies and dilutions used can be found in **Table 4**.

Flow cytometry and FACS. Samples were analysed by flow cytometry using FACS Canto II or FACS Calibur from BD Bioscience. For samples stained with more than one fluorophore-conjugated antibody, a cell-based compensation was performed with of FACS Diva Software. Controls performed for each experiment include untreated cells (no fixation, permeabilization or staining), an unstained control and cells stained for surface markers only (fluorescence minus one - FMO) and secondary antibody only to evaluate reliability of staining. Raw data extracted from FACS Canto II were evaluated using FlowJo Diagnostic Software version 10.

Macrophage activation control. Upregulation of phenotype-associated surface markers CD80, CD206 and CD163 were observed to monitor successful activation of macrophages. Therefore, fully differentiated and activated macrophages were washed twice with washing buffer and, subsequently, incubated for 15 min at 37 °C with 1 ml accutase to facilitate cell detachment. Cells were collected in 15 ml falcons by gently scraping off the cells from the bottom of the well. Subsequently, macrophages were fixed for 30 min in BD CellFix solution at room temperature to prevent attachment to Flow tubes. To check successful activation, a fraction of macrophages was incubated for 30 min with PE-labelled monoclonal antibodies for CD80 and CD206 or respective isotype controls, which were used at a concentration of 20 µg/mL. For some experiments, macrophages were labelled in parallel with APC-conjugated anti-CD206, FITC-conjugated anti-CD163 and PE-conjugated anti-CD80 or respective isotype controls.

Surface marker staining of leukocyte subsets. Peripheral blood monocytes, $CD4^+$ and $CD8^+$ T cells, Natural Killer (NK) cells, NK-T cells and B-cells were stained in the PBMC fraction

obtained after density gradient centrifugation. Peripheral blood granulocytes, eosinophils and neutrophils, were stained in the PMNL fraction. In some experiments, cultured monocyte purity was checked by staining with PerCP-conjugated mouse anti-human CD14 and anti-CD16 to differentiate between classical, intermediate and non-classical monocytes and, additionally, with anti-CD3 to estimate the fraction of contaminating T-lymphocytes. Cells were washed once in 5 ml PBS and spun down for 7 min at 400 x g. The pellet was resuspended in PBS, divided up at 3 million cells in 100 µl per FACS tube. All incubation steps were performed in the dark at room temperature followed by washing with 300 µl PBS^{--} /tube and centrifugation for 7 min at 400 x g. To differentiate between immune cells PBMCs were stained for 15 min at room temperature with cell-specific surface markers coupled to fluorescent dyes listed in **Table 5**.

hPGDS staining of human leukocytes. Macrophages (approximately 2 x 10^5/tube) were collected as described earlier, pre-fixed for 30 min in fixation buffer and used for hPGDS staining. Leukocytes previously stained with surface marker-specific antibodies, were fixed and permeablilized according to the manual using a Fixation/Permeablization Kit I from BD Bioscience. To block unspecific binding, macrophages were incubated with a 1:1 mixture of UV-block (BD Bioscience) and 5 % FCS in PBS and monocytes with FcX-receptor block (BioLegend) for 30 min. Subsequently, cells were stained for 30 min with 100 µl 1:100 dilution (5 µg/ml) of primary monoclonal mouse anti-human hPGDS antibody (Novus Bioscience) or the corresponding isotype control (mouse IgG) in permeabilization buffer as recommended, followed by incubation for 30 min with secondary antibody AF488-coupled rabbit anti-mouse IgG (1:5000). After two washing steps cells were resuspended in 250 µl fixation buffer.

Myeloid cell sorting from whole lung single cell suspension. Mice were anesthetized with an overdose of Ketamine/Xylazine before whole lungs were excised, inflated with 10 U/ml Dispase II (#04942078001, Roche, Basel, Switzerland) solution and trachea was closed by instillation of 500 µl of pre-warmed 1 % low-melt agarose solution (#A0701-25G, Sigma-Aldrich). Subsequently, lungs were placed into 50 ml falcon tubes containing 4 ml of Dispase II solution and incubated for 40 min at room temperature. Lung lobes were separated and dissociated with sterile scissors in DMEM media supplemented with DNase I (#LS002006, Worthington, Ohio, USA)

followed by for 8-10 min on an orbital shaker. Remaining tissue was gently loosened by pipetting, the solution was passed through a 100 µm cell strainer and washed with DMEM supplemented with 10 % FCS. Red blood cells were lysed (9 g NH_4Cl, 1 g $KHCO_3$, 37 mg EDTA in 100 ml Fresenius water) for 3 min on ice, lysis was stopped by adding excess PBS and cell suspension was passed through a 40 µm cell strainer. Total cell number and viability was obtained with Trypan blue using a Neubauer counting chamber. All centrifugation steps were performed using 400 x g for 5 min from now on. An average of 20-30 million cells were stained for each mouse, first with viability dye (1:1000 in PBS, Zombie aqua, BioLegend) for 20 min, washed with 300 µl PBS and spun down. Unspecific binding was blocked by incubation with mouse FcX block (1:100 in PBS with 2 % FCS, Biolegend) for 15 min at 4 °C. Cell populations were stained in 200 µl antibody cocktail as listed in **Table 7**. for 30 min at 4 °C, spun down and resuspended in complete medium (RPMI with 2.5 % FCS and 1 % Pen/Strep) at a cell density of 16 million/ml. Monocytes ($CD11b^+$, $Ly6G^-$, $Ly6C^+$), neutrophils ($CD11b^+$, $Ly6G^+$), macrophages ($CD11b^+$, $Ly6G^-$, $Ly6C^-$, $F4/80^+$) and mast cells ($CD11b^-$, $c\text{-}kit^+$) were sorted from viable $CD45^+$ cells with a FACSAria device (BD Biosciences, New Jersey, USA). Cells were spun down and resuspended in 250 µl RPMI medium supplemented with 2.5 % FCS and 1 % P/S, seeded into 48-well plates and incubated overnight in humidified atmosphere with 5 % CO_2 at 37 °C. A small aliquot of sorted cell populations were spun down using a cytospin3 device (Shandon, 600 rpm for 3 min) and stained with a standard Diff/Quik protocol (Hemacolor, Sigma-Aldrich) for morphological characterization.

hPGDS staining of murine myeloid subsets. A fraction of lung single cell suspensions obtained from vehicle or LPS-treated mice after population staining was divided up to FACS tubes (~ 250 000 cells/tube) for markers only (FMO), 2^{nd} only and hPGDS staining. Cells were fixed and permeabilized according to the manual using a Fixation/Permeablization Kit I from BD Bioscience and unspecific binding blocked by incubation with 50 µl of 1:100 dilution of mouse FcX block for 30 min. Subsequently, cells were stained with 50 µl of primary rabbit anti-hPGDS (LS Bio, 1:100 in perm/wash buffer) for 30 min at 4 °C. After washing, 100 µl Pacific blue-conjugated goat anti-rabbit secondary antibody (ThermoFisher Scientific, 1:500) was added for 30 min at 4 °C. hPGDS expression was determined with FACS Canto II and FlowJo Software by calculation of fold increase over FMO.

PGD_2 and PGE_2 detection in conditioned medium. For PGD_2 measurement, samples were defrosted quickly and mixed at a 1:1 ratio with the freshly prepared methyl-oximating reagent (0.1 g methoxylamine HCl, 0.82 g sodium acetate in 10 ml 1:10 solution of EtOH:H_2O) to generate a stable PGD_2-methoxime derivative. After vortexing, samples were heated at 60 °C for 30 min and stored at -20 °C until assaying. PGD_2-MOX ELISA was performed as stated in corresponding booklet including 2 non-specific binding wells (50 µl ELISA buffer + 50 µl MOX-medium), 2 maximum binding wells (B_0) and a PGD_2-MOX standard dilution assayed in duplicates ranging from 2.0 pg/ml to 250 pg/ml. The standards and the samples were diluted in MOX-medium (1:1 mixture of RPMI with 10 % FCS, 1 % P/S and methyl-oximating reagent) and assayed in duplicates at adequate dilutions. Additionally, methyl-oximated PGE_2, TBX_2 and medium containing supplements was tested to estimate non-specific binding. ELISA plates were incubated with samples, tracer and anti-serum at 4 °C overnight. Next day wells were washed 5 times with wash buffer using a microplate washer and subsequently incubated with 200 µl Ellman's reagent for 90 min at room temperature on a shaker in the dark and evaluated with a microplate spectrophotometer (BioRad) by measuring the absorbance at 410 nm. For detection of immunoreactive PGE_2 in conditioned medium a radioimmunoassay was used as described previously (272). Briefly, samples and standards (Sigma) were incubated with PGE_2 antiserum and [5,6,8,11,12,14,15(N)-3H]-PGE_2 (PerkinElmer, Germany) overnight at 4 °C. Unbound PGE_2 was removed by adding activated charcoal the next day followed by centrifugation at 4000 rpm for 15 min at 4 °C. Subsequently, supernatants were poured into scintillation tubes and scintillation cocktail (PerkinElmer) was added. Counts per minute were measured in a beta counter (HIDEX, Turku, Finland) and values were calculated in Sigma plot by employing a 4-parameter curve fit algorithm. IC_{50} of PGE_2 was 106.2 ± 10.6 pg/ml (n = 10) and detection limit, defined as 10 % inhibition of binding was at 11.2 ± 1.2 pg/ml.

Pierce BCA protein assay. Cell lysates from all wells with monocytes and macrophages for PGD_2 production were collected in 100 µl protein lysis buffer, in parallel with conditioned medium collection and stored at -70 °C. Lysates were thawed by vortexing at 4 °C for 30 min, spun down at 14 000 x rpm for 10 min and supernatant was transferred into a new tube. Protein content in these samples was determined by means of a BCA assay. A bovine serum albumin (BSA) standard

curve (0 - 1500 µg protein/ml) was prepared and assayed in duplicates. A 1:2 dilution of all samples was assayed in duplicates, while the ratio between working reagent and samples/standard was 1:20. The plate was incubated at 37 °C for 30 min and, subsequently, the absorbance at 562 nm was measured to determine protein concentration. Obtained mean values of protein content per well were used for normalization of PGD_2 values from the MOX-PGD_2 ELISA and PGE_2 RIA.

Determination of lipid mediators in conditioned medium with LC/MS. This analysis was performed at the Pharmazentrum Frankfurt/ZAFES, Institute of Clinical Pharmacology, Goethe University Frankfurt, Germany. Briefly, for the analysis of prostanoids in cell supernatants 230–285 µL of the samples (on ice water) were spiked with 20 µL of a solution of the isotopically labeled internal standards in ethanol (PGE_2-d4, PGD_2-d4, TXB_2-d4: 10 ng/mL). After addition of 20 µL pure ethanol and 100 µL of an aqueous EDTA solution (0.15 M), the sample was extracted twice using liquid-liquid extraction. For the extraction 600 µL of ethyl acetate were added and after mixing (1 min) and centrifugation (3 min at 20,000 x g, 4 °C) the supernatant was collected. The extraction was repeated and the supernatants were joined together before evaporation at 45 °C under a nitrogen stream. After reconstitution in 50 µL water:acetonitrile (8:2, v/v) containing 0.0025 % formic acid, samples were mixed, centrifuged (1 min at 20,000 x g) and transferred into vial inserts. The chromatographic separation was carried out using an Acquity UPLC BEH C18 column (2.1 x 100 mm, 1.7 µm, Waters Corporation, Milford Massachusetts, USA) under gradient conditions at 30 °C. Water and acetonitrile, both containing 0.0025% formic acid, were used as mobile phases and the run time was 13 min. The LC-MS/MS system consisted of a 1290 Infinity II HPLC pump and autosampler (G7120A + G7167B, Agilent Technologies, Santa Clara, California, USA) and of a hybrid triple quadrupole-ion trap mass spectrometer QTrap 6500+ (Sciex, Darmstadt, Germany) equipped with a Turbo-V-source operating in negative ESI mode. Analysis was done in MRM mode with a dwell time of 10 ms for all analytes. Injection volume was 10 µL. Data were acquired using Analyst Software V1.7.1 and quantified with MultiQuant Software V 3.0.3 (both Sciex, Darmstadt, Germany), using the internal standard method (isotope dilution mass spectrometry).

2.5 *In vivo* and *ex vivo* models

Animal housing. Three-month old BALB/c or C57BL/6j mice were used for indicated experiments. All animal care complied with national and international guidelines. Mice were housed under controlled conditions of temperature (21 ºC), air humidity (50 %) and a 12-hour light/dark cycle. Standard chow and water were provided *ad libitum*. Mice were randomly assigned before treatment.

LPS-induced lung inflammation model. Treatments in this mouse model were performed with the help of Katharina Jandl or Ilse Lanz. Acute pulmonary inflammation was induced in 3-month-old BALB/c mice (n = 5) by intranasal application of 1 mg LPS/kg body weight. For myeloid cell sort from whole lung single cell suspension, 3-month-old C57BL/6j mice (n = 6) were used. Previous LPS application mice were lightly anesthetized by intra peritoneal injection of 120 µl Ketamine/Xylazine (60 mg/kg body weight Ketasol, 6 mg/kg body weight Rompun in saline solution) solution. LPS solution was added dropwise to nostrils of mice to be inhaled. Broncho-alveolar fluid was collected 4 h after LPS application.

Ovalbumin-induced allergic airway inflammation. Treatments in this mouse model were conducted with the help of Robert Frei or Anna Theiler. Allergic lung inflammation was induced in 3-month old BALB/c mice (n = 5) by immunization with obalbumin (OVA). 10 µg of OVA adsorbed to $Al(OH)_3$ was injected i.p. on days 0 and 7. Mice were challenged by an OVA-aerosol in saline on days 14 and 16. Mononuclear alveolar cells were collected by broncho-alveolar lavage fluid on day 17.

Bleomycin-induced pulmonary fibrosis (chronic inflammation). Treatments in this mouse model were performed by Thomas Bärnthaler. Pulmonary fibrosis was caused as previously described (226). Briefly, 10 to 12-week-old C57BL/6j mice were anesthetized by intra peritoneal injection of Ketamine/Xylazine solution (75 mg/kg Ketasol, 7.5 mg/kg Rompun in saline) and bleomycin or vehicle (saline solution) was instilled intratracheally with a Hamilton syringe at a dose of 1.25 U/kg. Mice were monitored daily and sacrificed 21 days after bleomycin instillation.

Chicken chorioallantoic membrane (CAM) angiogenesis assay. The chicken CAM angiogenesis assay uses the chorioallantoic membrane, which is an extraembryonic membrane in the developing chick embryo underneath the eggshell. CAM is highly vascularized and serves as a respiratory organ. Deryugina et al. described in great detail how to perform the *ex ovo* CAM assay using collagen onplants (273). *Ex ovo* incubation of the eggs allows placing more than one onplant per egg and easy monitoring of the assay. Fertilized Lohman white chicken eggs were obtained (Schropper GmbH, A-2640 Gloggnitz – Aue) and at day 3 of incubation at 37 °C and 75 % relative humidity, the eggshell was carefully cut using a portable drill. The content of the egg was transferred to a sterile plastic weigh boat covered by a lid and incubated for additional 7 days. On day 10 the CAM is developed enough to carry collagen onplants and sustain angiogenesis. Double-gridded sandwiches were prepared using 3x3 mm nylon grids with 2x2 mm nylon grids on top, sterilized by UV-radiation prior to collagen mix addition. A mastermix for collagen onplants was prepared on ice containing 2 mg/ml collagen, which was divided up depending on groups tested and mixed with MDM-conditioned medium (minimum of 4 different donors) to reach the final volume. Subsequently, 30 µl of prepared collagen mixtures were added to nylon sandwiches and these were incubated for 1 h at 37 °C to facilitate collagen polymerization. For each experiment, n eggs with 6 onplants placed onto the CAM were used for different conditions. For representative images, 3 silicone rings per egg were placed onto the CAM and 20 µl of conditioned medium added. The chicken embryos were incubated for further 3 days and angiogenic properties of samples were evaluated on day 13 by counting positive panels showing small vessels that have grown into the nylon grid sandwich. Positive panels were counted by a blinded operator not familiar with tested substances. Images were taken from each silicone ring on day 13, resulting in 9 images from 3 different macrophage donors per condition.

2.6 Statistical analysis.

Data are shown as mean + or ± SEM for n observations, where n denotes independent experiments. Comparisons of groups were performed as appropriate with GraphPad Prism 8 software (La Jolla, CA, USA) using 1-way ANOVA followed by Tukey's or Sidak's *post hoc* test or 2-way ANOVA followed by Tukey's, Sidak's or Fisher's LSD *post hoc* test for independent or repeated measurements to determine the levels of significance for each group. The specific test

used for each graph is indicated in the figure legend. Outliers were removed after using ROUT or Grubb's test in GraphPad Prism (alpha = 0.2). Probability values of $P < 0.05$ were considered as statistically significant and are indicated in the figure legend.

3. Results

3.1. PART I: E-type 4 receptor mediates PGD_2-induced enhancement of pulmonary endothelial barrier function

Some parts of this section have been published in adapted form (2).

PGD_2 and DP1 agonist BW245c but not DP2 agonist DK-PGD_2 concentration-dependently enhanced human microvascular endothelial barrier. Our first aim was to evaluate the effect of PGD_2 and DP agonist stimulation on primary human microvascular endothelial cells from different origin. Kobayashi et al. showed that PGD_2 as well as DP1 agonist BW245c enhanced human dermal microvascular endothelial barrier *in vitro*, however, could only partially block this effect with DP1 antagonist BWA868c (68). We could reproduce their findings with PGD_2 and BW245c in primary human dermal microvascular endothelial cells, while DP2 agonist DK-PGD_2 had no effect (**Figure 7**A, B, C). In line with this, representative images for 5 independent experiments show that peripheral VE-cadherin staining increased upon PGD_2 and BW245c treatment (**Figure 7**D). To see whether this was a general microvascular effect caused by PGD_2 stimulation, we performed the same experiments with primary human pulmonary microvascular endothelial cells (HPMEC) and saw a similar pattern; however, the same concentration range resulted in lower maximal response in HPMEC (**Figure 7**E, F, G). In addition, peripheral VE-cadherin increased after stimulation with PGD_2 and BW245c also in pulmonary microvascular endothelial cells (**Figure 7**H).

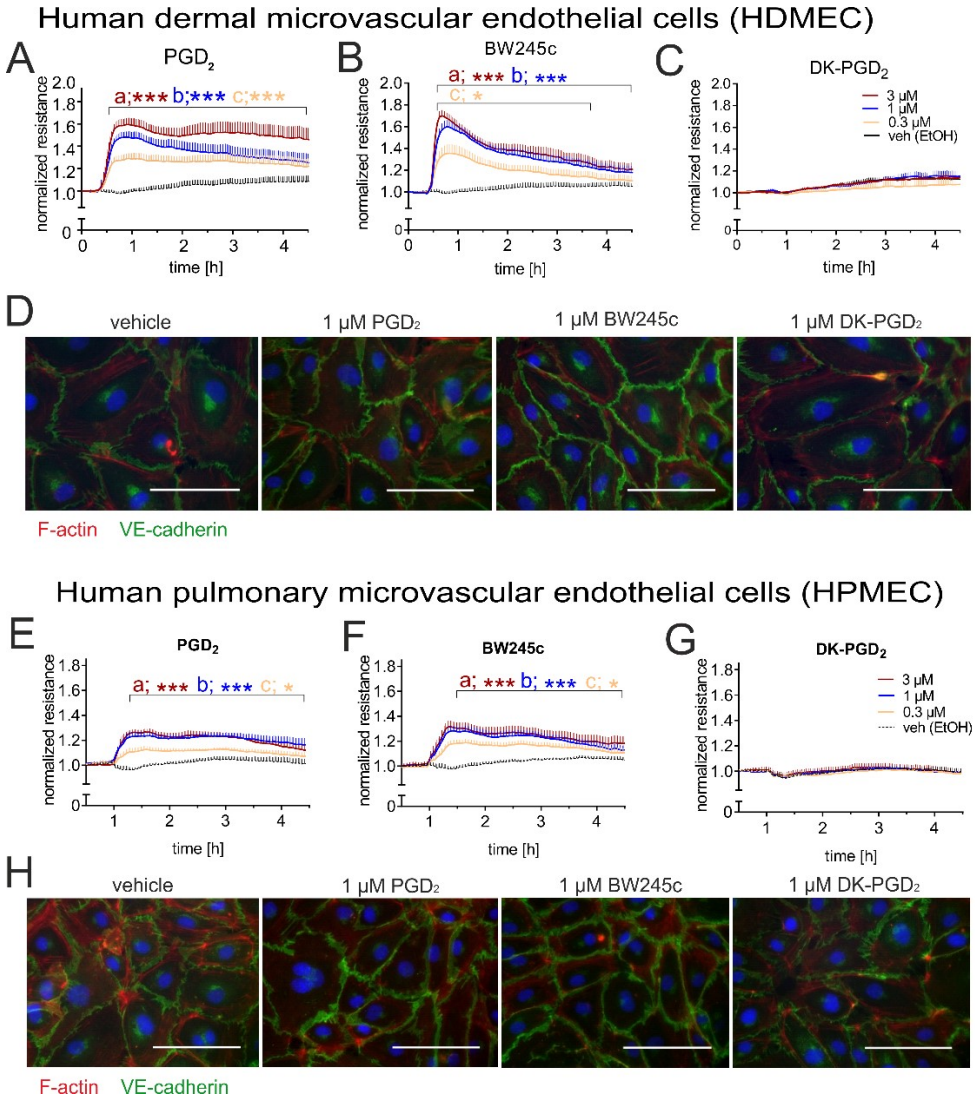

Figure 7. PGD_2 and DP1 agonist BW245c but not DP2 agonist DK-PGD_2 increase human microvascular endothelial barrier in a concentration-dependent manner. Human dermal (HDMEC) or pulmonary (HPMEC) microvascular endothelial cells were seeded onto 8W10E+ polycarbonate ECIS arrays and serum starved for 3 h. Changes in endothelial monolayer resistance, which is proportional to endothelial barrier function, were recorded in real time with an ECIS® Z-Theta device and the mean of duplicate measurements was plotted. In HPMECs (A) PGD_2 as well as (B) DP1 agonist BW245c increased the resistance of endothelial monolayers. (C) Stimulation with DP2 agonist DK-PGD_2 did not change the resistance. (E) PGD_2 and (F) BW245c, but not (G) DK-PGD_2, also increased the resistance in HPMEC. Immunofluorescent staining of VE-cadherin and F-actin in (D) HDMEC and (H) HPMEC, respectively, revealed a stronger VE-cadherin barrier in PGD_2 and BW245c-treated cells. Images are representative for 5 independent experiments (scale bar 100 µm). Data are shown as mean + SEM, n = 5. Two-way ANOVA for repeated measurements with Tukey's *post hoc* test, * $p<0.05$ and *** $p<0.001$, (a) veh (EtOH) vs. 3 µM agonist, (b) veh (EtOH) vs. 1 µM agonist, (c) veh (EtOH) vs. 0.3 µM agonist. Figure adapted from (2).

PGD_2 and DP1 agonist BW245c protect human microvascular endothelial cell barrier. During inflammation, exposure to barrier-disruptive agents i.e. thrombin, bacterial lipopolysaccharide or histamine facilitates extravasation of leukocytes and oedema formation. Since PGD_2 and BW245c improved microvascular endothelial barrier function in the previous experiment, we aimed to investigate whether pre-treatment of microvascular endothelial cells with PGD_2 and BW245c protected against thrombin-induced barrier disruption.

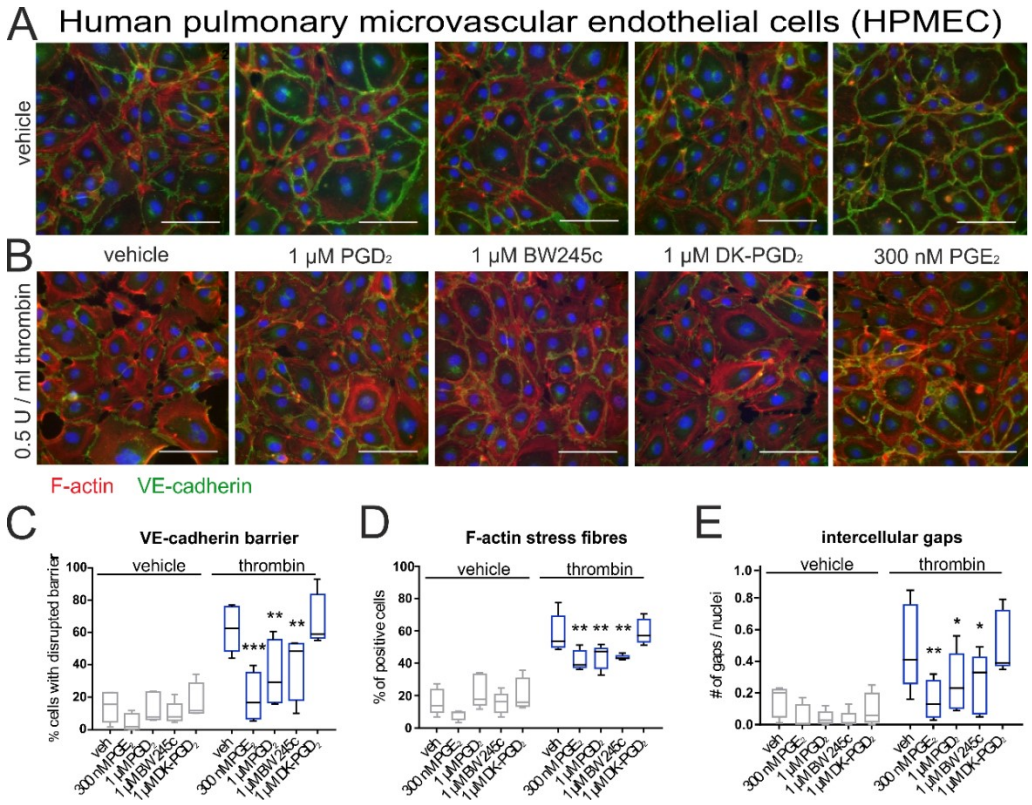

Figure 8. PGD_2 and DP_1 agonist BW245c but not DP2 agonist DK-PGD_2 protect HPMEC against thrombin-induced barrier disruption. Representative images for 5 independent experiments of confluent HPMEC stimulated with vehicle (EtOH), 1 µM PGD_2, BW245c, DK-PGD_2 or 300 nM PGE_2 for 15 min followed by incubation with (A) vehicle (a.d.) or (B) 0.5 U/ml thrombin for 15 min (scale bar 100 µm). Extent of barrier disruption was evaluated by quantifying (C) the percentage of cells with disrupted peripheral VE-cadherin staining, (D) the percentage of cells with actin stress fibres and (E) the ratio of intercellular gaps per nuclei. Data are displayed as box and whisker plot, n = 5. Two-way ANOVA with Fisher's LSD *post hoc* test, * $p<0.05$, ** $p<0.01$, *** $p<0.001$ difference between veh/thrombin vs. agonist. Figure adapted from (2).

In intact microvessels, F-actin filaments align at cellular periphery and inter-endothelial VE-cadherin forms a tight barrier as can be seen in vehicle-treated HPMEC (**Figure 8**A). Thrombin as a strong inducer of hyper-permeability caused the formation of F-actin stress fibres, cellular contraction and inter-endothelial gap formation as well as dissociation of VE-cadherin barrier (**Figure 8**B). Notably, pre-treatment of HPMEC with 1 µM PGD_2 or BW245c significantly protected the monolayer against gap formation and reduced the percentage of cells with disrupted VE-cadherin barrier or actin stress fibres (**Figure 8**C to D). DK-PGD_2 conferred no protective effect. Similar results could be obtained with HDMEC (**Figure 9**).

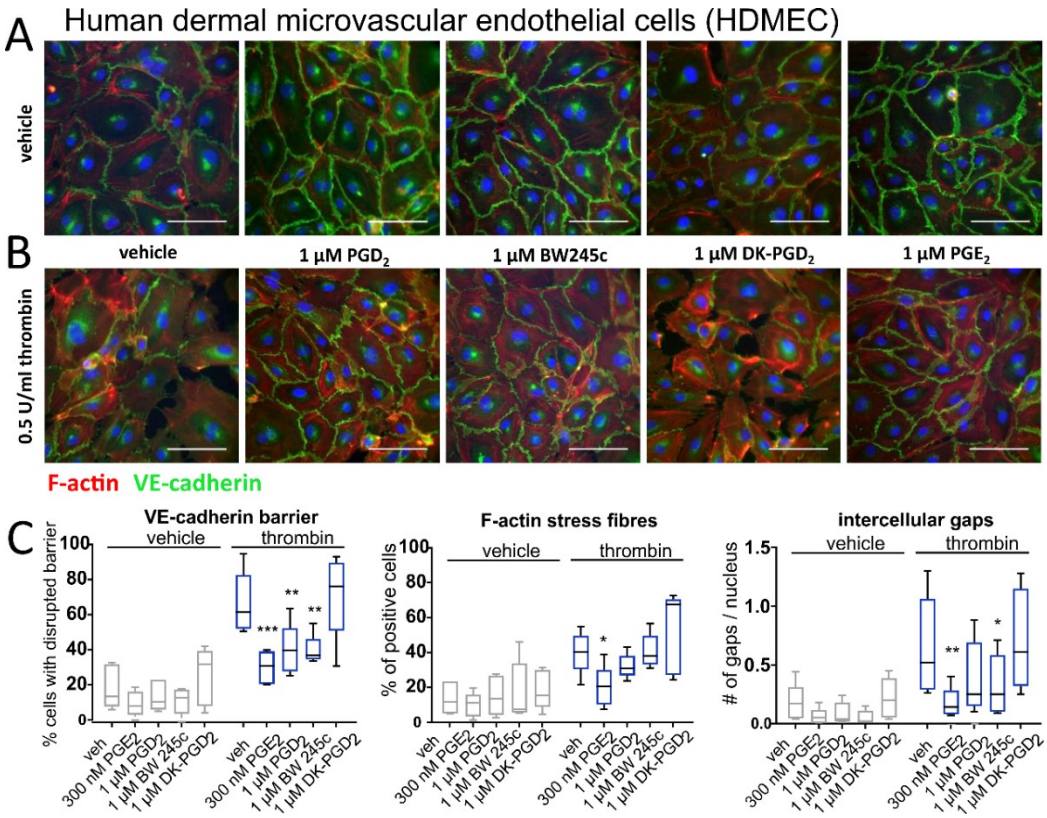

Figure 9. PGD_2 and DP_1 agonist BW245c but not DP2 agonist DK-PGD_2 protect HDMEC against thrombin-induced barrier disruption. Confluent HDMEC were stimulated with vehicle (EtOH), 1 µM PGD_2, BW245c, DK-PGD_2 or 300 nM PGE_2 for 15 min followed by incubation with (A) vehicle (a.d.) or (B) 0.5 U/ml thrombin for 15 min (scale bar 100 µm). Extent of barrier disruption was evaluated by quantifying (C) the percentage of cells with disrupted peripheral VE-cadherin staining, (D) the percentage of cells with actin stress fibres and (E) the ratio of intercellular gaps per nuclei. Data are displayed as box and whisker plot, n = 5. Two-way ANOVA with Fisher's LSD *post hoc* test, * $p<0.05$, ** $p<0.01$, *** $p<0.001$ difference between veh/thrombin vs. agonist. Images published in (2).

DP1 antagonism but not DP2 antagonism partially reduces PGD_2-induced barrier enhancement. The DP1 agonist mirrored all PGD_2 barrier effects, hence, we tested whether DP1 receptor activation was in fact responsible for the observed barrier fortification using a DP1 antagonist. Interestingly, blockade of DP1 receptor with MK0524 had no effect and BWA868c, another DP1 antagonist, only partially reduced the PGD_2-induced increase in HPMEC resistance (**Figure 10**A and B). As expected, DP2 blockade with Cay10471 did not affect PGD_2-induced barrier enhancement at all (**Figure 10**C). Under certain conditions, DP1-DP2 interaction has been shown to influence downstream signalling (274); however, synergistic blockade of DP1 and DP2 receptors on HPMEC did not reverse barrier increase either (**Figure 10**D). DP1 or DP2 antagonism had similar effects on HDMEC (**Figure 10**E and F).

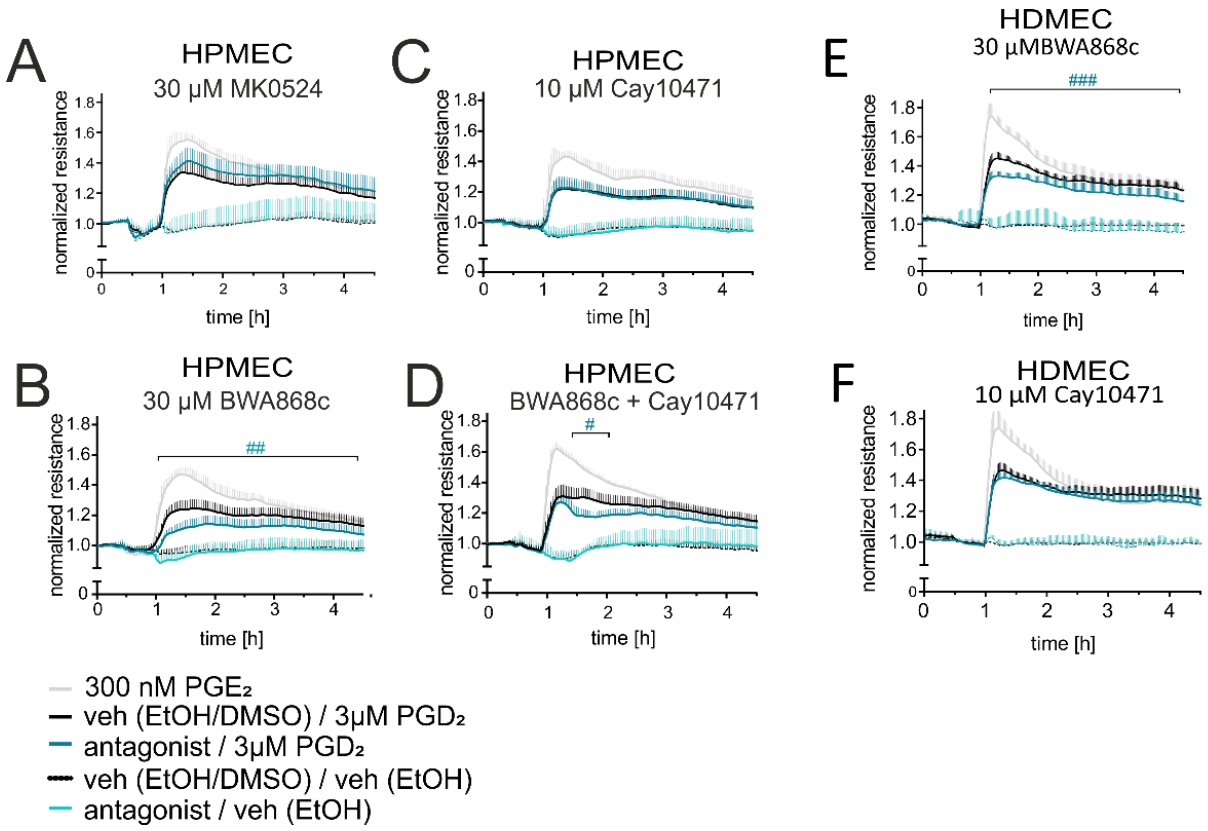

Figure 10. DP1 antagonist BWA886c but not DP2 antagonist Cay10471 partially reverses the PGD_2-induced barrier increase. (A) Pre-treatment with 30 µM of the DP1 antagonist MK0524 for 30 min did not affect PGD_2-induced increase in resistance. (B) 30 µM of the DP1 antagonist BWA868c partially, but significantly diminished the PGD_2-induced barrier increase. (C) 10 µM of the DP2 antagonist Cay10471 as well as (D) a combination of BWA868c

and Cay10471 had only minor effects. In HDMEC, similar effects could be observed for (E) 30 µM BWA868c and (F) 10 µM Cay10471. Data are displayed as mean + SEM, n = 5, two-way ANOVA for repeated measurements with Tukey's *post hoc* test, # $p<0.05$, ## $p<0.01$ difference between veh (DMSO) / 3 µM PGD_2 vs. antagonist / 3 µM PGD_2. Part of the Figure adapted from (2).

PGD_2 does not enhance HPMEC barrier function through activation of PPARγ, TP receptors or cyclooxygenases. It is known that PGD_2 is able to bind to PPARγ receptors, while PPARγ is important for continuous endothelial barrier function (83,87,105). Pre-treatment with PPAR-γ antagonist T0070907 had a considerable effect on endothelial barrier; however, blockade of PPARγ signalling with 30 µM T0070907 did not affect the delta increase of endothelial electrical resistance after PGD_2 stimulation (**Figure 11**A). Pre-treatment with 1 µM SQ 29,548, a TP receptor antagonist, likewise did not prevent the PGD_2-induced microvascular endothelial cell resistance (**Figure 11**B). Under some circumstances, PGD_2 may also relay its action by inducing other factors that cause autocrine stimulation of target cells i.e. lipid mediators; however, inhibition of cyclooxygenase-1/2 with 1 µM diclofenac did not impact the barrier response to PGD_2 (**Figure 11**C).

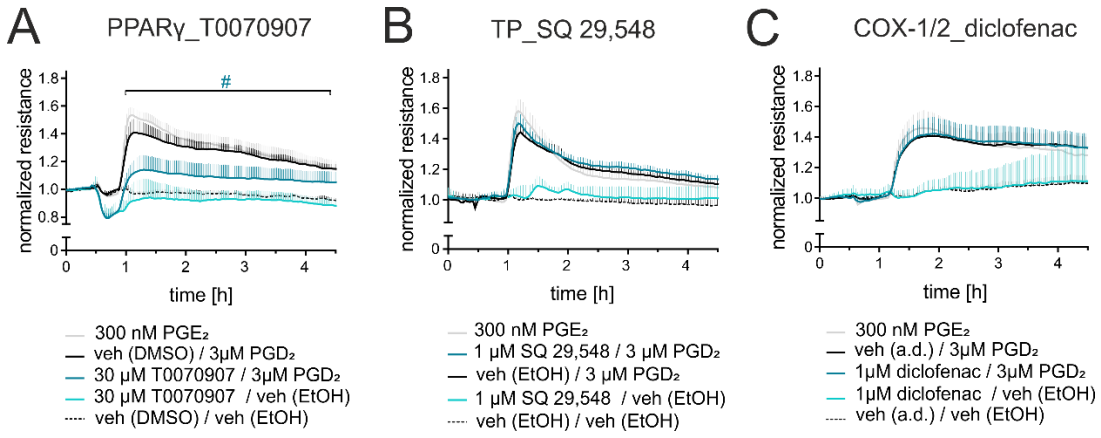

Figure 11. PGD_2 partially enhances microvascular barrier function through activation of PPARγ, but not via TP receptors and cyclooxygenases in HPMEC. (A) Pre-treatment with PPARγ antagonist T0070907 caused a transient drop of endothelial electrical resistance, and attenuated the PGD_2-induced barrier enhancement, while blockade of (B) TP receptors with 1 µM SQ 29,548 or (C) cyclooxygenase-1/2 with 1 µM diclofenac had no effect. Data are shown as mean + SEM, A and C: n = 5, B: n = 4, two-way ANOVA for repeated measurements with Tukey's post hoc test # $p<0.05$ difference between veh (DMSO) / 3 µM PGD_2 vs. antagonist / 3 µM PGD_2. Figure adapted from (2).

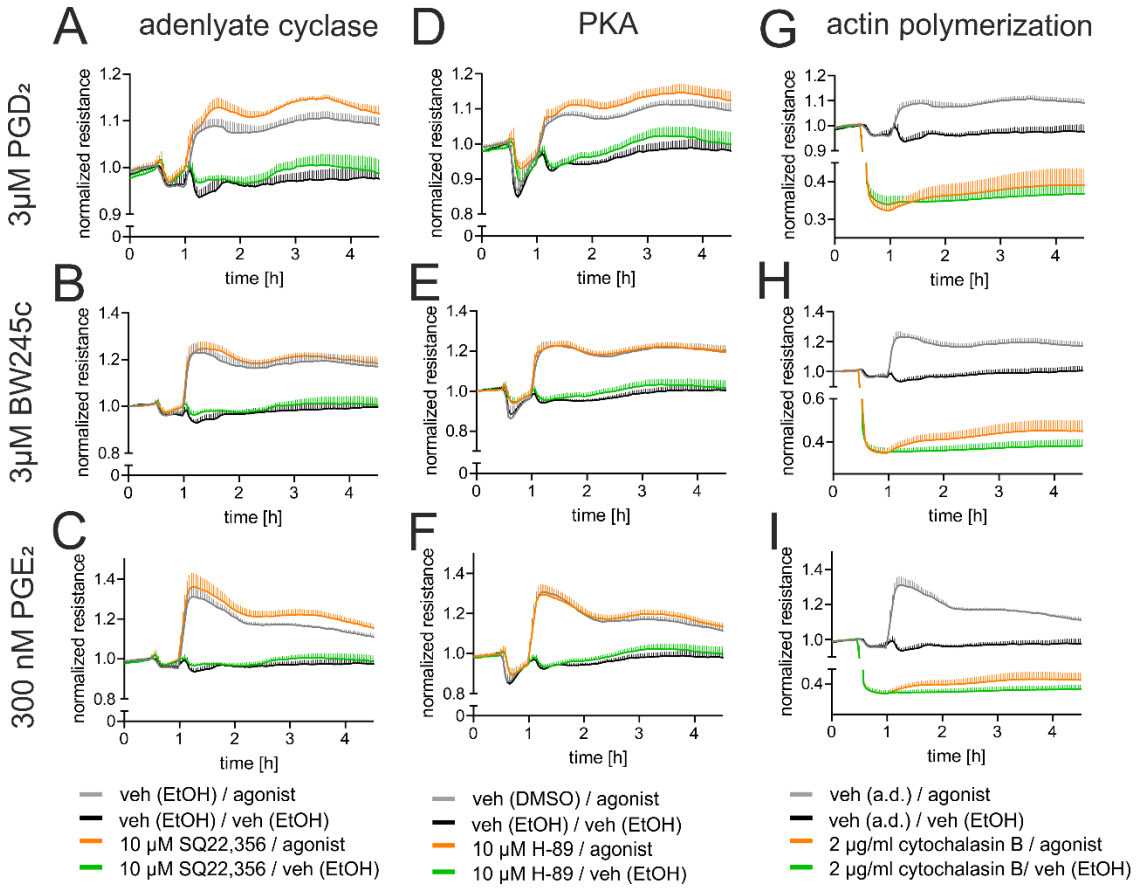

Figure 12. Inhibition of adenylate cyclase and PKA does not prevent PGD_2 or BW245c-induced HPMEC barrier enhancement. Pre-treatment of HPMEC with 10 µM adenylate cyclase inhibitor SQ 22,356 or PKA inhibitor H-89 did not ablate barrier enhancement by (A,D) PGD_2, (B,E) DP1 agonist BW245c or (C,F) PGE_2. Impairment of actin polymerization with 2 mg/ml cytochalasin B affected monolayer resistance but also reduced the extent of barrier enhancement by all agonists: (G) PGD_2, (H) BW245c and (I) PGE_2. Data are shown as mean + SEM, n = 5. Figure adapted from (2).

Inhibition of adenylate cyclase and PKA does not ablate PGD_2 or BW245c-induced HPMEC barrier enhancement. In a previous publication our group could show that PGE_2-EP4 mediated barrier enhancement is independent from cAMP/PKA but is reduced if actin polymerization is impaired (100). In contrast, Kobayashi et al. proposed that DP1-dependent barrier enhancement is dependent on cAMP/PKA (68). Therefore, we set out to study whether adenylate cyclase and PKA are involved in PGD_2 and BW245c-induced signalling in HPMEC. Surprisingly, we found that pre-treatment with 10 µM SQ 22,356, an adenylate cyclase inhibitor, or 10 µM H-89, an PKA inhibitor, did not significantly reverse the reactions to PGD_2 (**Figure**

12A,D) or BW245c (**Figure 12**B,E), very similar to PGE_2 (**Figure 12**C,F). Notably, pre-treatment with actin-depolymerizing agent cytochalasin B tremendously reduced the observed effects by PGD_2 (**Figure 12**G), BW245c (**Figure 12**H) and PGE_2 (**Figure 12**I). Similarly, pre-treatment with PLC inhibitor U-73112 significantly affected monolayer integrity, while preventing barrier enhancement by PGE_2, PGD_2 and BW245c (**Figure 13**A-C). Depletion of Ca^{2+} by EDTA caused a drop in endothelial resistance, while agonist treatment sped up resistance recovery rather than being affected by the previous Ca^{2+} depletion (**Figure 13**D-F). These observations were unexpected and raised the question, whether the DP1 receptor was not involved in PGD_2 induced HPMEC barrier improvement at all.

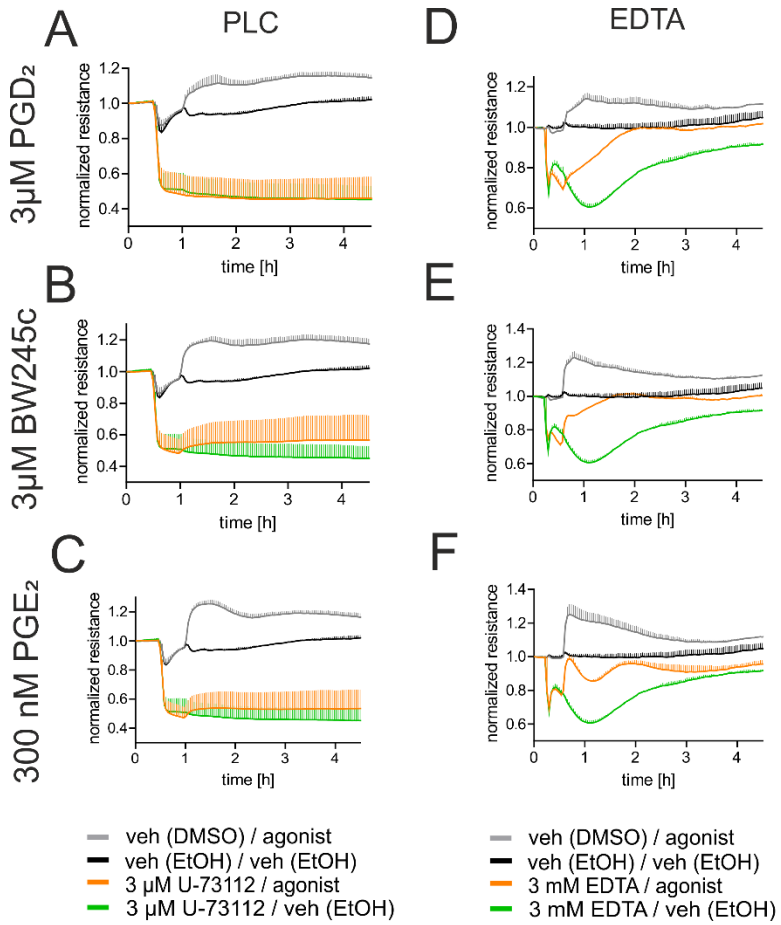

Figure 13. Investigation of phospholipase C and Ca^{2+} as potential mediators of PG-mediated barrier enhancement. Pre-treatment of HPMEC with 3 µM of PLC inhibitor U-73112 significantly affected endothelial resistance but also reduced (A) PGD_2, (B) BW245c and (C) PGE_2 elicited effects (n = 3). Pre-treatment with 3 mM of Ca^{2+} chelator EDTA also affected monolayer integrity, but stimulation with (D) PGD_2, (E) BW245c or (F) PGE_2 sped up recovery of endothelial resistance rather than diminishing the response (n = 2). Data are shown as mean + SEM.

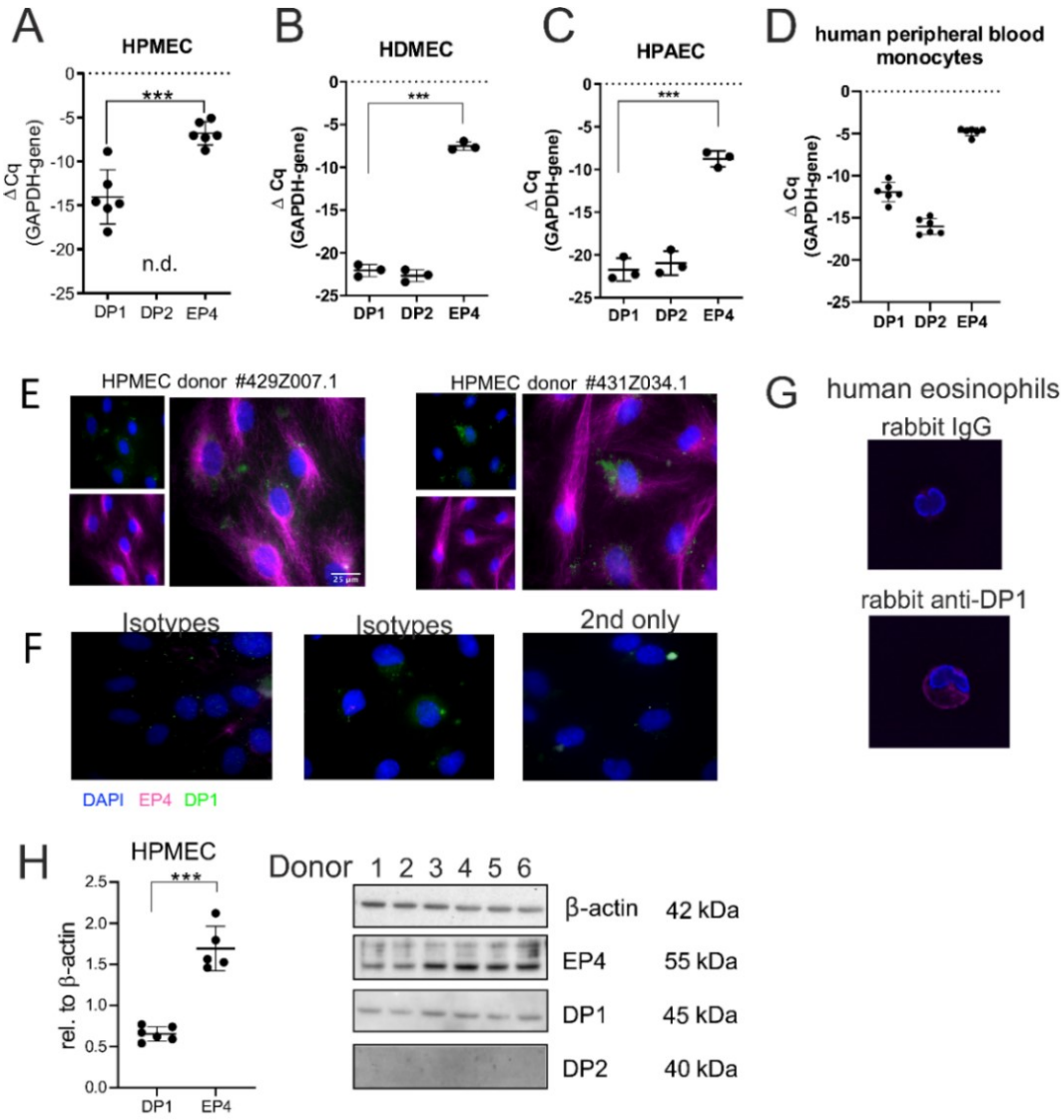

Figure 14. Human endothelial cells express very low levels of DP1 and DP2 but higher levels of EP4 receptor mRNA and protein. (A) Receptor mRNA expression in HPMEC was quantified by real time PCR (n = 6). EP4 receptor mRNA levels were significantly higher than DP1 mRNA levels, DP2 mRNA could not be detected. Similar levels of receptor mRNA expression were found in unstimulated (B) HDMEC (n = 3) and (C) HPAEC (n = 3). Here, DP1 mRNA was lower in comparison to HPMEC but DP2 mRNA could be detected. (D) Functionality of DP1 and DP2 primers was confirmed using human peripheral blood monocytes (n = 6). (E) Immunofluorescence staining (60x magnification) showed high expression levels of EP4 receptor throughout the cell in HPMEC, while DP1 receptor could hardly be seen (images from 2 different donors; representative of 3 independent experiments). (F) Staining controls (EP4/mouse and DP1/rabbit IgG and 2nd antibody-only) on HPMEC (representative of 3 independent experiments). (G) Additionally, functionality of DP1 antibody was validated using human eosinophils (representative for 3 donors, staining performed in independent experiments). (H) Potential differences in DP1, DP2 and EP4 receptor

protein levels were determined by Western blotting. Data are shown as mean ± SD, one data point represents one experiment or donor, one-way ANOVA with Tukey's *post hoc* test (qPCR) or Student's t-test (Western blot), n.d. – non detectable, ***p<0.001. Figure adapted from (2).

Human endothelial cells express very low basal levels of DP1 but much higher EP4 receptor mRNA and protein. To confirm that HPMEC expressed DP receptors, we first evaluated DP1, DP2 and EP4 receptor levels on mRNA level. Interestingly, human pulmonary and dermal microvascular cells as well as macrovascular pulmonary artery endothelial cells expressed very low basal levels of DP1 and DP2 mRNA (**Figure 14**A-C). To ensure functionality of primer pairs, DP1, DP2 and EP4 receptor mRNA expression levels were also determined in human monocytes, which are known to express all of these GPCR (**Figure 14**D). Interestingly, all cell types expressed significantly higher levels of EP4 receptor mRNA, as detection threshold (Cq) was reached several cycles earlier indicating much higher expression levels. Further, immunofluorescent staining of EP4 and DP1 receptors on HPMEC as well as Western blotting showed similar differences in expression levels also on protein level (**Figure 14**E and H, respectively). Representative images of isotype and 2nd only staining controls are shown in **Figure 14**F. Functionality of rabbit anti-DP1 receptor antibody was confirmed using human eosinophils (**Figure 14**G). This dataset indicates that EP4 receptors are of much higher importance for endothelial cell function compared to DP receptors.

Blockade of EP4 receptors abrogates PGD_2 and BW245c barrier enhancement and protection against thrombin-induced barrier disruption. Previously we described that PGE_2-EP4 activation has a strong barrier protective effect in HPMEC (100). Notably, PGE_2 was about 10x more potent than PGD_2 and BW245c in potentiating endothelial cell resistance but spatial-temporal responses were quite comparable – a high peak shortly after addition of stimulating agent followed by a slightly lower but sustained increase in endothelial resistance for several hours. With the knowledge that EP4 receptors are responsible for PGE_2-induced barrier enhancement and the much higher expression levels of EP4 as compared to DP1 receptors in human endothelial cells, as well as the independence from cAMP/PKA signalling of the observed effects, we decided to analyse the involvement of the PGE_2 receptor EP4 in the effects we have seen for PGD_2 and BW245c.

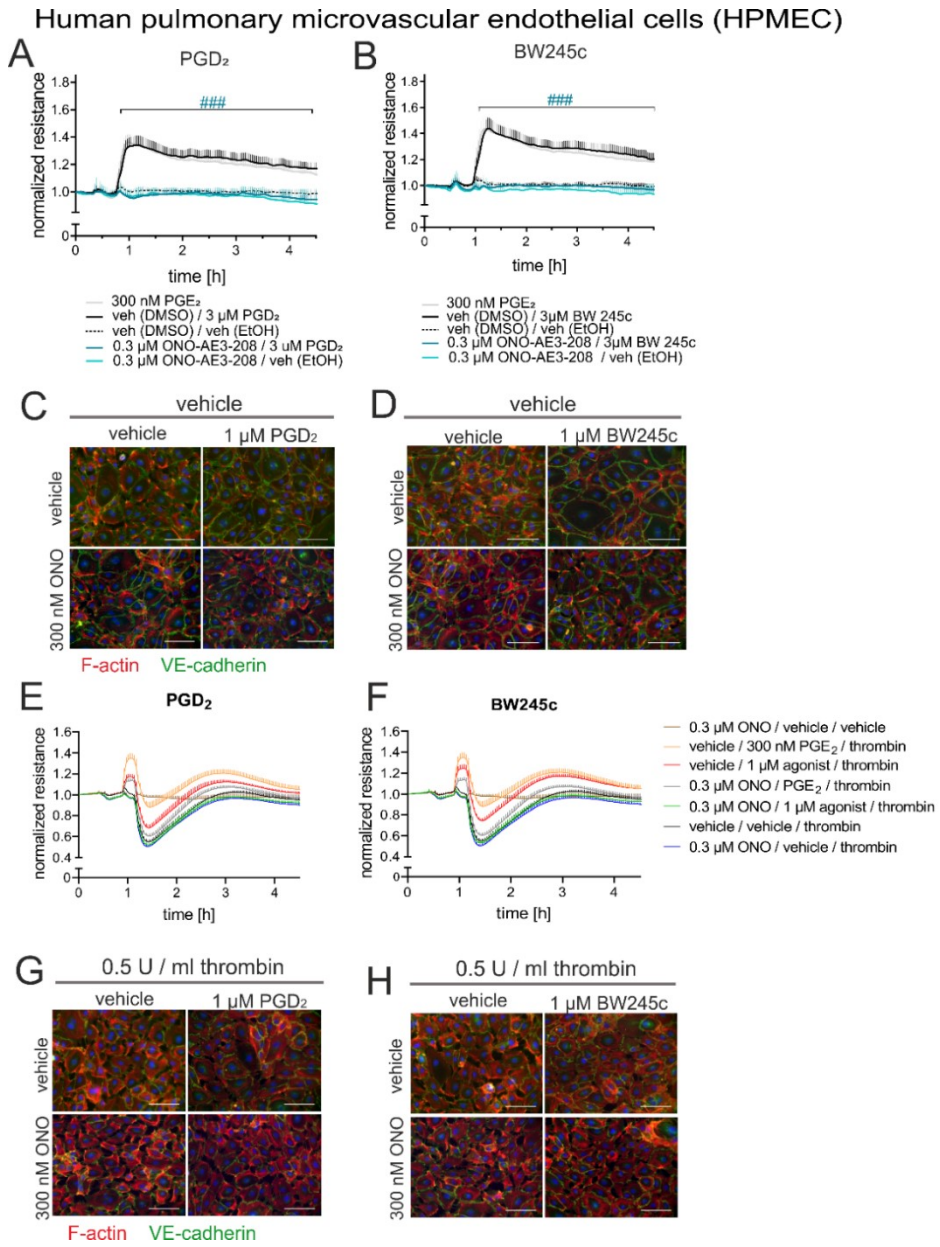

Figure 15. PGD_2 and BW245c barrier enhancement and protection against thrombin-induced barrier disruption is abolished after blockade EP4 receptors. Pre-treatment of HPMEC with 300 nM of ONO-AE3-208 (ONO; EP4 antagonist) for 30 min completely abolishes the barrier increase induced by 3 µM of (A) PGD_2 and (B) BW245c. VE-cadherin and F-actin staining revealed that pre-treatment with the EP4 antagonist before (C) PGD_2 or (D) BW245c stimulation inhibits VE-cadherin expression. Pre-treatment with 300 nM of ONO-AE3-208 also prevented the barrier protection against thrombin 1 µM induced by 3 µM of (E) PGD_2 and (F) BW245c. Immunofluorescent staining of VE-cadherin and F-actin showed that EP4 antagonism impairs increased VE-cadherin staining at cell periphery triggered by (G) PGD_2 or (H) BW245c in HPMEC (representative images for 5 independent experiments are shown, scale bar 100 µm). Data are displayed as mean + SEM, n = 5 - 6, two-way ANOVA for repeated measurements with Tukey's

post hoc test, ### p<0.001 difference between veh (DMSO) / 3 µM PGD_2 or BW245c vs. antagonist / 3 µM PGD_2 or BW245c. (ONO = ONO-AE3-208). Figure adapted from (2).

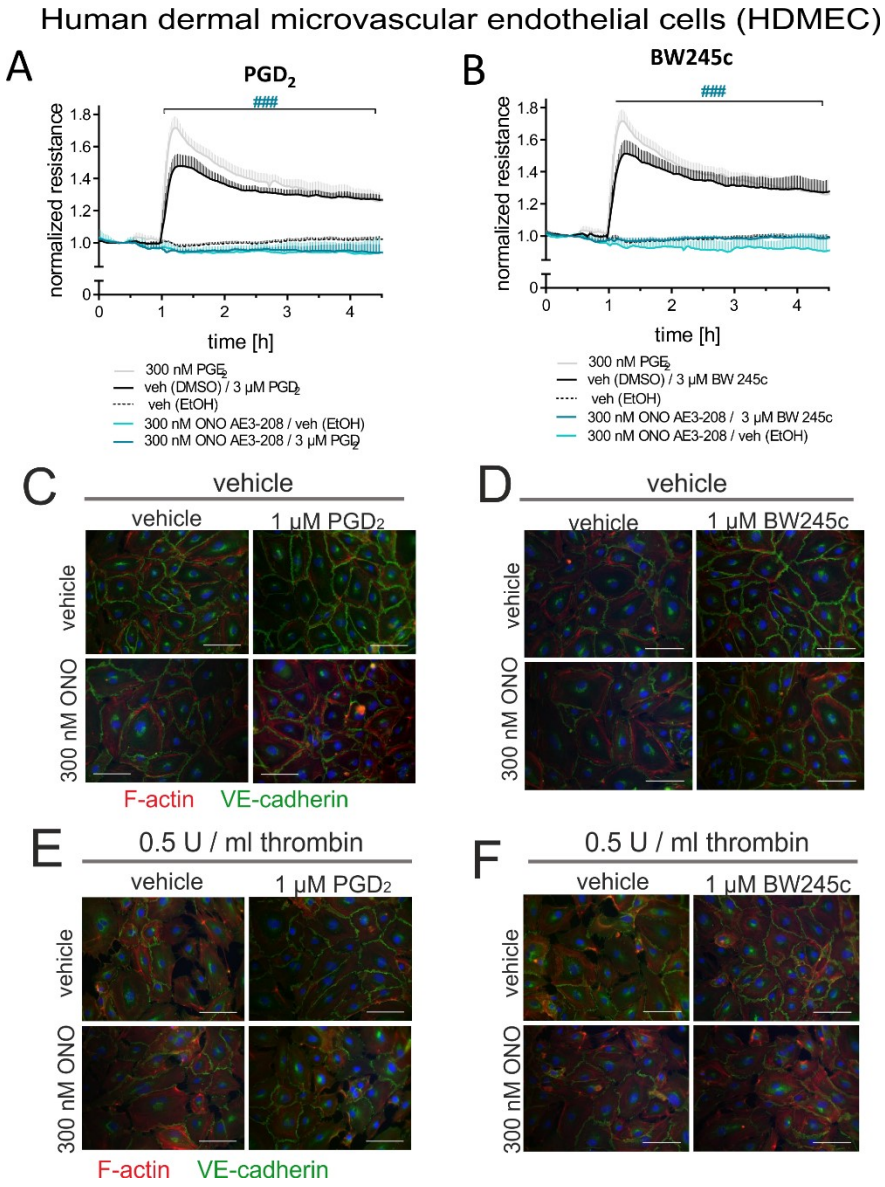

Figure 16. EP4 antagonism prevents PGD_2 and BW245c barrier enhancement and protection against thrombin-induced barrier disruption in HDMEC. Pre-treatment of HDMEC with 300 nM ONO-AE3-208 (ONO; EP4 antagonist) for 30 min completely abolished (A) PGD_2 as well as (B) BW245c-induced barrier increase. VE-Cadherin and F-actin staining revealed that pre-treatment with the EP4 antagonist before (C) PGD_2 or (D) BW245c stimulation inhibits enhancement of VE-Cadherin staining. In the thrombin barrier disruption assay, EP4 antagonism abolished the barrier protective effect by (E) PGD_2 or (F) BW245c in HDMEC (representative images of 5 independent experiments are shown, scale bar 100 µm). Data are displayed as mean + SEM, n = 5, two-way ANOVA for repeated measurements with Tukey's post hoc test, # p<0.05, ## p<0.01, ### p<0.001 difference between veh (DMSO) / 3 µM PGD_2 or BW245c vs. 300 nM ONO-AE3-208 / 3 µM PGD_2 or BW245c.

Indeed, blockade of EP4 receptors with 300 nM ONO-AE3-208, a specific EP4 receptor antagonist, completely abolished PGD_2 as well as BW245c-induced barrier stimulation in HPMEC (**Figure 15**A and B) and in HDMEC (**Figure 16**A and B). In addition to electrical resistance, ONO-AE3-208 diminished the barrier protective effect against thrombin (representative images are shown in **Figure 15** and **Figure 16**). In vehicle pre-treated cells, there was an increase in VE-cadherin staining at cell periphery after PGD_2 (**Figure 15**C) or BW245c (**Figure 15**D) treatment, however, if the cells were pre-treated with 300 nM ONO-AE3-208 this effect was not seen. Likewise, if EP4 receptors were blocked before stimulation with PGD_2 (**Figure 15**E) or BW245c (**Figure 15**F) there was no protection against thrombin-induced barrier disruption as there was no difference between inter-cellular gap formation and the proportion of cells with disrupted barrier. To further confirm this result, we used another EP4 antagonist, GW627368X, which blunted, but not completely abolished PGD_2 as well as BW245c-induced barrier enhancement (**Figure 17**). Notably, ONO-AE3-208 did not attenuate or sphingosine-1-phosphate induced barrier enhancement or the PGD_2-induced inhibition of platelet aggregation, which is mediated through DP1 (**Figure 18**A-D and E, respectively). This highlights the specificity of this antagonist.

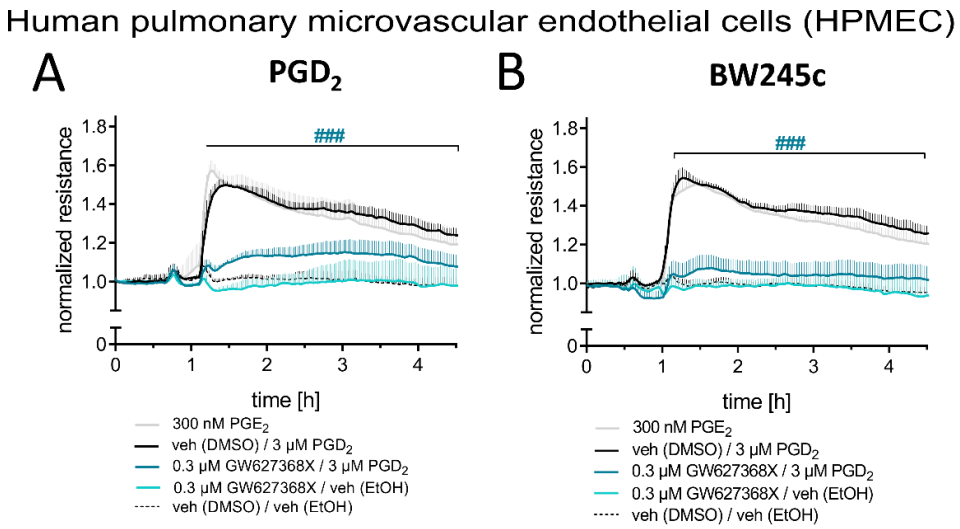

Figure 17. EP4 antagonist GW627368X strongly attenuates the barrier-protective effect of PGD_2 and BW245c. Pre-treatment of HPMEC with 300 nM GW6227368X for 30 min significantly reduced (A) PGD_2- as well as (B) BW245c-induced barrier increase. Data are displayed as mean + SEM, n = 5, two-way ANOVA for repeated measurements with Tukey's post hoc test, #p<0.05, #p0.01, ###p<0.001 difference between veh (DMSO)/ 3 µM PGD_2 or BW245c vs. 300 nM GW627368X/3 µM PGD_2 or BW245c. Figure adapted from (2).

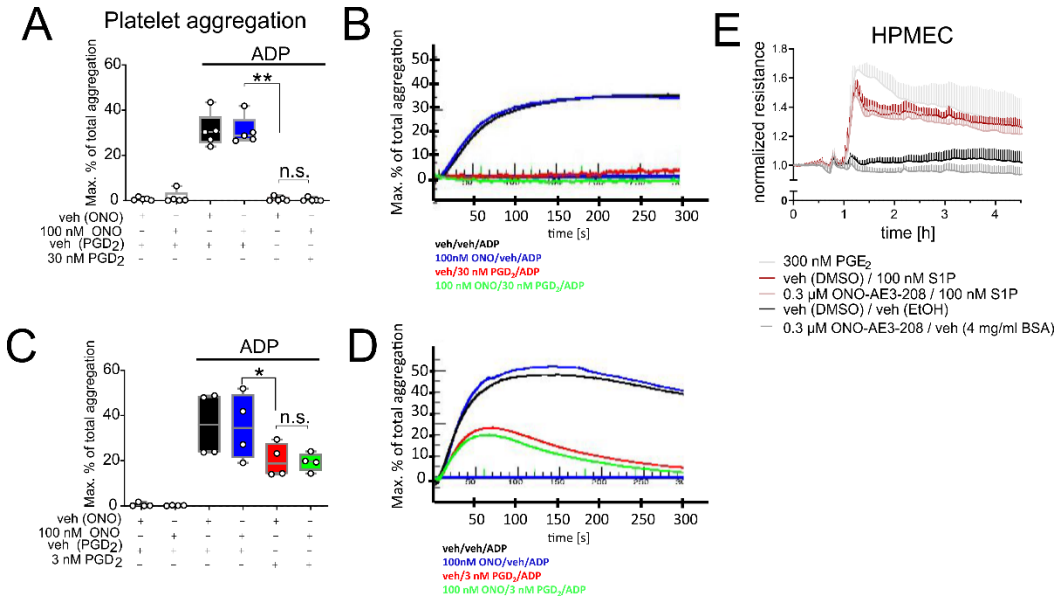

Figure 18. ONO-AE3-208 does not affect PGD_2-induced inhibition of platelet aggregation or S1P-induced barrier enhancement. Specificity of EP4 antagonist ONO-AE3-208 was confirmed using a platelet aggregation assay. (J) 30 nM or (K) 3 nM PGD_2-induced inhibition of platelet aggregation was not affected by pre-treatment with 100 nM ONO-AE3-208 (n = 4-5). On the right side, a representative graph from one donor is showing the aggregatory time course. (L) Pre-treatment of HPMEC with 0.3 µM ONO-AE3-208 for 30 min did not affect subsequent sphingosine-1-phosphate- (S1P) induced barrier enhancement (n = 4). Data are shown as mean + SEM or box and whisker plot, n numbers are indicated, platelet aggregation: one-way ANOVA for repeated measurements with Tukey's *post hoc* test. (ONO = ONO-AE3-208). Figure adapted from (2).

Transient EP4 receptor knock-down in HPMECs diminishes barrier enhancement by PGD_2 and BW245c. To rule out any non-specific effects of the EP4 antagonist, our next step was to knock-down the EP4 receptor in primary HPMEC using a siRNA approach already described before (99). HPMEC were incubated with transfection medium only, Lipofectamine only (mock-transfected), non-targeting control siRNA and EP4-targeting siRNA for 48 h and subsequently detached to be used for ECIS experiments or for transfection analysis with qPCR. EP4 knock-down completely abolished the PGD_2 and BW245c effect (**Figure 19**A and B, respectively). Transfection itself affected endothelial cell integrity to a certain extent as could be seen in control siRNA-transfected HPMEC; however, monolayer integrity was not affected.

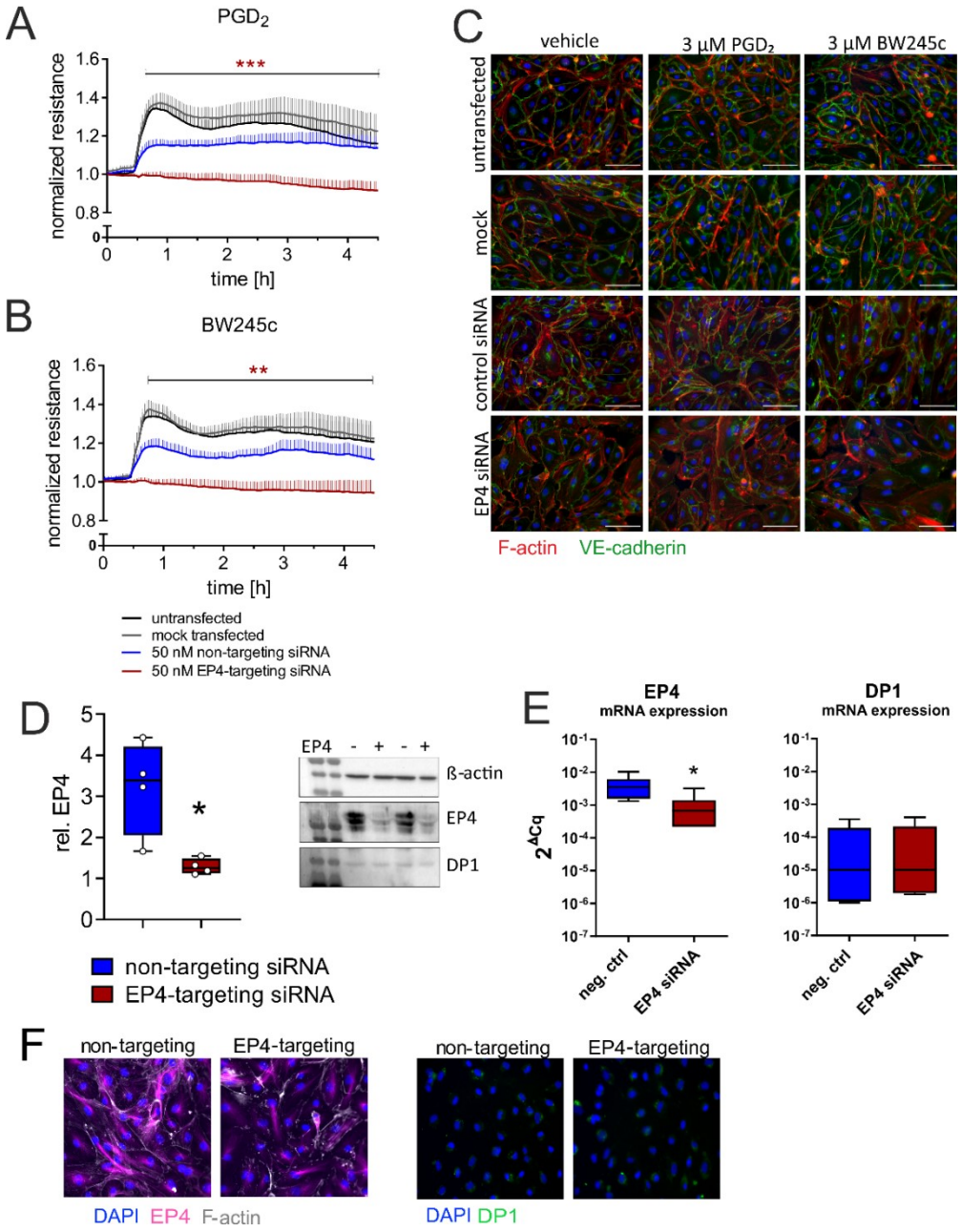

Figure 19. Transient knock-down of EP4 receptors abolished the PGD_2 and BW245c-induced HPMEC barrier enhancement. HPMECs were incubated for 48 h with transfection medium only, Lipofectamin (mock transfected), non-targeting control siRNA or PTGER4-targeting siRNA (EP4-targeting siRNA) and subsequently seeded onto 8W10E+ polycarbonate ECIS arrays for resistance measurements. EP4 knock-down completely prevented (A) PGD_2- and (B) BW245c-induced barrier enhancement. (C) VE-Cadherin and F-actin staining showed that transfection with EP4-targeting siRNA caused stress fibre formation in HPMEC, without compromising the cell monolayer, while the increase in VE-cadherin at cell periphery was attenuated after stimulation with PGD_2 and BW245c. Representative

images for 3 independent experiments are shown. EP4 knock-down efficiency was evaluated by (D) Western blotting (n = 4), (E) quantitative RT-PCR (n = 6) and (F) immunofluorescent staining of EP4 receptor and DP1 receptor as control (representative of 3 independent experiments). Data are shown as mean + SEM, ECIS experiments: two-way ANOVA for repeated measurements with Tukey's *post hoc* test or (D and E) Student's t-test, *p<0.05, **p<0.01, ***p<0.001 difference between control siRNA vs. EP4 siRNA-transfected cells. Figure adapted from (2).

Additionally, VE-cadherin and F-actin staining after transfection showed that reduction of EP4 receptor expression levels prevented PGD_2 or BW245c-induced enhancement of peripheral VE-cadherin staining (**Figure 19**C). Western blotting and RT qPCR confirmed significantly reduced EP4 mRNA content in cells transfected with EP4-targeting siRNA (**Figure 19**D and E, respectively), while DP1 receptor mRNA expression was unchanged. Sphingosine-1-phosphate barrier enhancement was unchanged in control siRNA and specifically siRNA-treated cells (**Figure 20**) further ruling out a non-specific effect of EP4 receptor knock-down.

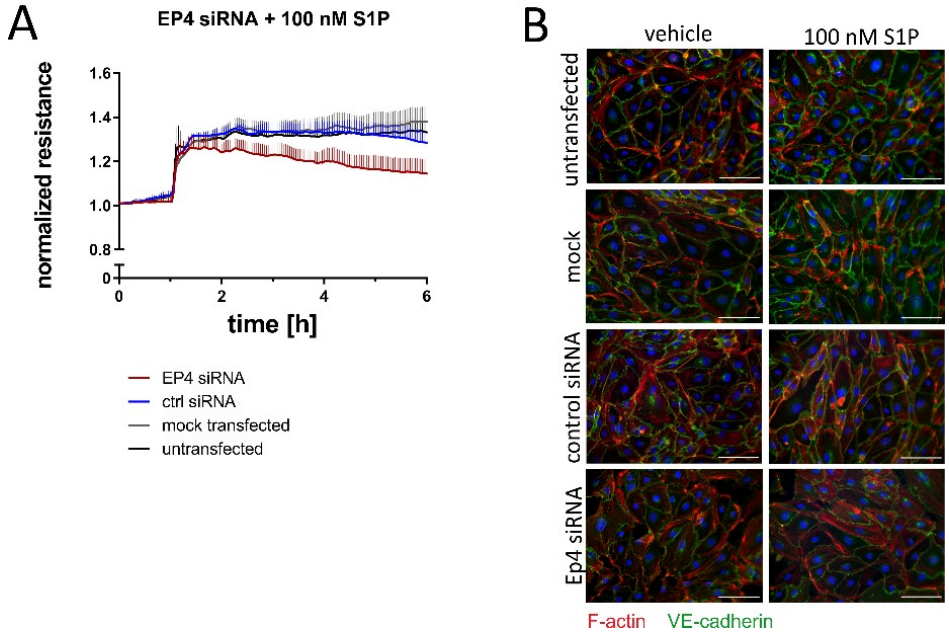

Figure 20. Transient knock-down of EP4 receptors in HPMEC does not affect the early phase of sphingosine-1-phosphate barrier enhancement. Primary HPMEC were transfected with PTGER4-specific or control siRNA for 48 h. To rule out a harmful or off-target effect of EP4 receptor knock down, cells were stimulated with sphingosine-1-phosphate. (A) EP4 receptor knock down did not reduce S1P-induced increase in endothelial resistance or (B) barrier protective effect against thrombin-induced barrier disruption (representative of 3 experiments). Data are shown as mean + SEM, n = 4. Figure adapted from (2).

PGE_2 and PGD_2 affect AKT phosphorylation but not VE-cadherin, focal adhesion kinase or paxillin phosphorylation in HPMEC. Rapid cytoskeletal rearrangement is often accomplished by modifications of the phosphorylation state of cytoskeletal or associated proteins. Since PG-induced effects peaked usually after 30 min, we assessed the phosphorylation state of VE-cadherin, focal adhesion kinase (FAK), paxillin (PAX) and protein kinase B (AKT) at this time point. Notably, PGE_2 and PGD_2 stimulation reduced AKT phosphorylation (S473), while pre-treatment with EP4 antagonist ONO-AE3-208 counteracted the PGD_2-elicited response (**Figure 21**A). This might be pivotal for the PGD_2 and PGE_2-induced protective effect as previous studies have reported that barrier disruptive agents like VEGF (275) or LPS (276) induced phosphorylation of AKT at S473 which resulted in endothelial permeability, contraction and migration. In contrast, stimulation of HPMEC with indicated concentrations of PGE_2 or PGD_2 for 30 min did not change the ratio of phosphorylated VE-cadherin, FAK or PAX to total protein (**Figure 21**C, B, D). A representative blot obtained from one donor is shown in **Figure 21**E.

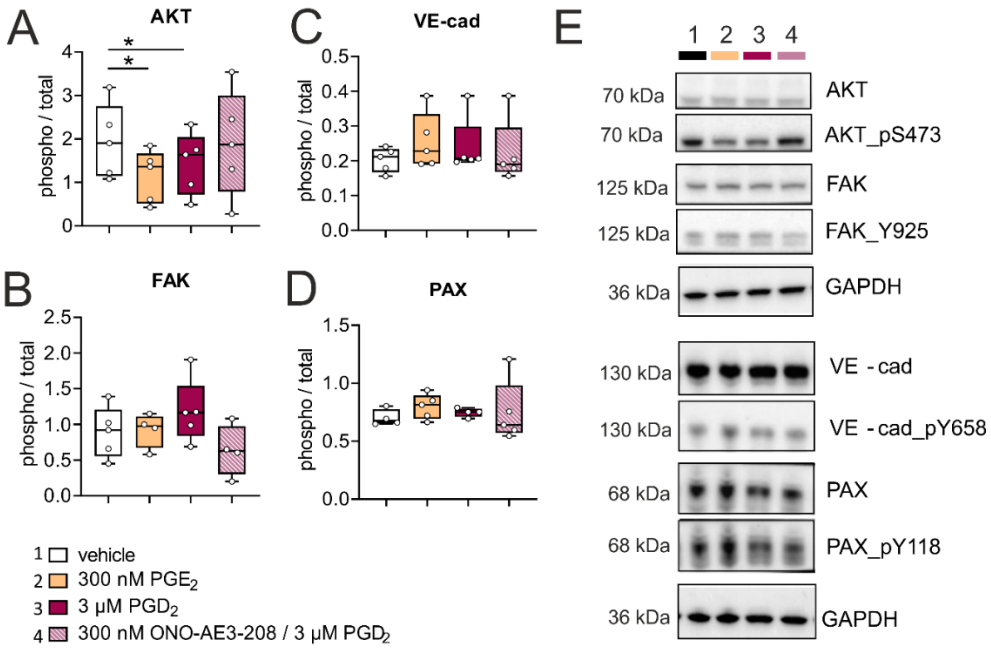

Figure 21. PGE_2 and PGD_2 reduce AKT phosphorylation but not VE-cadherin, focal adhesion kinase or paxillin phosphorylation in HPMEC. HPMEC were grown on gelatin-coated 6-well CellBind plates. Cells were starved in EBM-MV2 basal medium with 2 % FCS for 1 h, incubated with 300 nM EP4 antagonist ONO-AE3-208 or vehicle for 20 min and subsequently stimulated with agonists for 30 min. Amount of total protein and phosphorylated protein was

determined with respective antibodies (**Table 4**) and the ratio plotted. (A) Stimulation with 3 µM PGD_2 or 300 nM PGE_2 reduced the amount of phosphorylated AKT (S473) significantly. Pre-treatment with the EP4 antagonist reversed the PGD_2-induced reduction of AKT phosphorylation. Phosphorylation state of (B) focal adhesion kinase (FAK, Y925), (C) VE-cadherin (VE-cad, Y658) and (D) paxillin (PAX, Y118) were unchanged. (E) Representative Western blot obtained from one donor. Data are shown as box-and-whisker plot, n = 5, One-way ANOVA for repeated measurements with Dunn's *post hoc* test, * p <0.05. Figure adapted from (2).

PGD_2 and BW245c also promote human pulmonary artery endothelial cell barrier function through EP4-activation. Finally, we determined whether the barrier-enhancing effect of PGD_2 and EP4 receptors can also be seen in macrovascular endothelial cells, i.e. human pulmonary artery endothelial cells (HPAEC). Indeed, PGD_2 and BW245c triggered a concentration-dependent increase also in HPAEC comparable to HPMEC (**Figure 22**A and B). Blockade of EP4 receptors with 300 nM ONO-AE3-208 likewise diminished barrier enhancement by both, PGD_2 and BW245c (**Figure 22**C and D, respectively).

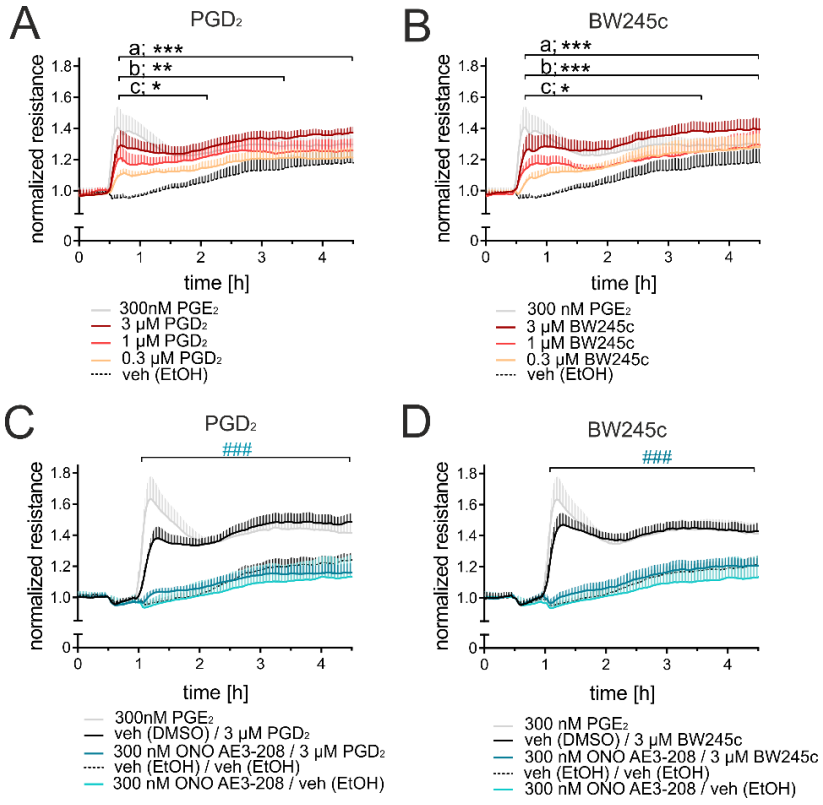

Figure 22. PGD_2 and BW245c also promote HPAEC barrier function through EP4-activation. (A) PGD_2 as well as (B) BW245c increased human pulmonary artery endothelial cell resistance in a concentration-dependent manner to

a comparable level as in HPMEC. Furthermore, EP4 blockade also prevented (C) PGD_2 and (B) BW245c triggered barrier enhancement. Data are displayed as mean + SEM, n = 5. Two-way ANOVA for repeated measurements with Tukey's post hoc test, (A and B) (a) veh (EtOH) vs. 3 µM agonist, (b) veh (EtOH) vs. 1 µM agonist, (c) veh (EtOH) vs. 0.3 µM agonist, * $p<0.05$, ** $p<0.01$, *** $p<0.001$. (C and D) ###$p<0.001$ difference between veh (DMSO) / 3 µM PGD_2 or BW245c vs. 300 nM ONO-AE3-208 / 3 µM PGD_2 or BW245c. Figure adapted from (2).

DP1 and EP4 receptor staining in human pulmonary vasculature. Staining and slide scanning was performed by Kerstin Schweighofer at the Ludwig Boltzmann Institute for Lung Vascular Research, Graz, Austria. To approach the subject of EP4 and DP1 receptor expression levels in pulmonary endothelial cells, we stained serial sections of healthy, non-tumorous, non-transplanted human lung tissue. Representative images of pulmonary microvasculature (PMV), arteries (PA) and veins (PV) are shown in **Figure 23**. Donors are referenced on the left side of the images. This staining suggests that also in human lung sections, DP1 receptor expression levels appear to be lower in comparison to EP4. Notably, endothelial cells in capillaries and veins showed more pronounced PG receptor staining as compared to arteries. There were some differences in staining intensity between the different donors, however, similar patterns could be found in all of the donor sections observed.

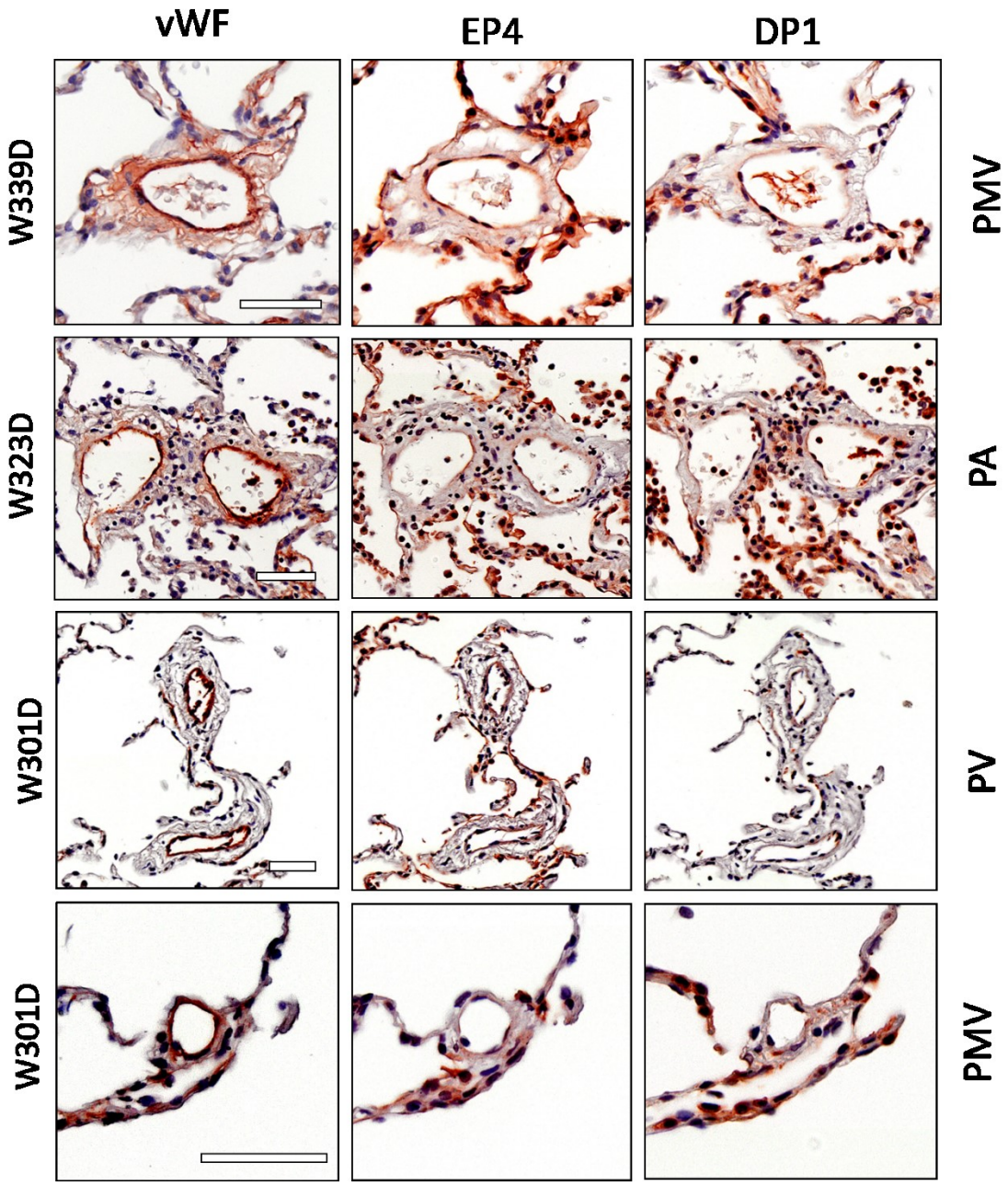

Figure 23. EP4 and DP1 receptor staining in human pulmonary vasculature. Serial sections obtained from non-tumorous, non-transplanted human lung tissue were stained with anti-EP4, anti-DP1 and anti-vWF (as endothelial cell marker). Representative images obtained from indicated donors (W#D) are shown. PMV – pulmonary microvasculature, PA – pulmonary artery, PV – pulmonary vein. Scale bar 50 µm.

3.2. PART II: Characterization of novel prostaglandin sources in LPS-induced inflammation

Mast cells are believed to be the main PGD_2 source; however, their involvement in acute inflammation is rather unlikely due to their low numbers in non-allergic settings. The specific action of PGD_2 in acute lung inflammation is not completely understood, albeit a role in driving inflammation and pathology has been proposed. A higher number of hematopoietic PGD synthase-expressing, infiltrating leukocytes were noted in lung histological sections of ARDS patients (67) and, by another study, urinary eicosanoids, including PGD_2 metabolites, were suggested as biomarkers for this condition (220). Mononuclear phagocytes, especially macrophages, play a central role in the modulation of inflammatory reactions. Besides being able to release a tremendous set of cytokines, these cells have also been associated with a repertoire of lipid mediators including prostaglandins, mainly PGE_2. Hence, we specifically aimed to characterize the potential of monocytes and macrophages as PGD_2 sources during pulmonary inflammation.

hPGDS expression in human circulating leukocytes and mononuclear phagocytes reveals potential PGD_2 sources. Our first aim was to evaluate hPGDS expression in human circulating leukocyte subsets using a flow cytometry approach to screen for potential other PGD_2 sources next to mast cells. Peripheral blood leukocytes from healthy donors were stained with specific cell surface markers in the PBMC or PMNL fraction and hPGDS expression was evaluated with a monoclonal anti-human hPGDS antibody (**Figure 24**A and B). The majority of monocytes stained positive but also about 70% of CD4 T-cells and, interestingly, NK and NK/T-cells stained highly positive for hPGDS. In addition, plasma cells appeared to express high levels of hPGDS. Highest hPGDS expression was found in monocyte-derived macrophages and IFN-γ/LPS or IL-4 activated macrophages (**Figure 24**C). These findings support our hypothesis that mononuclear phagocytes potentially act as PGD_2 sources in non-allergic lung inflammation.

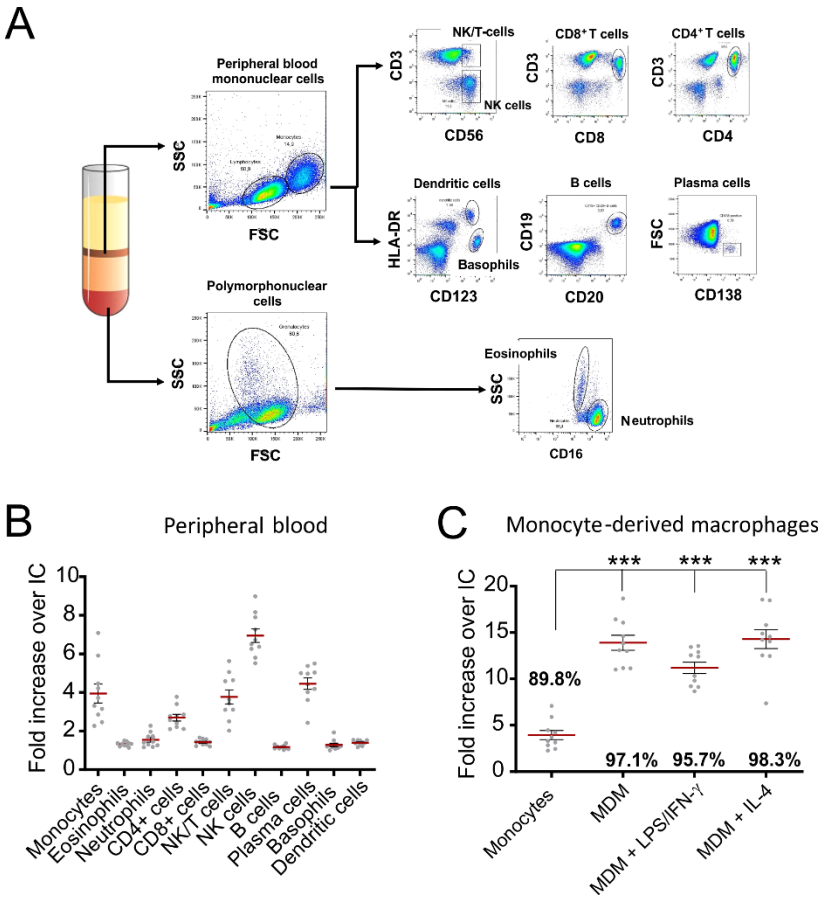

Figure 24. Screening for hPGDS expression in circulating leukocytes and monocyte-derived macrophages. (A) Gating strategy for human leukocytes, which were stained in the PMNL or PBMC fraction of peripheral blood from human donors. (B) Monocytes, $CD4^+$ T-cells, NK/T and NK cells as well as plasma cells stained positive for hPGDS. (C) Monocyte-derived macrophages (MDM) express significantly higher levels of hPGDS than peripheral blood monocytes. Activation of MDM with IFN-γ or IL-4 for 48 h did not significantly change hPGDS expression. Data are shown as scatter plot ± SEM, n = 10, One-way ANOVA with Turkey's *post hoc* test (*** $p<0.001$), percentage of positive cells is denoted in C.

Murine monocytes, macrophages, neutrophils and mast cells sorted from the mouse lung express hPGDS on mRNA and protein level. Aware of the fact that resident pulmonary leukocytes in the healthy lung might differ from circulating subsets, we next set out to evaluate hPGDS expression in murine leukocytes sorted from the lung. One of the first populations recruited to the lung by activated macrophages and monocytes are neutrophils, which appear in high numbers. As mentioned above, mast cells are considered as the main PGD2 source. Therefore, we included neutrophils as well as mast cells in our experimental settings for comparison. Whole lungs were digested with dispase II and stained with cell surface markers to enable the enrichment of following leukocyte subsets by FACS starting from viable, CD45+ cells: neutrophils (CD11b+, Ly6G+), monocytes (Ly6c+, CD11b+), mast cells (CD11b-, c-kit+) and macrophages (F4/80+, CD11blow-high) (**Figure 25**A and B).

We started with determining hPGDS protein expression levels in the individual immune cell populations. Flow cytometry revealed significantly higher expression of hPGDS in monocytes in comparison to macrophages and mast cells sorted from the lung (**Figure 25**C). Further, neutrophils expressed similar hPGDS levels to monocytes in the healthy lung. Leukocyte populations obtained after sorting were rested overnight to ensure an inactivated state. All investigated immune cells expressed comparable levels of hPGDS mRNA (**Figure 25**D); thus, similar levels to mast cells. To extend these findings, we also determined LPGDS mRNA expression, the second rate-limiting PGD2 production enzyme next to hPGDS, in the sorted populations (**Figure 25**E); however, mRNA levels were below detection level in most samples indicating that hPGDS is more prominently expressed and undoubtedly more important in immune populations.

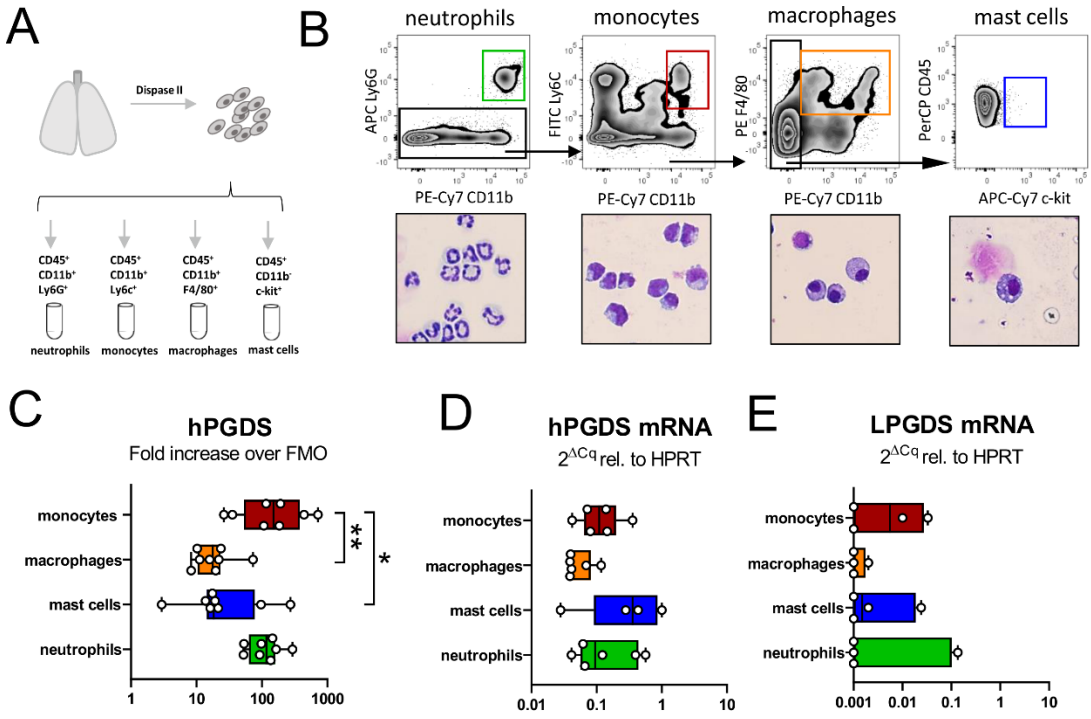

Figure 25. Murine leukocytes sorted from healthy lungs express hPGDS mRNA and protein. (A) Schematic of experimental approach. Total lung was extracted and digested with dispase II. (B) Neutrophils, monocytes, macrophages and mast cells were sorted from whole lung single cell suspension according to displayed gating strategy and RNA extracted from Trizol lysates. Representative images of populations obtained after sorting have been stained with Diff/Quik are shown (pooled from 2 mice, n = 4). (C) Flow cytometric evaluation of hPGDS expression indicated that Ly6c^{+} monocytes expressed significantly higher levels of hPGDS compared to other populations. (D) hPGDS mRNA could be detected at similar levels in all leukocyte subsets investigated. (E) LPGDS mRNA was not in the

detectable range for most samples. Data are shown as box-and-whisker plots with one data point representing one mouse, n = 4-8, outliers were removed after a ROUT test (α = 0.02), one-way ANOVA for repeated measurements with Sidak's *post hoc* test, * $p<0.05$, ** $p<0.01$.

hPGDS *in situ* hybridization in different models of murine pulmonary inflammation shows most hPGDS$^+$ CD68$^+$ cells in pulmonary fibrosis.

Next, we decided to probe for hPGDS expression in paraffin-embedded lung sections collected in preceding studies from murine models of LPS-induced acute lung injury/inflammation (BALB/c), OVA-induced allergic lung inflammation (BALB/c) and bleomycin-induced pulmonary fibrosis (B57BL/6). *In situ* hybridization in control vehicle-treated mice showed that few cells express detectable levels of hPGDS mRNA in the healthy lung. Remarkably, in all investigated inflammatory models, allergic or non-allergic as well as acute or sustained, detectable hPGDS mRNA levels in the lung were more prominent than in control lungs (**Figure 26**). This could be either due to infiltration of leukocytes or upregulation in resident cells. Co-staining with CD68 enabled us to evaluate whether CD68$^+$ monocytes/macrophages expressed hPGDS on mRNA level and the distribution of hPGDS expression in each inflammatory model. In bleomycin-induced fibrosis there were clearly more CD68$^+$ hPGDS mRNA$^+$ cells present and expression levels increased also in the parenchyma and potentially in other infiltrating cells. In OVA-induced allergic inflammation, hPGDS mRNA was highly upregulated in bronchial epithelial cells, which had been noted in other allergic mouse models before (277), and also hPGDS mRNA$^+$ infiltrating cells could be observed. Unexpectedly, hardly any CD68$^+$ cells stained positive with the hPGDS probe in LPS-treated lungs. As mentioned above, these sections were from preceding studies, from different strains of mice, and notably hardly any alveolar macrophages could be found in these lung sections because broncho-alveolar lavage was performed prior to embedding. This was different in bleomycin-treated lungs, which were not subjected to BAL. Yet, these observation suggest that hPGDS expression, and potentially PGD_2 production, is involved in pulmonary inflammation not only in an allergic environment but may also be important in acute lesions.

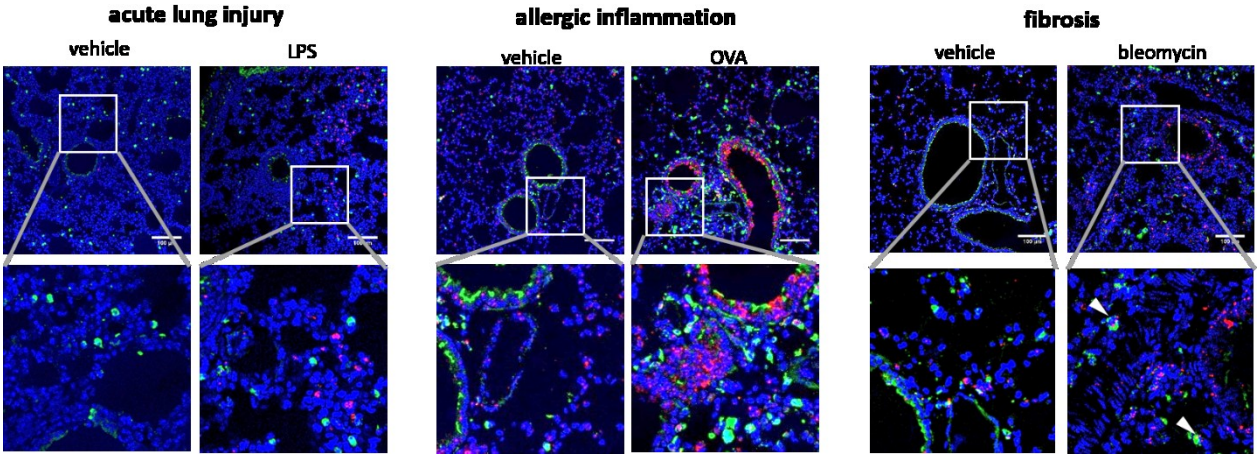

Figure 26. hPGDS *in situ* hybridization in murine LPS-induced acute lung injury, OVA-induced allergic inflammation and bleomycin-induced fibrosis. BALB/c mice received intra-nasal 1 µg/kg LPS or were challenged with OVA as described in the methods section to result in acute lung injury or allergic inflammation, respectively. Pulmonary fibrosis was modelled in C57BL/6 mice by intra-tracheal instillation of 1.5 U bleomycin. HPGDS *in situ* hybridization (red) was performed on mouse lung paraffin sections and macrophage/monocyte populations were co-stained with anti-CD68 (green). Scale bar: 100 µm, enlarged regions are shown below original images, n = 3 mice for each condition. $hPGDS^+$ $CD68^+$ cells are indicated with white arrows.

Evaluation of monocytes and macrophages as prostanoid sources in bleomycin-induced pulmonary fibrosis. As we observed a marked increase in hPGDS mRNA expressing $CD68^+$ cells in the bleomycin-induced pulmonary fibrosis model, we decided to explore the capacity for PG production of monocytes and macrophages in this model. On day 21 after bleomycin-instillation a pronounced pulmonary fibrosis had developed in the lungs, which can be seen in representative images in **Figure 27**C. Whole lungs were extracted and pulmonary neutrophil, monocyte, mast cell and macrophage populations sorted as described in **Figure 25**. Macrophages were clearly the most abundant cell type in the lung, whereby bleomycin-mice had significantly elevated macrophage numbers (**Figure 27**D). Monocyte and neutrophil numbers were comparable and not significantly changed in fibrotic lungs (**Figure 27**E and G, respectively). Mast cell numbers were low, but significantly increased in fibrotic lungs (**Figure 27**F). Directly after sorting, cells were resuspended in culture medium, incubated overnight (18 h) and lipid mediator content in conditioned medium was evaluated with LC/MS. PGE_2 (**Figure 27**I) as well as PGD_2 (**Figure 27**H) could be detected in macrophage-conditioned medium at remarkably high levels already in control (vehicle-treated) mice; however, no significant increase in bleomycin mice could be observed. No PGD_2 could be

measured in monocyte, neutrophil and mast cell-conditioned medium. Similar results were obtained for TBX_2, whereby mast cells from bleomycin-mice produced less TBX_2 than vehicle-treated mice (**Figure 27**J). These data suggest that macrophages may supply constant, basal levels of PGs in fully established lung fibrosis; however, it would be interesting to evaluate their PG production potential in the early, inflammatory state of fibrotic development in future studies.

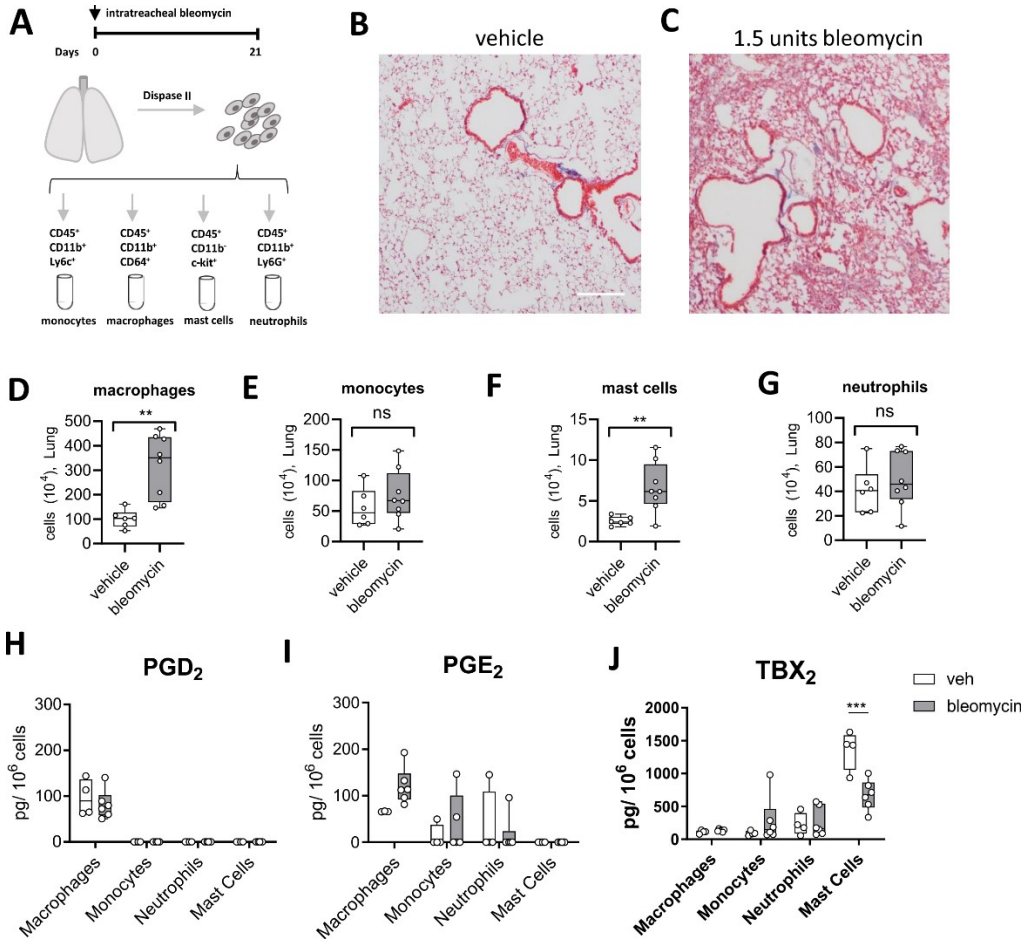

Figure 27. Evaluation of myeloid cells as prostaglandin source in bleomycin-induced pulmonary fibrosis. (A) Experimental setup. Lung cells from vehicle or bleomycin-treated mice were sorted from perfused, whole lung single cell suspensions. Representative images (n = 3) of lung pathology obtained by Masson's Trichrome staining of (B) vehicle treated or (C) intra-tracheal instillation of 1.5 units bleomycin. (D) Macrophage and (F) mast cell numbers were significantly higher in bleomycin-treated animals. (E) Monocyte and (G) neutrophil counts were unchanged between groups. Conditioned medium from sorted cells collected after 18 h without additional stimulation was analysed by LC/MS and (H) PGD_2, (I) PGE_2 and (J) TBX_2 levels obtained. Data are displayed as box-and-whisker plots, n = 5-8, Student's t-test or two-way ANOVA with Fisher's LSD *post hoc* test, ** $p<0.01$. *** $p<0.001$.

Mononuclear cells collected with BALF from LPS-induced acute pulmonary inflammation but not OVA-induced allergic inflammation release PGD_2. To evaluate the extent of PGD_2 production by alveolar mononuclear cells in ongoing type-1 and type-2 inflammation, we used two different murine models of pulmonary inflammation: an LPS-induced model of acute lung inflammation and an ovalbumin (OVA)-induced model of allergic lung inflammation (Schematics in **Figure 28**A and B). In contrast to established pulmonary fibrosis, where inflammation takes place primarily in the parenchyma, in LPS and OVA models inflammation of the airways and alveoli is predominant. Therefore, cells were collected with broncho-alveolar lavage (BAL) fluid either 4 h after LPS instillation or one day after the second OVA-aerosol challenge and total cell number was determined (**Figure 28**E). Haematoxylin and eosin staining revealed similar levels of leukocyte infiltration and plasma extravasation around airways and vessels (**Figure 28**C and D). Significantly more infiltrating cells could be detected in BAL fluid obtained from LPS-induced lung inflammation. Using a morphological approach, i.e. cell size and nucleus morphology, the percentage of mononuclear cells in BALF was determined. In naïve mice the mononuclear cell fraction comprised about 90 % of total cells, while in BALF obtained from OVA and LPS models the percentage was significantly lower indicating a tremendous lymphocyte and granulocyte influx (**Figure 28**F). The mononuclear cell fraction was enriched using differential adhesion, and non-adherent cells were washed off after 1 h. Representative images of the enriched cell fraction can be seen in **Figure 28**G. Mononuclear cells enriched from BALF after LPS-induced acute lung injury produced significant amounts of PGD_2 after 18 h incubation without further stimulation; in contrast, cells from OVA-induced allergic inflammation released negligible amounts of PGD_2 (**Figure 28**H). This clearly confirms that in non-allergic inflammation, i.e. initiated by bacterial LPS, mononuclear phagocytes contribute significant levels of PGD_2 and are able to modulate inflammation in return.

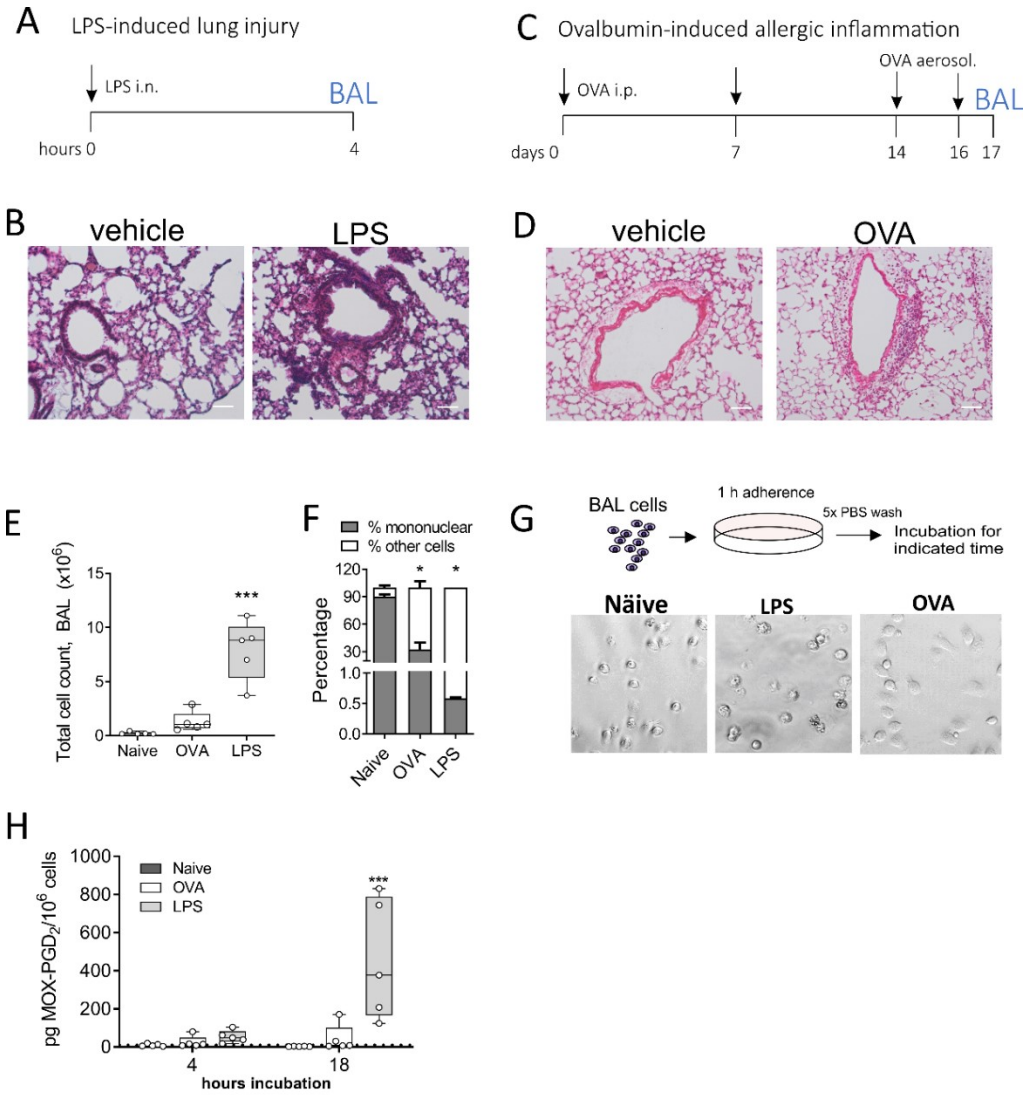

Figure 28. Alveolar mononuclear phagocytes isolated from LPS- but not OVA-challenged mouse lung release high amounts of PGD_2. (A) Scheme of LPS-induced lung inflammation model and (C) OVA-induced allergic inflammation model. Alveolar cells were collected by bronchoalveolar lavage (BAL) at indicated time points. Lung histology for both pulmonary inflammation models, (B) LPS-induced acute and (D) OVA-induced allergic inflammation, are shown (H&E staining, representative of 3 mice each). (E) In BAL fluid obtained from LPS-induced lung inflammation there were significantly more cells present. (F) The percentage of mononuclear cells in BALF was determined upon morphological differences. (G) BAL cells were seeded into CellBind plates and non-adherent cells washed off after 1 h adherence. Enriched mononuclear cell fraction was incubated for indicated time points. Representative images of resulting enriched mononuclear populations are shown. (H) Mononuclear phagocytes from LPS-induced lung inflammation released significantly more PGD_2 after 18 h in culture. Data are shown as bar chart + SEM or box-and-whisker plot. n = 5, One-way ANOVA with Tukey's *post hoc* test (C and D) or two-way ANOVA with Tukey's *post hoc* test (D), * $p<0.05$, *** $p<0.001$.

***Ex vivo* LPS/IFN-γ stimulated murine monocytes and macrophages sorted from the healthy lung release significant amounts of prostaglandins.** Building up on our finding that broncho-alveolar mononuclear cells enriched from LPS-induced lung inflammation release significant amounts of PGD2, we now were interested whether (i) monocytes or macrophages are the source and (ii) how they compare to mast cells as PGD2 producers. We applied our previous approach (**Figure 25**) and again sorted monocytes, macrophages, mast cells and neutrophils from healthy, whole lungs.

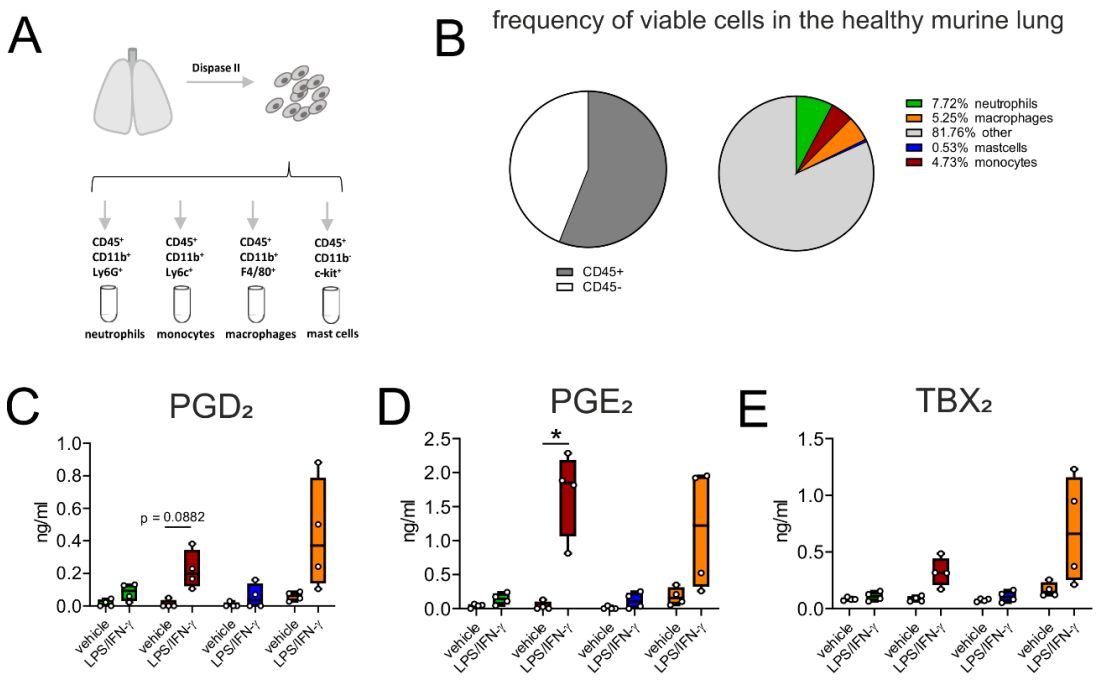

Figure 29. *Ex vivo* LPS/IFN-γ stimulated murine monocytes and macrophages sorted from the healthy lung release significant amounts of prostaglandins. Data obtained from the same mice as in **Figure 25**. (A) Neutrophils, monocytes, macrophages and mast cells were sorted from total lung single cell suspensions as described previously. (B) Mean value obtained for all mice are shown to visualize the proportion of $CD45^+$ cells and the ratio of viable leukocyte populations obtained in this experiment after dispase II digestion and surface marker staining. (C) After sorting, leukocyte populations were divided up and one part stimulated with 50 ng/ml LPS and 10 ng/ml IFN-γ, while the other part was cultured in medium only for 18 h. This stimulation induced (C) PGD_2 and, more potently, (D) PGE_2 release by murine monocytes and macrophages, but only to a minor extent in neutrophils or mast cells sorted from the lung. (E) TBX_2 release was increased by trend in monocyte- and macrophage-conditioned medium. Data are shown as box-and-whisker plot or pie chart, n = 4, each dot represents data obtained from one mouse. Two-way ANOVA with Sidak's *post hoc* test, * $p<0.05$.

In **Figure 29**B the frequency of sorted populations in the healthy murine lung can be seen. About the same numbers of viable neutrophils, monocytes and macrophages but only very low numbers of mast cells could be recovered. Directly after sorting, cells were split in half and resuspended in culture medium with or without 50 ng/ml LPS and 10 ng/ml IFN-γ and incubated overnight (18 h). Lipid mediator content in conditioned medium was determined using LC/MS, whereby values obtained for PGD_2, PGE_2 and TBX_2 for each population were plotted as ng/ml (**Figure 29**C, D, E). Notably, this means that values were not normalized to cell number and, hence, represent the actual number of cells obtained for one lung. Indeed, in monocyte and macrophage-conditioned medium most PGD_2 could be detected, which indicates that both populations contribute to elevated levels in LPS-induced lung inflammation (**Figure 29**C). Even higher levels of PGE_2 could be detected in monocyte and macrophage-conditioned medium after activation with LPS/IFN-γ (**Figure 29**D). At this time point (18 h after activation), monocytes clearly favoured PGE_2 release under these conditions.

Human peripheral blood monocytes and monocyte-derived macrophages release PGD_2 and PGE_2 after LPS/IFN-γ, but not IL-4 stimulation. So far, we could convincingly show that murine monocytes and macrophages express hPGDS and release significant amounts of PGD_2 in LPS-induced type-1, but not OVA-induced allergic (type-2) inflammation. Next, we aimed to confirm that these observations also apply to human peripheral blood monocytes and monocyte-derived macrophages. To explore this, circulating monocytes were enriched by differential adhesion using the peripheral blood mononuclear cell (PBMC) fraction obtained from healthy blood donors and, either directly used for experiments, or differentiated with M-CSF into monocyte-derived macrophages for 6-8 days. Cells were either activated with LPS/IFN-γ, as classical type-1 inflammatory stimulus, or IL-4, to simulate a type-2 cytokine-biased environment seen in allergic pulmonary inflammation. PGD_2 levels were determined using a MOX-PGD_2 ELISA Kit, while PGE_2 levels were measured with a radio-immunoassay (RIA) and the values were normalized to total mg protein per well (as determined with a BCA kit) to exclude variations in cell numbers. Indeed, we could detect significant amounts of PGD_2 and PGE_2 in conditioned medium from both cell types after LPS/IFN-γ stimulation (**Figure 30**A and B) but not IL-4 stimulation (**Figure 30**D and E). Both cell types, monocytes and macrophages, released up to 10x

more PGE_2, whereby PGE_2 levels steadily increased up to 200 ng PGE_2 /mg protein 48 h after activation. An interesting observation was also that monocytes as well as monocyte-derived macrophages release PGD_2 and PGE_2 with different kinetics; PGD_2 peaks between 8 and 24 h after activation, while PGE_2 levels rise up to 48 h after activation. To prove successful activation, human MDM were stained with anti-CD80 for a pro-inflammatory or anti-CD206 antibodies for an anti-inflammatory polarization; LPS/IFN-γ and IL-4 successfully upregulated CD80 and CD206, respectively (**Figure 30**C and F). These observations are in line with what we observed for murine pulmonary leukocytes and shows that also human monocyte- and macrophage-derived PGD_2 production can be triggered by LPS/IFN-γ but not IL-4.

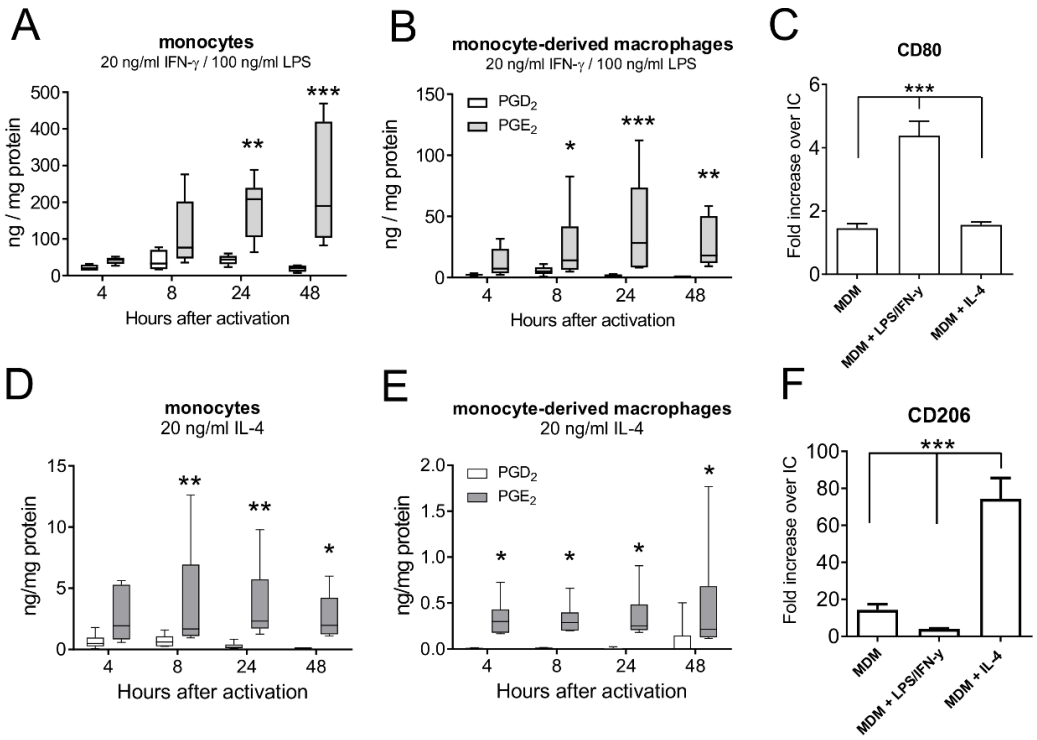

Figure 30. Human peripheral blood monocytes and monocyte-derived macrophages release prostaglandins after stimulation with LPS/IFN-γ but not IL-4. Human peripheral blood monocytes were enriched by differential adhesion from the PBMC fraction of human donors and either directly activated with LPS/IFN-γ or first differentiated into monocyte-derived macrophages (MDM). Conditioned medium was collected at indicated time points after activation and PG content determined and normalized to total protein per well. (A) Human peripheral blood monocytes and (B) MDM released PGD_2 and PGE_2 upon stimulation with LPS/IFN-γ. Significantly more PGE_2 could be detected at later time points (>24 h). (C) Stimulation with LPS/IFN-γ upregulated CD80 expression in MDM (n = 10). (D)

Monocytes and (E) MDM stimulated with IL-4 released negligible amounts of PGE_2 and PGD_2. (F) Stimulation with IL-4 successfully upregulated CD206 expression in MDM (n = 10). Data are shown as histogram + SEM or box-and whisker plot. n = 6, One-way ANOVA with Sidak's *post hoc* test (C and F) or two-way ANOVA for repeated measurements with Sidak's *post hoc* test (A, B, D, E), * $p<0.05$, ** $p<0.01$, *** $p<0.001$.

Human monocytes surpass monocyte-derived macrophages as prostaglandin sources after LPS/IFN-γ at all time points. Remarkably, human monocytes seem to exceed monocyte-derived macrophages as prostaglandin sources at all time points investigated. Monocytes released significantly higher levels of PGD_2 (**Figure 31**A) as well as PGE_2 (**Figure 31**B) in comparison to monocyte-derived macrophages after stimulation. We could measure values of up to 50 ng MOX-PGD_2 / mg protein at 8 and 24 h after activation, while PGD_2 levels dropped after 48 h. In our *ex vivo* approach looking into murine pulmonary monocytes and macrophages, we could see that these populations release comparable levels of PGD_2 after LPS/IFN-γ stimulations. These results suggest that human monocytes may even surpass monocyte-derived macrophages as PG sources under certain circumstances.

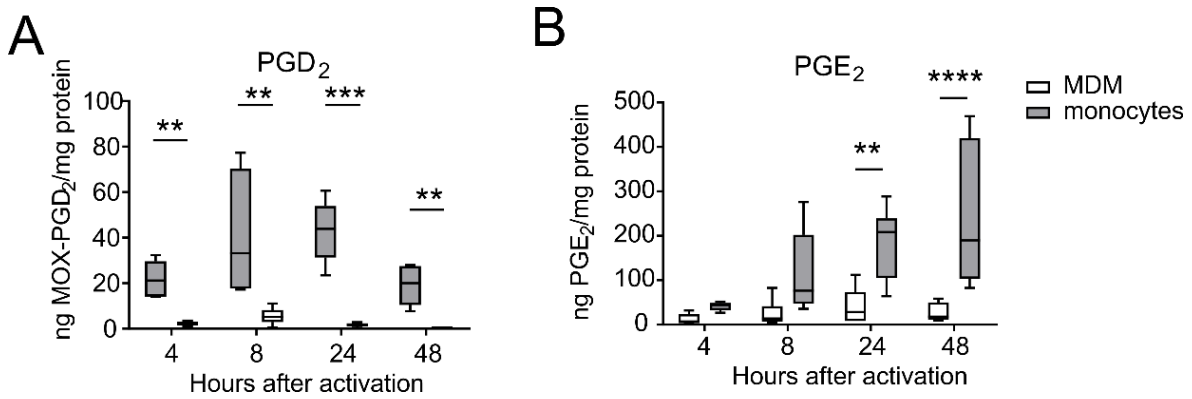

Figure 31. Human peripheral blood monocytes surpass monocyte-derived macrophages as prostaglandin sources at all observed time points. (A) PGD_2 release by human monocytes peaked between 8 and 24 h after activation with LPS/IFN-γ. At all time-points monocytes released higher amounts of PGD_2 normalized to total protein per well. (B) Monocyte-derived PGE_2 levels increased for up to 48 h after activation. At 24 h and 48 h after activation, monocytes exceeded human MDM in PGE_2 production. Data are shown as box-and-whisker plot, n = 6, two-way ANOVA for repeated measurements with Sidak's *post hoc* test, ** $p<0.01$, *** $p<0.001$. Same data as in **Figure 30**.

Monocyte-derived PGE_2 affects endothelial cell barrier function. Considering the facts that (i) PGE_2 as well as PGD_2 improve pulmonary microvascular endothelial barrier function, (ii) a disrupted endothelial barrier may lead to pulmonary oedema during acute inflammation, and (iii) human monocytes produce both prostaglandins in high amounts, we were interested to see whether monocyte-derived prostaglandins affect pulmonary microvascular endothelial barrier function.

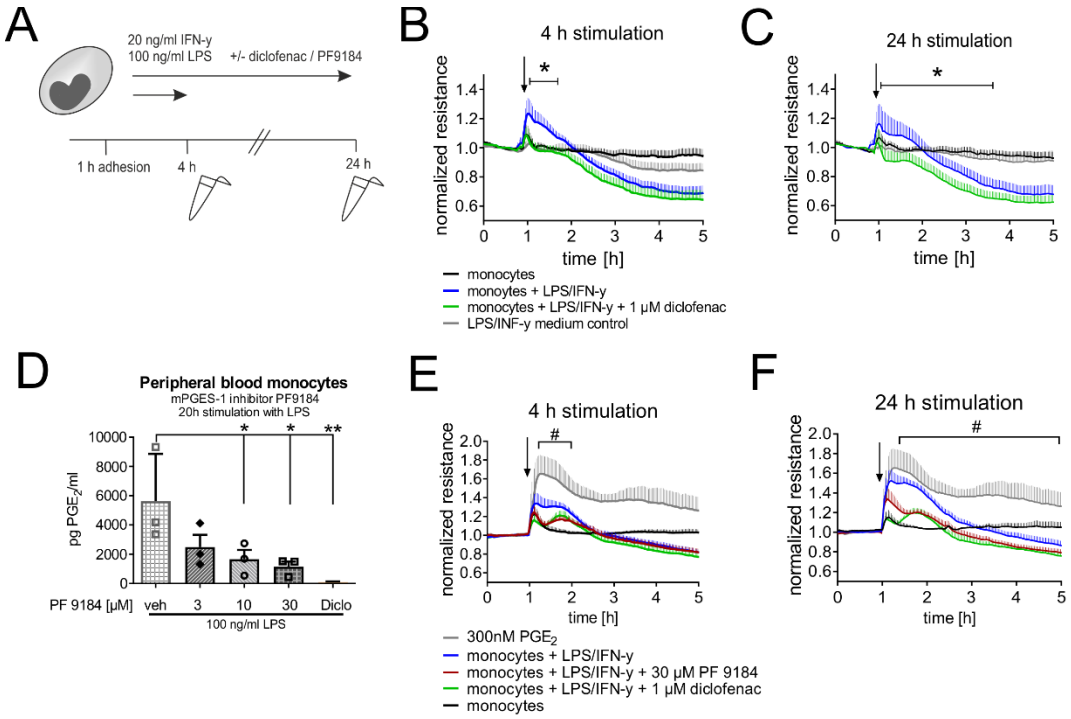

Figure 32. Peripheral blood monocyte-derived PGE_2 affects HPMEC barrier function. (A) Experimental setup: Human monocytes were stimulated for 4 or 24 h with LPS/IFN-γ and conditioned medium was collected for ECIS experiments. As controls, cell-free wells were incubated with stimulation media. Initial barrier enhancing effect by monocyte-conditioned medium (diluted 1:20) was reduced at (B) 4 and (C) 24 h after activation when COX-1/2 were blocked in monocytes with diclofenac. (D) Specific blockade of mPGES-1 with PF9184 in monocytes was evaluated using PGE_2 RIA (n = 3). Incubation of monocytes with PF9184 showed that PGE_2 is mostly responsible for the barrier enhancing effect at (D) 4 h but also at (E) 24 h. Data shown as mean + SEM, n = 3-6, One-way ANOVA with Sidak's *post hoc* test or two-way ANOVA with Tukey's *post hoc* test, * $p<0.05$, ** $p<0.01$, $p<0.001$ (B, C) and # $p<0.05$ comparison between monocytes + LPS/IFN-γ and monocytes + PF 9184 + LPS/IFN-γ.

Indeed, monocyte-conditioned medium after stimulation with LPS/IFN-γ caused a characteristic bi-phasic effect. In the first 2 h after addition of media, there was an increase, followed by a robust drop of endothelial resistance. This was true for media collected after 4 h as

well as 24 h of treatment, while barrier enhancing effect was diminished when cyclooxygenase function was blocked with diclofenac **Figure 32**B and C, respectively). The drop in endothelial resistance could not be reversed by inhibition of prostaglandin synthesis but rather sped up loss of endothelial barrier. In the next experiment, mPGES-1 was blocked in monocytes resulting in reduced PGE_2 levels in conditioned media (**Figure 32**D). In turn, loss of mPGES-1 function resulted in reduction of primary barrier enhancement, indicating that barrier enhancement was mainly mediated by PGE_2 (**Figure 32**E and F).

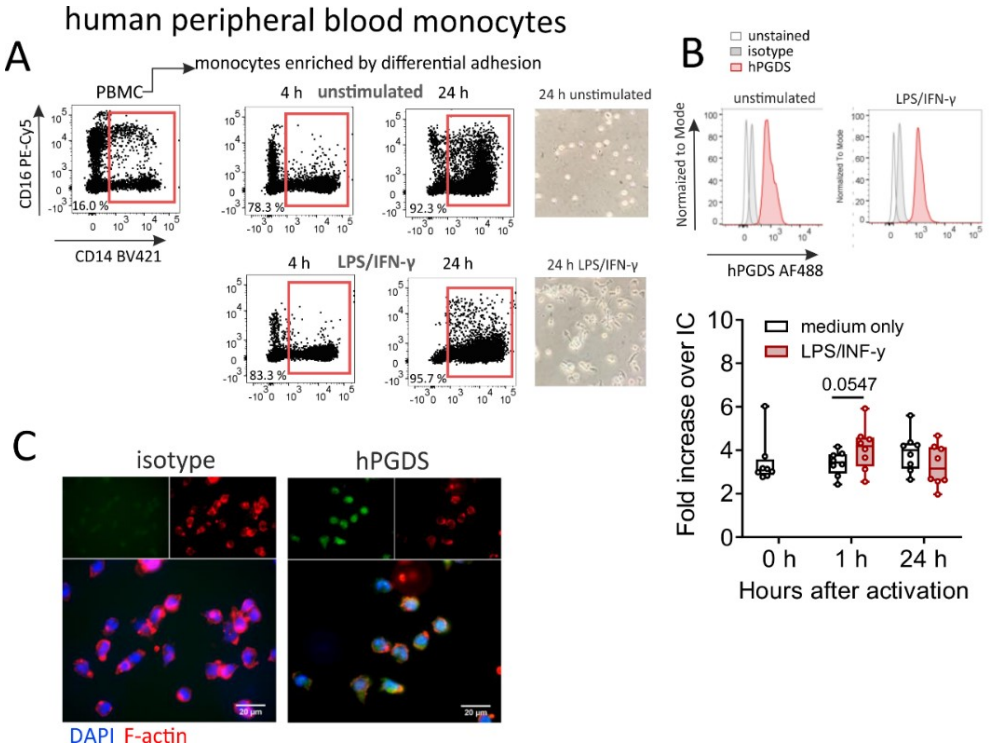

Figure 33. Human peripheral blood monocytes constitutively express hPGDS. (A) Peripheral blood monocytes in the PBMC fraction of human donors were enriched by differential adhesion and either left unstimulated or activated with LPS/IFN-γ for 4 or 24 h. Flow cytometric characterization and representative light microscopy images of monocytes from one donor are shown. CD14 vs. CD16 surface expression revealed that LPS/IFN-γ stimulation resulted in primarily classical $CD14^+$ monocytes after 24 h in culture. (B) The majority of monocytes express hPGDS; however, stimulation did not increase hPGDS expression at the 24 h time point. At 1 h after activation, hPGDS expression tended to increase. (C) Representative images for hPGDS staining in unstimulated human monocytes (scale bar 20 µm). For all experiments n = 5. Data are shown as box-and-whisker plot. 1 h time point: paired Wilcoxon test.

Human peripheral blood monocytes and monocyte-derived macrophages constitutively express hPGDS. We continued with our *in vitro* approach to reconstitute LPS-induced inflammation and used it to further explore hPGDS expression and regulation after pro-inflammatory stimulation in human peripheral blood monocytes and monocyte-derived macrophages. IFN-γ/LPS activation induced a morphological change of peripheral blood monocytes (elongated shape) and treated cells were mainly $CD14^+CD16^-$, while untreated cells maintained the classical distribution of $CD14^+CD16^-$ and $CD14^+CD16^+$ monocytes (**Figure 33**A). Only a minority of cells (less than 1.5 %) were $CD3^+$ indicating a high purity of monocytes after 24 h in culture. Using a flow cytometry approach, we could see that circulating $CD14^+$ monocytes constitutively express hPGDS, while expression levels shifted 1 h after activation and went back to baseline 24 h after activation with LPS/IFN-γ (**Figure 33**B). Activation of monocyte-derived macrophages with LPS/IFN-γ also caused a change in morphology, i.e. elongated or detached morphology, and upregulated CD80 expression verifying successful induction of an inflammatory phenotype (**Figure 34**A). CD163 was not significantly affected by LPS/IFN-γ stimulation. Already at basal state, human monocyte-derived macrophages express substantial levels of hPGDS, which were unchanged after pro-inflammatory activation (LPS/IFN-γ) for 48 h (**Figure 34**B). Representative immunofluorescence images demonstrate that unstimulated human monocytes and monocyte-derived macrophages robustly express hPGDS (**Figure 33**C and **Figure 34**C, respectively).

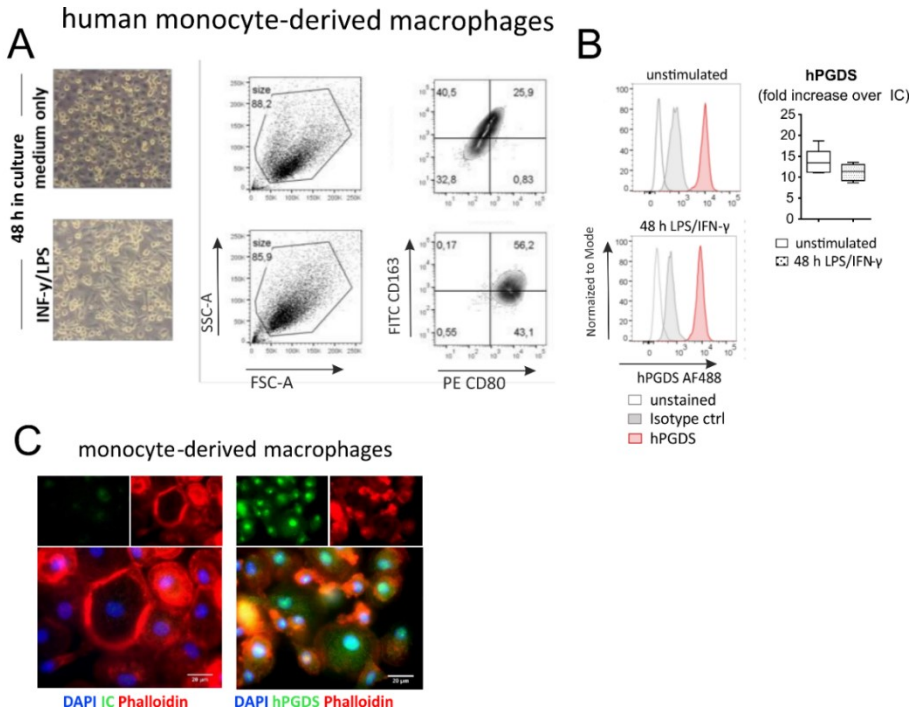

Figure 34. Human monocyte-derived macrophages constitutively express hPGDS. (A) Peripheral blood monocytes in the PBMC fraction of human donors were enriched by differential adhesion and differentiated into monocyte-derived macrophages by incubation with rh M-CSF for a week. Flow cytometric analysis of CD80 and CD163 expression as activation control and representative light microscopy images of macrophages from one donor are shown. (B) Human monocyte-derived macrophages stained highly positive for hPGDS, but pro-inflammatory stimulation for 48 h did not upregulate hPGDS. (C) Representative images for hPGDS staining in unstimulated human monocyte-derived macrophages (scale bar 20 µm). For all experiments n = 5. Data are shown as box-and-whisker plot. Paired Wilcoxon test.

In human mononuclear phagocytes, LPS/IFN-γ activation initiates rapid COX-2 upregulation, while hPGDS is downregulated after 24 h on mRNA level. As we could not see a change in hPGDS expression at the 24 h or 48 h time point after activation of monocytes and macrophages, respectively, we next set out to investigate the time-dependent expression of enzymes involved in prostaglandin production. Activation with LPS/IFN-γ caused a tremendous upregulation of COX-2 mRNA transcription in human monocytes, which was still significantly upregulated after 24h (**Figure 35**A). HPGDS mRNA expression did not increase after LPS/IFN-γ stimulation, but, on the contrary, hPGDS was downregulated 24 h after activation (**Figure 35**A).

Only very low or undetectable levels of LPGDS mRNA for quantification were present in peripheral blood monocytes (**Figure 35**A and B). Additionally, we were interested in how the rate-limiting enzyme of PGE_2, the enantiomer of PGD_2 and also a result of the arachidonic acid/COX pathway, was regulated in comparison to hPGDS. Microsomal PGE synthase 1 (mPGES-1) is the most prominent PGE_2 producing enzyme in LPS-activated monocytes and macrophages according to literature (168). Here, we saw a slight increase of mPGES-1 mRNA in activated monocytes 4 h after activation. On protein level, we could see a potent upregulation of COX-2 and, interestingly, a significant upregulation of hPGDS in monocytes 8 h after activation (**Figure 35**B).

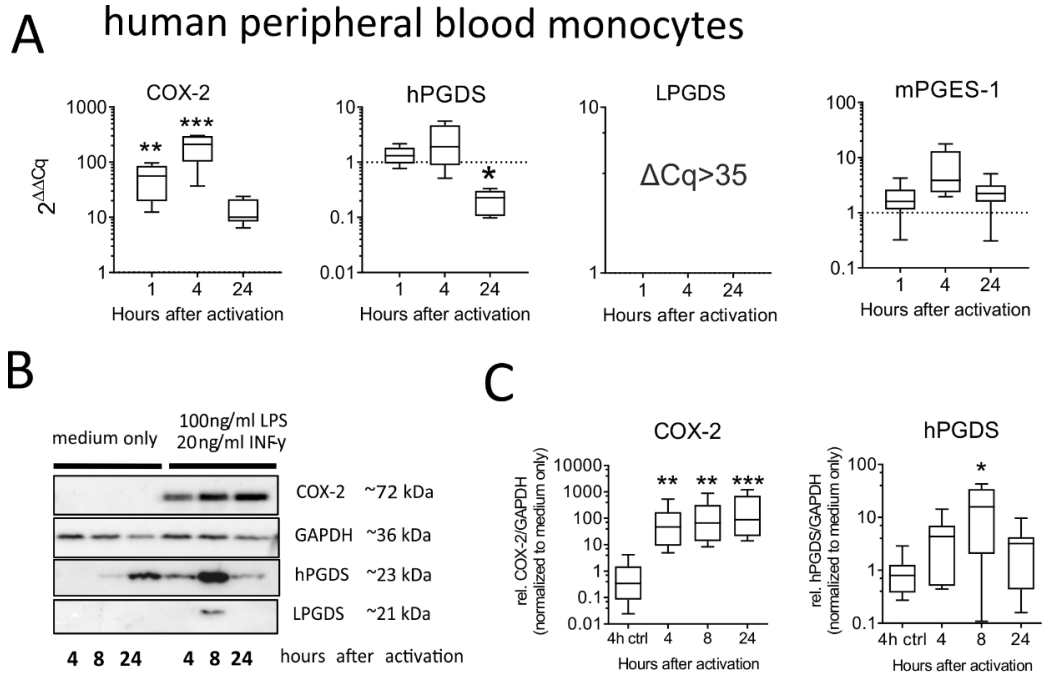

Figure 35. LPS/IFN-γ stimulation initiates rapid COX-2 upregulation, whereby hPGDS is downregulated on mRNA level 24 h after activation in peripheral blood monocytes. Plotted values were obtained after normalization to 1 h or 4 h medium only controls for qPCR and Western blot, respectively. (A) COX-2 mRNA expression is highly upregulated after stimulation with LPS/IFN-γ, while hPGDS mRNA levels decrease 24 h after activation (n = 7) and LPGDS mRNA could not be detected in these cells (n = 5). mPGES-1 mRNA levels did not significantly increase within 24 h after activation. (B) Representative Western blot from one human monocyte donor. (C) COX-2 and hPGDS densitometric results obtained by Western blotting were normalized to GAPDH values and their respective controls (n = 8). Data are displayed as box-and-whisker plot, significance was determined by comparison with the median of 1 h or 4 h controls. Friedman test for repeated measurements with Dunn's *post hoc* test, * $p<0.05$, ** $p<0.01$, *** $p<0.001$.

In monocyte-derived macrophages, we could see a similar picture: Pro-inflammatory stimulation caused the upregulation of COX-2, which indicated the initiation of prostaglandin production (**Figure 36**A). As seen with monocytes, hPGDS was not upregulated on mRNA level, but rather downregulated 24 h after stimulation. We could see a significant upregulation of mPGES-1 mRNA levels after 24 h as well as low, but consistent expression of LPGDS mRNA (**Figure 36**A). On protein level, COX-2 was highly upregulated 4 and 8 h, while hPGDS was significantly upregulated 4 h after LPS/IFN-γ activation in monocyte-derived macrophages (**Figure 36**B and C). These data indicate that PG production is initiated rapidly by COX-2 upregulation which provides high amounts of PGH_2, the substrate for both, hPGDS and mPGES-1. A downregulation of hPGDS mRNA indicates a possible negative feedback loop limiting PGD_2, while favouring PGE_2 production at later time points. Discrepancies between mRNA and protein expression levels of hPGDS suggest that there might be another level of regulation, e.g. miRNAs.

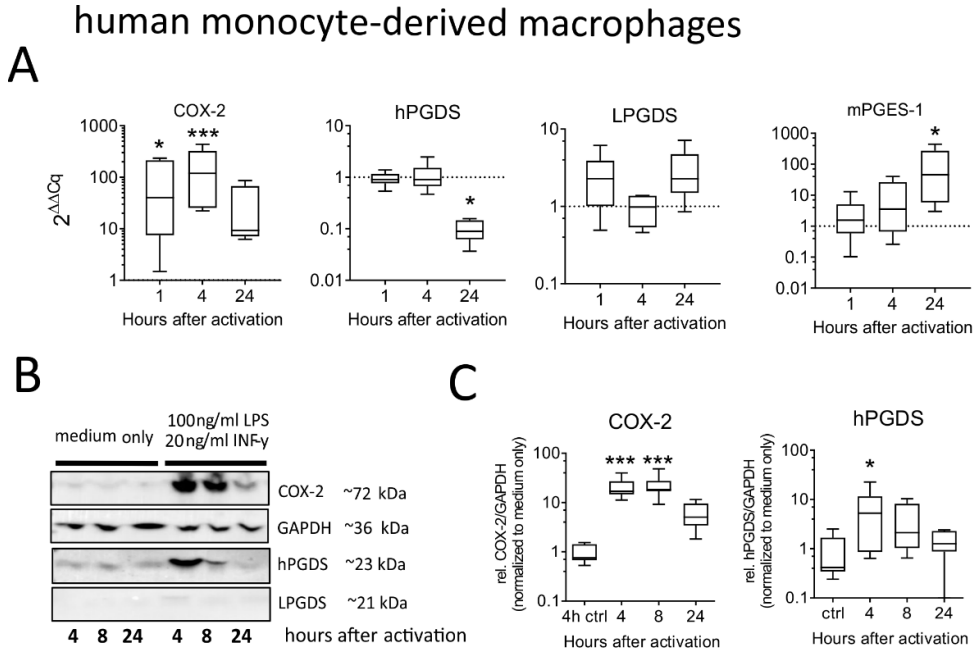

Figure 36. LPS/IFN-γ stimulation initiates rapid COX-2 upregulation, whereby hPGDS is downregulated on mRNA level 24 h after activation in human MDM. Plotted values were obtained after normalization to 1 h or 4 h medium only controls for qPCR and Western blot, respectively. (A) COX-2, hPGDS, LPGDS and mPGES-1 mRNA levels in human MDM after LPS/IFN-γ stimulation. MDM did express low levels of LPGDS, which were unchanged after activation. (n = 6). After 24 h, hPGDS was significantly downregulated, while for mPGES-1 it was the opposite. (B) Representative Western blot from one MDM donor. (C) COX-2 and hPGDS volumetric results obtained by

Western blotting were normalized to GAPDH values and to their respective controls (n = 7). Data are displayed as box-and-whisker plot, significance was determined by comparison with the median of 1 h or 4 h controls. Friedman test for repeated measurements with Dunn's *post hoc* test, * $p<0.05$, ** $p<0.01$, *** $p<0.001$.

In mice, hPGDS protein and mRNA are robustly expressed, but downregulated with time in leukocytes sorted from LPS-induced lung inflammation. To translate the knowledge gained about regulation of PG enzymes in human monocytes and macrophages after LPS/IFN-γ stimulation into an *in vivo* context, we decided to evaluate hPGDS, COX-2 and mPGES-1 expression in murine monocytes, macrophages, neutrophils and mast cells sorted 4 h after LPS-induced lung inflammation or from vehicle treated mice. We applied the same approach as described before for **Figure 25**. Expression levels of hPGDS in all immune populations determined by flow cytometry were the comparable in PBS and LPS-treated mice. Notably, hPGDS expression tended to be reduced in populations from LPS-treated mice compared to PBS-controls (**Figure 37**B). This correlates well with our observations for human monocytes, where we also did not see a significant upregulation of hPGDS on protein level 4 h after activation. Sorted neutrophils, monocytes, macrophages and mast cells were cultured overnight and collected for RNA quantification after 18 h. At this timepoint (approximately 28 h after LPS or PBS instillation), COX-2 was still significantly upregulated in macrophages (**Figure 37**C), where neutrophils and mast cells expressed the highest levels. Similar to human monocytes, monocytes sorted from LPS-lungs, showed a tendency to express less hPGDS compared to controls (**Figure 37**D). The main PGE_2 synthase mPGES-1 was not significantly changed in macrophages and neutrophils (**Figure 37**E). In sum, as observed with human phagocytes, also in pulmonary murine monocytes and macrophages hPGDS is not upregulated after *in vivo* LPS-stimulation, but rather downregulated at a later time point.

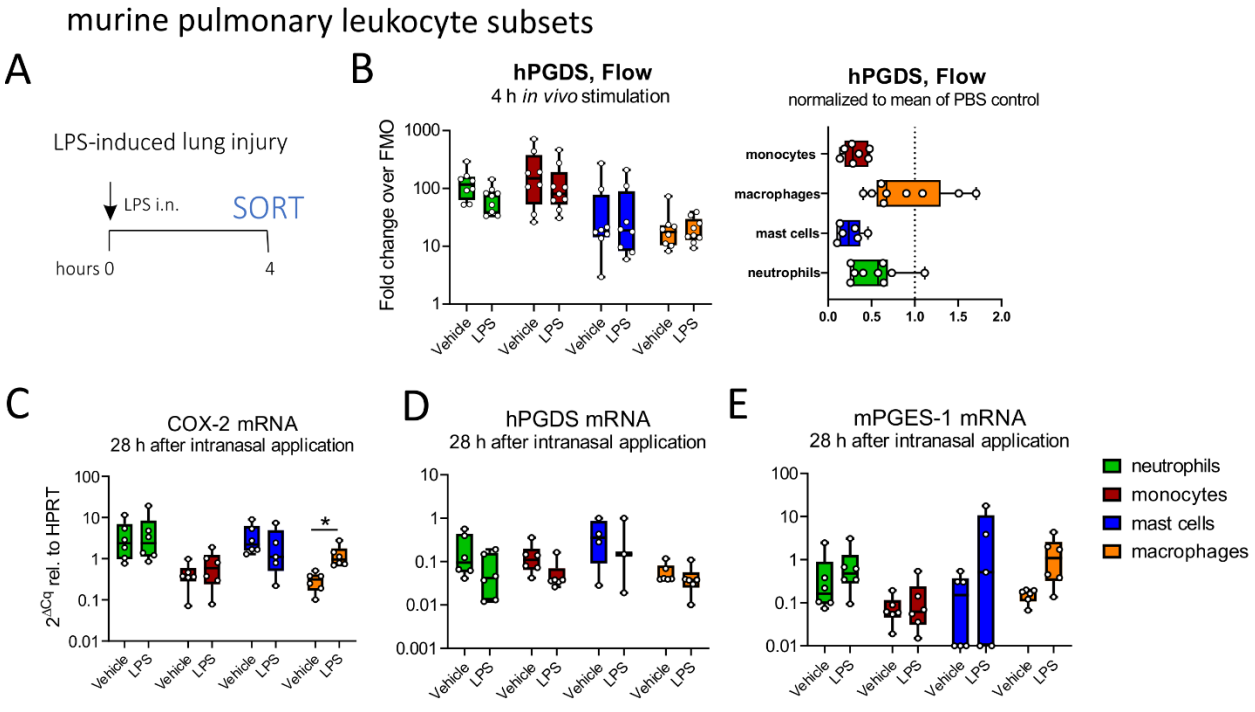

Figure 37. hPGDS protein and mRNA are robustly expressed, but downregulated with time in leukocytes sorted from LPS-induced lung inflammation. (A) Mice received either intranasal LPS (1 mg/kg) or PBS (vehicle) as control and whole lungs were extracted 4 h after treatment and digested with dispase II. Neutrophils, monocytes, macrophages and mast cells were sorted from whole lung single cell suspension according to gating strategy shown in **Figure 25**. (B) Before sorting, an aliquot was taken for flow cytometric evaluation of hPGDS expression. LPS-induced lung inflammation did not result in increased hPGDS expression. Normalization to the mean value obtained from PBS controls for each population rather revealed a reduction. Cells were rested overnight to check transcriptional changes of PG production-related enzymes. At this time point, (C) COX-2 mRNA was still significantly upregulated in macrophages. (D) hPGDS was reduced by trend in neutrophils and Ly6c^{+} monocytes, while (E) mPGES-1 was upregulated by trend in neutrophils and macrophages. Data are shown as box-and-whisker plots with one data point representing one mouse. One-way ANOVA with Tukey's *post hoc* test or Student's t-test, * $p<0.05$.

Neutrophils sorted from mice with LPS-induced pulmonary inflammation release significant levels of PGD_2. Finally, we were interested whether our finding of monocytes exceeding macrophages as PG producers was translatable to an *in vivo* setting. Again, acute pulmonary inflammation was induced in C57BL/6 mice by intranasal application of 1 mg/kg LPS. After digestion, cells were stained as described previously and prepared for sorting (**Figure 25**). Leukocyte numbers per lung were determined by multiplying the percentage of viable cells for

each cell type with the total cell count determined by Trypan blue. As expected, LPS instillation caused a significant neutrophilic inflammation, whereby also monocyte numbers were increased by trend (**Figure 38**C and D, respectively). Only a few mast cells could be detected, while their number was even lower after LPS stimulation (**Figure 38**F), which supports our hypothesis of these cell type being negligible as PGD_2 source in acute inflammation. When cells were cultured directly after sorting from PBS and LPS-lungs, neutrophils showed the most potent increase in PGD_2 and PGE_2 levels, while no PGD_2 could be detected in monocytes (**Figure 38**G and H). A high number of neutrophils may be necessary to achieve such a significant effect, but this indicates that murine neutrophils may contribute to elevated PG levels in acute pulmonary inflammation.

Murine monocytes and macrophages require the presence of LPS/IFN-γ to induce PG production, while repeated stimulation reduces PGD_2 but not PGE_2 release. We were intrigued by the observation that murine neutrophils sorted from LPS-stimulated lungs exceeded all other populations as PG sources, while human and murine monocytes and macrophages, that so clearly were releasing relevant levels after LPS/IFN-γ stimulation in the previous experiments, were not. We assumed that we needed to adapt our experimental approach to (i) overcome potential loss of activation or hyperactivation due to processing and sorting of cells and to (ii) check whether LPS/IFN-γ needs to be constantly present to elicit a PG release. Consequently, populations obtained after sorting for PBS or LPS-lungs received additional LPS/IFN-γ *in vitro* overnight and PG content in conditioned medium was evaluated. Indeed, monocytes required the presence of LPS/IFN-γ for PGD_2 release (**Figure 39**). Notably, PGD_2 levels were elevated more prominently in cells obtained from PBS-treated mice, while populations sorted from mice that had received LPS for 4 h released lower levels of PGD_2 (**Figure 39**A). Interestingly, PGE_2 production by monocytes and macrophages seemed unaffected and was comparable in cells obtained from mice that received PBS or LPS for 4 h (**Figure 39**B). This suggests that repeated stimulation of monocytes and macrophages with LPS may naturally favour the release of PGE_2, potentially due to a negative feedback loop causing the downregulation of hPGDS. TBX_2 release by investigated populations was changed in a similar manner as PGD_2 (**Figure 39**C).

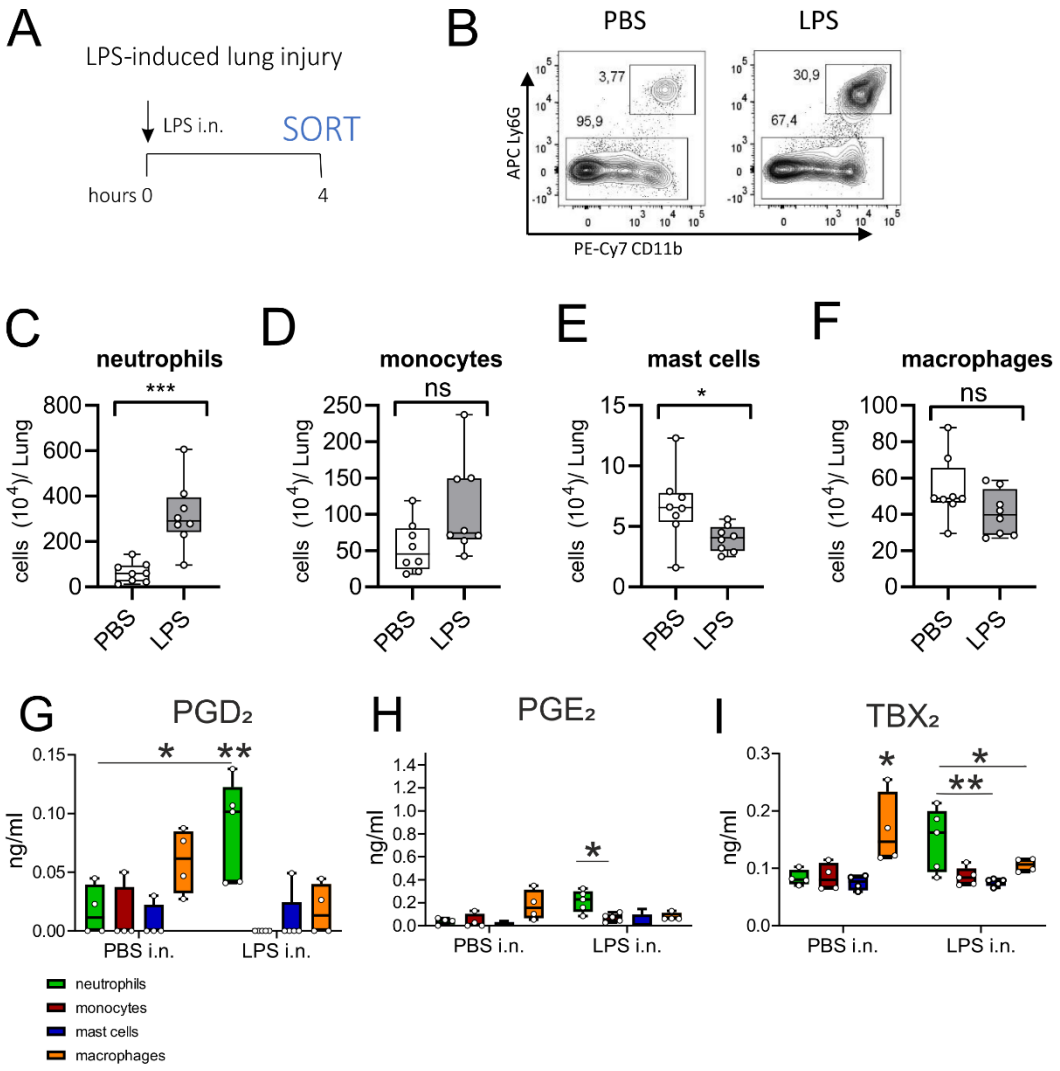

Figure 38. Neutrophils sorted from mice with LPS-induced pulmonary inflammation released significant levels of PGD_2. (A) Schematic of LPS-induced acute pulmonary inflammation. Total lung was extracted 4 h after LPS (1 mg/kg) or PBS instillation and digested with dispase II. Leukocytes were sorted from whole lung single cell suspension according to gating strategy displayed in **Figure 25**. (B) Representative blot showing neutrophilic inflammation in animals treated with intranasal LPS. (C) Intranasal LPS significantly increased neutrophil numbers in the whole lung. (D) $Ly6C^+$ monocyte numbers were not significantly increased, however, (E) mast cell numbers were decreased after LPS instillation. (F) Macrophage numbers were not significantly changed. (G) PGD_2 levels in neutrophil-conditioned medium was significantly higher in cells sorted from LPS-lungs. (H) PGE_2 levels in neutrophil-conditioned medium were higher than observed for monocytes, macrophages and mast cells. (I) Macrophages from PBS-stimulated mice released significant levels of TBX_2 in comparison to other populations. Highest levels were observed in neutrophil-conditioned medium from the LPS group. Data are shown as box-and-whisker plot, n = 4-8. Student's t-test (C-F) or two-way ANOVA with Tukey's *post hoc* test (G-I), * $p<0.05$, ** $p<0.01$, *** $p<0.001$.

Further, PGD_2 and PGE_2 levels after additional *in vitro* stimulation were normalized to total cell number obtained for each population after sorting to gauge the proximate PG production potential of each cell type (**Figure 39**D). There is a huge statistical variation in the results obtained for mast cells, most likely due to extremely few sorted cells per mouse, which questions their relevance in this model. Interestingly, monocytes and macrophages showed a tendency of producing most PGD_2 per cell. This effect was even more pronounced for PGE_2. Hence, in an *in vivo* situation where LPS is present and inflammation still ongoing, monocytes and macrophages may still be the most important PG sources, whereby PGD_2 and PGE_2 release seems to be tightly regulated.

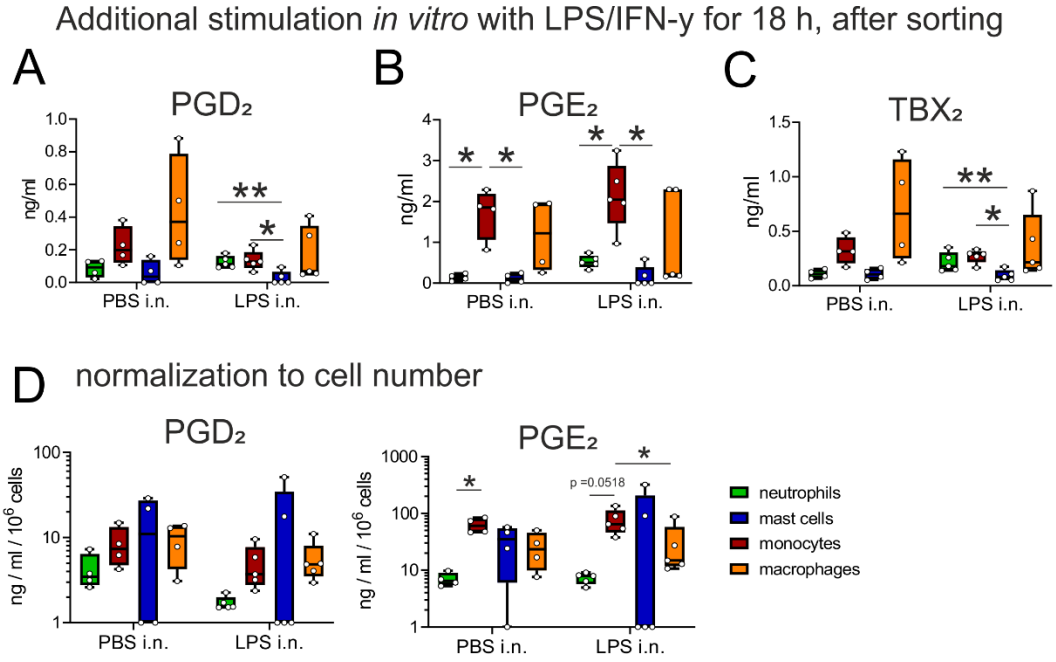

Figure 39. Lipid mediator profile of murine pulmonary leukocyte subsets sorted from LPS-induced lung injury and controls after additional *in vitro* LPS/IFN-γ stimulation. Data obtained from the same mice as in **Figure 38** (G-I). After sorting, leukocyte populations were stimulated with 50 ng/ml LPS and 10 ng/ml IFN-γ for 18 h. (A) PGD_2, (B) PGE_2 and (C) TBX_2 levels detected in conditioned medium collected from indicated pulmonary populations. PGD_2 release was blunted in leukocytes that had been sorted from mice that received intranasal LPS, while PGE_2 release was not affected or even increased by trend. (D) PGD_2 and PGE_2 levels (from additionally *in vitro* stimulated cells) were normalized to total cell number obtained for each population after sorting to gauge the proximate PG production potential of each cell type. Data are shown as box-and-whisker plot with one data point representing one mouse. PBS: n = 4, LPS: n = 5. i.n. stands for intranasal. Two-way ANOVA with Tukey's *post hoc* test, * $p<0.05$, ** $p<0.01$.

Human neutrophils neither express relevant levels of hPGDS nor release PGD_2 after LPS stimulation *in vitro*. Lastly, we were interested whether also human neutrophils are able to produce PGD_2 under certain circumstances; however, using the same culture conditions as used for human monocytes, we could not measure PGD_2 in human neutrophil-conditioned medium at different time points after LPS stimulation (**Figure 40**B). Notably, immunofluorescence imaging showed that unstimulated human peripheral blood neutrophils do not express hPGDS (**Figure 40**A). As shown previously (**Figure 29**), *in vitro* stimulation of murine neutrophils from the healthy lung with LPS/IFN-γ did not significantly increase PGD_2 or PGE_2 levels. Merely an *in vivo* activation, as achieved with the LPS-induced lung inflammation, resulted in induction of significant PG release. These results point out that neutrophil PG production may not be initiated by LPS/IFN-γ alone but additional factors present in acute lung inflammation may be needed.

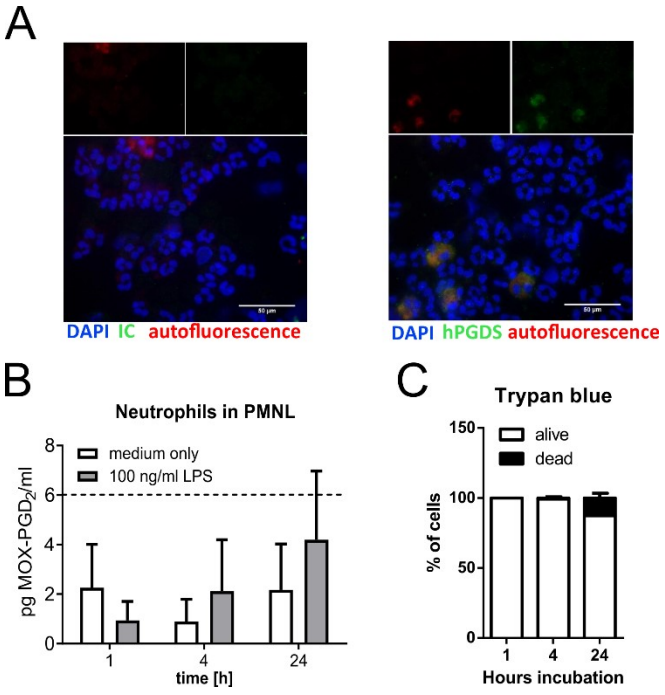

Figure 40. Human neutrophils neither express relevant levels of hPGDS nor release PGD_2 after LPS stimulation *in vitro*. (A) Immunofluorescence staining with isotype control or hPGDS-specific antibody in PMNL fraction of heathy human donors. hPGDS-specific staining is shown in green; neutrophils were not positive. Autofluorescent eosinophils stained faintly positive for hPGDS. (n = 3, scale bar 50 µm) (B) LPS (100 ng/ml) stimulation of human neutrophils in the PMNL fraction of healthy donors did not result in PGD_2 levels above detection threshold (dotted line) (n = 4). (C) Viability of cells was determined with Trypan blue at the moment of conditioned medium collection (n = 4). Data are displayed as bar chart, mean + SEM.

Collectively, this dataset highlights the importance of monocytes and macrophages as PG sources in acute pulmonary inflammation. In established allergic or fibrotic lung disease other cell types may be more relevant. Release of enantiomers PGD_2 and PGE_2 by phagocytes seems to be tightly regulated by COX-2 upregulation and PGD_2 production limited by downregulation of hPGDS in the late phase of inflammation.

3.3. PART III: PGD_2-DP2 activation on human IL-4 polarized monocyte-derived macrophages abrogates angiogenic potential of conditioned medium

The central players of pulmonary immune response are macrophages that adapt rapidly and either promote or counteract inflammation. During the resolution phase of inflammation, macrophages polarize to M2-like macrophages that release anti-inflammatory mediators but also interact with non-immune cells like endothelial cells to influence tissue remodelling and regeneration. It remains unknown whether the presence of lipid mediators like PGD_2 during resolution impact M2-like macrophage function and, consequently, tissue remodelling.

PGD_2 significantly promotes HPMEC wound healing capacity, while PGD_2 stimulation of human MDM delays wound closure. Vasculopathy or dysregulated neovascularization is a common feature of chronic pulmonary disorders and deregulated activation of macrophages may affect endothelial cell regeneration and function. PGD_2 has been reported to activate pulmonary macrophages and aggravate pulmonary inflammation (67). Also, we know from Part I that PGD_2 strengthens HPMEC barrier and, hence, we were interested how PGD_2 influences HPMEC wound closure. To explore this, HPMEC were treated with 1 µM PGD_2 after wounding and monitored for 24 h. Indeed, a beneficial effect on HPMEC wound closure by PGD_2, measured as recovery of electrical resistance with an ECIS device, could be observed (**Figure 41**A and B). Next, we were interested in whether DP receptor activation changes macrophage secretome in a way that endothelial cell wound healing is affected. Interestingly, human monocyte-derived macrophage conditioned medium (diluted 1:4 in EBM basal medium with 2 % FCS) did not significantly improve HPMEC wound closure; however, PGD_2 treatment of macrophages delayed wound healing to a small extent (**Figure 41**C and D). The observed differences may seem negligible, yet wound healing and tissue regeneration are processes that progress over a long time. Thus, effects may add up over time to significantly impact regenerative progression. Consequently, we decided to follow up on this notion and further explore the effect of PGD_2 stimulation on human MDM and their effect on endothelial cell function.

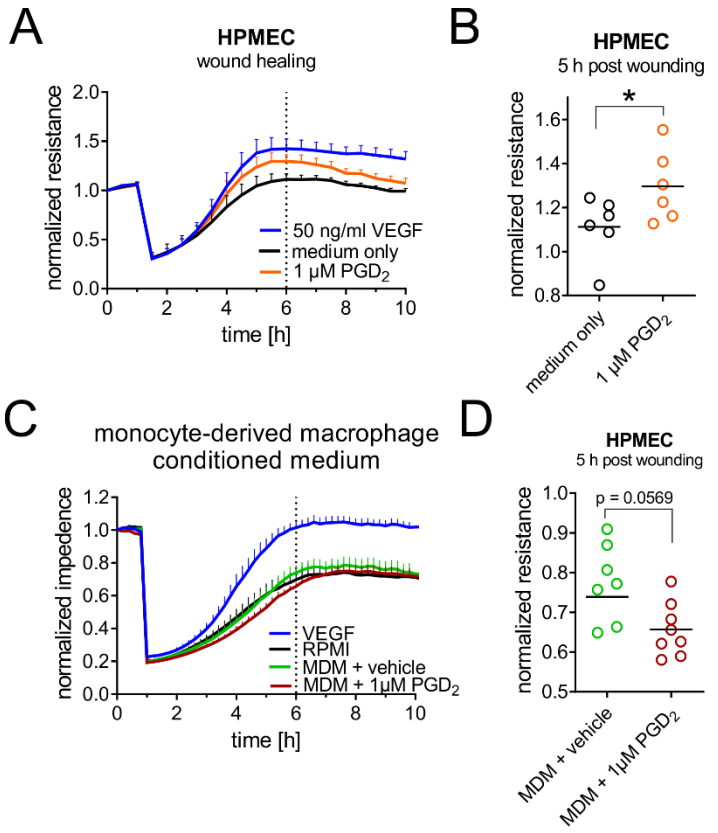

Figure 41. PGD_2 significantly promotes HPMEC wound healing capacity, while PGD_2 stimulation of human MDM delays wound closure. (A) HPMEC treatment with 1 µM PGD_2 at the time of wounding accelerated the recovery, even exceeding starting conditions (n = 6). (B) Five h post wounding, HPMEC wells treated with 1 µM PGD_2 showed significantly higher normalized resistance values (n = 6). (C and D) Conditioned medium from human MDM that had been treated with 1 µM PGD_2 (1:4 dilution) reduced this effect by trend 5 h post wounding (n = 7). Mean + SEM, paired t-test, * $p<0.05$.

PGD_2 modifies primary human M2-like monocyte-derived macrophage morphology, but not CD206, CD80 or CD163 expression. Alternatively activated (M2-like) macrophages are key mediators of the resolution and regeneration phase of inflammation. Therefore, we were curious whether DP receptor activation on M2-like macrophages modulates HPMEC function more prominently. Various subdivisions of the M2-like phenotype exist due to differential polarization stimuli. Here, we differentiated monocyte-derived macrophages with M-CSF and additionally activated the cells with IL-4 or IL-10, often referred to as M2a or M2c macrophages, respectively. Macrophage morphology is a good indicator of polarization state and often correlates with functional divergence. It is known that pro-inflammatory LPS/IFN-γ activation causes elongation of cells and formation of cell aggregates (278), which we could confirm in our model. IL-4 or IL-10 activated macrophages were enlarged and flattened, while IL-10-activated cells had an elongated or round morphology. To ensure a successful activation of MDM to M2a or M2c, we additionally evaluated phenotypic surface marker expression in vehicle-treated macrophages after collection of conditioned medium. M-CSF-differentiated MDM already express basal levels of

CD206 and CD163, while CD206 was significantly upregulated in M2a and CD163 in M2c macrophages, respectively (**Figure 42** A and B). Interestingly, PGD_2 treatment during macrophage polarization caused an increase of cell aggregates in alternatively activated macrophages, especially IL-4 activated cells, as well as more elongated cells, which would indicate a change in polarization state of treated cells to a pro-inflammatory phenotype (**Figure 42**C). A schematic representation of MDM stimulation and PGD_2 treatment is shown in **Figure 42**D. To elaborate on these observations, macrophages were collected after collection of conditioned medium and the effect of PGD_2 on activation marker CD80, CD206 and CD163 expression was analysed. Notably, the effects of PGD_2 treatment on surface marker expression levels seem to be minor as no significant differences could be observed (**Figure 42**E).

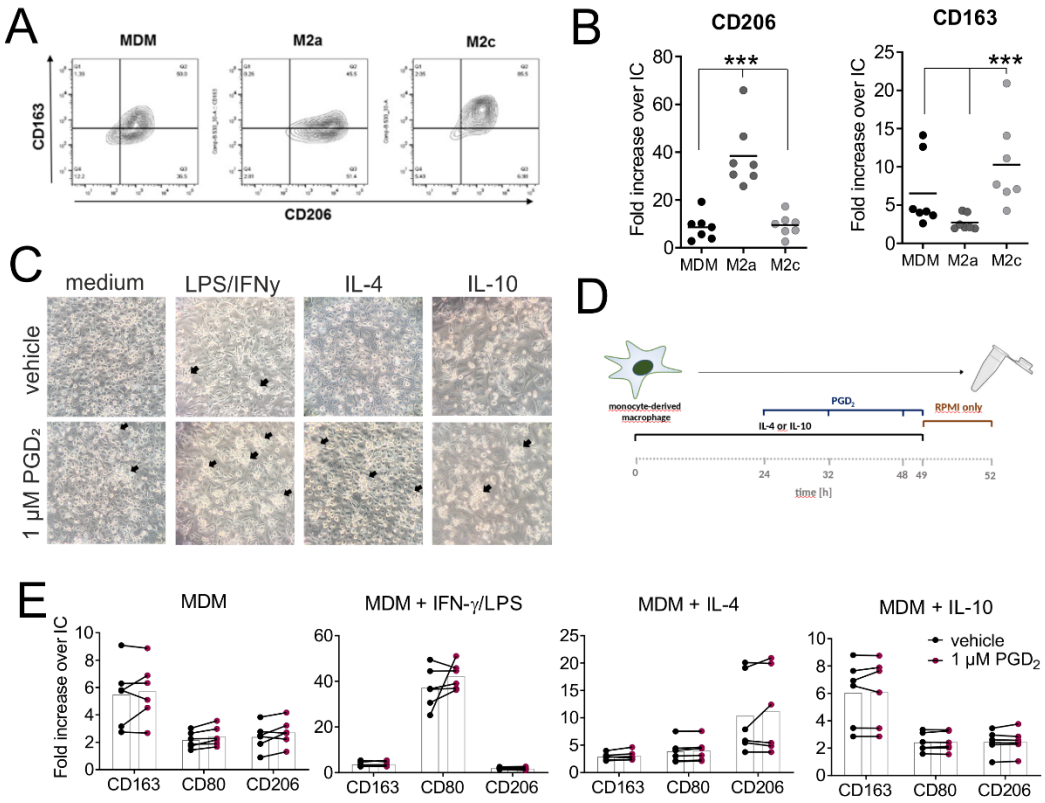

Figure 42. **PGD_2 modifies primary human M2-like monocyte-derived macrophage morphology, but not CD206, CD80 or CD163 expression**. (A) Contour plots of CD163 and CD206 receptor expression in MDM, M2a (IL-4) and M2c (IL-10) macrophages obtained by flow cytometry. Cut-off was determined with respective isotype controls. (B) CD206 was significantly upregulated by IL-4 in M2a macrophages, while M2c macrophages showed an upregulation of CD163 by IL-10 polarization (n = 7). (C) Representative images of vehicle or 1 µM PGD_2-treated human MDM,

M1 (LPS/IFN-γ), M2a and M2c macrophages. Arrows indicate cell clusters typical for LPS/IFN-γ activated MDM. (D) Schematic representation of primary human macrophage activation and PGD_2 treatment. . (E) PGD_2 stimulation of MDM during activation with different cytokines did not affect CD163, CD80 and CD206 expression (n = 6). One-way or two-way ANOVA for repeated measurements with Tukey's *post hoc* test, *** $p<0.001$)

PGD_2-primed M2-like macrophages differentially regulate HPMEC wound healing. Efficient inflammatory resolution does not only include efferocytosis of apoptotic immune cells by macrophages but also relies on efficient tissue regeneration, i.e. ECM deposition, regulated re-growth of vasculature and restoration of epithelial and endothelial barrier. In macrophages, efferocytosis initiates the release of anti-inflammatory and angiogenic factors such as IL-10, VEGF and TGF-β, while at the same time impairing TNF-α, IL-6 and IL-1β (279). Consequently, we now set out to look more thoroughly into how M2-like macrophages affect pulmonary microvascular endothelial recovery after wounding. As we saw different effects of IL-4 and IL-10 activated macrophage conditioned medium on eosinophils in the previous experiment, we assumed that potentially also macrophages derived from atopic and non-atopic donors may display altered function. To follow up on this hypothesis, human MDM differentiated from atopic or non-atopic donors were stimulated three consecutive times with PGD_2 during polarization with IL-4 or IL-10 as shown in **Figure 42**D. Indeed, conditioned media collected from these cells was able to influence HPMEC wound healing. This was partly dependent on IL-4 or IL10-induced polarization but, remarkably, MDM originating from atopic or non-atopic monocytes resulted in a different effect. Only PGD_2 treatment of non-atopic M2c improved HPMEC wound healing, while non-atopic M2a conferred a similar wound healing effect with and without treatment (**Figure 43**B and A, respectively). HPMEC treated with conditioned media from M2a and M2c derived from atopic donors recovered earlier, while PGD_2 treatment of atopic M2a delayed the recovery (**Figure 43**C). These results suggest that already in circulation, monocytes of atopic subjects are primed somehow, which persists in monocyte-derived macrophages modulating their function. Further, the differential effects on HPMEC wound healing may be due to a change in cell death, migration or proliferation. Therefore, we looked at changes in cell cycle, however, direct PGD_2 treatment (**Figure 44**B) or atopic M2-like macrophage CM did not influence HPMEC cell cycle within 24 h stimulation (**Figure 44**C).

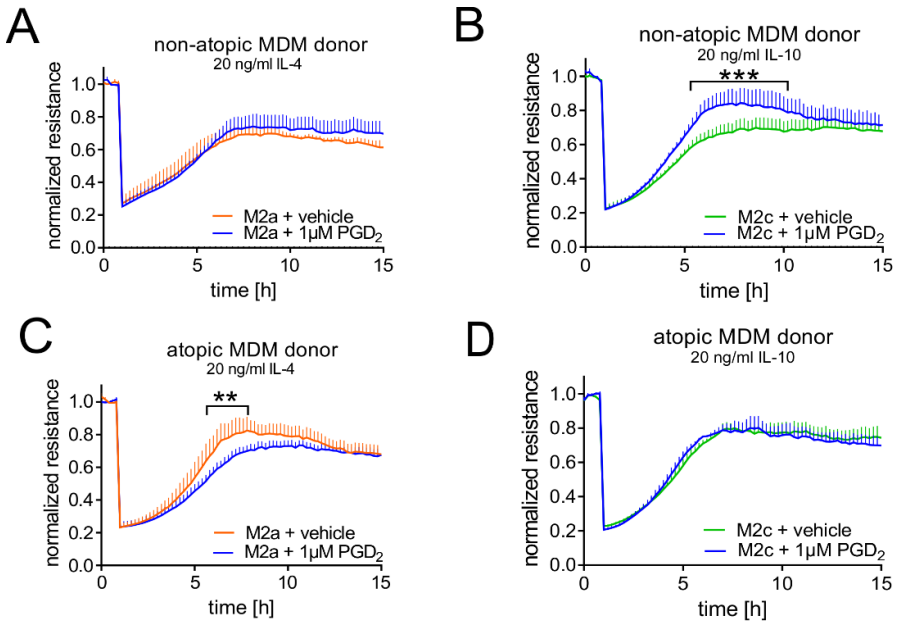

Figure 43. PGD_2-primed M2-like macrophages differentially regulate HPMEC wound healing. Conditioned medium was generated as described in **Figure 42**. (A) PGD_2 stimulation did not change HPMEC wound healing response by conditioned medium (diluted 1:4) from non-atopic MDM donors activated with IL-4. (B) In contrast, PGD_2 stimulation resulted in enhanced wound healing response to conditioned medium from non-atopic MDM donors activated with IL-10. (C) PGD_2 stimulation of atopic IL-4 activated macrophages significantly reduced wound healing response, while (D) no effect could be seen with conditioned medium from atopic IL-10 activated macrophages. Two-way ANOVA for repeated measurements with Sidak's *post hoc* test, ** $p<0.01$, *** $p<0.001$, n = 5; mean + SEM.

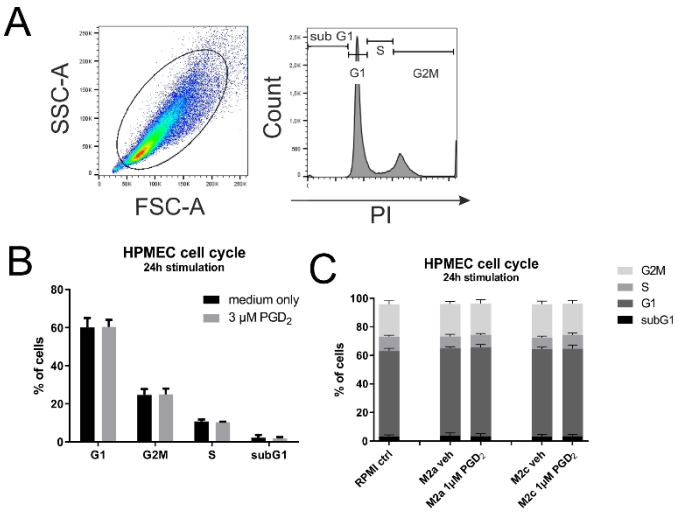

Figure 44. Atopic M2-like macrophage conditioned medium does not influence HPMEC cell cycle within 24 h. (A) Representative pseudo-colour plot of HPMEC and gating strategy to determine the proportion of cells in subG1, G1, S and G2M phase of cell cycle with propidium iodide (PI). (B) Stimulation with 3 µM PGD_2 did not affect HPMEC cell cycle. (C) No shift in cell cycle phases could be observed between HPMEC incubated with RPMI control, M2a or M2c conditioned medium (1:10 in EBM-2 incomplete medium) (n = 4; mean + SEM).

PGD_2 stimulation of IL-4 polarized MDM reduces sprouting of HPMEC and angiogenesis in the CAM angiogenesis assay. We continued to investigate the effect of PGD_2-primed M2 macrophages on endothelial cell function, by focusing on IL-4 polarized human MDM, as this is the major phenotype seen in chronic pulmonary inflammation, i.e. allergic asthma (195). Tissue regeneration and wound healing is dependent on tightly regulated, but at the same time efficient, angiogenesis. Sprouting angiogenesis harbours the initiation of neo-vascularization; hence, our next aim was to explore the effect of PGD_2-stimulated M2a macrophages on 3D endothelial sprouting. Human microvascular endothelial cell spheroids (~1000 cells per spheroid) were generated using the hanging drop technique and seeded within a collagen matrix. After collagen polymerization, spheroids were stimulated for 16 h with medium only (as negative control), a combination of 25 ng/ml VEGF-A, 10 ng/ml basic FGF and 10 ng/ml TNF-α (as positive control) or macrophage conditioned medium (1:5) in sprouting medium (M199 medium (Lonza) supplemented with 10 % human AB serum (Gibco) and 10% new born calf serum (Gibco)). Indeed, conditioned medium from IL-4 polarized human MDM increased cumulative sprout length by trend compared to negative control. Critically, treatment of these IL-4 polarized MDM with PGD_2 significantly blunted sprout formation (**Figure 45**A) as can also be seen in the representative pictures obtained for one endothelial cell donor (**Figure 45**B). This a completely novel observation as it has not been considered before that PGD_2 may impact the angiogenic capacity of macrophages.

To follow up on these results, we conducted an *ex vivo* angiogenesis assay using the chicken chorioallantoic membrane (CAM) model. Representative images for one out of three macrophage donors (3 eggs with 3 silicone rings per condition for each donor) are shown in **Figure 45**C. Treatment was applied to silicone rings that have been directly placed onto the CAM and incubated for 72 h. The regions treated with the positive control (25 ng/ml VEGF, 10 ng/ml bFGF, 10 ng/ml TNF-α) showed an increased number of small vessels sprouting from medium sized vessels in comparison to the chorioallantoic membrane outside of silicone rings. Similar effects could be seen with M2a conditioned medium. In contrast, conditioned medium from M2a treated with 1 µM PGD_2 caused a reduction of the smallest vessels sprouting from medium vessels. To quantify this, we used collagen onplants on nylon grids, either containing a certain volume of the positive control (VEGF, bFGF, TNF-α) or conditioned medium, that were placed onto the CAM and incubated for 72 h. On the third day, we quantified the number of positive panels, i.e. panels showing small

vessels that had grown into the nylon grid sandwich, counted by a blinded operator while embryos were provided by another person not familiar with tested substances. The positive control yielded about 40 % positive panels, while application of M2a conditioned media had a comparable effect. Notably, PGD_2 treated macrophage-conditioned medium significantly reduced the number of positive panels (**Figure 45**E), which further reinforced our hypothesis that DP receptor activation on macrophages affects vascular regeneration. However, no differences between atopic and non-atopic MDM donors could be seen (data not shown).

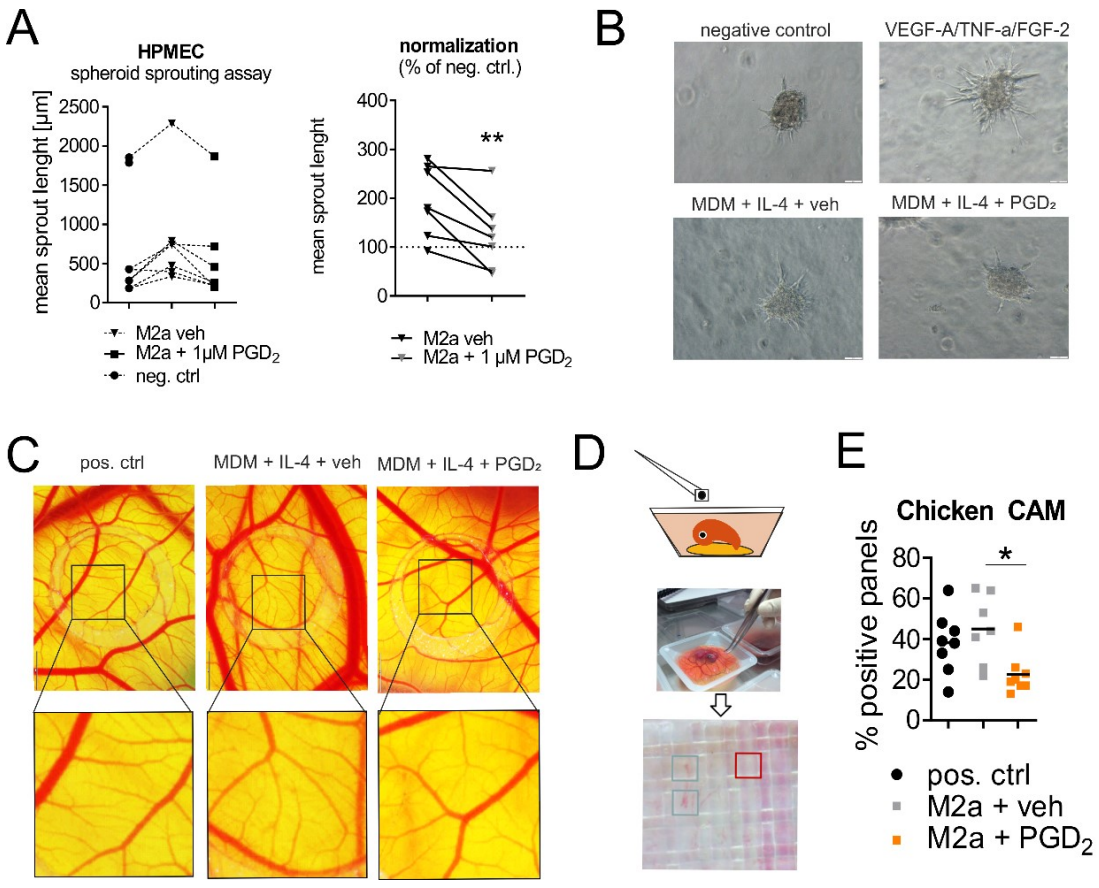

Figure 45. PGD_2 stimulation of human IL-4 polarized macrophages impairs sprouting angiogenesis. Human monocyte-derived macrophages were stimulated as indicated in **Figure 42**. After stimulation, cells were incubated for 3 h in RPMI only and this conditioned medium was used for sprouting experiments (diluted 1:5) (A) M2a-conditioned medium induces sprouting angiogenesis to an extent comparable with the positive control in human pulmonary microvascular endothelial cells, while macrophage treatment with 1 µM PGD_2 diminished this effect (n = 7). (B) Representative light microscopy images obtained for HPMEC spheroids. (C) Representative images for direct

application of positive control/conditioned medium onto chicken chrorioallantoic membrane (CAM) (n = 9, 3 eggs for 3 MDM donors). (D) Schematic describing the placement of collagen onplants onto chicken CAM for evaluation of angiogenic potential. Vessel growth into nylon grids (green boxes) were enumerated to calculate the percentage of positive panels. Red box: negative panel. (E) Quantification of vessel growth into collagen grids containing treatments (n = 7 eggs, 4 MDM donors). Paired t-test or one-way ANOVA for repeated measurements with Tukey's *post hoc* test, * $p<0.05$, ** $p<0.01$. Positive control: 25 ng/ml VEGF-A, 10 ng/ml TNF-α, 10 ng/ml bFGF.

Repeated PGD_2 stimulation during polarization of MDM derived from healthy or atopic donors results only in minor changes of their angiogenic secretome. As we saw a potent inhibitory effect on endothelial cell sprouting and *ex vivo* angiogenesis of PGD_2-stimulated, IL-4-polarized macrophage-conditioned medium, we next used a Western blot-based ProteomeProfiler angiogenesis array (R&D Biosystems) to determine changes in the angiogenic secretome. This assay allows parallel evaluation of 55 different angiogenesis-related proteins in cell lysates or conditioned medium. The angiogenesis kit membranes were incubated with conditioned medium (500 µl) from vehicle or 1 µM PGD_2-treated IL4-polarized human MDM and vehicle treated controls. ProteomeProfiler plots from one donor of PGD_2-treated M2a conditioned medium are shown. In **Figure 46**C, a selection of results obtained from 3 donors (2 healthy, 1 atopic) were plotted to observe differences in expression levels. As we had seen a different effect of MDM derived from atopic versus healthy donors on endothelial wound healing in combination with PGD_2, we decided to present data from both, an atopic and a non-atopic donor, for comparison. Densitometric values obtained from membranes were normalized to respective vehicle treated M2a values and the changes were displayed in a heat map as fold change over M2a vehicle control (**Figure 46**D). These data did not result in significant hits; however, several proteins appeared to be differentially regulated between the atopic and non-atopic donor, which had been differentiated and stimulated in parallel. Firstly, serpin E1 and MCP-1 were downregulated, while VEGF, uPA, thrombospondin-2, PDGF-AA, TGF-β1, endostatin and amphiregulin were upregulated by trend in both donors after PGD_2 stimulation. Notably, serpin F1, serpin B5, PIGF, leptin, angiostatin, angiopoietin-1/2 were regulated by trend in an opposing way in macrophages from atopic and non-atopic donors. Due to considerable differences between donors, we will have to increase our n numbers to enable a reliable readout. At this moment, no specific conclusion can be drawn from these data.

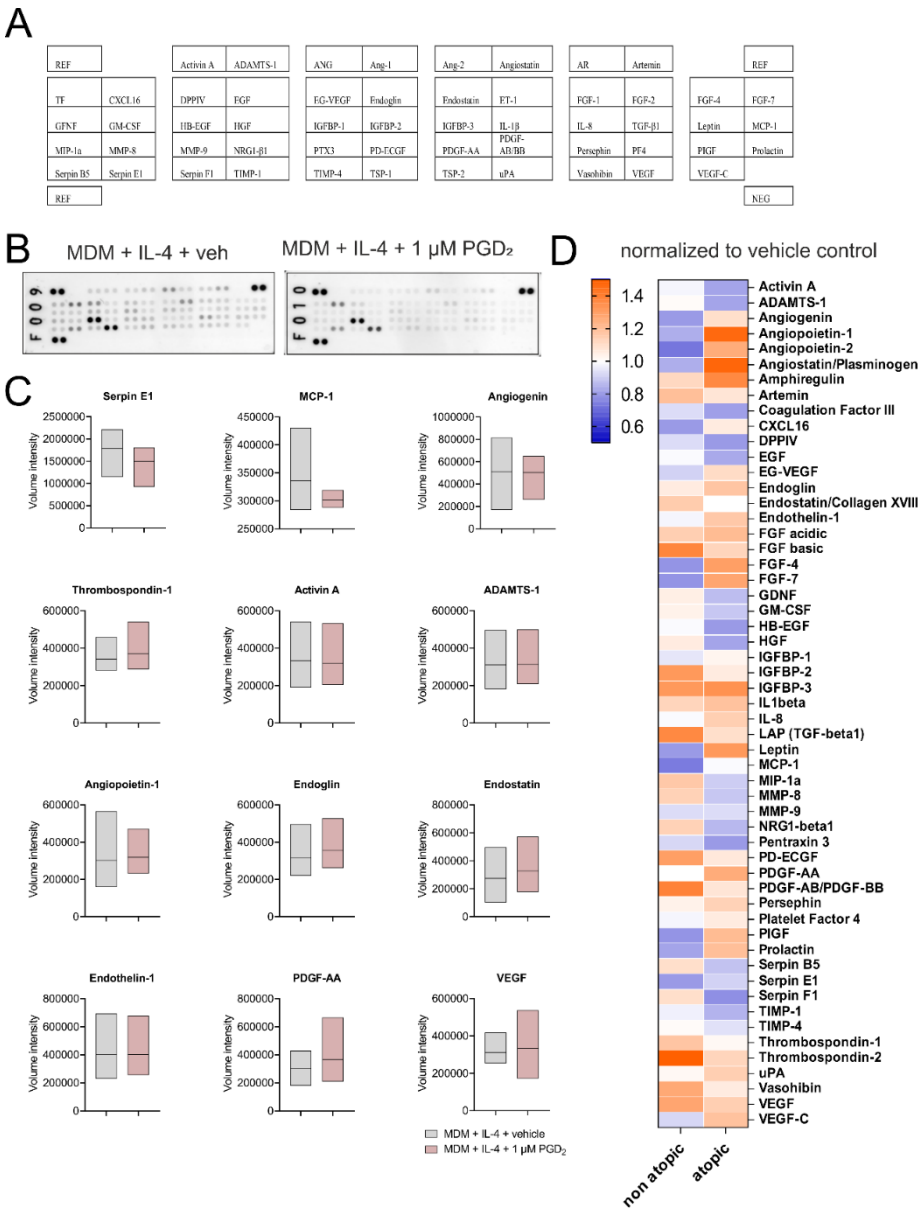

Figure 46. Repeated PGD_2 stimulation during polarization of MDM derived from healthy or atopic donors results only in minor changes of their angiogenic secretome. Human monocyte-derived macrophages were stimulated as indicated in **Figure 42**. After stimulation, cells were incubated for 3 h in RPMI only and this conditioned medium was used (500 µl, 1:3). (A) Coordinates for Human Angiogenesis Array (R&D Systems). (B) Representative blots obtained for MDM + IL4 vehicle control and cells additionally stimulated with 1 µM PGD_2. (C) Volume intensity values for selected factors were plotted for statistical evaluation. Data are shown as MIN-MAX plots, n = 3. (D) Heat map shows values obtained from one non-atopic and one atopic donor normalized to MDM + IL-4 vehicle control, differentiated and treated in parallel, for comparison.

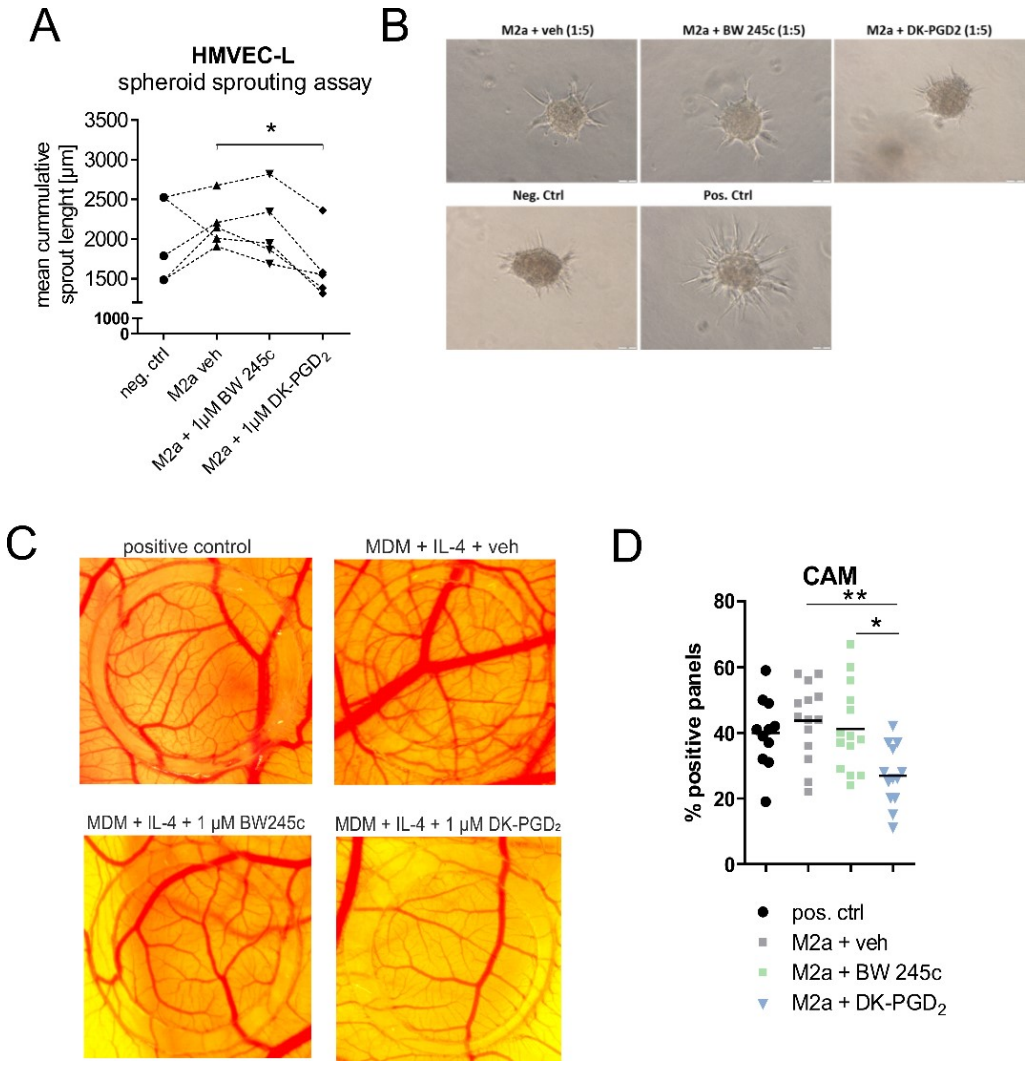

Figure 47. DP2 activation on human IL-4 polarized macrophages impairs sprouting angiogenesis. Human monocyte-derived macrophages were stimulated as indicated in **Figure 42**. After stimulation, cells were incubated for 3 h in RPMI only and this conditioned medium was used for experiments (1:5 dilution) (A) M2a-conditioned medium induces sprouting angiogenesis in human pulmonary microvascular endothelial cells, while treatment with 1 µM DK-PGD_2 (DP2 agonist) reversed this result. BW 245c (DP1 agonist) had no effect (n = 5). (B) Representative light microscopy images obtained for HPMEC spheroids. (C) Representative images for direct application of positive control/conditioned medium onto chicken chrorioallantoic membrane (CAM) (n = 3 x 3-4 eggs for 4 MDM donors). (D) Quantification of vessels grown into collagen grids containing treatments (each individual dot represents one egg, 4 MDM donors). One-way ANOVA for repeated measurements with Tukey's *post hoc* test, * $p<0.05$, ** $p<0.01$. Positive control: 25 ng/ml VEGF-A, 10 ng/ml TNF-α, 10 ng/ml bFGF.

DP2 activation on human MDM in the presence of IL-4 reduces angiogenic properties of conditioned media. Our data showed that PGD_2 treatment of human macrophages changes their ability to modulate angiogenic endothelial cell function. To evaluate which DP receptor is responsible for these effects, we treated human MDM with 1 µM DP1 agonist BW245c or DP2 agonist DK-PGD_2 during polarization with IL-4. BW245c treatment did not change the positive effect of M2a-conditioned medium on human microvascular endothelial cell sprouting, while DP2 activation significantly reduced cumulative sprout length (**Figure 47**A). Representative images are shown in **Figure 47**B. We could observe the same effect on *ex vivo* angiogenesis in the CAM assay, where DP2 receptor activation on macrophages was clearly responsible for the reduction of vessel ingrowth (**Figure 47**C and D). Here, we could not see differences between conditioned medium from atopic and non-atopic MDM donors (data not shown). These results show that DP2 activation on human MDM was responsible for impaired angiogenesis by macrophage-conditioned medium.

Conditioned medium from DP receptor agonist-treated, IL-4 polarized human monocyte-derived macrophages differentially affects HPMEC resistance. Reduced endothelial barrier function is a typical feature of endothelial dysfunction and is also considered as an indicator of neovascularization, e.g. a strong endothelial barrier function and reduced vascular permeability has been shown to limit angiogenesis (32). To observe the effect of macrophage-conditioned medium on HPMEC barrier, IL-4 polarized macrophages were stimulated with DP1 receptor agonist BW245c (1 µM) or DP2 receptor agonist DK-PGD_2 (1 µM) according to the same scheme as mentioned in **Figure 42**. Interestingly, microvascular endothelial cells treated with conditioned medium from M2a with activated DP2 receptors (diluted 1:5 in EBM basal medium with 2 % FCS) elevated endothelial barrier most potently (**Figure 48**). Notably, M2a-conditioned medium did not reduce barrier function, as would have been expected for a pro-angiogenic stimulus.

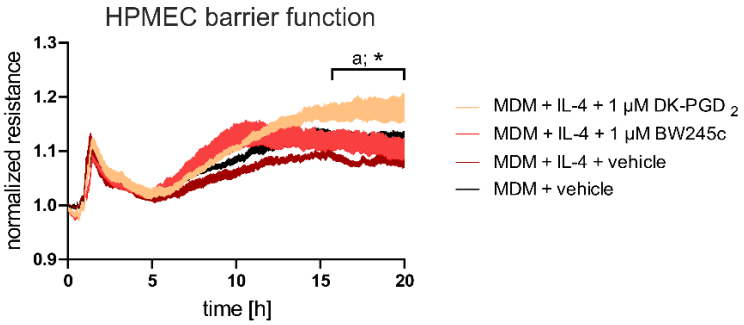

Figure 48. DP receptor activation on human IL-4 polarized macrophages increases microvascular endothelial resistance. Human monocyte-derived macrophages were stimulated as indicated in **Figure 42**. After stimulation, cells were incubated for 3 h in RPMI only and this conditioned medium was used for ECIS experiments (1:5). Data shown as mean + SEM, n = 4, two-way ANOVA for repeated measurements with Tukey's *post hoc* test, a: *p<0.05 difference between MDM + IL-4 + vehicle and MDM + IL-4 + DK-PGD_2.

DP1 and DP2 receptor activation on human IL-4 polarized macrophages differentially affect angiogenic secretome of macrophages. To further explore the involvement of DP1 and DP2 receptors on MDM-induced angiogenic effects, we performed the ProteomeProfiler assay with conditioned media from one atopic and two non-atopic MDM donors stimulated with DP agonists and normalized the results to the densitometric values obtained for vehicle treated M2a. This allowed us to observe which genes were regulated by BW245c (DP1) or DK-PGD_2 (DP2) in IL-4 primed macrophages. The heat map shown in **Figure 49**B shows the mean values calculated from three MDM donors. Several proteins appeared differentially regulated by DP1 or DP2 activation, some only by trend due to variations between human MDM donors. Preliminary observations include that DP1 receptor activation induced VEGF, uPA, endoglin, TIMP-4, thrombospondin-1/2, PGDF amongst others, while DP2 activation had the opposite effect. Further, DP2 receptor activation with DK-PGD_2 significantly reduced endoglin and angiopoietin-1 expression, while PDGF-AB and endostatin were reduced by trend (**Figure 49**C). Other potential downregulated candidates were ADAMTS-1, VEGF and endothelin. Interestingly, activin-A, which is overexpressed in severe asthma and has anti-angiogenic effects (280), was upregulated by trend in conditioned media from DK-PGD_2-stimulated M2a macrophages. Due to considerable differences between donors, we will have to increase our n numbers to enable a reliable readout. At this moment, no specific conclusion can be drawn from these data.

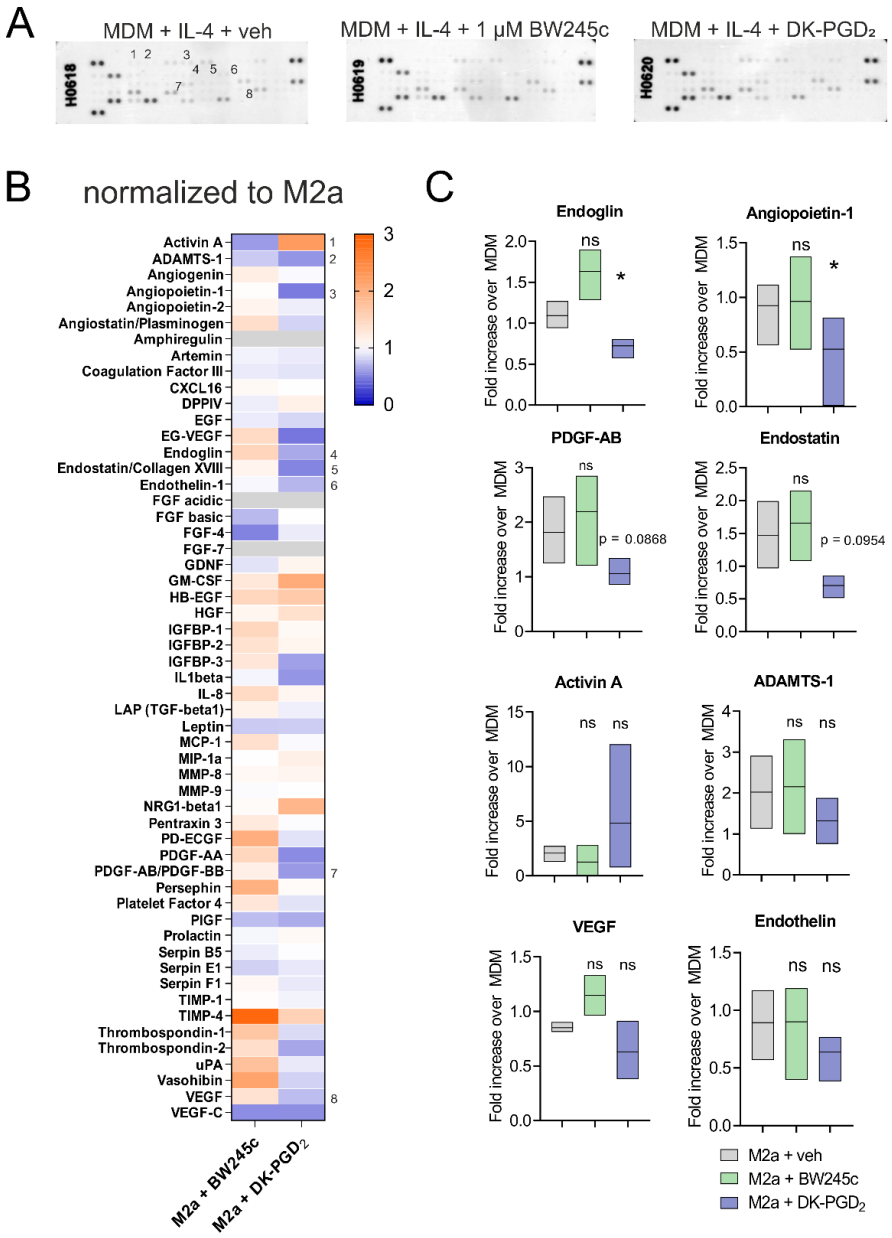

Figure 49. DP1 or DP2 receptor activation on human IL-4 polarized macrophages differentially affects angiogenic secretome of macrophages. Human monocyte-derived macrophages were stimulated as indicated in **Figure 42**. After stimulation, cells were incubated for 3 h in RPMI only and this conditioned medium was used (500 µl, 1:3). (A) Representative blots obtained for MDM + IL4 vehicle control, BW245c and DK-PGD$_2$ stimulated cells (B) Heat map shows mean fold increase values (2 non-atopic and 1 atopic donor) normalized to MDM + IL-4 vehicle control. Eight promising factors are indicated in corresponding blots. (C) Values obtained after normalization to MDM control for selected factors were plotted for statistical evaluation. Data are shown as MIN-MAX plots, n = 3, One-way ANOVA for repeated measurements with Fisher's LSD *post hoc* test, * $p<0.05$. Heatmap: values outside the defined range are shown in grey.

4. Discussion

In the development of novel anti-inflammatory agents, reduction of PGD_2 production or blockade of PGD_2 signalling has been of great interest; however, PGD_2-induced signalling has proven to be more complex than previously thought. Its action depends on many factors including the target cells, its concentration, and activation of various GPCRs (1,83). Opposing effects of PGD_2 have been interrelated with singular or combined activation of DP receptors (82), a biphasic pattern of increased PGD_2 levels in the early phase as well as the late phase of inflammation (281) acting on a variety of target cells while bioactive PGD_2 metabolites add additional modulations (10). The application of different experimental models hinders general conclusions, thus, further complicating a definite classification of PGD_2 as either pro- or anti-inflammatory lipid mediator. This thesis focuses on expanding the knowledge of PGD_2-elicited effects on the innate immune response in the lung. We could (i) show that PGD_2 is able to activate EP4 receptors on human endothelial cells and, in this manner, limits endothelial permeability, (ii) explore hPGDS expression, the rate-limiting enzyme for PGD_2 production, in human and murine leukocyte subsets and characterize human monocytes as potent PGD_2 sources in presence of LPS/IFN-γ and (iii) reveal that DP2 activation on human IL-4 polarized monocyte-derived macrophages compromises their angiogenic potential.

4.1 PART I: E-type receptor 4 mediates PGD_2 enhancement of pulmonary endothelial barrier function

The aim of Part I was to clarify how PGD_2 influences barrier function in human pulmonary endothelial cells. Endothelial cell integrity and intact barrier function are crucial to limit leukocyte and plasma extravasation during inflammation. Most anti-inflammatory effects of PGD_2 have been attributed to DP1 receptor activation on immune, epithelial or endothelial cells (48,56,68,71). In contrast, PGD_2-DP1 activation has also been shown to induce cough in guinea pigs (72) as well as increased mucus production and airway hyper-reactivity in a mouse model of allergic asthma (73), hence, making it a controversial therapeutic target.

In acute and chronic inflammatory reactions, endothelial cell activation leading to sustained microvascular leakage is one of the primary causes of leukocyte extravasation and oedema

formation (115,282). A previous study suggested that PGD_2, in comparison to other arachidonic acid-derived lipid mediators, had only a minor effect on pulmonary artery endothelial cell barrier (283). Here, we could show that primary HPMEC barrier integrity improved after PGD_2 or BW245c stimulation, although to a lesser extent than in HDMEC (2). The underlying reasons for stronger effects in HDMEC, even though HPMEC and HDMEC express similar EP4 receptor mRNA levels, might be due to differences in intracellular signal transduction or different expression levels of barrier-associated proteins, e.g. VE-cadherin, already in basal state. In HPMEC, stimulation with PGD_2 or the DP1 agonist BW245c but not the DP2 antagonist, DK-PGD_2 counteracted thrombin-induced barrier disruption as evaluated by quantification of stress fibre and gap formation and the extent of VE-cadherin barrier disruption. Notably, the PGD_2-elicited response in HPMEC was only partially reversed by pre-incubation with the DP1 receptor antagonist BWA868c, which was consistent with previous findings in HDMEC (68). In fact, a BWA868c concentration of 30 µM was required to achieve a small inhibitory effect against 3 µM PGD_2 stimulation. This was an unexpected observation as we could show in a previous study, that a BWA868 concentration of 100 nM was sufficient to diminish inhibition of platelet aggregation by 30 nM PGD_2 (284), implying a much greater importance of this signalling in platelet biology. Furthermore, pre-treatment of cells with MK0524, an antagonist and inverse agonist of the DP1 receptor, did not diminish but rather enhance the PGD_2 effect, which largely excludes the involvement of DP1 receptors. DP1 and DP2 receptors may form DP2/DP1 heteromers and modulate each other's signalling properties (274). Therefore, antagonism of both receptors might be required to inhibit downstream signalling; however, in primary human microvascular endothelial cells the combined blockade of DP1 and DP2 receptors did not inhibit the PGD_2-induced effect.

As PGD_2 is a highly promiscuous ligand and can bind to a number of other receptors, we checked whether PPARγ or TP receptor signalling was involved. TP receptor blockade did not affect PGD_2-induced barrier enhancement in microvascular endothelial cells. Pre-treatment with the PPARγ antagonist T0070907 caused a transient reduction of endothelial resistance, most likely due to modulating tight junction proteins, as previously suggested (106). Stimulation with PGD_2 increased HPMEC resistance but the delta-increase was reduced in comparison to vehicle pre-treated cells. As previously mentioned, we observed an increase in VE-cadherin staining in PGD_2-

treated endothelial cells, while inhibition of PPARγ signalling might interfere with this effect. To see whether this is a direct PGD_2-PPARγ-induced effect still requires further investigation; however, we do not believe that this is the main pathway included in this effect.

Interestingly, we found that PGD_2 and BW245c-provoked barrier enhancement was unchanged after adenylate cyclase or PKA inhibition (2). This contradicts the proposed cAMP/PKA signalling pathway for DP1 receptor-mediated barrier enhancement (68). In contrast, PGE_2-EP4 induced barrier protection is independent from cAMP/PKA (100). These observations strengthen our notion that the PGD_2 and BW245c effect is unlikely to be mediated through a DP1-dependent mechanism. On the contrary, as we knew that also PGE_2-EP4 induced barrier enhancement is independent from cAMP/PKA, we hypothesised that the EP4 receptor might be involved in PGD_2-induced effects as well. Also, PGE_2 like PGD_2/BW245c-induced effects were tremendously reduced when actin polymerization was impaired.

Further, we used PGE_2 as positive control throughout our experiments and saw the same pattern of changes in trans-endothelial resistance and VE-cadherin staining, albeit to a lower extent, after PGD_2/BW245c treatment. This strengthened out notion that PGD_2 might also be able to act through activation of EP4 receptors. Findings by Lydford et al. support this, as they indirectly concluded from pharmacological studies using rabbit saphenous vein that (i) the DP1 antagonist BWA868c has some affinity for EP4 receptors and (ii) PGD_2 as well as BW245c-induced vasorelaxation was likely to be mediated through EP4 receptor activation (108). The partial inhibition of barrier enhancement by BWA868c is, thus, most likely due to inhibition of EP4 receptor signalling. Indeed, blockade of EP4 receptors using two distinct EP4 antagonists fully reversed PGD_2-induced barrier enhancement in both, pulmonary microvascular and arterial endothelial cells (2). This concept is supported by two previous reports that PGD_2 may bind to and activate EP4 receptors overexpressed in HEK cells with low affinity: competition in radio-ligand binding PGD_2-EP4 Ki 1483 ± 189 nM (PGE_2-EP4 Ki 0.79 ± 0.07 nM) (83) or PGD_2-EP4 mediated cAMP production EC_{50} 1664 nM (PGE_2-EP4 EC_{50} 0.3 nM) (107). These data suggest that the affinity of PGD_2 to human EP4 receptors is approximately 1500-fold lower than of PGE_2. In contrast, PGD_2 relaxed rabbit saphenous vein with 200-fold lower potency (EC_{50}) than did PGE_2 (108), while from our results we estimate that the difference in potency with regard to TEER enhancement is close to 30-fold (2).

Our experiments did not reveal any obvious differences in EP4 mRNA expression levels between the different cell types, and also pulmonary artery and microvascular responses to PGD_2 and BW245c were similar. We observed very low mRNA expression of DP1 and DP2 receptors but much higher levels of EP4 receptor mRNA in primary human endothelial cells, which underlines the greater influence of EP4 receptors in endothelial cell function. A previous study used immunohistochemistry as well as mRNA expression analysis to show higher EP4 expression in human pulmonary veins in comparison to arteries (285), which might be a relevant factor in an *in vivo* setting. We could see a similar pattern in human lung sections stained with anti-EP4 antibodies, which suggests a potentially greater influence of EP4 receptors on venous endothelial cell function. Further, immunohistochemistry of human lung sections revealed distinct DP1 receptor staining in endothelial cells, but less pronounced than EP4 (2). Hence, it has to be considered that the DP1 receptor might play a stronger role *in vivo* than the observed effects in our *in vitro* test system.

Finally, we could demonstrate unambiguously the involvement of the EP4 receptor in primary human microvascular cells, via EP4 receptor knock down experiments, which resulted in the total loss of PGD_2 and BW245c-elicited effects (2). Even though the knock down was incomplete (30 % remaining mRNA) the barrier enhancement by PGD_2 and BW245c was eradicated. An explanation for this may be the rather low affinity of these ligands to EP4, such that a combination of high receptor expression levels and relatively high levels of agonist may be essential for an efficient cellular response.

To further explore the mechanistic details of the observed PGD_2-EP4 mediated effect, we checked phosphorylation of proteins involved in cytoskeletal rearrangement. Kinase-induced protein phosphorylation is an important regulator of endothelial permeability as reviewed in (286). As an example, it has been reported that Src-dependent tyrosine phosphorylation of focal adhesion kinase and VE-cadherin disrupted adherens junctions of human brain and pulmonary microvascular endothelial cells (287,288). However, phosphorylation state of VE-cadherin, focal adhesion kinase and paxillin, a protein involved in tethering actin filaments to adherens junctions, were unchanged after PGD_2 or PGE_2 treatment. Vascular permeability may also be modulated by other mechanisms targeting cytoskeletal integrity and contractility including activation of downstream GTPases, e.g. Rho-dependent actin stress fibre formation followed by Rac-dependent cell rounding and

retraction. Konya et al. could not reverse PGE_2 induced barrier effects with PI3K, PKC, endothelial NO synthase (eNOS) or Rac-1 inhibition (100), therefore, we decided to focus on other possibilities. Interestingly, barrier disruptive agents, including VEGF (275) and LPS (276), induce phosphorylation of AKT (i.e. PI3K and eNOS activation), which has been linked to endothelial cell permeability, increased contractility and migration. Significantly, stimulation of HPMEC with PGE_2 and PGD_2 for 30 min reduced AKT phosphorylation. Thus, we suggest that PGE_2, PGD_2 and BW245c enhance endothelial barrier by decreasing phosphorylation of AKT and downstream substrates, possibly including eNOS. Notably, endothelial NO synthase-derived nitric oxide has been shown to induce transient vascular permeability by regulating changes in cytoskeletal rearrangement (289). As PGD_2 and PGE_2 rather limit PI3K and eNOS activity than activate their function, this is most likely the reason Konya et al. did not see a difference with these inhibitors.

As mentioned above, many of the anti-inflammatory effects for PGD_2 were attributed to DP1 receptor activation. Since its discovery in 1983, BW245c has been the most commonly used DP1 agonist in cellular, preclinical and clinical studies (72,290–293) and its specificity has been thoroughly studied (83). DP1 receptor or hematopoietic PGD synthase knock-out mice in combination with BW245 treatment revealed reproducible, protective effects against vascular leakage, tumour angiogenesis and inflammation (48,123,294,295). In mice, DP1 receptor signalling results predominantly in anti-inflammatory effects; yet, there are indications that prostanoid receptor signalling varies vastly among different species. Certain discrepancies concerning the role of DP1 receptor activation in human and murine eosinophil function has been described (34); DP1 receptor activation has been shown to attenuate eosinophilic inflammation in a murine model of chronic allergic lung inflammation (294) but at the same time prolongs human eosinophil survival (36). Further, PGE_2 induces relaxation by activation of EP2 receptor in mice, guinea pigs and monkey trachea, while in human and rat the relaxation is EP4 receptor mediated (296). Following this line of thought, our results indicate that EP4, but not DP1, is the primary receptor responsible for PGD_2-induced improvement of barrier function in human endothelial cells.

One may speculate, however, that in the context of severe pulmonary inflammatory responses, such as acute lung injury or exacerbations of chronic inflammation, PGD_2-EP4-induced enhancement of endothelial barrier may have a pivotal role in limiting oedema formation. Bacterial products i.e. LPS have been shown to induce PGD_2 production in murine bone marrow-derived

macrophages (168) and we saw that also human monocytes and macrophages are able to release significant amounts of PGD_2, which may be able to influence inflammation in return. Interestingly, in a low-dose LPS model of acute lung injury, PGD_2 exacerbated pulmonary inflammation in mice (67), while PGD_2 limited inflammation in the same model using a higher LPS dose (48). One possible reason for this could be that high levels of PGD_2 trigger the physiologic response to limit inflammation by strengthening the endothelial barrier, resulting in limited oedema formation and risk of sepsis. In allergic asthma, mast cell-derived PGD_2 recruits eosinophils and Th2 cells via DP2 activation (297), while PGD_2 levels from other sources, e.g. monocytes/macrophages, might activate EP4 receptors on endothelial cells and prevent excess oedema formation under certain circumstances.

One limitation of these observations is that conclusions are drawn solely from *in vitro* data. Both in our experience and in literature there are profound differences in mouse and human prostaglandin receptors concerning expression pattern and ligand selectivity (69,296,298–300). While previously published studies have proposed that DP1 receptors are mediating the PGD_2 enhancement of endothelial barrier function in mice (68,103,104,223), our data convincingly show that it is the EP4 receptor in human pulmonary endothelial cells (2). With this in mind, we do not expect that animal models are suitable to further explore the role of EP4 receptors in PGD_2-mediated barrier enhancement. Further studies will be needed in humans and/or primates to advance this concept.

4.2 PART II: Characterization of novel prostaglandin sources in LPS-induced inflammation

Mast cells have been considered as the primary PGD_2 source in allergic inflammation; however, which immune cells express the hematopoietic PGD synthase and are able to produce PGD_2 during acute inflammation, i.e. bacterial or viral infection, has not been thoroughly described yet. Bacterial products, including LPS, have been shown to induce PGD_2 production in murine bone marrow-derived macrophages (168), which are able to modulate inflammation in return. The aim of the second project was to investigate the major source of PGD_2 during acute pulmonary inflammation. Using a flow cytometry approach, we could identify human monocytes, NK cells, NK/T cells, plasma cells and Th4 cells as potential PGD_2 sources as the majority of these cell types stained positive for hPGDS, the rate-limiting enzyme of PGD_2 production in peripheral tissue.

Remarkably, monocyte-derived macrophages expressed the highest levels of hPGDS by far, independent from polarization state. In lung sections of patients suffering from acute lung injury, Jandl et al. observed that a majority of $hPGDS^+$ cells had mononuclear phagocyte morphology (67). During inflammation, monocyte-derived macrophages may outnumber tissue resident macrophages thereby impacting the course of the inflammatory response and outcome (301). Hence, we were interested in the potential of human monocytes and monocyte-derived macrophages to influence PGD_2 levels during the acute inflammatory phase. Using a flow cytometry approach and immunofluorescence staining we could show that the majority of peripheral blood monocytes constitutively express the hematopoietic PGD synthase, while only a small increase in expression could be seen after pro-inflammatory stimulation. On protein level, hPGDS expression was upregulated after 8 h incubation, however to a much smaller extent than COX-2. In unstimulated monocytes an unexpected upregulation after 24 h incubation could be seen. This could be caused by an adhesion-induced effect or initiation of differentiation into a macrophage-like phenotype. Interestingly, hPGDS mRNA transcription was not upregulated after pro-inflammatory stimulation but was rather downregulated after 24 h incubation, when COX-2 mRNA levels were still significantly elevated. These data suggest a possible negative feedback loop of PGD_2 or PGE_2 on monocytes causing a downregulation of hPGDS mRNA expression after an acute response. The microsomal PGE synthase has been described in literature as the rate-limiting enzyme of PGE_2 production in mononuclear cells, but its mRNA expression was not remarkably changed in comparison to control monocytes. In macrophages, stimulation with IFN-γ/LPS caused an upregulation of hPGDS on protein level after 4 h, while mRNA levels were downregulated after 48 h. In sum, we saw a downregulation of hPGDS mRNA levels after 24 h, which seems to be a regulatory step to limit PGD_2 production and elevate PGE_2 levels by shuffling COX-2-derived PGH_2 into respective pathways. We assume that the discrepancies between hPGDS mRNA and protein level may be due to another level of regulation i.e. subcellular location of hPGDS or miRNAs.

In pulmonary inflammation, PGD_2 and PGE_2 often act as opposing mediators whereby the PGD_2 to PGE_2 ratio can be a pivotal factor in the prognosis of respiratory inflammation (9). Simultaneous evaluation of secreted PGD_2 and PGE_2 in monocyte and MDM-conditioned medium allows the determination of the PGD_2 to PGE_2 ratio. Both, monocytes and MDM released PGD_2

after pro-inflammatory stimulation with the peak after 8 to 24 h while the most striking finding was that monocytes released significantly more PGD_2 at all observed time points. Until now, monocytes have not been considered as relevant PGD_2 source, but these findings suggest an active role in modulating PGD_2 levels. Upon stimulation, monocytes as well as MDM released tremendous amounts of PGE_2 with levels increasing up to 48 h after activation when PGD_2 levels are already fading. Notably, monocytes released also higher amounts of PGE_2 than MDM, which further emphasizes their importance as effector cells.

In the course of this work, we could see that both, PGE_2 and PGD_2, had strong effects on endothelial barrier function which in turn modulates inflammatory progression. As we discovered that monocytes produce both prostaglandins in excess after pro-inflammatory stimulation with bacterial LPS, we were interested in whether this might be another way monocyte-derived PGs modulate acute inflammation. Indeed, monocyte-conditioned media had an interesting bi-phasic effect on endothelial barrier function – a robust increase in the first two h of stimulation followed by a drop in barrier resistance. Blockade of cyclooxygenases with diclofenac as well as inhibition on microsomal PGE synthase-1 revealed that the barrier enhancing effect was mediated primarily through PGE_2. Potential factors for the subsequent drop in barrier function could be TNF-α or VEGF. There is evidence that DP1 receptor activation on macrophages induces TNF-α production (67), which is likely the case for monocytes as well. A possible additional factor could be that LPS/IFN-γ stimulation induces PGE_2 but also PGD_2 that acts in an autocrine fashion to induce TNF-α. However, this requires further investigation.

Resident cell populations in the lung often differ in phenotype and function from respective circulating populations (302). We sorted neutrophils, macrophages, monocytes and mast cells from the healthy murine lung and could see that pulmonary monocytes expressed most hPGDS. To get a better understanding of the *in vivo* situation, we had a look at the pattern of hPGDS mRNA expression with help of *in situ* hybridization in different models of murine pulmonary inflammation. Remarkably, in all three models of pulmonary inflammation, LPS-induced acute, OVA-induced allergic and bleomycin-induced fibrotic inflammation, we could see an increase in the hPGDS signal, whereby the most prominent change was present in the OVA-induced allergic inflammation. In OVA-induced allergic inflammation, hPGDS mRNA was highly upregulated in bronchial epithelial cells, an effect that had been noted in another allergic mouse model before

(277). Interestingly, in bleomycin-induced fibrosis there were clearly more $CD68^+$ hPGDS $mRNA^+$ cells present, and expression levels increased also in the parenchyma and potentially in other infiltrating cells. In this model, we could also see an increase in macrophage and mast cell numbers by flow. A crucial role for infiltrating macrophages in driving fibrotic inflammation has been described recently (303). Additionally, we could measure relatively high levels of PGD_2 and PGE_2 in macrophage-conditioned medium already in basal conditions, suggesting that pulmonary macrophages might continuously supply prostaglandins to a certain extent in this model. A recent publication could show that elevating PGE_2 levels ameliorates pulmonary fibrosis and may be beneficial to treat this disease (226), therefore, macrophages may be potential candidates to target in the future.

To follow up on the hypothesis that monocytes are potent prostaglandin sources in acute, but not allergic inflammation, we evaluated their potential in an acute LPS-induced pulmonary inflammation and compared the outcome to OVA-induced allergic inflammation. In both mouse models, monocytes/macrophages have been considered central players of inflammatory or pathological outcome (67,195). Our data clearly showed a potent PGD_2 release by mononuclear phagocytes from LPS-lungs, while cells from established OVA-induced allergic inflammation did not. In this manner, we could translate the findings for human monocytes and macrophages after LPS/IFN-γ or IL-4 stimulation and confirm it in an *in vivo* setting. This clearly outlines that in non-allergic inflammation, i.e. initiated by bacterial LPS, mononuclear phagocytes contribute significant levels of PGD_2 and are able to modulate inflammation in return, while in an allergic environment other cell types, i.e. mast cells, are more important.

We continued working with the LPS-induced pulmonary inflammation model to characterize PG production and sources. Intranasal instillation of 1 mg/kg LPS induced a potent neutrophilic inflammation after 4 h, while monocyte numbers increased only by trend. Interestingly, mast cell numbers were abated in LPS-induced inflammation. Notably, monocytes showed highest levels of hPGDS expression followed by neutrophils in healthy lungs. Leukocyte populations obtained from LPS-stimulated mice did not express higher levels of hPGDS, which could be due to collection at an inappropriate time point, as in human monocytes we saw most hPGDS upregulation after 8 h stimulation, while these cells were isolated after 4 h of *in vivo* LPS stimulation. Another relevant factor might be that LPS stimulation is required constantly and upregulation was terminated due to

lack of continuous TLR4 stimulation. We had similar concerns when analysing data obtained from LC/MS of conditioned medium. If leukocytes were directly cultured after sorting without additional stimulation, monocytes released hardly any detectable levels of PGD_2, PGE_2 or TBX_2. Macrophages fared slightly better, however with these experimental settings neutrophils isolated after 4 h of LPS-induced pulmonary inflammation produced significant amounts of PGD_2 and also PGE_2. The other half of cells were stimulated *in vitro* with a low dose of LPS/IFN-γ. Interestingly, this initiated the release of PGD_2 and PGE_2 by monocytes and macrophages obtained from vehicle mice. Another relevant observation was that monocytes and macrophages obtained from LPS-induced pulmonary inflammation released notably less PGD_2 after *in vitro* stimulation, while PGE_2 levels even increased slightly. Considering the fact that we were looking at quite a late time point for acute, non-lethal inflammation (>24 h after initial LPS administration), this supports our theory of a negative feedback loop concerning PGD_2 production in monocytes. Proposedly, when the cells were stimulated with another dose of LPS, this feedback loop was already in process, thereby, favouring PGE_2 production. Consistently, hPGDS mRNA was downregulated in monocytes collected this time point. Further, these data suggest that monocytes and macrophages may require the presence of LPS to produce prostaglandins and resign production as soon as the threat fades. In contrast, neutrophil activation appears to be longer-lasting, i.e. cells remain activated until they undergo apoptosis, and therefore, these cells may not need a direct LPS stimulation to release PGs. What rules in favour of this statement is that *in vitro* stimulation of murine neutrophils from the healthy lung with LPS/IFN-γ did not significantly increase PGD_2 or PGE_2 levels. Solely an *in vivo* activation, as achieved with the LPS-induced lung inflammation, resulted in induction of significant PG release. These results point out that neutrophil PG production may not be initiated by LPS at all, but rather through other, secondary factors present in acute lung inflammation. In line with this, we could not measure PGD_2 in human neutrophil-conditioned medium after stimulation with LPS. As a result, we would like to speculate that neutrophil activation happens in an indirect manner, e.g. by factors secreted by activated macrophages as suggested previously (67). After normalization of the LC/MS data to individual cell numbers of each population, it appears that monocytes, mast cells and macrophages are able to release higher PG levels per cell than neutrophils. Hence, in an *in vivo* situation where LPS is present and inflammation still ongoing monocytes and macrophages may still be the central PG sources. In the future we would like to

explore how the PGD_2 level changes in the lung during inflammation, whether PGD_2 release can be successfully blocked by inhibition of hPGDS and if the inflammatory response can be limited in this manner.

4.3 PART III: PGD_2-DP2 activation on human IL-4 polarized monocyte-derived macrophages abrogates angiogenic potential of conditioned medium

Recent findings that human MDM express DP receptors and PGD_2 impacts their function in acute lung injury (67) opened up new questions of how the PGD_2-DP1-DP2 axis influences macrophage function in other (patho-) physiological settings. As a result, the third part of my thesis was dedicated to how the PGD_2-DP1-DP2 axis on monocyte-derived macrophages affects their ability to regulate the pulmonary vasculature. First, we evaluated the direct PGD_2 effect on HPMEC where we could see a beneficial effect on wound healing, however, no change in cell cycle after 24 h stimulation could be observed. Mechanistically, this would exclude an effect of PGD_2 on proliferation but leaves migration as potential mechanism for improved wound closure. We know, however, from the results of Part I that PGD_2 increases HPMEC barrier function, therefore, we cannot exclude cytoskeletal rearrangement or other changes of cell shape as potential mechanism. A hallmark of chronic lung disease is dysregulated angiogenesis and vascularisation (207); our results indicate a potential role of PGD_2 in driving endothelial cell wound healing, maybe also influencing angiogenesis in some way.

Alternatively-activated macrophages are responsible for effective inflammatory resolution including efferocytosis, tissue regeneration and release of anti-inflammatory mediators (219). Next, we were interested whether PGD_2 affects M2-like macrophages and in turn microvascular endothelial cell function. Interestingly, PGD_2 did not potentiate MDM-stimulated wound healing, but rather had a small reducing effect. Therefore, DP receptor activation on MDM did somehow limit wound closure of HPMEC. To follow up on these findings, we decided to switch to a slightly different *in vitro* model by activating human MDM with IL-4 or IL-10 to two different subtypes of M2-like macrophages, sometimes referred to as M2a and M2c, respectively. There is evidence that IL-4 and IL-10-activated macrophages act counteractively during chronic pulmonary inflammation, e.g. allergic asthma (195); whereby IL-4 polarized macrophages comprise an inactive, detrimental phenotype and are present in excess in allergic subjects. After 24 h of

activation with IL-4 or IL-10, macrophages were stimulated three consecutive times within 24 h with PGD_2 to simulate a prolonged challenge with the agonist. This treatment did not change expression of CD206, CD80 or CD163, which are commonly used to determine changes in polarization state of macrophages (152); however, morphology of M2-like macrophages changed towards a more pro-inflammatory, detached phenotype as smaller, rounded cells, often close to each other, were visible. An interesting follow up would be to look into cellular metabolism to see if PGD_2 stimulation initiates a more glycolysis-favouring phenotype of macrophages, which has been associated with a pro-inflammatory phenotype (304). Even though we could not pin down a phenotypic change of macrophages stimulated with PGD_2, we decided to evaluate whether the conditioned medium, collected from monocytes differentiated from atopic (house dust mite) or non-atopic donors, had a differential effect on HPMEC wound healing. Primarily we were interested in whether (i) IL-4 and IL-10 activated macrophages had opposing effects on pulmonary endothelial cells and (ii) whether monocytes from atopic donors had already been primed and potentially favoured certain functions after differentiation into macrophages. We could not see an overall increase in wound healing by IL-4 activated MDM (M2a)-conditioned medium in comparison to RPMI only; however, PGD_2 treatment of macrophages derived from an atopic donor delayed wound closure to an extent comparable to non-atopic M2a macrophages. This was an intriguing observation, because M2-like macrophages are responsible for the initiation of the resolution phase and tissue regeneration (194). Insufficient or de-regulated neovascularization may also contribute to tissue remodelling and impair functional recovery (207). IL-10 activated MDM (M2c)-conditioned medium showed a different pattern, whereby PGD_2-treatment of non-atopic M2c boosted HPMEC wound healing capacity to levels seen with atopic donors (in which additional PGD_2 had no effect). This suggests that PGD_2 stimulation may influence M2c macrophage function in a way that they assume a more M2a-like polarization state; nevertheless, to substantiate this hypothesis further investigation will be required. Collectively, these observations advocate a pivotal role of macrophage polarization in combination with elevated PGD_2 levels in pulmonary inflammation.

The first step of neo-vascularization is sprout formation from existent vessels (273); hence, next we were interested in whether macrophage-conditioned medium directly affects this process. Looking into the angiogenic potential of MDM-conditioned medium, we could finally see a

compelling effect on pulmonary microvascular sprout formation but also in an *ex vivo* assay using the chicken chorioallantoic membrane assay. Remarkably, PGD_2-primed IL-4 polarized macrophage-conditioned medium prevented HPMEC sprouting but also *ex vivo* angiogenesis. To identify which angiogenic factors are affected after PGD_2 treatment and potential differences between atopic and non-atopic donors, we performed a Western blot-based assay, ProteomeProfiler from R&D systems, which did not yet result in one single pathway due to the low numbers of biological replicates in this study: We obtained results from 3 donors so far, two non-atopic and one atopic donor, which limits the power of conclusions drawn from this experiment. Nevertheless, certain differences could be seen in the atopic donor compared to the non-atopic donor that had been treated in parallel. Serpin E1, a serine protease inhibitor, and MCP-1, a monocyte chemoattractant, were reduced after PGD_2 treatment in both, atopic and non-atopic donors by trend. Angiostatin and angiopoietin-1 were elevated in conditioned medium from the atopic MDM donor after stimulation with IL-4 and PGD_2.

It has been shown that both, DP1 and DP2, are expressed on human monocyte-derived macrophages (67). Here, we could show that DP2 receptor activation on IL-4 polarized macrophages was responsible for reduced sprout formation *in vitro* as well as angiogenic potential of conditioned medium in the CAM assay. Interestingly, in a short-term experiment using resistance measurement of HPMEC monolayers, we saw that stimulation of M2a macrophages with DP2 agonist DK-PGD_2 increased endothelial resistance significantly. It has previously been suggested that an increase in barrier function may prevent angiogenesis and metastasis (305,306), which could be another factor how DP2 activation on macrophages limits angiogenesis. As we did not observe obvious differences between MDM obtained from atopic or non-atopic donors in the sprouting or CAM assay (data not shown), results were presented as a combination of data obtained from one atopic and two non-atopic donors. Angiopoietin-1 and VEGF are potent angiogenic factors, complementing each other's function, while both were elevated in broncho-alveolar lavage fluid of asthmatics (307). Stimulation of IL-4 polarized human macrophages with DP2 agonist DK-PGD_2 reduced angiopoietin-1 significantly and VEGF by trend, which makes them potential candidates for the reduced angiogenic activity observed in our experiments. PDGF has also been related to pro-angiogenic activity, however, it is better known for mediating differentiation and recruitment of vascular smooth muscle cells and pericytes (308), which are supporting cells

necessary for the formation of functional, non-leaky vessels. DP2 activation on macrophages had a tendency to reduce PDGF expression, which might affect the formation of functional vessels. Interestingly, activin-A, a factor overexpressed in severe asthma and with anti-angiogenic action (280), was more prominent in conditioned media from DK-PGD_2-stimulated M2a macrophages. Similarly, endoglin was significantly reduced after DK-PGD_2 treatment. Endoglin functions as a membrane co-receptor of the TGF-β family, whereby high levels of the soluble glycoprotein after cleavage from the membrane-anchoring part has been associated with anti-angiogenic activity (309), increased vascular permeability and endothelial dysfunction (310). DP2 activation also affected endostatin levels, a factor considered as anti-inflammatory mediator. Collectively, DP2 receptor activation on M2 macrophages seems to interfere with the expression of several proteins, both, pro- and anti-inflammatory, able to cause endothelial and/or vascular dysfunction. This assay was performed for screening purpose only, therefore, the n number is very low. The variation between donors substantial and as a result we will follow up these preliminary observations with additional methods, i.e. qPCR and Western blot. Even though most studies indicate that an excess formation of new vessels is contributing to asthma pathology and airway remodelling, most agree that there is a tremendous dysregulation of pro- to anti-inflammatory factors BAL fluid and lung tissue (116,280,307,311). Our findings show that DP2 receptor activation on macrophages might contribute to this imbalance. Blockade of DP2 receptors has been considered as therapeutic approach for COPD and pulmonary fibrosis next to allergic asthma (79). Thus, the DP2-M2a-triggered effect on neovascularization could be another interesting aspect to consider for future therapy.

5. Conclusion

In the course of this PhD thesis we could describe for the first time that PGD_2 enhances the barrier function of human pulmonary endothelial cells by activating EP4 receptors, but not classical PGD_2 receptors, DP1 and DP2, or TP receptors. PGD_2 and BW245c elicited barrier protective effects that were independent from cAMP/PKA, the proposed mechanism for DP1 receptor-induced barrier enhancement. In contrast, we could show that phosphorylation of AKT was reduced by PGD_2-EP4 activation. These findings thus reveal yet another way of how PGD_2 might modulate inflammation and raises the question, whether some of the anti-inflammatory effects observed with PGD_2 and DP1 agonist BW245c might be due to EP4 receptor activation.

Further, we identified human monocytes as novel PGD_2 source after activation with bacterial LPS, but not IL-4. Human monocytes even surpassed PGD_2 and PGE_2 levels released by monocyte-derived macrophages. Downregulation of hPGDS appears to be regulating the switch from initial PGD_2 to pro-resolving PGE_2 production. We could translate these findings with an *in vivo* approach using a murine model of LPS-induced acute lung inflammation and confirmed that monocytes are able to release relevant levels of PGD_2, notably, only in the presence of LPS. Alveolar mononuclear phagocytes from OVA-induced allergic inflammation did not release significant levels of PGD_2, confirming that phagocytes do not act as PG sources in established, allergic inflammation. Interestingly, murine neutrophils from LPS-challenged mice released significant levels of PGD_2, partly attributable to their high number in the inflamed lung. Whether blockade of monocyte/macrophage derived PGD_2 is beneficial in limiting pulmonary inflammation remains to be examined.

Last but not least, we found that DP2 receptor activation on IL-4 polarized human monocyte-derived macrophages reduced their ability to release factors that stimulate sprout formation of human pulmonary microvascular endothelial cells and angiogenesis in the chicken CAM assay. This project requires further investigation towards the regulated factors responsible for reduced angiogenesis and, potentially, endothelial and vascular dysfunction. Dysregulated angiogenesis and resulting vascular dysfunction often contribute to airway and tissue remodelling, thus, this mechanism opens up a novel therapeutic option to aid the resolution of acute and chronic airway inflammation.

Collectively, we could highlight potential novel PGD_2 sources that might serve as therapeutic targets during acute pulmonary inflammation. Specifically targeting hPGDS-dependent PGD_2 production, which has been shown to contribute to a pro-inflammatory milieu, could potentially alleviate symptoms and tissue damage. Even though we could see a beneficial role of PGD_2 on endothelial barrier function and potentially oedema formation, PGE_2 release would be unaffected by hPGDS inhibition and still able to convey the EP4-mediated barrier enhancement. Also, we could convincingly show that DP2 receptor activation on macrophages modulates their angiogenic potential and opens up speculations about its role in tissue regeneration and remodelling during sustained pulmonary inflammation.

6. References

1. Rittchen S, Heinemann A. Therapeutic Potential of Hematopoietic Prostaglandin D2 Synthase in Allergic Inflammation. Cells. 2019;8(6):619.
2. Rittchen S, Rohrer K, Platzer W, Knuplez E, Bärnthaler T, Marsh LM, et al. Prostaglandin D2 strengthens human endothelial barrier by activation of E-type receptor 4. Biochem Pharmacol [Internet]. 2020 Oct;114277. Available from: https://doi.org/10.1016/j.bcp.2020.114277
3. Smith WL, Urade Y, Jakobsson PJ. Enzymes of the cyclooxygenase pathways of prostanoid biosynthesis. Chem Rev. 2011;111(10):5821–65.
4. King LS, Fukushima M, Banerjee M, Kang KH, Newman JH, Biaggioni I. Pulmonary vascular effects of prostaglandin D2, but not its systemic vascular or airway effects, are mediated through thromboxane receptor activation. Circ Res. 1991;68(2):352–8.
5. Burke JE, Dennis EA. Phospholipase A 2 structure/function, mechanism, and signaling. J Lipid Res. 2009;50(SUPPL.):237–42.
6. Qiu ZH, de Carvalho MS, Leslie CC. Regulation of phospholipase A2 activation by phosphorylation in mouse peritoneal macrophages. J Biol Chem [Internet]. 1993 Nov 15 [cited 2016 Jul 3];268(32):24506–13. Available from: http://www.ncbi.nlm.nih.gov/pubmed/8227003
7. Dubois RN, Abramson SB, Crofford L, Gupta RA, Simon LS, Van De Putte LB, et al. Cyclooxygenase in biology and disease. FASEB J. 1998;12(12):1063–73.
8. Ricciotti E, Fitzgerald GA. Prostaglandins and inflammation. Arterioscler Thromb Vasc Biol. 2011;31(5):986–1000.
9. Yoshimura T, Yoshikawa M, Otori N, Haruna S, Moriyama H. Correlation between the Prostaglandin D2/E2 Ratio in Nasal Polyps and the Recalcitrant Pathophysiology of Chronic Rhinosinusitis Associated with Bronchial Asthma. Allergol Int [Internet]. 2008;57(4):429–36. Available from: http://www.sciencedirect.com/science/article/pii/S132389301530808X
10. Schuligoi R, Schmidt R, Geisslinger G, Kollroser M, Peskar BA, Heinemann A. PGD2 metabolism in plasma: Kinetics and relationship with bioactivity on DP1 and CRTH2 receptors. Biochem Pharmacol. 2007;74(1):107–17.

11. Song W-L, Ricciotti E, Liang X, Grosser T, Grant GR, FitzGerald GA. Lipocalin-Like Prostaglandin D Synthase but Not Hemopoietic Prostaglandin D Synthase Deletion Causes Hypertension and Accelerates Thrombogenesis in Mice. J Pharmacol Exp Ther [Internet]. 2018 Dec;367(3):425–32. Available from: http://jpet.aspetjournals.org/lookup/doi/10.1124/jpet.118.250936
12. Yu R, Xiao L, Zhao G, Christman JW, van Breemen RB. Competitive Enzymatic Interactions Determine the Relative Amounts of Prostaglandins E2 and D2. J Pharmacol Exp Ther. 2011;339(2):716–25.
13. Urade Y, Eguchi N. Lipocalin-type and hematopoietic prostaglandin D synthases as a novel example of functional convergence. Prostaglandins Other Lipid Mediat. 2002;68–69:375–82.
14. Uchida Y, Urade Y, Mori S, Kohzuma T. UV resonance Raman studies on the activation mechanism of human hematopoietic prostaglandin D2 synthase by a divalent cation, Mg2+. J Inorg Biochem [Internet]. 2010;104(3):331–40. Available from: http://dx.doi.org/10.1016/j.jinorgbio.2009.12.003
15. Inoue T, Irikura D, Okazaki N, Kinugasa S, Matsumura H, Uodome N, et al. Mechanism of metal activation of human hematopoietic prostaglandin D synthase. Nat Struct Mol Biol [Internet]. 2003 Apr;10(4):291–6. Available from: http://dx.doi.org/10.1038/nsb907
16. Pinzar E, Miyano M, Kanaoka Y, Urade Y, Hayaishi O. Structural basis of hematopoietic prostaglandin D synthase activity elucidated by site-directed mutagenesis. J Biol Chem. 2000;275(40):31239–44.
17. Tippin BL, Levine AJ, Materi AM, Song W-L, Keku TO, Goodman JE, et al. Hematopoietic prostaglandin D synthase (HPGDS): A high stability, Val187Ile isoenzyme common among African Americans and its relationship to risk for colorectal cancer. Prostaglandins Other Lipid Mediat [Internet]. 2012 Jan;97(1–2):22–8. Available from: http://www.ncbi.nlm.nih.gov/pubmed/25133997
18. Aritake K, Kado Y, Inoue T, Miyano M, Urade Y. Structural and functional characterization of HQL-79, an orally selective inhibitor of human hematopoietic prostaglandin D synthase. J Biol Chem. 2006;281(22):15277–86.
19. Zhao G, Yu R, Deng J, Zhao Q, Li Y, Joo M, et al. Pivotal role of reactive oxygen species

in differential regulation of lipopolysaccharide-induced prostaglandins production in macrophages. Mol Pharmacol [Internet]. 2013;83(1):167–78. Available from: http://www.pubmedcentral.nih.gov/articlerender.fcgi?artid=3533474&tool=pmcentrez&rendertype=abstract

20. Ishii T. Close teamwork between Nrf2 and peroxiredoxins 1 and 6 for the regulation of prostaglandin D2 and E2 production in macrophages in acute inflammation. Free Radic Biol Med [Internet]. 2015 Nov;88(Part B):189–98. Available from: http://dx.doi.org/10.1016/j.freeradbiomed.2015.04.034
21. Chatterjee S, Feinstein SI, Dodia C, Sorokina E, Lien YC, Nguyen S, et al. Peroxiredoxin 6 phosphorylation and subsequent phospholipase A2activity are required for agonist-mediated activation of NADPH oxidase in mouse pulmonary microvascular endothelium and alveolar macrophages. J Biol Chem. 2011;286(13):11696–706.
22. Kim KH, Sadikot RT, Xiao L, Christman JW, Freeman ML, Chan JY, et al. Nrf2 is essential for the expression of lipocalin-prostaglandin D synthase induced by prostaglandin D2. Free Radic Biol Med [Internet]. 2013;65:1134–42. Available from: http://dx.doi.org/10.1016/j.freeradbiomed.2013.08.192
23. Luna-Gomes T, Magalhaes KG, Mesquita-Santos FP, Bakker-Abreu I, Samico RF, Molinaro R, et al. Eosinophils as a Novel Cell Source of Prostaglandin D2: Autocrine Role in Allergic Inflammation. J Immunol [Internet]. 2011;187(12):6518–26. Available from: http://www.jimmunol.org/cgi/doi/10.4049/jimmunol.1101806
24. Jowsey IR, Thomson a M, Flanagan JU, Murdock PR, Moore GB, Meyer DJ, et al. Mammalian class Sigma glutathione S-transferases: catalytic properties and tissue-specific expression of human and rat GSH-dependent prostaglandin D2 synthases. Biochem J [Internet]. 2001;359(Pt 3):507–16. Available from: http://www.pubmedcentral.nih.gov/articlerender.fcgi?artid=1222171&tool=pmcentrez&rendertype=abstract
25. Balzar S, Fajt ML, Comhair SAA, Erzurum SC, Bleecker E, Busse WW, et al. Mast cell phenotype, location, and activation in severe asthma: Data from the Severe Asthma Research Program. Am J Respir Crit Care Med. 2011;183(3):299–309.
26. Kawakami T, Ando T, Kimura M, Wilson BS, Kawakami Y. Mast cells in atopic dermatitis.

Curr Opin Immunol. 2009;21(6):666–78.

27. Amin K. The role of mast cells in allergic inflammation. Respir Med [Internet]. 2012;106(1):9–14. Available from: http://dx.doi.org/10.1016/j.rmed.2011.09.007
28. Lewis RA, Soter NA, Diamond PT, Austen KF, Oates JA, Roberts LJ. Prostaglandin D2 generation after activation of rat and human mast cells with anti-IgE. J Immunol [Internet]. 1982 Oct 15 [cited 2016 Jul 22];129(4):1627–31. Available from: http://www.ncbi.nlm.nih.gov/pubmed/11535533
29. Dwyer DF, Barrett NA, Austen KF. Expression profiling of constitutive mast cells reveals a unique identity within the immune system. Nat Immunol [Internet]. 2016 Jul 2;17(7):878–87. Available from: http://www.nature.com/articles/ni.3445
30. Baothman BK, Smith J, Kay LJ, Suvarna SK, Peachell PT. Prostaglandin D2generation from human lung mast cells is catalysed exclusively by cyclooxygenase-1. Eur J Pharmacol [Internet]. 2018;819(November 2017):225–32. Available from: https://doi.org/10.1016/j.ejphar.2017.12.005
31. Okano M, Fujiwara T, Sugata Y, Gotoh D, Masaoka Y, Sogo M, et al. Presence and characterization of prostaglandin D2–related molecules in nasal mucosa of patients with allergic rhinitis. Am J Rhinol [Internet]. 2006;20(3):342–8. Available from: http://openurl.ingenta.com/content/xref?genre=article&issn=1050-6586&volume=20&issue=3&spage=342
32. Murata T, Aritake K, Matsumoto S, Kamauchi S, Nakagawa T, Hori M, et al. Prostagladin D2 is a mast cell-derived antiangiogenic factor in lung carcinoma. Proc Natl Acad Sci. 2011;108(49):19802–7.
33. Fulkerson PC, Rothenberg ME. Targeting eosinophils in allergy, inflammation and beyond. Nat Rev Drug Discov [Internet]. 2013 Jan 21;12(2):117–29. Available from: http://www.nature.com/doifinder/10.1038/nrd3838
34. Peinhaupt M, Sturm EM, Heinemann A. Prostaglandins and Their Receptors in Eosinophil Function and As Therapeutic Targets. Front Med. 2017;4(July):1–12.
35. Lamkhioued B, Aldebert D, Gounni AS, Delaporte E, Goldman M, Capron A, et al. Synthesis of cytokines by eosinophils and their regulation. Int Arch Allergy Immunol. 1995;107(1–3):122–3.

36. Peinhaupt M, Roula D, Theiler A, Sedej M, Schicho R, Marsche G, et al. DP1 receptor signaling prevents the onset of intrinsic apoptosis in eosinophils and functions as a transcriptional modulator. J Leukoc Biol. 2018;104(1):159–71.
37. Schuligoi R, Sturm E, Luschnig P, Konya V, Philipose S, Sedej M, et al. CRTH2 and D-type prostanoid receptor antagonists as novel therapeutic agents for inflammatory diseases. Pharmacology. 2010;85(6):372–82.
38. Radnai B, Zs, Sturm EM, Stancic A, Jandl K, Labocha S, et al. Eosinophils contribute to intestinal inflammation via chemoattractant receptor-homologous molecule expressed on Th2 Cells, CRTH2, in experimental crohn's disease. J Crohn's Colitis. 2016;10(9):1087–95.
39. Feng X, Ramsden MK, Negri J, Baker MG, Payne SC, Borish L, et al. Eosinophil production of PGD2 in Aspirin-Exacerbated Respiratory Disease. J Allergy Clin Immunol [Internet]. 2016;138(4):1089–97. Available from: http://linkinghub.elsevier.com/retrieve/pii/S0091674916304407
40. Miyake K, Karasuyama H. Emerging roles of basophils in allergic inflammation. Allergol Int. 2017;66(3):382–91.
41. Koshino T, Arai Y, Miyamoto Y, Sano Y, Itami M, Teshima S, et al. Airway basophil and mast cell density in patients with bronchial asthma: relationship to bronchial hyperresponsiveness. J Asthma [Internet]. 1996 [cited 2019 Jan 9];33(2):89–95. Available from: http://www.ncbi.nlm.nih.gov/pubmed/8609103
42. Kepley CL, McFeeley PJ, Oliver JM, Lipscomb MF. Immunohistochemical detection of human basophils in postmortem cases of fatal asthma. Am J Respir Crit Care Med [Internet]. 2001 Sep 15 [cited 2019 Jan 9];164(6):1053–8. Available from: http://www.ncbi.nlm.nih.gov/pubmed/11587996
43. Satoh T, Ito Y, Miyagishi C, Yokozeki H. Basophils Infiltrate Skin Lesions of Eosinophilic Pustular Folliculitis (Ofuji's Disease). Acta Derm Venereol [Internet]. 2011;91(3):371–2. Available from: http://www.medicaljournals.se/acta/content/?doi=10.2340/00015555-1052
44. Marone G, Galdiero MR, Pecoraro A, Pucino V, Criscuolo G, Triassi M, et al. Prostaglandin D2 receptor antagonists in allergic disorders: safety, efficacy, and future perspectives. Expert Opin Investig Drugs [Internet]. 2018;28(1):73–84. Available from:

https://doi.org/10.1080/13543784.2019.1555237

45. Ugajin T, Satoh T, Kanamori T, Aritake K, Urade Y, Yokozeki H. FcεRI, but Not FcγR, Signals Induce Prostaglandin D2 and E2 Production from Basophils. Am J Pathol. 2011;179(2):775–82.
46. Pellefigues C, Dema B, Lamri Y, Saidoune F, Chavarot N, Lohéac C, et al. Prostaglandin D2amplifies lupus disease through basophil accumulation in lymphoid organs. Nat Commun. 2018;9(1):725.
47. Rosales C. Neutrophil: A cell with many roles in inflammation or several cell types? Front Physiol. 2018;9(FEB):1–17.
48. Murata T, Aritake K, Tsubosaka Y, Maruyama T, Nakagawa T, Hori M, et al. Anti-inflammatory role of PGD2 in acute lung inflammation and therapeutic application of its signal enhancement. Proc Natl Acad Sci [Internet]. 2013 Mar 26;110(13):5205–10. Available from: http://www.pubmedcentral.nih.gov/articlerender.fcgi?artid=3612619&tool=pmcentrez&rendertype=abstract
49. Hirai H, Tanaka K, Yoshie O, Ogawa K, Kenmotsu K, Takamori Y, et al. Prostaglandin D2 selectively induces chemotaxis in T helper type 2 cells, eosinophils, and basophils via seven-transmembrane receptor CRTH2. J Exp Med [Internet]. 2001 Jan 15 [cited 2016 Jul 6];193(2):255–61. Available from: http://www.ncbi.nlm.nih.gov/pubmed/11208866
50. Maric J, Ravindran A, Mazzurana L, Van Acker A, Rao A, Kokkinou E, et al. Cytokine-induced endogenous production of PGD2 is essential for human ILC2 activation. J Allergy Clin Immunol [Internet]. 2018;143(2019):2202–14. Available from: http://www.ncbi.nlm.nih.gov/pubmed/30578872%0Ahttps://linkinghub.elsevier.com/retrieve/pii/S009167491832774X
51. Tanaka K, Ogawa K, Sugamura K, Nakamura M, Takano S, Nagata K. Cutting Edge: Differential Production of Prostaglandin D2 by Human Helper T Cell Subsets. J Immunol [Internet]. 2000;164(5):2277–80. Available from: http://www.jimmunol.org/cgi/content/abstract/164/5/2277
52. Mitson-Salazar A, Yin Y, Wansley DL, Young M, Bolan H, Arceo S, et al. Hematopoietic prostaglandin D synthase defines a proeosinophilic pathogenic effector human TH2 cell

subpopulation with enhanced function. J Allergy Clin Immunol [Internet]. 2016;137(3):907-918.e9. Available from: http://dx.doi.org/10.1016/j.jaci.2015.08.007

53. Tait Wojno ED, Monticelli LA, Tran S V, Alenghat T, Osborne LC, Thome JJ, et al. The prostaglandin D2 receptor CRTH2 regulates accumulation of group 2 innate lymphoid cells in the inflamed lung. Mucosal Immunol [Internet]. 2015 Nov 8;8(6):1313–23. Available from: http://www.nature.com/articles/mi201521
54. Maric J, Ravindran A, Mazzurana L, Björklund ÅK, Van Acker A, Rao A, et al. Prostaglandin E2 suppresses human group 2 innate lymphoid cell function. J Allergy Clin Immunol [Internet]. 2018 May [cited 2019 Jan 21];141(5):1761-1773.e6. Available from: http://www.ncbi.nlm.nih.gov/pubmed/29217133
55. Gour N, Lajoie S. Epithelial Cell Regulation of Allergic Diseases. Curr Allergy Asthma Rep [Internet]. 2016 Sep 17 [cited 2019 Feb 17];16(9):65. Available from: http://www.ncbi.nlm.nih.gov/pubmed/27534656
56. Werder RB, Lynch JP, Simpson JC, Zhang V, Hodge NH, Poh M, et al. PGD2/DP2 receptor activation promotes severe viral bronchiolitis by suppressing IFN- production. Sci Transl Med. 2018;10(440):eaao0052.
57. Jakiela B, Gielicz A, Plutecka H, Hubalewska-Mazgaj M, Mastalerz L, Bochenek G, et al. Th2-type cytokine induced mucous metaplasia decreases susceptibility of human bronchial epithelium to rhinovirus infection. Am J Respir Cell Mol Biol [Internet]. 2014 Mar 3 [cited 2019 Feb 17];51:229–41. Available from: http://www.atsjournals.org/doi/abs/10.1165/rcmb.2013-0395OC
58. Taba Y, Sasaguri T, Miyagi M, Abumiya T, Miwa Y, Ikeda T, et al. Fluid shear stress induces lipocalin-type prostaglandin D(2) synthase expression in vascular endothelial cells. Circ Res [Internet]. 2000 May 12 [cited 2019 Jan 22];86(9):967–73. Available from: http://www.ncbi.nlm.nih.gov/pubmed/10807869
59. Omori K, Morikawa T, Kunita A, Nakamura T, Aritake K, Urade Y, et al. Lipocalin-type prostaglandin D synthase-derived PGD 2 attenuates malignant properties of tumor endothelial cells. J Pathol [Internet]. 2018 Jan 1 [cited 2019 Jan 22];244(1):84–96. Available from: http://doi.wiley.com/10.1002/path.4993
60. Chiba Y, Suto W, Sakai H. Augmented Pla2g4c/Ptgs2/Hpgds axis in bronchial smooth

muscle tissues of experimental asthma. PLoS One. 2018;13(8):1–20.

61. Basith S, Cui M, Macalino SJY, Park J, Clavio NAB, Kang S, et al. Exploring G protein-coupled receptors (GPCRs) ligand space via cheminformatics approaches: Impact on rational drug design. Front Pharmacol. 2018;9(MAR):1–26.
62. Sriram K, Insel PA. G protein-coupled receptors as targets for approved drugs: How many targets and how many drugs? Mol Pharmacol. 2018;93(4):251–8.
63. Kamato D, Thach L, Bernard R, Chan V, Zheng W, Kaur H, et al. Structure, Function, Pharmacology, and Therapeutic Potential of the G Protein, Gα/q,11. Front Cardiovasc Med. 2015;2(March):1–11.
64. Weis WI, Kobilka BK. The Molecular Basis of G Protein–Coupled Receptor Activation. Annu Rev Biochem [Internet]. 2018 Jun 20;87(1):897–919. Available from: https://linkinghub.elsevier.com/retrieve/pii/S0031938416312148
65. Smrcka A V. G protein βγ subunits: Central mediators of G protein-coupled receptor signaling. Cell Mol Life Sci [Internet]. 2008 Jul 19;65(14):2191–214. Available from: http://link.springer.com/10.1007/s00018-008-8006-5
66. Campbell AP, Smrcka A V. Targeting G protein-coupled receptor signalling by blocking G proteins. Nat Rev Drug Discov [Internet]. 2018;17(11):789–803. Available from: http://dx.doi.org/10.1038/nrd.2018.135
67. Jandl K, Stacher E, Bálint Z, Sturm EM, Maric J, Peinhaupt M, et al. Activated prostaglandin D2 receptors on macrophages enhance neutrophil recruitment into the lung. J Allergy Clin Immunol [Internet]. 2016;137:833–43. Available from: http://linkinghub.elsevier.com/retrieve/pii/S0091674915017388
68. Kobayashi K, Tsubosaka Y, Hori M, Narumiya S, Ozaki H, Murata T. Prostaglandin D2-DP signaling promotes endothelial barrier function via the cAMP/PKA/Tiam1/Rac1 pathway. Arterioscler Thromb Vasc Biol. 2013;33(3):565–71.
69. Narumiya S, Sugimoto Y, Ushikubi F. Prostanoid receptors: Structures, properties, and functions. Physiol Rev [Internet]. 1999 Oct [cited 2016 Jul 6];79(4):1193–226. Available from: http://www.ncbi.nlm.nih.gov/pubmed/10508233
70. Giles H, Leff P, Bolofo ML, Kelly MG, Robertson AD. The classification of prostaglandin DP-receptors in platelets and vasculature using BW A868C, a novel, selective and potent

competitive antagonist. Br J Pharmacol [Internet]. 1989 Feb [cited 2016 Jul 6];96(2):291–300. Available from: http://www.ncbi.nlm.nih.gov/pubmed/2924081

71. Hammad H, Kool M, Soullié T, Narumiya S, Trottein F, Hoogsteden HC, et al. Activation of the D prostanoid 1 receptor suppresses asthma by modulation of lung dendritic cell function and induction of regulatory T cells. J Exp Med [Internet]. 2007;204(2):357–67. Available from: http://www.jem.org/lookup/doi/10.1084/jem.20061196
72. Maher SA, Birrell MA, Adcock JJ, Wortley MA, Dubuis ED, Bonvini SJ, et al. Prostaglandin D2 and the role of the DP1 , DP2 and TP receptors in the control of airway reflex events. Eur Respir J [Internet]. 2015 Apr [cited 2019 Feb 20];45(4):1108–18. Available from: http://www.ncbi.nlm.nih.gov/pubmed/25323233
73. Matsuoka T, Hirata M, Tanaka H, Takahashi Y, Murata T, Kabashima K, et al. Prostaglandin D2 as a mediator of allergic asthma. Science (80-). 2000;287(5460):2013–7.
74. Arimura A, Yasui K, Kishino J, Asanuma F, Hasegawa H, Kakudo S, et al. Prevention of allergic inflammation by a novel prostaglandin receptor antagonist, S-5751. J Pharmacol Exp Ther [Internet]. 2001 Aug [cited 2016 Jul 6];298(2):411–9. Available from: http://www.ncbi.nlm.nih.gov/pubmed/11454901
75. Sandig H, Andrew D, Barnes AA, Sabroe I, Pease J. 9α,11β-PGF2 and its stereoisomer PGF 2α are novel agonists of the chemoattractant receptor, CRTH2. FEBS Lett. 2006;580(2):373–9.
76. Gazi L, Gyles S, Rose J, Lees S, Allan C, Xue L, et al. Δ12-Prostaglandin D2 is a potent and selective CRTH2 receptor agonist and causes activation of human eosinophils and Th2 lymphocytes. [1] K Asosingh al, “Endothelial cells innate response to allergens Initiat atopic asthma,” J Clin Invest, vol 128, no 7, pp 3116–3128, 2018Prostaglandins Other Lipid Mediat. 2005;75(1–4):153–67.
77. Kostenis E, Ulven T. Emerging roles of DP and CRTH2 in allergic inflammation. Trends Mol Med [Internet]. 2006 Apr [cited 2016 Jul 6];12(4):148–58. Available from: http://linkinghub.elsevier.com/retrieve/pii/S1471491406000438
78. Stubbs VELL, Schratl P, Hartnell A, Williams TJ, Peskar BA, Heinemann A, et al. Indomethacin causes prostaglandin D2-like and eotaxin-like selective responses in eosinophils and basophils. J Biol Chem [Internet]. 2002 Jul 19 [cited 2016 Jul

6];277(29):26012–20. Available from: http://www.jbc.org/cgi/doi/10.1074/jbc.M201803200

79. Jandl K, Heinemann A. The therapeutic potential of CRTH2/DP2 beyond allergy and asthma. Prostaglandins Other Lipid Mediat [Internet]. 2017;3(137):42–8. Available from: https://doi.org/10.1016/j.prostaglandins.2017.08.006
80. Shichijo M, Sugimoto H, Nagao K, Inbe H, Encinas JA, Takeshita K, et al. Chemoattractant receptor-homologous molecule expressed on Th2 cells activation in vivo increases blood leukocyte counts and its blockade abrogates 13,14-dihydro-15-keto-prostaglandin D2-induced eosinophilia in rats. J Pharmacol Exp Ther [Internet]. 2003 Nov [cited 2016 Jul 6];307(2):518–25. Available from: http://www.ncbi.nlm.nih.gov/pubmed/12975488
81. Chen G, Zuo S, Tang J, Zuo C, Jia D, Liu Q, et al. Inhibition of CRTH2-mediated Th2 activation attenuates pulmonary hypertension in mice. J Exp Med [Internet]. 2018;215:2175–95. Available from: http://www.jem.org/lookup/doi/10.1084/jem.20171767
82. Sedej M, Schröder R, Bell K, Platzer W, Vukoja A, Kostenis E, et al. D-type prostanoid receptor enhances the signaling of chemoattractant receptor-homologous molecule expressed on T H2 cells. J Allergy Clin Immunol. 2012;129(2).
83. Abramovitz M, Adam M, Boie Y, Carrière MC, Denis D, Godbout C, et al. The utilization of recombinant prostanoid receptors to determine the affinities and selectivities of prostaglandins and related analogs. Biochim Biophys Acta - Mol Cell Biol Lipids. 2000;1483(2):285–93.
84. Suganami A, Fujino H, Okura I, Yanagisawa N, Sugiyama H, Regan JW, et al. Human DP and EP2 prostanoid receptors take on distinct forms depending on the diverse binding of different ligands. FEBS J [Internet]. 2016 Nov;283(21):3931–40. Available from: http://doi.wiley.com/10.1111/febs.13899
85. Tanimoto J, Fujino H, Takahashi H, Murayama T. Human EP2 prostanoid receptors exhibit more constraints to mutations than human DP prostanoid receptors. FEBS Lett [Internet]. 2015;589(6):766–72. Available from: http://dx.doi.org/10.1016/j.febslet.2015.02.006
86. Harris SG, Phipps RP. The nuclear receptor PPAR gamma is expressed by mouse T lymphocytes and PPAR gamma agonists induce apoptosis. Eur J Immunol.

2001;31(4):1098–105.

87. Li J, Guo C, Wu J. 15-Deoxy-Δ- 12,14 -Prostaglandin J2 (15d-PGJ2), an Endogenous Ligand of PPAR- γ : Function and Mechanism. PPAR Res [Internet]. 2019 Aug 1;2019:1–10. Available from: https://www.hindawi.com/journals/ppar/2019/7242030/

88. Lee HS, Yun SJ, Ha JM, Jin SY, Ha HK, Song SH, et al. Prostaglandin D2 stimulates phenotypic changes in vascular smooth muscle cells. Exp Mol Med [Internet]. 2019;51(11). Available from: http://dx.doi.org/10.1038/s12276-019-0330-3

89. Larsson AK, Hagfjärd A, Dahlén SE, Adner M. Prostaglandin D 2 induces contractions through activation of TP receptors in peripheral lung tissue from the guinea pig. Eur J Pharmacol [Internet]. 2011;669(1–3):136–42. Available from: http://dx.doi.org/10.1016/j.ejphar.2011.07.046

90. Stevens T. Functional and molecular heterogeneity of pulmonary endothelial cells. Proc Am Thorac Soc. 2011;8(6):453–7.

91. Goldenberg NM, Kuebler WM. Endothelial Cell Regulation of Pulmonary Vascular Tone, Inflammation, and Coagulation. In: Comprehensive Physiology [Internet]. Hoboken, NJ, USA: John Wiley & Sons, Inc.; 2015 [cited 2018 Jan 11]. p. 531–59. Available from: http://doi.wiley.com/10.1002/cphy.c140024

92. Sayner SL. Emerging themes of cAMP regulation of the pulmonary endothelial barrier. Am J Physiol Cell Mol Physiol [Internet]. 2011 May;300(5):L667–78. Available from: https://www.physiology.org/doi/10.1152/ajplung.00433.2010

93. Rahimi N. Defenders and challengers of endothelial barrier function. Front Immunol. 2017;8(DEC):1–10.

94. Brasch J, Harrison OJ, Ahlsen G, Carnally SM, Henderson RM, Honig B, et al. Structure and Binding Mechanism of Vascular Endothelial Cadherin: A Divergent Classical Cadherin. J Mol Biol [Internet]. 2011 Apr;408(1):57–73. Available from: https://www.ncbi.nlm.nih.gov/pmc/articles/PMC3624763/pdf/nihms412728.pdf

95. Noda K, Zhang J, Fukuhara S, Kunimoto S, Yoshimura M, Mochizuki N. Vascular Endothelial-Cadherin Stabilizes at Cell–Cell Junctions by Anchoring to Circumferential Actin Bundles through α- and β-Catenins in Cyclic AMP-Epac-Rap1 Signal-activated Endothelial Cells. Nusrat A, editor. Mol Biol Cell [Internet]. 2010 Feb 15;21(4):584–96.

Available from: https://www.molbiolcell.org/doi/10.1091/mbc.e09-07-0580

96. Gavard J. Endothelial permeability and VE-cadherin. Cell Adh Migr. 2014;8(2):158–64.
97. Simmons S, Erfinanda L, Bartz C, Kuebler WM. Novel mechanisms regulating endothelial barrier function in the pulmonary microcirculation. J Physiol. 2019;597(4):997–1021.
98. Ono S, Egawa G, Kabashima K. Regulation of blood vascular permeability in the skin. Inflamm Regen. 2017;37(1):1–8.
99. Theiler A, Konya V, Pasterk L, Maric J, Bärnthaler T, Lanz I, et al. The EP1/EP3 receptor agonist 17-pt-PGE2 acts as an EP4 receptor agonist on endothelial barrier function and in a model of LPS-induced pulmonary inflammation. Vascul Pharmacol. 2016;87:180–9.
100. Konya V, Üllen A, Kampitsch N, Theiler A, Philipose S, Parzmair GP, et al. Endothelial E-type prostanoid 4 receptors promote barrier function and inhibit neutrophil trafficking. J Allergy Clin Immunol. 2013;131(2):532–40.
101. Konya V, Maric J, Jandl K, Luschnig P, Aringer I, Lanz I, et al. Activation of EP4 receptors prevents endotoxin-induced neutrophil infiltration into the airways and enhances microvascular barrier function. Br J Pharmacol. 2015;172(18):4454–68.
102. Konya V, Marsche G, Schuligoi R, Heinemann A. E-type prostanoid receptor 4 (EP4) in disease and therapy. Pharmacol Ther [Internet]. 2013 Jun;138(3):485–502. Available from: https://linkinghub.elsevier.com/retrieve/pii/S0163725813000752
103. Nakamura T, Fujiwara Y, Yamada R, Fujii W, Hamabata T, Lee MY, et al. Mast cell–derived prostaglandin D2attenuates anaphylactic reactions in mice. J Allergy Clin Immunol. 2017;140(2):630-632.e9.
104. Horikami D, Toya N, Kobayashi K, Omori K, Nagata N, Murata T. L-PGDS-derived PGD2 attenuates acute lung injury by enhancing endothelial barrier formation. J Pathol. 2019;248(3):280–90.
105. Qu A, Shah YM, Manna SK, Gonzalez FJ. Disruption of endothelial peroxisome proliferator-activated receptor γ accelerates diet-induced atherogenesis in LDL receptor-null mice. Arterioscler Thromb Vasc Biol [Internet]. 2012 Jan;32(1):65–73. Available from: https://www.ahajournals.org/doi/10.1161/ATVBAHA.111.239137
106. Zhao Y, Wei X, Song J, Zhang M, Huang T, Qin J. Peroxisome Proliferator-Activated Receptor γ Agonist Rosiglitazone Protects Blood–Brain Barrier Integrity Following Diffuse

Axonal Injury by Decreasing the Levels of Inflammatory Mediators Through a Caveolin-1-Dependent Pathway. Inflammation. 2019;42(3):841–56.

107. Leduc M, Breton B, Galés C, Le Gouill C, Bouvier M, Chemtob S, et al. Functional selectivity of natural and synthetic prostaglandin EP 4 receptor ligands. J Pharmacol Exp Ther. 2009;331(1):297–307.
108. Lydford SJ, McKechnie KCW, Left P. Interaction of BW A868C, a Prostanoid DP-Receptor Antagonist, with Two Receptor Subtypes in the Rabbit Isolated Saphenous Vein. Prostaglandins [Internet]. 1997 Jan;53(1):59–62. Available from: https://linkinghub.elsevier.com/retrieve/pii/S0090698096000007
109. Song WL, Stubbe J, Ricciotti E, Alamuddin N, Ibrahim S, Crichton I, et al. Niacin and biosynthesis of PGD 2 by platelet COX-1 in mice and humans. J Clin Invest. 2012;122(4):1459–68.
110. Nakamura T, Murata T. Regulation of vascular permeability in anaphylaxis. Br J Pharmacol. 2018;175(13):2538–42.
111. Birukov KG, Karki P. Injured lung endothelium: mechanisms of self-repair and agonist-assisted recovery (2017 Grover Conference Series). Pulm Circ [Internet]. 2018 Jan 20;8(1):204589321775266. Available from: http://journals.sagepub.com/doi/10.1177/2045893217752660
112. Green CE, Turner AM. The role of the endothelium in asthma and chronic obstructive pulmonary disease (COPD). Respir Res [Internet]. 2017;18(1):1–14. Available from: http://dx.doi.org/10.1186/s12931-017-0505-1
113. Grand RJAA, TURNELL AS, Grabham PW. Cellular consequences of thrombin-receptor activation. Biochem J [Internet]. 1996 Jan 15;313(2):353–68. Available from: https://portlandpress.com/biochemj/article/313/2/353/32395/Cellular-consequences-of-thrombinreceptor
114. Vouret-Craviari V, Boquet P, Pouysségur J, Van Obberghen-Schilling E. Regulation of the actin cytoskeleton by thrombin in human endothelial cells: Role of Rho proteins in endothelial barrier function. Mol Biol Cell. 1998;9(9):2639–53.
115. Benson BL, Li L, Myers JT, Dorand RDi, Gurkan UA, Huang AY, et al. Biomimetic post-capillary venule expansions for leukocyte adhesion studies. Sci Rep [Internet]. 2018;8(1):1–

15. Available from: http://dx.doi.org/10.1038/s41598-018-27566-z

116. Kropski JA, Richmond BW, Gaskill CF, Foronjy RF, Majka SM. Deregulated angiogenesis in chronic lung diseases: A possible role for lung mesenchymal progenitor cells (2017 Grover Conference Series). Pulm Circ. 2018;8(1).

117. Niethamer TK, Stabler CT, Leach JP, Zepp JA, Morley MP, Babu A, et al. Defining the role of pulmonary endothelial cell heterogeneity in the response to acute lung injury. Elife. 2020;9:1–28.

118. Ebina M, Shimizukawa M, Shibata N, Kimura Y, Suzuki T, Endo M, et al. Heterogeneous Increase in CD34-positive Alveolar Capillaries in Idiopathic Pulmonary Fibrosis. Am J Respir Crit Care Med [Internet]. 2004 Jun;169(11):1203–8. Available from: http://www.atsjournals.org/doi/abs/10.1164/rccm.200308-1111OC

119. Koyama S, Sato E, Haniuda M, Numanami H, Nagai S, Izumi T. Decreased level of vascular endothelial growth factor in bronchoalveolar lavage fluid of normal smokers and patients with pulmonary fibrosis. Am J Respir Crit Care Med [Internet]. 2002 Aug;166(3):382–5. Available from: http://www.atsjournals.org/doi/abs/10.1164/rccm.2103112

120. Maloney JP, Gao L. Proinflammatory Cytokines Increase Vascular Endothelial Growth Factor Expression in Alveolar Epithelial Cells. Mediators Inflamm [Internet]. 2015;2015:1–7. Available from: http://www.hindawi.com/journals/mi/2015/387842/

121. Voelkel NF, Gomez-Arroyo J, Mizuno S. COPD/Emphysema: The Vascular Story. Pulm Circ [Internet]. 2011 Jul;1(3):320–6. Available from: http://journals.sagepub.com/doi/10.4103/2045-8932.87295

122. Zanini A, Chetta A, Imperatori AS, Spanevello A, Olivieri D. The role of the bronchial microvasculature in the airway remodelling in asthma and COPD. Respir Res [Internet]. 2010 Dec 29;11(1):132. Available from: http://respiratory-research.biomedcentral.com/articles/10.1186/1465-9921-11-132

123. Murata T, Lin MI, Aritake K, Matsumoto S, Narumiya S, Ozaki H, et al. Role of prostaglandin D2 receptor DP as a suppressor of tumor hyperpermeability and angiogenesis in vivo. Proc Natl Acad Sci U S A. 2008;105(50):20009–14.

124. Nandi P, Girish G V., Majumder M, Xin X, Tutunea-Fatan E, Lala PK. PGE2 promotes breast cancer-associated lymphangiogenesis by activation of EP4 receptor on lymphatic

endothelial cells. BMC Cancer [Internet]. 2017 Dec 5;17(1):11. Available from: http://bmccancer.biomedcentral.com/articles/10.1186/s12885-016-3018-2

125. Namkoong S, Lee S-J, Kim C-K, Kim Y-M, Chung H-T, Lee H, et al. Prostaglandin E2 stimulates angiogenesis by activating the nitric oxide/cGMP pathway in human umbilical vein endothelial cells. Exp Mol Med [Internet]. 2005 Dec 1;37(6):588–600. Available from: http://www.nature.com/articles/emm200572
126. Zhang Y, Daaka Y. PGE2 promotes angiogenesis through EP4 and PKA Cγ pathway. Blood [Internet]. 2011 Nov 10;118(19):5355–64. Available from: https://ashpublications.org/blood/article/118/19/5355/29412/PGE2-promotes-angiogenesis-through-EP4-and-PKA-Cγ
127. Rosales C, Uribe-Querol E. Phagocytosis: A Fundamental Process in Immunity. Biomed Res Int [Internet]. 2017;2017:1–18. Available from: https://www.hindawi.com/journals/bmri/2017/9042851/
128. Murray PJ, Wynn TA. Protective and pathogenic functions of macrophage subsets. Nat Rev Immunol [Internet]. 2011;11(11):723–37. Available from: http://www.pubmedcentral.nih.gov/articlerender.fcgi?artid=3422549&tool=pmcentrez&rendertype=abstract%5Cn%3CGo to ISI%3E://000296584700011
129. Iwasaki A, Medzhitov R. Toll-like receptor control of the adaptive immune responses. Nat Immunol [Internet]. 2004 Oct [cited 2016 Jun 19];5(10):987–95. Available from: http://www.nature.com/doifinder/10.1038/ni1112
130. Serbina N V, Jia T, Hohl TM, Pamer EG. Monocyte-mediated defense against microbial pathogens. Annu Rev Immunol [Internet]. 2008 [cited 2016 Jul 3];26:421–52. Available from: http://www.ncbi.nlm.nih.gov/pubmed/18303997
131. Gordon S, Plüddemann A. Tissue macrophages: Heterogeneity and functions. BMC Biol. 2017;15(1):1–18.
132. Condon TV, Sawyer RT, Fenton MJ, Riches DWH. Lung dendritic cells at the innate-adaptive immune interface. J Leukoc Biol [Internet]. 2011 Nov;90(5):883–95. Available from: http://doi.wiley.com/10.1189/jlb.0311134
133. Ziegler-Heitbrock L, Ancuta P, Crowe S, Dalod M, Grau V, Hart DN, et al. Nomenclature of monocytes and dendritic cells in blood. Blood [Internet]. 2010 Oct 21 [cited 2016 Jul

3];116(16):e74-80. Available from: http://www.ncbi.nlm.nih.gov/pubmed/20628149

134. Wolf AA, Yáñez A, Barman PK, Goodridge HS. The Ontogeny of Monocyte Subsets. Front Immunol [Internet]. 2019 Jul 17;10. Available from: https://www.frontiersin.org/article/10.3389/fimmu.2019.01642/full
135. Tsou C-L, Peters W, Si Y, Slaymaker S, Aslanian AM, Weisberg SP, et al. Critical roles for CCR2 and MCP-3 in monocyte mobilization from bone marrow and recruitment to inflammatory sites. J Clin Invest [Internet]. 2007 Apr 2;117(4):902–9. Available from: http://www.jci.org/cgi/doi/10.1172/JCI29919
136. Kratofil RM, Kubes P, Deniset JF. Monocyte conversion during inflammation and injury. Arterioscler Thromb Vasc Biol. 2017;37(1):35–42.
137. Jakubzick C, Gautier EL, Gibbings SL, Sojka DK, Schlitzer A, Johnson TE, et al. Minimal Differentiation of Classical Monocytes as They Survey Steady-State Tissues and Transport Antigen to Lymph Nodes. Immunity [Internet]. 2013 Sep;39(3):599–610. Available from: https://linkinghub.elsevier.com/retrieve/pii/S107476131300335X
138. Rodero MP, Poupel L, Loyher PL, Hamon P, Licata F, Pessel C, et al. Immune surveillance of the lung by migrating tissue monocytes. Elife. 2015;4(JULY 2015):1–23.
139. Baharom F, Thomas S, Rankin G, Lepzien R, Pourazar J, Behndig AF, et al. Dendritic Cells and Monocytes with Distinct Inflammatory Responses Reside in Lung Mucosa of Healthy Humans. J Immunol. 2016;196(11):4498–509.
140. Fogg D, Sibon C, Miled C, Jung S,Aucouturier, Dan R. Littman, Ana Cumano FG. A clonogenic bone marrow progenitor specific for macrophages and dendritic cells. Science (80-). 2006;311(March):83–8.
141. Mosser DM. The many faces of macrophage activation. J Leukoc Biol. 2003;73(February):209–12.
142. Dziarski R, Gupta D. Role of MD-2 in TLR2- and TLR4-mediated recognition of Gram-negative and Gram-positive bacteria and activation of chemokine genes. J Endotoxin Res [Internet]. 2000 [cited 2016 Jul 2];6(5):401–5. Available from: http://www.ncbi.nlm.nih.gov/pubmed/11521063
143. Schildberger A, Rossmanith E, Eichhorn T, Strassl K, Weber V. Monocytes, peripheral blood mononuclear cells, and THP-1 cells exhibit different cytokine expression patterns

following stimulation with lipopolysaccharide. Mediators Inflamm. 2013;2013.

144. Plevin RE, Knoll M, McKay M, Arbabi S, Cuschieri J. The Role of Lipopolysaccharide Structure in Monocyte Activation and Cytokine Secretion. SHOCK [Internet]. 2016 Jan;45(1):22–7. Available from: https://linkinghub.elsevier.com/retrieve/pii/S0031938416312148

145. Endo Y, Blinova K, Romantseva T, Golding H, Zaitseva M. Differences in PGE2 production between primary human monocytes and differentiated macrophages: role of IL-1β and TRIF/IRF3. PLoS One [Internet]. 2014 [cited 2016 Jul 14];9(5):e98517. Available from: http://www.ncbi.nlm.nih.gov/pubmed/24870145

146. Byrne AJ, Powell JE, O'Sullivan BJ, Ogger PP, Hoffland A, Cook J, et al. Dynamics of human monocytes and airway macrophages during healthy aging and after transplant. J Exp Med. 2020;217(3):1–11.

147. Morales-Nebreda L, Misharin A V., Perlman H, Scott Budinger GR. The heterogeneity of lung macrophages in the susceptibility to disease. Eur Respir Rev [Internet]. 2015;24(137):505–9. Available from: http://dx.doi.org/10.1183/16000617.0031-2015

148. Sen D, Jones SM, Oswald EM, Pinkard H, Corbin K, Krummel MF. Tracking the spatial and functional gradient of monocyte-to-macrophage differentiation in inflamed lung. PLoS One. 2016;11(10):1–19.

149. Eligini S, Crisci M, Bono E, Songia P, Tremoli E, Colombo GI, et al. Human monocyte-derived macrophages spontaneously differentiated in vitro show distinct phenotypes. J Cell Physiol. 2013;228(7):1464–72.

150. Guilliams M, van de Laar L. A Hitchhiker's Guide to Myeloid Cell Subsets: Practical Implementation of a Novel Mononuclear Phagocyte Classification System. Front Immunol [Internet]. 2015;6(August):406. Available from: http://journal.frontiersin.org/article/10.3389/fimmu.2015.00406/abstract

151. Xue J, Schmidt S V., Sander J, Draffehn A, Krebs W, Quester I, et al. Transcriptome-Based Network Analysis Reveals a Spectrum Model of Human Macrophage Activation. Immunity [Internet]. 2014 Feb;40(2):274–88. Available from: https://linkinghub.elsevier.com/retrieve/pii/S107476131400034X

152. Jaguin M, Houlbert N, Fardel O, Lecureur V. Polarization profiles of human M-CSF-

generated macrophages and comparison of M1-markers in classically activated macrophages from GM-CSF and M-CSF origin. Cell Immunol. 2013;281(1):51–61.

153. Murray PJ. On macrophage diversity and inflammatory metabolic timers. Nat Rev Immunol [Internet]. 2020 Feb 5;20(2):89–90. Available from: http://www.nature.com/articles/s41577-019-0260-2
154. Kim S, Elkon KB, Ma X. Transcriptional Suppression of Interleukin-12 Gene Expression following Phagocytosis of Apoptotic Cells. Immunity [Internet]. 2004 Nov;21(5):643–53. Available from: https://linkinghub.elsevier.com/retrieve/pii/S1074761304003000
155. Ariel A, Serhan CN. New Lives Given by Cell Death: Macrophage Differentiation Following Their Encounter with Apoptotic Leukocytes during the Resolution of Inflammation. Front Immunol [Internet]. 2012;3. Available from: http://journal.frontiersin.org/article/10.3389/fimmu.2012.00004/abstract
156. Zhou D, Huang C, Lin Z, Zhan S, Kong L, Fang C, et al. Macrophage polarization and function with emphasis on the evolving roles of coordinated regulation of cellular signaling pathways. Cell Signal [Internet]. 2014;26(2):192–7. Available from: http://dx.doi.org/10.1016/j.cellsig.2013.11.004
157. Gordon S. Alternative activation of macrophages. Nat Rev Immunol. 2003;3(1):23–35.
158. Kopf M, Schneider C, Nobs SP. The development and function of lung-resident macrophages and dendritic cells. Nat Immunol [Internet]. 2015 Dec 18 [cited 2016 Jun 27];16(1):36–44. Available from: http://www.nature.com/doifinder/10.1038/ni.3052
159. van Furth R, Cohn ZA. The origin and kinetics of mononuclear phagocytes. J Exp Med [Internet]. 1968 Sep 1 [cited 2016 Jun 27];128(3):415–35. Available from: http://www.ncbi.nlm.nih.gov/pubmed/5666958
160. Epelman S, Lavine KJ, Randolph GJ. Origin and Functions of Tissue Macrophages. Immunity [Internet]. 2014;41(1):21–35. Available from: http://dx.doi.org/10.1016/j.immuni.2014.06.013
161. Guilliams M, De Kleer I, Henri S, Post S, Vanhoutte L, De Prijck S, et al. Alveolar macrophages develop from fetal monocytes that differentiate into long-lived cells in the first week of life via GM-CSF. J Exp Med [Internet]. 2013;210(10):1977–92. Available from: http://jem.rupress.org/content/210/10/1977

162. Snelgrove RJ, Goulding J, Didierlaurent AM, Lyonga D, Vekaria S, Edwards L, et al. A critical function for CD200 in lung immune homeostasis and the severity of influenza infection. Nat Immunol. 2008;9(9):1074–83.
163. Hussell T, Bell TJ. Alveolar macrophages: Plasticity in a tissue-specific context. Nat Rev Immunol. 2014;14(2):81–93.
164. Fathi M, Johansson A, Lundborg M, Orre L, Skold CM, Camner P. Functional and morphological differences between human alveolar and interstitial macrophages. Exp Mol Pathol. 2001;70(2):77–82.
165. Cai Y, Sugimoto C, Arainga M, Alvarez X, Didier ES, Kuroda MJ. In vivo characterization of alveolar and interstitial lung macrophages in rhesus macaques: implications for understanding lung disease in humans. J Immunol [Internet]. 2014;192(6):2821–9. Available from: http://www.jimmunol.org/content/192/6/2821.full
166. Urade Y, Ujihara M, Horiguchi Y, Ikai K, Hayaishi O. The major source of endogenous prostaglandin D2 production is likely antigen-presenting cells. Localization of glutathione-requiring prostaglandin D synthetase in histiocytes, dendritic, and Kupffer cells in various rat tissues. J Immunol [Internet]. 1989 Nov 1 [cited 2019 Jan 14];143(9):2982–9. Available from: http://www.ncbi.nlm.nih.gov/pubmed/2509561
167. Norwitz ER, Bernal AL, Starkey PM. Prostaglandin production by human peripheral blood monocytes changes with in vitro differentiation. Prostaglandins. 1996;51(5):339–49.
168. Xiao L, Ornatowska M, Zhao G, Cao H, Yu R, Deng J, et al. Lipopolysaccharide-Induced Expression of Microsomal Prostaglandin E Synthase-1 Mediates Late-Phase PGE2 Production in Bone Marrow Derived Macrophages. PLoS One. 2012;7(11):e50244.
169. Yoon YS, Lee YJ, Choi YH, Park YM, Kang JL. Macrophages programmed by apoptotic cells inhibit epithelial-mesenchymal transition in lung alveolar epithelial cells via PGE2, PGD2, and HGF. Sci Rep [Internet]. 2016;6(January):1–18. Available from: http://dx.doi.org/10.1038/srep20992
170. Kong D, Shen Y, Liu G, Zuo S, Ji Y, Lu A, et al. PKA regulatory IIα subunit is essential for PGD $_2$ -mediated resolution of inflammation. J Exp Med [Internet]. 2016;213(10):2209–26. Available from: http://www.jem.org/lookup/doi/10.1084/jem.20160459
171. Virtue S, Masoodi M, de Weijer BAM, van Eijk M, Mok CYL, Eiden M, et al. Prostaglandin

profiling reveals a role for haematopoietic prostaglandin D synthase in adipose tissue macrophage polarisation in mice and humans. Int J Obes [Internet]. 2015;39(7):1151–60. Available from: http://www.nature.com/doifinder/10.1038/ijo.2015.34

172. Henkel FDR, Friedl A, Haid M, Thomas D, Bouchery T, Haimerl P, et al. House dust mite drives pro-inflammatory eicosanoid reprogramming and macrophage effector functions. Allergy [Internet]. 2018;74(74):1090–101. Available from: https://onlinelibrary.wiley.com/doi/abs/10.1111/all.13700
173. Lee J, Kim TH, Murray F, Li X, Choi SS, Broide DH, et al. Cyclic AMP concentrations in dendritic cells induce and regulate Th2 immunity and allergic asthma. Proc Natl Acad Sci [Internet]. 2015;112(5):1529–34. Available from: http://www.pnas.org/lookup/doi/10.1073/pnas.1417972112
174. Shimura C, Satoh T, Igawa K, Aritake K, Urade Y, Nakamura M, et al. Dendritic cells express hematopoietic prostaglandin D synthase and function as a source of prostaglandin D2 in the skin. Am J Pathol [Internet]. 2010;176(1):227–37. Available from: http://dx.doi.org/10.2353/ajpath.2010.090111
175. Moghaddami M, Ranieri E, James M, Fletcher J, Cleland LG. Prostaglandin D(2) in inflammatory arthritis and its relation with synovial fluid dendritic cells. Mediators Inflamm [Internet]. 2013 [cited 2016 Jul 23];2013:329494. Available from: http://www.ncbi.nlm.nih.gov/pubmed/23737645
176. Gosset P, Pichavant M, Faveeuw C, Bureau F, Tonnel AB, Trottein F. Prostaglandin D2 affects the differentiation and functions of human dendritic cells: Impact on the T cell response. Eur J Immunol. 2005;35(5):1491–500.
177. Duque GA, Descoteaux A. Macrophage cytokines: Involvement in immunity and infectious diseases. Front Immunol. 2014;5(OCT):1–12.
178. Glaser, Coulter, Shields, Touzelet, Power, Broadbent. Airway Epithelial Derived Cytokines and Chemokines and Their Role in the Immune Response to Respiratory Syncytial Virus Infection. Pathogens [Internet]. 2019 Jul 19;8(3):106. Available from: https://www.mdpi.com/2076-0817/8/3/106
179. LeMessurier KS, Tiwary M, Morin NP, Samarasinghe AE. Respiratory Barrier as a Safeguard and Regulator of Defense Against Influenza A Virus and Streptococcus

pneumoniae. Front Immunol. 2020;11(February).

180. Jaworska J, Coulombe F, Downey J, Tzelepis F, Shalaby K, Tattoli I, et al. NLRX1 prevents mitochondrial induced apoptosis and enhances macrophage antiviral immunity by interacting with influenza virus PB1-F2 protein. Proc Natl Acad Sci [Internet]. 2014 May 20;111(20):E2110–9. Available from: http://www.pnas.org/cgi/doi/10.1073/pnas.1322118111

181. Puttur F, Gregory LG, Lloyd CM. Airway macrophages as the guardians of tissue repair in the lung. Immunol Cell Biol [Internet]. 2019 Mar 15;97(3):246–57. Available from: https://onlinelibrary.wiley.com/doi/abs/10.1111/imcb.12235

182. Aegerter H, Kulikauskaite J, Crotta S, Patel H, Kelly G, Hessel EM, et al. Influenza-induced monocyte-derived alveolar macrophages confer prolonged antibacterial protection. Nat Immunol [Internet]. 2020 Feb 13;21(2):145–57. Available from: http://dx.doi.org/10.1038/s41590-019-0568-x

183. Coulombe F, Jaworska J, Verway M, Tzelepis F, Massoud A, Gillard J, et al. Targeted prostaglandin E2 inhibition enhances antiviral immunity through induction of type I interferon and apoptosis in macrophages. Immunity [Internet]. 2014 Apr;40(4):554–68. Available from: https://linkinghub.elsevier.com/retrieve/pii/S1074761314001095

184. Talmi-Frank D, Altboum Z, Solomonov I, Udi Y, Jaitin DA, Klepfish M, et al. Extracellular Matrix Proteolysis by MT1-MMP Contributes to Influenza-Related Tissue Damage and Mortality. Cell Host Microbe [Internet]. 2016 Oct;20(4):458–70. Available from: https://linkinghub.elsevier.com/retrieve/pii/S1931312816303821

185. Herold S, Steinmueller M, von Wulffen W, Cakarova L, Pinto R, Pleschka S, et al. Lung epithelial apoptosis in influenza virus pneumonia: the role of macrophage-expressed TNF-related apoptosis-inducing ligand. J Exp Med [Internet]. 2008 Dec 22;205(13):3065–77. Available from: https://rupress.org/jem/article/205/13/3065/47162/Lung-epithelial-apoptosis-in-influenza-virus

186. Knapp S, Leemans JC, Florquin S, Branger J, Maris NA, Pater J, et al. Alveolar Macrophages Have a Protective Antiinflammatory Role during Murine Pneumococcal Pneumonia. Am J Respir Crit Care Med [Internet]. 2003 Jan 15;167(2):171–9. Available from: http://www.atsjournals.org/doi/abs/10.1164/rccm.200207-698OC

187. Jiang Z, Zhou Q, Gu C, Li D, Zhu L. Depletion of circulating monocytes suppresses IL-17 and HMGB1 expression in mice with LPS-induced acute lung injury. Am J Physiol - Lung Cell Mol Physiol. 2017;312(2):L231–42.

188. Barr LC, Brittan M, Morris AC, McAuley DF, McCormack C, Fletcher AM, et al. A Randomized Controlled Trial of Peripheral Blood Mononuclear Cell Depletion in Experimental Human Lung Inflammation. Am J Respir Crit Care Med [Internet]. 2013 Aug 15;188(4):449–55. Available from: http://www.atsjournals.org/doi/abs/10.1164/rccm.201212-2334OC

189. Kapellos TS, Bassler K, Aschenbrenner AC, Fujii W, Schultze JL. Dysregulated Functions of Lung Macrophage Populations in COPD. J Immunol Res [Internet]. 2018;2018:1–19. Available from: https://www.hindawi.com/journals/jir/2018/2349045/

190. Byrne AJ, Maher TM, Lloyd CM. Pulmonary Macrophages: A New Therapeutic Pathway in Fibrosing Lung Disease? Trends Mol Med [Internet]. 2016 Apr;22(4):303–16. Available from: https://linkinghub.elsevier.com/retrieve/pii/S1471491416000344

191. Fricker M, Gibson PG. Macrophage dysfunction in the pathogenesis and treatment of asthma. Eur Respir J [Internet]. 2017 Sep 12;50(3):1700196. Available from: http://erj.ersjournals.com/lookup/doi/10.1183/13993003.00196-2017

192. Herold S, Mayer K, Lohmeyer J. Acute Lung Injury: How Macrophages Orchestrate Resolution of Inflammation and Tissue Repair. Front Immunol [Internet]. 2011;2. Available from: http://journal.frontiersin.org/article/10.3389/fimmu.2011.00065/abstract

193. Bosurgi L, Cao YG, Cabeza-Cabrerizo M, Tucci A, Hughes LD, Kong Y, et al. Macrophage function in tissue repair and remodeling requires IL-4 or IL-13 with apoptotic cells. Science (80-) [Internet]. 2017 Jun 9;356(6342):1072–6. Available from: https://www.sciencemag.org/lookup/doi/10.1126/science.aai8132

194. Oishi Y, Manabe I. Macrophages in inflammation, repair and regeneration. Int Immunol [Internet]. 2018 Aug 25;30(11):511–28. Available from: https://academic.oup.com/intimm/advance-article/doi/10.1093/intimm/dxy054/5079207

195. Draijer C, Boorsma CE, Robbe P, Timens W, Hylkema MN, Ten Hacken NH, et al. Human asthma is characterized by more IRF5+ M1 and CD206+ M2 macrophages and less IL-10+ M2-like macrophages around airways compared with healthy airways. J Allergy Clin

Immunol. 2017;140(1):280-283.e3.

196. Ogawa Y, Duru E, Ameredes B. Role of IL-10 in the Resolution of Airway Inflammation. Curr Mol Med [Internet]. 2008 Aug 1;8(5):437–45. Available from: http://www.eurekaselect.com/openurl/content.php?genre=article&issn=1566-5240&volume=8&issue=5&spage=437

197. Jetten N, Verbruggen S, Gijbels MJ, Post MJ, De Winther MPJ, Donners MMPC. Anti-inflammatory M2, but not pro-inflammatory M1 macrophages promote angiogenesis in vivo. Angiogenesis [Internet]. 2014 Jan 8;17(1):109–18. Available from: http://link.springer.com/10.1007/s10456-013-9381-6

198. Corliss BA, Azimi MS, Munson JM, Peirce SM, Murfee WL. Macrophages: An Inflammatory Link Between Angiogenesis and Lymphangiogenesis. Microcirculation [Internet]. 2016 Feb;23(2):95–121. Available from: http://doi.wiley.com/10.1111/micc.12259

199. Zajac E, Schweighofer B, Kupriyanova TA, Juncker-Jensen A, Minder P, Quigley JP, et al. Angiogenic capacity of M1- and M2-polarized macrophages is determined by the levels of TIMP-1 complexed with their secreted proMMP-9. Blood [Internet]. 2013 Dec 12;122(25):4054–67. Available from: https://ashpublications.org/blood/article/122/25/4054/32050/Angiogenic-capacity-of-M1-and-M2polarized

200. Brecht K, Weigert A, Hu J, Popp R, Fisslthaler B, Korff T, et al. Macrophages programmed by apoptotic cells promote angiogenesis via prostaglandin E 2 . FASEB J. 2011;25(7):2408–17.

201. Monticelli LA, Sonnenberg GF, Abt MC, Alenghat T, Ziegler CGK, Doering TA, et al. Innate lymphoid cells promote lung-tissue homeostasis after infection with influenza virus. Nat Immunol [Internet]. 2011 Nov;12(11):1045–54. Available from: http://www.ncbi.nlm.nih.gov/pubmed/21946417

202. Ding L, Liu T, Wu Z, Hu B, Nakashima T, Ullenbruch M, et al. Bone Marrow CD11c + Cell–Derived Amphiregulin Promotes Pulmonary Fibrosis. J Immunol [Internet]. 2016 Jul 1;197(1):303–12. Available from: http://www.jimmunol.org/lookup/doi/10.4049/jimmunol.1502479

203. Boorsma CE, Draijer C, Melgert BN. Macrophage heterogeneity in respiratory diseases. Mediators Inflamm. 2013;2013.

204. Golpon HA, Fadok VA, Taraseviciene-Stewart L, Scerbavicius R, Sauer C, Welte T, et al. Life after corpse engulfment: phagocytosis of apoptotic cells leads to VEGF secretion and cell growth. FASEB J [Internet]. 2004 Nov 2;18(14):1716–8. Available from: https://onlinelibrary.wiley.com/doi/abs/10.1096/fj.04-1853fje

205. Okuma T, Terasaki Y, Kaikita K, Kobayashi H, Kuziel WA, Kawasuji M, et al. C-C chemokine receptor 2 (CCR2) deficiency improves bleomycin-induced pulmonary fibrosis by attenuation of both macrophage infiltration and production of macrophage-derived matrix metalloproteinases. J Pathol. 2004;204(5):594–604.

206. Hamacher J, Lucas R, Lijnen HR, Buschke S, Dunant Y, Wendel A, et al. Tumor Necrosis Factor-α and Angiostatin Are Mediators of Endothelial Cytotoxicity in Bronchoalveolar Lavages of Patients with Acute Respiratory Distress Syndrome. Am J Respir Crit Care Med [Internet]. 2002 Sep;166(5):651–6. Available from: http://www.atsjournals.org/doi/abs/10.1164/rccm.2109004

207. Voelkel NF, Douglas IS, Nicolls M. Angiogenesis in Chronic Lung Disease. [cited 2018 Jan 22]; Available from: https://www.ncbi.nlm.nih.gov/pmc/articles/PMC4396181/pdf/nihms-50137.pdf

208. Yu X, Buttgereit A, Lelios I, Utz SG, Cansever D, Becher B, et al. The Cytokine TGF-β Promotes the Development and Homeostasis of Alveolar Macrophages. Immunity [Internet]. 2017 Nov;47(5):903-912.e4. Available from: https://linkinghub.elsevier.com/retrieve/pii/S1074761317304612

209. Chen G, Khalil N. TGF-β1 increases proliferation of airway smooth muscle cells by phosphorylation of map kinases. Respir Res [Internet]. 2006 Dec 3;7(1):2. Available from: http://respiratory-research.biomedcentral.com/articles/10.1186/1465-9921-7-2

210. Rafii R, Juarez MM, Albertson TE, Chan AL. A review of current and novel therapies for idiopathic pulmonary fibrosis. J Thorac Dis [Internet]. 2013 Feb;5(1):48–73. Available from: http://www.ncbi.nlm.nih.gov/pubmed/23372951

211. Morris DG, Huang X, Kaminski N, Wang Y, Shapiro SD, Dolganov G, et al. Loss of integrin αvβ6-mediated TGF-β activation causes Mmp12-dependent emphysema. Nature [Internet].

2003 Mar;422(6928):169–73. Available from: http://www.nature.com/articles/nature01413

212. Byers DE, Holtzman MJ. Alternatively Activated Macrophages and Airway Disease. Chest. 2011;140(3):768–74.
213. Singh D, Agusti A, Anzueto A, Barnes PJ, Bourbeau J, Celli BR, et al. Global Strategy for the Diagnosis, Management, and Prevention of Chronic Obstructive Lung Disease: the GOLD science committee report 2019. Eur Respir J [Internet]. 2019 May;53(5):1900164. Available from: http://erj.ersjournals.com/lookup/doi/10.1183/13993003.00164-2019
214. Dharmage SC, Perret JL, Custovic A. Epidemiology of Asthma in Children and Adults. Front Pediatr [Internet]. 2019 Jun 18;7. Available from: https://www.frontiersin.org/article/10.3389/fped.2019.00246/full
215. Villar J, Pérez-Méndez L, Kacmarek RM. Current definitions of acute lung injury and the acute respiratory distress syndrome do not reflect their true severity and outcome. Intensive Care Med [Internet]. 1999 Sep [cited 2016 Jun 12];25(9):930–5. Available from: http://www.ncbi.nlm.nih.gov/pubmed/10501747
216. Spadaro S, Park M, Turrini C, Tunstall T, Thwaites R, Mauri T, et al. Biomarkers for Acute Respiratory Distress syndrome and prospects for personalised medicine. J Inflamm (United Kingdom). 2019;16(1):1–11.
217. Gonzales JN, Lucas R, Verin AD. The Acute Respiratory Distress Syndrome: Mechanisms and Perspective Therapeutic Approaches. Austin J Vasc Med [Internet]. 2015 Jun 4 [cited 2016 Jun 12];2(1). Available from: http://www.ncbi.nlm.nih.gov/pubmed/26973981
218. Fanelli V, Vlachou A, Ghannadian S, Simonetti U, Slutsky AS, Zhang H. Acute respiratory distress syndrome: new definition, current and future therapeutic options. J Thorac Dis [Internet]. 2013 Jun [cited 2016 Jun 12];5(3):326–34. Available from: http://www.ncbi.nlm.nih.gov/pubmed/23825769
219. Aggarwal NR, King LS, D'Alessio FR. Diverse macrophage populations mediate acute lung inflammation and resolution. Am J Physiol Lung Cell Mol Physiol [Internet]. 2014;306:L709--25. Available from: http://www.ncbi.nlm.nih.gov/pubmed/24508730
220. Higashi A, Higashi N, Tsuburai T, Takeuchi Y, Taniguchi M, Mita H, et al. Involvement of eicosanoids and surfactant protein D in extrinsic allergic alveolitis. Eur Respir J. 2005;26(6):1069–73.

221. Rajakariar R, Hilliard M, Lawrence T, Trivedi S, Colville-nash P, Bellingan G, et al. Hematopoietic prostaglandin D 2 synthase controls through PGD 2 and 15-deoxy 12 – 14 PGJ 2. Pnas. 2007;104(52):20979–84.

222. Gao Y, Zhang H, Luo L, Lin J, Li D, Zheng S, et al. Resolvin D1 Improves the Resolution of Inflammation via Activating NF-κB p50/p50–Mediated Cyclooxygenase-2 Expression in Acute Respiratory Distress Syndrome. J Immunol. 2017;199(6):2043–54.

223. Sarashina H, Tsubosaka Y, Omori K, Aritake K, Nakagawa T, Hori M, et al. Opposing immunomodulatory roles of prostaglandin D2 during the progression of skin inflammation. J Immunol [Internet]. 2014;192(1):459–65. Available from: http://www.ncbi.nlm.nih.gov/pubmed/24298012

224. Raghu G, Remy-Jardin M, Myers JL, Richeldi L, Ryerson CJ, Lederer DJ, et al. Diagnosis of idiopathic pulmonary fibrosis An Official ATS/ERS/JRS/ALAT Clinical practice guideline. Am J Respir Crit Care Med. 2018;198(5):e44–68.

225. Marshall RP, Bellingan G, Webb S, Puddicombe A, Goldsack N, McAnulty RJ, et al. Fibroproliferation occurs early in the acute respiratory distress syndrome and impacts on outcome. Am J Respir Crit Care Med. 2000;162(5):1783–8.

226. Bärnthaler T, Theiler A, Zabini D, Trautmann S, Stacher-Priehse E, Lanz I, et al. Inhibiting eicosanoid degradation exerts antifibrotic effects in a pulmonary fibrosis mouse model and human tissue. J Allergy Clin Immunol [Internet]. 2019 Dec; Available from: https://linkinghub.elsevier.com/retrieve/pii/S0091674919316252

227. Ando M, Murakami Y, Kojima F, Endo H, Kitasato H, Hashimoto A, et al. Retrovirally introduced prostaglandin D2 synthase suppresses lung injury induced by bleomycin. Am J Respir Cell Mol Biol. 2003;28(5):582–91.

228. Kida T, Ayabe S, Omori K, Nakamura T, Maehara T, Aritake K, et al. Prostaglandin D2 attenuates bleomycin-induced lung inflammation and pulmonary fibrosis. PLoS One. 2016;11(12):1–11.

229. Ueda S, Fukunaga K, Takihara T, Shiraishi Y, Oguma T, Shiomi T, et al. Deficiency of CRTH2, a prostaglandin D 2 receptor, aggravates bleomycin-induced pulmonary inflammation and fibrosis. Am J Respir Cell Mol Biol. 2019;60(3):289–98.

230. Barnes PJ. New therapies for asthma: is there any progress? Trends Pharmacol Sci [Internet].

2010 Jul 1 [cited 2019 Feb 20];31(7):335–43. Available from: https://www.sciencedirect.com/science/article/pii/S0165614710000787?via%3Dihub

231. Fajt ML, Gelhaus SL, Freeman B, Uvalle CE, Trudeau JB, Holguin F, et al. Prostaglandin D2 pathway upregulation: Relation to asthma severity, control, and TH2 inflammation. J Allergy Clin Immunol [Internet]. 2013;131(6):1504-1512.e12. Available from: http://dx.doi.org/10.1016/j.jaci.2013.01.035
232. Kolmert J, Gómez C, Balgoma D, Sjödin M, Bood J, Konradsen JR, et al. Urinary Leukotriene E4 and Prostaglandin D2 Metabolites Increase in Adult and Childhood Severe Asthma Characterized by Type-2 Inflammation. Am J Respir Crit Care Med. 2020;1–67.
233. al Jarad N, Hui K, Barnes N. Effects of a thromboxane receptor antagonist on prostaglandin D2 and histamine induced bronchoconstriction in man. Br J Clin Pharmacol. 1994;37(1):97–100.
234. Christ AN, Labzin L, Bourne GT, Fukunishi H, Weber JE, Sweet MJ, et al. Development and Characterization of New Inhibitors of the Human and Mouse Hematopoietic Prostaglandin D2 Synthases. J Med Chem [Internet]. 2010 Aug 12;53(15):5536–48. Available from: https://doi.org/10.1021/jm100194a
235. Santus P, Radovanovic D. Prostaglandin D2 receptor antagonists in early development as potential therapeutic options for asthma. Expert Opin Investig Drugs. 2016;25(9):1083–92.
236. Kupczyk M, Kuna P. Targeting the PGD2/CRTH2/DP1 Signaling Pathway in Asthma and Allergic Disease: Current Status and Future Perspectives. Drugs. 2017;77(12):1281–94.
237. James KM, Gebretsadik T, Escobar GJ, Wu P, Carroll KN, Li SX, et al. Risk of childhood asthma following infant bronchiolitis during the respiratory syncytial virus season. J Allergy Clin Immunol. 2013;132(1):227–9.
238. Kajiwara D, Aoyagi H, Shigeno K, Togawa M, Tanaka K, Inagaki N, et al. Role of hematopoietic prostaglandin D synthase in biphasic nasal obstruction in guinea pig model of experimental allergic rhinitis. Eur J Pharmacol [Internet]. 2011;667(1–3):389–95. Available from: http://dx.doi.org/10.1016/j.ejphar.2011.05.041
239. Nabe T, Kuriyama Y, Mizutani N, Shibayama S, Hiromoto A, Fujii M, et al. Inhibition of hematopoietic prostaglandin D synthase improves allergic nasal blockage in guinea pigs. Prostaglandins Other Lipid Mediat [Internet]. 2011;95(1–4):27–34. Available from:

http://dx.doi.org/10.1016/j.prostaglandins.2011.05.001

240. Cosio MG, Saetta M, Agusti A. Immunologic Aspects of Chronic Obstructive Pulmonary Disease. N Engl J Med [Internet]. 2009 Jun 4;360(23):2445–54. Available from: http://www.nejm.org/doi/abs/10.1056/NEJMra0804752

241. Ives SJ, Harris RA, Witman MAH, Fjeldstad AS, Garten RS, McDaniel J, et al. Vascular Dysfunction and Chronic Obstructive Pulmonary Disease. Hypertension [Internet]. 2014 Mar;63(3):459–67. Available from: https://www.ahajournals.org/doi/10.1161/HYPERTENSIONAHA.113.02255

242. Titz B, Boué S, Phillips B, Talikka M, Vihervaara T, Schneider T, et al. Effects of cigarette smoke, cessation, and switching to two heat-not-burn tobacco products on lung lipid metabolism in C57BL/6 and Apoe-/- mice-an integrative systems toxicology analysis. Toxicol Sci. 2016;149(2):441–57.

243. Dagouassat M, Gagliolo JM, Chrusciel S, Bourin MC, Duprez C, Caramelle P, et al. The cyclooxygenase-2-prostaglandin e2 pathway maintains senescence of chronic obstructive pulmonary disease fibroblasts. Am J Respir Crit Care Med. 2013;187(7):703–14.

244. Stebbins KJ, Broadhead AR, Baccei CS, Scott JM, Truong YP, Coate H, et al. Pharmacological blockade of the DP2 receptor inhibits cigarette smoke-induced inflammation, mucus cell metaplasia, and epithelial hyperplasia in the mouse lung. J Pharmacol Exp Ther [Internet]. 2010 Mar [cited 2016 Jun 12];332(3):764–75. Available from: http://www.ncbi.nlm.nih.gov/pubmed/19996299

245. Snell N, Foster M, Vestbo J. Efficacy and safety of AZD1981, a CRTH2 receptor antagonist, in patients with moderate to severe COPD. Respir Med [Internet]. 2013 Nov;107(11):1722–30. Available from: https://linkinghub.elsevier.com/retrieve/pii/S0954611113002187

246. Wendell SG, Fan H, Zhang C. G protein–coupled receptors in asthma therapy: Pharmacology and drug actions. Pharmacol Rev. 2020;72(1):1–49.

247. Kao CC, Parulekar AD. Journal of Asthma and Allergy Dovepress Spotlight on fevipiprant and its potential in the treatment of asthma: evidence to date. J Asthma Allergy [Internet]. 2019;12–3. Available from: www.dovepress.com

248. Hardman C, Chen W, Luo J, Batty P, Chen YL, Nahler J, et al. Fevipiprant, a selective prostaglandin D2 receptor 2 antagonist, inhibits human group 2 innate lymphoid cell

aggregation and function. J Allergy Clin Immunol. 2019;143(6):2329–33.

249. Shamri R, Dubois G, Erpenbeck VJ, Mankuta D, Sandham DA, Levi-Schaffer F. Fevipiprant, a DP2 receptor antagonist, inhibits eosinophil migration towards mast cells. Clin Exp Allergy [Internet]. 2019;49(2):255–7. Available from: http://www.ncbi.nlm.nih.gov/pubmed/30379368

250. Saunders R, Kaul H, Berair R, Gonem S, Singapuri A, Sutcliffe AJ, et al. DP 2 antagonism reduces airway smooth muscle mass in asthma by decreasing eosinophilia and myofibroblast recruitment. Sci Transl Med. 2019;11(479):1–12.

251. Bateman ED, Guerreros AG, Brockhaus F, Holzhauer B, Pethe A, Kay RA, et al. Fevipiprant, an oral prostaglandin DP2 receptor (CRTh2) antagonist, in allergic asthma uncontrolled on low-dose inhaled corticosteroids. Eur Respir J [Internet]. 2017;50(2). Available from: http://dx.doi.org/10.1183/13993003.00670-2017

252. Barnes N, Pavord I, Chuchalin A, Bell J, Hunter M, Lewis T, et al. A randomized, double-blind, placebo-controlled study of the CRTH2 antagonist OC000459 in moderate persistent asthma. Clin Exp Allergy [Internet]. 2012 Jan;42(1):38–48. Available from: http://doi.wiley.com/10.1111/j.1365-2222.2011.03813.x

253. Kuna P, Bjermer L, Tornling G. Two Phase II randomized trials on the CRTh2 antagonist AZD1981 in adults with asthma. Drug Des Devel Ther [Internet]. 2016 Aug;Volume 10:2759–70. Available from: https://www.dovepress.com/two-phase-ii-randomized-trials-on-the-crth2-antagonist-azd1981-in-adul-peer-reviewed-article-DDDT

254. Diamant Z, Sidharta PN, Singh D, O'Connor BJ, Zuiker R, Leaker BR, et al. Setipiprant, a selective CRTH2 antagonist, reduces allergen-induced airway responses in allergic asthmatics. Clin Exp Allergy [Internet]. 2014 Aug;44(8):1044–52. Available from: http://doi.wiley.com/10.1111/cea.12357

255. Hall IP, Fowler A V., Gupta A, Tetzlaff K, Nivens MC, Sarno M, et al. Efficacy of BI 671800, an oral CRTH2 antagonist, in poorly controlled asthma as sole controller and in the presence of inhaled corticosteroid treatment. Pulm Pharmacol Ther [Internet]. 2015 Jun;32:37–44. Available from: https://linkinghub.elsevier.com/retrieve/pii/S1094553915000383

256. Busse WW, Wenzel SE, Meltzer EO, Kerwin EM, Liu MC, Zhang N, et al. Safety and

efficacy of the prostaglandin D2 receptor antagonist AMG 853 in asthmatic patients. J Allergy Clin Immunol [Internet]. 2013 Feb;131(2):339–45. Available from: https://linkinghub.elsevier.com/retrieve/pii/S0091674912016570

257. Kerstjens HAM, Gosens R. Comment Prostaglandin D 2 : the end of a story or just the beginning ? Lancet Respir [Internet]. 2020;5(20):10–1. Available from: http://dx.doi.org/10.1016/S2213-2600(20)30449-5
258. Kamanna VS, Ganji SH, Kashyap ML. The mechanism and mitigation of niacin-induced flushing. Int J Clin Pract [Internet]. 2009 Sep;63(9):1369–77. Available from: http://doi.wiley.com/10.1111/j.1742-1241.2009.02099.x
259. Dishy V, Liu F, Ebel DL, Atiee GJ, Royalty J, Reilley S, et al. Effects of aspirin when added to the prostaglandin d2 receptor antagonist laropiprant on niacin-induced flushing symptoms. J Clin Pharmacol. 2009;49(4):416–22.
260. Van Hecken A, Depré M, De Lepeleire I, Thach C, Oeyen M, Van Effen J, et al. The effect of MK-0524, a prostaglandin D2 receptor antagonist, on prostaglandin D2-induced nasal airway obstruction in healthy volunteers. Eur J Clin Pharmacol. 2007;63(2):135–41.
261. Philip G, van Adelsberg J, Loeys T, Liu N, Wong P, Lai E, et al. Clinical studies of the DP1 antagonist laropiprant in asthma and allergic rhinitis. J Allergy Clin Immunol [Internet]. 2009;124(5):942-948.e9. Available from: http://dx.doi.org/10.1016/j.jaci.2009.07.006
262. Okubo K, Hashiguchi K, Takeda T, Baba K, Kitagoh H, Miho H, et al. A randomized controlled phase II clinical trial comparing ONO-4053, a novel DP1 antagonist, with a leukotriene receptor antagonist pranlukast in patients with seasonal allergic rhinitis. Allergy Eur J Allergy Clin Immunol. 2017;72(10):1565–75.
263. Lee K, Lee SH, Kim TH. The biology of prostaglandins and their role as a target for allergic airway disease therapy. Int J Mol Sci. 2020;21(5).
264. Aldous S, Fennle M, Jiang J, John S, Mu L, Pedgrift B, et al. Patent US,8258,130 B2 - Pyrimidine hydrazide compounds as PGDS inhibitors [Internet]. United States Patent; 2012. p. Sep. 4. Available from: https://patents.google.com/patent/US8258130/un
265. VanDeusen C (Sanofi/Paris). Patent US 9,937,175 B2 - Phenyloxadialzole derivatives as PGDS inhibitors [Internet]. United States Patent; 2018. p. Apr. 10. Available from: http://www.freepatentsonline.com/9937175.pdf

266. Astex Therapeutics Limited G, Glaxosmith Kline Intelectual G. Patent WO 2017/103851 A1 - Quinoline-3-carboxamides as h-pgds inhibitors [Internet]. Patent Cooperation Treaty; 2017. p. Jun. 22. Available from: https://patents.google.com/patent/WO2017103851A1/pt
267. Zai Lab Pty. Ltd. Study of the Tolerability and Pharmacokinetic of ZL-2102 With an Investigation of Food Effect in Healthy Male Subjects [Internet]. 2015 [cited 2019 Mar 7]. Available from: https://clinicaltrials.gov/ct2/show/NCT02397005
268. Takeshita E, Komaki H, Shimizu-Motohashi Y, Ishiyama A, Sasaki M, Takeda S. A phase I study of TAS-205 in patients with Duchenne muscular dystrophy. Ann Clin Transl Neurol. 2018;5(11):1338–49.
269. Hoffmann J, Wilhelm J, Marsh LM, Ghanim B, Klepetko W, Kovacs G, et al. Distinct differences in gene expression patterns in pulmonary arteries of patients with chronic obstructive pulmonary disease and idiopathic pulmonary fibrosis with pulmonary hypertension. Am J Respir Crit Care Med. 2014;190(1):98–111.
270. Blacher S, Erpicum C, Lenoir B, Paupert J, Moraes G, Ormenese S, et al. Cell invasion in the spheroid sprouting assay: A spatial organisation analysis adaptable to cell behaviour. PLoS One. 2014;9(5):1–10.
271. Curcic S, Holzer M, Pasterk L, Knuplez E, Eichmann TO, Frank S, et al. Secretory phospholipase A 2 modified HDL rapidly and potently suppresses platelet activation. Sci Rep. 2017 Dec 1;7(1).
272. Schuligoi R. Effect of colchicine on nerve growth factor-induced leukocyte accumulation and thermal hyperalgesia in the rat. Naunyn Schmiedebergs Arch Pharmacol [Internet]. 1998;358(2):264–9. Available from: http://www.ncbi.nlm.nih.gov/pubmed/9750013
273. Deryugina EI, Quigley JP. Chapter 2 Chick Embryo Chorioallantoic Membrane Models to Quantify Angiogenesis Induced by Inflammatory and Tumor Cells or Purified Effector Molecules. Methods Enzymol. 2008;444(08):21–41.
274. Sedej M, Schröder R, Bell K, Platzer W, Vukoja A, Kostenis E, et al. D-type prostanoid receptor enhances the signaling of chemoattractant receptor–homologous molecule expressed on TH2 cells. J Allergy Clin Immunol [Internet]. 2012 Feb;129(2):492-500.e9. Available from: https://linkinghub.elsevier.com/retrieve/pii/S0091674911013157
275. Lal BK, Varma S, Pappas PJ, Hobson RW, Durán WN. VEGF increases permeability of the

endothelial cell monolayer by activation of PKB/akt, endothelial nitric-oxide synthase, and MAP kinase pathways. Microvasc Res. 2001;62(3):252–62.

276. Xu H, Song J, Gao X, Xu Z, Xu X, Xia Y, et al. Paeoniflorin attenuates lipopolysaccharide-induced permeability of endothelial cells: involvements of F-actin expression and phosphorylations of PI3K/Akt and PKC. Inflammation [Internet]. 2013 Feb;36(1):216–25. Available from: http://www.ncbi.nlm.nih.gov/pubmed/23053726
277. Werder RB, Lynch JP, Simpson JC, Zhang V, Hodge NH, Poh M, et al. PGD2/DP2 receptor activation promotes severe viral bronchiolitis by suppressing IFN- production. Sci Transl Med. 2018;10(440).
278. Zajac E, Schweighofer B, Kupriyanova TA, Juncker-Jensen A, Minder P, Quigley JP, et al. Angiogenic capacity of M1- and M2-polarized macrophages is determined by the levels of TIMP-1 complexed with their secreted proMMP-9. Blood. 2013 Dec;122(25):4054–67.
279. Elliott MR, Koster KM, Murphy PS. Efferocytosis Signaling in the Regulation of Macrophage Inflammatory Responses. J Immunol. 2017;198(4):1387–94.
280. Samitas K, Poulos N, Semitekolou M, Morianos I, Tousa S, Economidou E, et al. Activin-A is overexpressed in severe asthma and is implicated in angiogenic processes. Eur Respir J [Internet]. 2016;47(3):769–82. Available from: http://dx.doi.org/10.1183/13993003.00437-2015
281. Gilroy DW, Colville-Nash PR, Willis D, Chivers J, Paul-Clark MJ, Willoughby DA. Inducible cyclooxygenase may have anti-inflammatory properties. Nat Med. 1999;5(6):698–701.
282. Claesson-Welsh L. Vascular permeability—the essentials. Ups J Med Sci [Internet]. 2015 Jul 3;120(3):135–43. Available from: http://www.tandfonline.com/doi/full/10.3109/03009734.2015.1064501
283. Ke Y, Oskolkova O V., Sarich N, Tian Y, Sitikov A, Tulapurkar ME, et al. Effects of prostaglandin lipid mediators on agonist-induced lung endothelial permeability and inflammation. Am J Physiol - Lung Cell Mol Physiol. 2017;313(4):L710–21.
284. Schuligoi R, Sedej M, Waldhoer M, Vukoja A, Sturm EM, Lippe IT, et al. Prostaglandin H2 induces the migration of human eosinophils through the chemoattractant receptor homologous molecule of Th2 cells, CRTH2. J Leukoc Biol. 2008;85(1):136–45.

285. Foudi N, Kotelevets L, Louedec L, Leséche G, Henin D, Chastre E, et al. Vasorelaxation induced by prostaglandin E 2 in human pulmonary vein: Role of the EP 4 receptor subtype. Br J Pharmacol. 2008;154(8):1631–9.

286. Barabutis N, Verin A, Catravas JD. Regulation of pulmonary endothelial barrier function by kinases. Am J Physiol Lung Cell Mol Physiol [Internet]. 2016;311(5):L832–45. Available from: http://www.ncbi.nlm.nih.gov/pubmed/27663990

287. Roberts TK, Eugenin EA, Lopez L, Romero IA, Weksler BB, Couraud PO, et al. CCL2 disrupts the adherens junction: Implications for neuroinflammation. Lab Investig. 2012;92(8):1213–33.

288. Wang L, Bittman R, Garcia JGN, Dudek SM. Junctional complex and focal adhesion rearrangement mediates pulmonary endothelial barrier enhancement by FTY720 S-phosphonate. Microvasc Res [Internet]. 2015;99:102–9. Available from: http://dx.doi.org/10.1016/j.mvr.2015.03.007

289. Di Lorenzo A, Lin MI, Murata T, Landskroner-Eiger S, Schleicher M, Kothiya M, et al. eNOS-derived nitric oxide regulates endothelial barrier function through VE-cadherin and Rho GTPases. J Cell Sci [Internet]. 2013 Dec 15;126(Pt 24):5541–52. Available from: http://www.ncbi.nlm.nih.gov/pubmed/24046447

290. Koch KA, Wessale JL, Moreland R, Reinhart GA, Cox BF. Effects of BW245C, a prostaglandin DP receptor agonist, on systemic and regional haemodynamics in the anaesthetized rat. Clin Exp Pharmacol Physiol [Internet]. 2005 Nov [cited 2020 Jan 21];32(11):931–5. Available from: http://doi.wiley.com/10.1111/j.1440-1681.2005.04287.x

291. Ahmad AS. PGD2 DP1 receptor stimulation following stroke ameliorates cerebral blood flow and outcomes. Neuroscience. 2014 Oct 1;279:260–8.

292. Town HH, Casals-Stenzel J, Schillinger E. Pharmacological and cardiovascular properties of a hydantoin derivative, BW 245 C, with high affinity and selectivity for PGD2receptors. Prostaglandins. 1983;25(1):13–28.

293. Nakajima M, Goh Y, Azuma I, Hayaishi O. Effects of prostaglandin D2 and its analogue, BW245C, on intraocular pressure in humans. Graefe's Arch Clin Exp Ophthalmol. 1991 Sep;229(5):411–3.

294. Maehara T, Nakamura T, Maeda S, Aritake K, Nakamura M, Murata T. Epithelial cell-

derived prostaglandin D2 inhibits chronic allergic lung inflammation in mice. FASEB J. 2019;33(7):8202–10.

295. Tsubosaka Y, Maehara T, Imai D, Nakamura T, Kobayashi K, Nagata N, et al. Hematopoietic prostaglandin D synthase-derived prostaglandin D2 ameliorates adjuvant-induced joint inflammation in mice. FASEB J. 2019;33(6):6829–37.
296. Buckley J, Birrell MA, Maher SA, Nials AT, Clarke DL, Belvisi MG. EP4 receptor as a new target for bronchodilator therapy. Thorax. 2011;66(12):1029–35.
297. Spik I, Brenuchon C, Angeli V, Staumont D, Fleury S, Capron M, et al. Activation of the Prostaglandin D2 Receptor DP2/CRTH2 Increases Allergic Inflammation in Mouse. J Immunol [Internet]. 2005;174(6):3703–8. Available from: http://www.jimmunol.org/cgi/doi/10.4049/jimmunol.174.6.3703
298. Armstrong RA, Lawrence RA, Jones RL, Wilson NH, Collier A. Functional and ligand binding studies suggest heterogeneity of platelet prostacyclin receptors. Br J Pharmacol [Internet]. 1989 Jul;97(3):657–68. Available from: http://doi.wiley.com/10.1111/j.1476-5381.1989.tb12001.x
299. Alexander SPH, Christopoulos A, Davenport AP, Kelly E, Mathie A, Peters JA, et al. THE CONCISE GUIDE TO PHARMACOLOGY 2019/20: G protein-coupled receptors. Br J Pharmacol [Internet]. 2019 Dec 11;176(S1). Available from: https://onlinelibrary.wiley.com/doi/abs/10.1111/bph.14748
300. Norel X, Sugimoto Y, Ozen G, Abdelazeem H, Amgoud Y, Bouhadoun A, et al. International Union of Basic and Clinical Pharmacology. CIX. Differences and Similarities between Human and Rodent Prostaglandin E 2 Receptors (EP1–4) and Prostacyclin Receptor (IP): Specific Roles in Pathophysiologic Conditions. Ohlstein EH, editor. Pharmacol Rev [Internet]. 2020 Oct 22;72(4):910–68. Available from: http://pharmrev.aspetjournals.org/lookup/doi/10.1124/pr.120.019331
301. Italiani P, Boraschi D. Development and Functional Differentiation of Tissue-Resident Versus Monocyte-Derived Macrophages in Inflammatory Reactions. In: Results and problems in cell differentiation [Internet]. 2017 [cited 2018 Jan 19]. p. 23–43. Available from: http://www.ncbi.nlm.nih.gov/pubmed/28455704
302. Kopf M, Schneider C, Nobs SP. The development and function of lung-resident

macrophages and dendritic cells. Nat Immunol [Internet]. 2015;16(1):36–44. Available from: http://www.ncbi.nlm.nih.gov/pubmed/25521683

303. Birnhuber A, Egemnazarov B, Biasin V, Bonyadi Rad E, Wygrecka M, Olschewski H, et al. CDK4/6 inhibition enhances pulmonary inflammatory infiltration in bleomycin-induced lung fibrosis. Respir Res. 2020;21(1):4–8.
304. Artyomov MN, Sergushichev A, Schilling JD. Integrating immunometabolism and macrophage diversity. Semin Immunol [Internet]. 2016 Oct;28(5):417–24. Available from: https://linkinghub.elsevier.com/retrieve/pii/S1044532316301051
305. Holash J, Maisonpierre PC, Compton D, Boland P, Alexander CR, Zagzag D, et al. Vessel cooption, regression, and growth in tumors mediated by angiopoietins and VEGF. Science (80-). 1999;284(5422):1994–8.
306. Weis S, Cui J, Barnes L, Cheresh D. Endothelial barrier disruption by VEGF-mediated Src activity potentiates tumor cell extravasation and metastasis. J Cell Biol. 2004;167(2):223–9.
307. Simcock DE, Kanabar V, Clarke GW, O'Connor BJ, Lee TH, Hirst SJ. Proangiogenic activity in bronchoalveolar lavage fluid from patients with asthma. Am J Respir Crit Care Med. 2007;176(2):146–53.
308. Hellström M, Kalén M, Lindahl P, Abramsson A, Betsholtz C. Role of PDGF-B and PDGFR-β in recruitment of vascular smooth muscle cells and pericytes during embryonic blood vessel formation in the mouse. Development. 1999;126(14):3047–55.
309. Hawinkels LJAC, Kuiper P, Wiercinska E, Verspaget HW, Liu Z, Pardali E, et al. Matrix metalloproteinase-14 (MT1-MMP)-mediated endoglin shedding inhibits tumor angiogenesis. Cancer Res. 2010;70(10):4141–50.
310. Vitverova B, Blazickova K, Najmanova I, Vicen M, Hyšpler R, Dolezelova E, et al. Soluble endoglin and hypercholesterolemia aggravate endothelial and vessel wall dysfunction in mouse aorta. Atherosclerosis. 2018;271:15–25.
311. Asai K, Kanazawa H, Otani K, Shiraishi S, Hirata K, Yoshikawa J. Imbalance between vascular endothelial growth factor and endostatin levels in induced sputum from asthmatic subjects. J Allergy Clin Immunol. 2002;110(4):571–5.

Appendix

7.1 Materials & Equipment

Table 1. *List of endothelial cell donors. HPMEC – human pulmonary microvascular endothelial cells, HDMEC – human dermal microvascular endothelial cells, HPAEC – human pulmonary artery endothelial cells*

DONOR #	TYPE	COMPANY
525116	HPMEC	Lonza
612039	HPMEC	Lonza
560121	HPMEC	Lonza
560758	HPMEC	Lonza
429Z007.1	HPMEC	PromoCell
431Z036.1	HPMEC	PromoCell
435Z034.2	HDMEC	PromoCell
423Z018.1	HDMEC	PromoCell
28074	HPAEC	Lonza
21304	HPAEC	Lonza
27930	HPAEC	Lonza

Table 2. List of agonists, antagonists, inhibitors and stimulation agents.

Agonists						
NAME	**Target**	**Company**	**Cat#**	**stock [c]**	**diluent**	**used at**
PGD_2	DP1, DP2	CaymanChem	12010	30 mM	EtOH	100 nM - 3 µM
PGE_2	EP1-4	CaymanChem	14010	30 mM	EtOH	100 nM - 3 µM
DK-PGD_2	DP2	CaymanChem	12610	30 mM	EtOH	100 nM - 3 µM
BW245c	DP1	CaymanChem	12050	30 mM	EtOH	100 nM - 3 µM
S1P	S1PRs	Sigma-Aldrich	73914	125 µM	0.1% BSA in a.d.	100 nM
Antagonists						
NAME	**Target**	**Company**	**Cat#**	**stock [c]**	**diluent**	**used at**
ONO-AE3-208	EP4	CaymanChem	14522	10 mM	EtOH	300 nM
BWA868c	DP1	CaymanChem	12060	30 mM	EtOH	30 µM
Cay10471	DP2	CaymanChem	10006735	10 mM	EtOH	10 µM
MK 0524	DP1	CaymanChem	10009835	30 mM	EtOH	30 µM

T0070907	PPARy	CaymanChem	10026	100 mM	DMSO	30 µM
GW 627368X	EP4	CaymanChem	10009162	10 mM	DMSO	300 nM
SQ 29,548	TP	CaymanChem	19025	100 mM	EtOH	10 µM
Inhibitors						
NAME	**Target**	**Company**	**Cat#**	**stock [c]**	**diluent**	**used at**
HQL-79	hPGDS	CaymanChem	10134	10 mM	DMSO	100 µM
HPGDS Inhibitor I	hPGDS	CaymanChem	16256	10 mM	DMSO	100 µM
TFC 007	hPGDS	Bio-techne Ltd.	5108/10	100mM	DMSO	50 µM
PF 9184	mPGES-1	Bio-techne Ltd.	5917	30 mM	DMSO	30 µM
Diclofenac	COX-2	Sigma-Aldrich	D6899	3 mM	a.d.	1 µM
SQ 22,356	AC	Sigma-Aldrich	S153	100 mM	DMSO	10 µM
Cytochalasin B	Actin	Sigma-Aldrich	C6762	25 mg/ml	a.d.	2 mg/ml
H-89	PKA	CaymanChem	10010556	30 mM	DMSO	10 µM
U-73112	PLC	Sigma-Aldrich	662035	3 mM	DMSO	3 µM
Biologicals and stimulation agents						
NAME	**Target**	**Company**	**Cat#**	**stock [c]**	**diluent**	**used at**
rh IL-4	MDM	Immunotools	11340043	20 ug/ml	0.1% BSA in a.d.	20 nM
rh IL-10	MDM	Immunotools	11340105	20 ug/ml	0.1% BSA in a.d.	20 nM
rh M-CSF	Monocytes	PeproTech	AF-300	100 ug/ml	0.1% BSA in a.d.	100 nM
rh IFN-y	Mono, MDM	Immunotools	11343534	20 ug/ml	0.1% BSA in a.d.	20 nM
rh Thrombin	Endothelium	Sigma-Aldrich	T7009	500 U/ml	a.d.	0.5 U/ml
rh FGF-2	Endothelium	Sigma-Aldrich	SRP-4037	100 µg/ml	5mM Tris pH 7.6	10 ng/ml
rh TNF-a	Endothelium	Reliatech	300-028	10 µg/ml	a.d.	10 ng/ml
rh VEGF 165	Endothelium	Reliatech	300-076	25 µg/ml	a.d.	25 ng/ml
Lipopolysaccharide from E. *coli*	Mono, MDM	Sigma-Aldrich	L2880	5 mg/ml	a.d.	100 ng/ml

Table 3. List of primers used for murine myeloid populations.

Gene	NCBI ID	primerbank ID	Forward primer	Reverse primer
HPRT1	15452		AGGCCAGACTTTGTTGGATTTGAA	CAACTTGCGCTCATCTTAGGCTTT
HPGDS	54486	254281299c1	AAGCTGACTGGCCTAAAATCAAG	CTCTGGTGGATTGTAAGTCCTTC
mPGES1	64292	11967941a1	GGATGCGCTGAAACGTGGA	CAGGAATGAGTACACGAAGCC
COX2	19225	31981525a1	TGAGCAACTATTCCAAACCAGC	GCACGTAGTCTTCGATCACTATC
LPGDS	19215	2317286a1	TGCAGCCCAACTTTCAACAAG	TGGTCTCACACTGGTTTTTCCT

Table 4. List of antibodies used to determine phospho-proteins by Western blotting. BioTechne (Minnesota, USA), Cell Signaling (Massachusets, USA), Jackson ImmunoResearch (Pennsylvania, USA). FAK – focal adhesion kinase, GAPDH – glyceraldehyde-3-phosphate dehydrogenase, VE-cad – vascular endothelial cadherin, PAX – paxillin, AKT – protein kinase B, p – phosphorylated.

Target	Cat#	dilution	diluent	host	Company
GAPDH	2118S	1:5000	5 % milk in TBST	rabbit	Cell Signaling
FAK	3285	1:1000	5 % milk in TBST	rabbit	Cell Signaling
pFAK_Y925	3284	1:1000	5 % BSA in TBST	rabbit	Cell Signaling
VE-Cad	2500	1:1000	2.5 % BSA in TBST	rabbit	Cell Signaling
pVE-Cad_Y658	44-1144G	1:1000	2.5 % BSA in TBST	rabbit	ThermoFisher
PAX	12065	1:1000	2.5 % BSA in TBST	rabbit	Cell Signaling
pPAX_Y118	2541	1:1000	2.5 % BSA in TBST	rabbit	Cell Signaling
AKT	9272	1:1000	2.5 % BSA in TBST	rabbit	Cell Signaling
pAKT_S473	4058	1:1000	2.5 % BSA in TBST	rabbit	Cell Signaling
HRP anti-rabbit	111-035-045	1:5000	5 % milk in TBST	goat	Jackson Immuno

Table 5. Surface marker staining for differentiation of human leukocytes.

	Gate	Blocking	Markers
MDM	-	UV-block/ 5 % FCS in PBS	-
Inflammatory macrophages	-	UV-block/ 5 % FCS in PBS	CD80
Alternative macrophages	-	UV-block/ 5 % FCS in PBS	CD206
Monocytes	PBMC/ Monocytes	UV-block/ 5 % FCS in PBS	$CD14^+$
Eosinophils	PMNL/ Granulocytes	FcX block	$CD16^-$

Neutrophils	PMNL/ Granulocytes	FcX block	$CD16^+$
$CD4^+$ T cells	PBMC/ Lymphocytes	FcX block	$CD3^+$ $CD4^+$
$CD8^+$ T cells	PBMC/ Lymphocytes	FcX block	$CD3^+$ $CD8^+$
NK/T cells	PBMC/ Lymphocytes	FcX block	$CD3^-$ $CD56^+$
NK cells	PBMC/ Lymphocytes	FcX block	$CD3^+$ $CD56^+$
B cells	PBMC/ Lymphocytes	FcX block	$CD19^+$ $CD20^+$
Plasma Cells	PBMC/ Lymphocytes	FcX block	$CD138^+$
Dendritic cells	PBMC	FcX block	$HLA\text{-}DR^+$ $CD123^+$
Basophils	PBMC	FcX block	$HLA\text{-}DR^-$ $CD123^+$

Table 6. List of antibodies.

Antibodies for Flow cytometry			
	Company	**Cat.#**	**dilution**
APC mouse anti-human CD123	BD Bioscience	560087	1:5
PE Isotype Control IgG1 kappa	BD Bioscience	559320	1:5
PE mouse anti-human CD138	BD Bioscience	561704	1:5
PE mouse anti-human CD206	BD Bioscience	555954	1:5
PE mouse anti-human CD4	BD Pharmingen	561843	1:5
PE mouse anti-human CD8	BD Pharmingen	560949	1:5
PE mouse anti-human CD80	BD Bioscience	557227	1:5
PE mouse anti-human HLA/DR	BD Bioscience	556653	1:5
PE-Cy5 mouse anti-human CD16	BioLegend	302010	1:20
PE-Cy5.5 mouse anti-human CD3	BD Bioscience	555334	1:5
PE-Cy7 mouse anti-human CD20	BD Pharmingen	560735	1:20
PE-Cy7 mouse anti-human CD56	BD Pharmingen	560916	1:20
PerCP mouse anti-human CD14	BD Bioscience	2240746	1:50
V450 mouse anti-human CD19	BD Horizon	560354	1:20
FITC anti-mouse Ly6C	BioLegend	128005	1:600
APC anti-mouse Ly6G	BioLegend	127613	1:400
PE-Cy7 anti-mouse CD11b	BioLegend	561098	1:200
PerCP anti-mouse CD45	BioLegend	103129	1:300
PE anti-mouse F4/80	BioLegend	565410	1:50

APC-Cy7 anti-mouse c-kit	BioLegend	105825	1:100
Primary antibodies			
Mouse anti-hPGDS (IgG1)	Novus Bioscience	MAB6487	1:100
Mouse IgG1 isotype control	Novus Bioscience	MAB002	
Rabbit anti-hPGDS	EuBio	LS-B6886	1:100
Rabbit anti-LPGDS	Novus Bioscience	NBP1-79280	1:200
rabbit IgG isotype control	Abcam	ab27478	
goat anti-VE-cadherin	SantaCruz	sc-9989	1:200
rabbit anti-CD68	Abcam	ab125212	1:200
rabbit anti-EP4	SantaCruz	sc-20677	1:200
mouse anti-EP4	SantaCruz	sc-55596	1:200
rabbit anti-EP4	Abcam	ab133170	1:200
rabbit anti-DP1	CaymanChem	101640	1:200
rat anti-CRTH2	SantaCruz	sc-21798	1:200
mouse anti-β-actin	BioTechne	NB600-501	1:5000
Rabbit anti-human GAPDH	New England Biolabs	2118S	1:5000
HRP-conjugated antibodies			
goat anti-rabbit HRP	Jackson ImmunoResearch	111-035-045	1:5000
goat anti-mouse HRP	Jackson ImmunoResearch	115-035-062	1:5000
goat anti-rat HRP	Jackson ImmunoResearch	112-035-003	1:5000
Alexa Fluor-conjugated secondary antibodies			
AF488 rabbit anti-mouse	ThermoFisher	A-11059	
AF488 goat anti-mouse	ThermoFisher	A-10667	1:500
AF647 goat anti-mouse	ThermoFisher	A-21235	1:500
AF647 donkey anti-rabbit	ThermoFisher	A-32795	1:500
AF Pacific blue goat anti-rabbit	ThermoFisher	P-10994	1:500
Others			
TexasRed-X Phalloidin	ThermoFisher	T7471	1:40
TruStain FcX (anti-mouse CD16/32)	BioLegend	101320	1:20
TruStain FcX (human Fc receptor)	BioLegend	422302	1:100
Zombie aqua viability dye	BioLegend	423101	1:1000

Table 7. Myeloid panel for murine lung single cell suspension.

	Company	**Category #**	**Dilution**
FITC anti-mouse Ly6C	BioLegend	128005	1:600
APC anti-mouse Ly6G	BioLegend	127613	1:400

PE-Cy7 anti-mouse CD11b	BioLegend	561098	1:200
PerCP anti-mouse CD45	BioLegend	103129	1:200
PE anti-mouse F4/80	BioLegend	565410	1:50
APC-Cy7 anti-mouse c-kit	BioLegend	105825	1:100
Zombie aqua viability dye	BioLegend	423101	1:500

Table 8. List of chemicals and reagents.

Cell culture		
	Company	**Cat #**
L-Cystein	Sigma	C7352
EBM-MV medium	PromoCell	C-22221
EBM-MV medium	Lonza	CC-3202
Microvascular EC kit	PromoCell	C-22121
Microvascular EC kit	Lonza	CC-4147
0.04 % Trypsin/EDTA solution	PromoCell	C41010
0.025 % Trypsin/EDTA solution	Lonza	CC-5012
Trypsin neutralizing solution	PromoCell	C-41110
Trypsin neutralizing solution	Lonza	CC-5002
Cell attachment factor solution	PeloBiotech	PB123-100
Gelatin from bovine skin, type B, powder	Sigma-Aldrich	G9391
Trypsin/EDTA solution	PAN Biotechnology	P10-023100
Accutase	Sigma-Aldrich	A6864
Histopaque-1077	Sigma-Aldrich	10771
Phosphate buffered saline (PBS) with or w/o Ca2+ and Mg2+	ThermoFisher	14190144
Hank's buffered saline solution (HBSS) w/o Ca2+ and Mg2+	ThermoFisher	14170112
New born calf serum	ThermoFisher	16010159
Fetal Bovine Serum	Gibco Life Technologies	11573397
RPMI 1640 with stable Glutamine	Gibco Life Technologies	11875093
Human Serum from human male AB plasma	Sigma-Aldrich	H4522
MEM non-essential Amino Acid solution	Sigma-Aldrich	M7145
Sodium Pyruvate Solution	Sigma-Aldrich	S8636
Penicillin/Streptomycin (100x)	PAN Biotechnology	P0607100
D(+) Glucose	Sigma-Aldrich	G8270
Dextrane	Sigma-Aldrich	31392
Methylcellulose	Sigma-Aldrich	M0512
NaCO3	Sigma-Aldrich	E005761

Rat-tail collagen type I	Corning	354236
Monocyte Isolation Kit II	Miltenyi	130-091-153
Eosinophil isolation Kit	Miltenyi	130-092-010
HEPES Buffer Solution 1M	PAN Biotechnology	P05-01100
Lipofectamin RNAiMAX	ThermoFisher	13778075
PTGER4 FlexiTube-Gene Solution	Qiagen	1027416
Negative control siRNA duplex	Qiagen	1027310
OptiMEM I reduced serum medium	ThermoFisher	31985062
Molecular biological methods		
CellFix	BD Immunocytometry Systems	340181
Dako Antibody Diluent	Dako	S3023
FACSFlow	BD Immunocytometry Systems	324003
Fixation/Permeabilization Kit	BD Biosciences	BDB554714
Fresenius double-distilled water	Fresenius Kabi Austria	
iScript cDNA Synthesis Kit	BioRad	1708890
High capacity cDNA synthesis kit	ThermoFisher	4368814
SsoAdvanced Universal SYBR Green Supermix	BioRad	1725271
Goat Serum	Sigma	G9023
TriReagent	ThermoFisher	AM9738
Formaledhyde solution 37 %	CarlRoth	CP10.1
Bovine Serum Albumin	Sigma-Aldrich	A7906
Triton X-100	Fluka BioChemika	00212
DAPI mounting medium	Vectashield	H-1200
Diff-Quik staining Kit	Lactan	
Clarity™ Western ECL Blotting Substrate	BioRad	1705061
Ammonium Chloride for lysis buffer	CarlRoth	5470.1
RNAscope 2.5 HD	Biotechne	322360
RNAscope Probe- Mm-Hpgds	Biotechne	413391
Animal experiments		
Ketasol (115,3 mg/ml Ketaminhydrochlorid)	aniMedica, OGRIS Pharma V, Austria	05.611.1110
Rompun (20 mg/ml Xylazine)	Bayer, Vienna, Austria	(01)04007221017981
Isofluorane	Baxter	HDG9623
Saline solution for injection	Fresenius Kabi Austria	
Dispase II	Roche	4942078001
Low melt agarose solution	Sigma-Aldrich	A0701
DNAse I	Worthington	LS002006

Table 9. List of equipment.

Devices	Company
Axiocert 40 CFL microscope	Carl Zeiss Microscopy GmbH
Olympus IX70 fluorescence microscope	Olympus
Inverted microscope CKX41	Olympus
CFX Connect Real-Time PCR Detection System	BioRad
ChemiDoc Touch System	BioRad
ELx50 microplate washer	BioTek
FACS Canto II	BD Biosciences
FACS Aria IIIu	BD Biosciences
ECIS® Z-Theta device	Applied Biophysics
iBlot Gel Transfer Device	ThermoFisher
4-channel platelet aggregometer APACT4004	LabiTec
Microplate Spectrophotometer xMark	BioRad
Cytospin3	Shandon
Nikon A1 Confocal Microscope	Nikon
Equipment	
CellBind culture plates/flasks	Corning
Lab-Tek II CC2 8-chamber well slide	ThermoFisher
8W10E+ or 96W20idf polycarbonate arrays	Applied Biophysics
iBlot Transfer Stacks	ThermoFisher
Novex WedgeWell, 4-20% Tris Glycine Mini Gels	ThermoFisher
Cell strainer (100 µm, 70 µm, 40 µm)	Falcon
MACS Multistand Separator	Miltenyi Biotech
Others	
PGD_2-MOX ELISA Kit	CaymanChem
Pierce BCA Protein Assay Kit	ThermoFisher